

FINAL REPORT

Integrating Uncertainty Analysis in the Risk Characterization of In-Place Remedial Strategies for Contaminated Sediments

SERDP Project ER-1371

March 2009

Peter Adriaens
Steven J. Wright
The University of Michigan

Cyndee L. Gruden
University of Toledo

John Wolfe
Todd Redder
Noemi Barabas
Joseph DePinto
LimnoTech, Inc.



Strategic Environmental Research and
Development Program

Report Documentation Page			Form Approved OMB No. 0704-0188		
Public reporting burden for the collection of information is estimated to average 1 hour per response, including the time for reviewing instructions, searching existing data sources, gathering and maintaining the data needed, and completing and reviewing the collection of information. Send comments regarding this burden estimate or any other aspect of this collection of information, including suggestions for reducing this burden, to Washington Headquarters Services, Directorate for Information Operations and Reports, 1215 Jefferson Davis Highway, Suite 1204, Arlington VA 22202-4302. Respondents should be aware that notwithstanding any other provision of law, no person shall be subject to a penalty for failing to comply with a collection of information if it does not display a currently valid OMB control number.					
1. REPORT DATE MAR 2009		2. REPORT TYPE N/A		3. DATES COVERED -	
4. TITLE AND SUBTITLE Integrating Uncertainty Analysis in the Risk Characterization of In-Place Remedial Strategies for Contaminated Sediments				5a. CONTRACT NUMBER	
				5b. GRANT NUMBER	
				5c. PROGRAM ELEMENT NUMBER	
6. AUTHOR(S)				5d. PROJECT NUMBER	
				5e. TASK NUMBER	
				5f. WORK UNIT NUMBER	
7. PERFORMING ORGANIZATION NAME(S) AND ADDRESS(ES) The University of Michigan				8. PERFORMING ORGANIZATION REPORT NUMBER	
9. SPONSORING/MONITORING AGENCY NAME(S) AND ADDRESS(ES)				10. SPONSOR/MONITOR'S ACRONYM(S)	
				11. SPONSOR/MONITOR'S REPORT NUMBER(S)	
12. DISTRIBUTION/AVAILABILITY STATEMENT Approved for public release, distribution unlimited					
13. SUPPLEMENTARY NOTES The original document contains color images.					
14. ABSTRACT					
15. SUBJECT TERMS					
16. SECURITY CLASSIFICATION OF:			17. LIMITATION OF ABSTRACT UU	18. NUMBER OF PAGES 268	19a. NAME OF RESPONSIBLE PERSON
a. REPORT unclassified	b. ABSTRACT unclassified	c. THIS PAGE unclassified			

This report was prepared under contract to the Department of Defense Strategic Environmental Research and Development Program (SERDP). The publication of this report does not indicate endorsement by the Department of Defense, nor should the contents be construed as reflecting the official policy or position of the Department of Defense. Reference herein to any specific commercial product, process, or service by trade name, trademark, manufacturer, or otherwise, does not necessarily constitute or imply its endorsement, recommendation, or favoring by the Department of Defense.

EXECUTIVE SUMMARY

Background: In-place management of sediments, such as accomplished through capping technologies, has the potential to provide an important alternative and complement to sediment removal. Despite the development and increasing availability of technologies on the market, their efficient application is hindered by large uncertainties due to a lack of scientifically substantiated causal relationships. While there is a substantial body of reference material on field performance for such technologies, in order to integrate and generalize those lessons in practical decision-making at new sites, basic scientific relationships and uncertainties must be better quantified. For example, how is the system (sediment with monitored natural recovery or cap) response controlled by its biogeochemical and hydrodynamic properties? In addition, the ultimate effects of system characteristics on the pertinent risk end-points are not known in the context of in-place sediment remediation. These questions have not yet been addressed in an integrated fashion, with all components evaluated within the same system, from bench-scale to field scale. Therefore, the propagation of uncertainties associated with transitioning bench-scale measurements to field conditions needs to be quantified.

Goal and Approach: The overarching goal of this work was to characterize and bound the uncertainties associated with the impact of sediment processes (with focus on ebullition and advection) on the long-term performance of in situ capping strategies. The approach was a combination of experimental work and modeling to enable evaluation of the impact of ebullition and advection on both sediment bed stability and contaminant fluxes (here: PAH) from the sediment. The experiments were focused on the quantification of ebullition metrics, PAH flux measurements, and sediment resuspension measurements conducted in batch systems and flume configurations using sediments collected from the Anacostia River Capping Project. These site-specific data were aimed at narrowing the process uncertainties as they are currently reported in the literature. A geostatistical model was developed and applied to enable comparison of microbial data collected at the field and laboratory scales. The integrative modeling approach evolved from a generic water quality model to a custom-designed sediment flux model (SFM) that allowed for the integration of data collected at various scales, to link the flume and field aspects of the study.

Results: For the Anacostia River, findings from site-specific field and laboratory studies and the uncertainty analysis conducted with the SFM have shown that microbial gas-generated ebullition is likely not a significant process affecting contaminant flux through cap layers at the site, while groundwater seepage is likely to be an important long-term process in areas where there is a net advective flux of water from the sediment bed to the overlying water column. The current findings suggest that additional site characterization of the Anacostia River capping site should consider studies aimed at reducing the uncertainty and spatial variability in groundwater seepage rates. Monte Carlo-based predictions of PAH flux obtained for the sensitivity and uncertainty analyses provide valuable insight into the relative importance and sensitivity of model input parameters and the impact of the basis for value distributions. The outcome of these modeling analyses demonstrates that: (i) Model-predicted fluxes are strongly dependent on multiple process rates and physical parameters. Therefore, there is a clear need to evaluate the combined effect of input parameter uncertainties on uncertainties in expected fluxes and cap performance; (ii) Partitioning and other chemical-specific characteristics of a particular contaminant play a critical role in determining the extent to which that contaminant can be mobilized and

transported to the sediment-water interface; (iii) Significant reductions in input parameter uncertainties can be expected by incorporating site-specific field studies and in-situ/laboratory experiments, as opposed to relying exclusively on ranges available in literature for key process parameters; (iv) Laboratory-based data can be used to reduce the spatial estimation variance of sediment attributes (v) Significant (i.e., orders of magnitude) reductions in mean/median and interquartile range (IQR) for predicted total PAH flux can be obtained when relying on site-specific datasets to reduce parameter uncertainty for the Anacostia River; and (vi) An integrated capping model framework, such as the SFM, can be used to effectively compare relative performance across multiple capping technologies, as well as to evaluate the effect of combined parameter uncertainties on predicted contaminant flux from the sediment bed to the water column.

Implications: The combination of targeted site-specific experimental and generalizable modeling tools represents a step forward in terms of tools available for evaluating the performance of various capping technologies. The SFM developed here contains a similar level of sediment process complexity embodied within other available models, but is a user-friendly tool that is specifically designed to simulate the effect of capping actions on contaminant flux. Particularly important and unique to the model structure is the ability to simulate multiple “sediment” materials, which allows for an explicit representation of the physical properties not only of the parent bed material, but also sand cap, AquaBlok, coke breeze, and potentially other cap materials.

TABLE OF CONTENTS

1. Project Background	1
1.1 introduction.....	1
1.2 Objective	1
2. Review and Evaluation of Significance and Uncertainty of Sediment – Water Exchange Processes at Contaminated Sediment Sites	4
2.1 Partitioning	5
2.2 Particle Deposition and Erosion.....	6
2.3 Non-Resuspension Related Mass transfer Processes.....	8
2.3.1 Gas Ebullition	8
2.3.2 Groundwater Seepage	9
2.3.3 Diffusive Mass Transfer and Bioturbation	10
2.4 Biotransformation	11
2.5 Overall Significance and Relative Uncertainty	12
3. Water Quality Model Framework for Uncertainty Quantification and Propagation	15
3.1 Water Quality Analysis Simulation Program (WASP).....	16
3.1.1 Model Description and Parameterization	16
3.1.2 Parameterization.....	16
3.1.3 Preliminary Assessment of Uncertainty Quantification and Propagation	18
3.2 Sediment Flux Model (SFM)	21
3.2.1 Differences Between WASP and SFM	22
3.2.2 Model Conceptual Design	22
3.2.3 Model Process Representation	24
4. Spatial Distribution of Sediment Microbial Characteristics in Field and Laboratory Settings.	29
4.1 Microbial Abundance and Activity Measurement	29
4.1.1 Materials and Methods	29
4.1.2 Results and Discussion.....	31
4.1.3 Extraction of Data for Integration Modeling.....	35
4.2 Microbial Ebullition Measurements	36
4.2.1 Experimental Approach	36
4.2.2 Results and Discussion.....	37
<u>Biogas dependence on temperature.....</u>	39
4.2.3 Data Extraction for Integration Modeling	40
4.3 Spatial Modeling of Sediment Microbial Characteristics.....	40
4.3.1 Description of Modeling Tools	40
4.3.2 Data Treatment and Variogram Development	43
4.3.3 Results and Discussion.....	45
4.4 Overall Significance and Impact on Uncertainty	47
5. Impact of Advection and Ebullition on the Physical Stability of Sediments	48
5.1 Experimental Approach.....	48
5.1.1 Description of Environmental Apparatus	48

5.1.2 Experimental Procedures	50
5.1.3 Modeling Considerations	56
5.2 Results and Discussion	61
5.2.1 Ebullition Forcings	63
5.2.2 Advective Forcings	66
5.2.3 Aquablok™ Cap Experiments	68
5.3 Overall Significance and Impact on Uncertainty	72
6. Impact of Advection and Ebullition on the Chemical Stability of PAH in Sediments	74
6.1 Experimental Approach	74
6.1.1 Description of Experimental Apparatus	74
6.1.2 Experimental Conditions and Preliminary Analysis	75
6.2 Results and Discussion	77
6.2.1 SPMD-PAH Concentrations under Control Conditions	77
6.2.2 PAH Fluxes in the Presence of Ebullition	78
6.2.3 PAH Fluxes in the Presence of Advection	80
6.3 Overall Significance and Impact on Uncertainty	83
7. Integration of Flume and Field Data Using Uncertainty Modeling	84
7.1 Sediment Flux Model Confirmation	84
7.1.1 Flux Chamber Experiments	84
7.1.2 Anacostia River Pilot Capping Study	86
7.2 Model Uncertainty Analysis	88
7.2.1 Monte Carlo Sensitivity Analysis	89
7.2.2 Monte Carlo Uncertainty Analysis	95
7.3 Summary of Findings	102
7.4 “Sediment Flux Model” – Future Improvements	102
8. References	104
9. Appendices	104
Appendix A. Literature Review “Review and Evaluation of Significance and Uncertainty of Sediment – Water Exchange Processes at Contaminated Sediment Sites”	
Appendix B. Excel Spreadsheets of Flux Calculations	
Appendix C. List of Publications and Presentations	

LIST OF FIGURES

Figure 1-1.	<i>Project framework</i>	2
Figure 1-2.	<i>Project Flow Chart</i>	3
Figure 2-1.	<i>Surface sediment processes that affect natural attenuation and in situ remediation.</i>	5
Figure 3-1.	<i>Tiered Model Complexity</i>	15
Figure 3-2.	<i>Basic model segmentation of WASP for the Anacostia River.</i>	17
Figure 3-3.	<i>Uncertainty propagation of PAH fluxes for strongly sorbing compounds</i>	19
Figure 3-4.	<i>Uncertainty propagation of PAH fluxes for mildly sorbing compounds</i>	20
Figure 3-5.	<i>Contaminant transport process flow chart</i>	21
Figure 3-6.	<i>Sediment Flux Model Process Diagram</i>	23
Figure 4-1.	<i>Sediment Tank Reactor</i>	29
Figure 4-2.	<i>Sampling schemes in the field (A) and the laboratory tank reactor (B)</i>	30
Figure 4-3.	<i>The average number of total and active bacteria per gram dry sediment across cap type. (■) active numbers (□) total numbers</i>	31
Figure 4-4.	<i>Average metabolic response (AMR) across cap types. (▲) No cap, (■) Aquablok™ cap, (□) Sand cap</i>	31
Figure 4-5.	<i>Dendrogram for DGGE from bacteria in sediments.</i>	32
Figure 4-6.	<i>Microbial abundance and activity in unamended sediment flux chamber</i>	33
Figure 4-7.	<i>Total and active microorganisms at fine scale spatial resolution in the flux tank</i>	34
Figure 4-8.	<i>Microbial activity as measured using CTC for 65% (top) and 0.7% (bottom) active sediment samples</i>	35
Figure 4-9.	<i>Total and active microorganisms in sand (A), Aquablok (B) and uncapped (C) sediments (left to right, 5 cm increments below the cap)</i>	35
Figure 4-10.	<i>Distribution of gas production from Anacostia River sediments</i>	37
Figure 4-11.	<i>Time trends of dinitrogen (left) and carbon dioxide in sediments</i>	38
Figure 4-12.	<i>Biogas and composition rate (mL/gdw/d and $\mu\text{mole/gdw/d}$, respectively) in 80 days incubation experiment with 2% HRC at room temperature in three depths, 1-10 cm (top), 10-20 cm (middle) and 20-30 cm (bottom): (a) biogas; (b) nitrogen; (c) carbon dioxide; (d) methane. (▲) No-cap, (□) Sand-cap (ave\pmst. dev., n=3).</i>	38
Figure 4-13.	<i>Biogas rate (mL/gdw/d) in time distribution for the first 14 day incubation experiment when biogas stopped and no measurable biogas volume for several days in three depths: (a) No-cap; (b) Sand-cap. (Δ) 0-10 cm, (□) 10-20 cm, (▲) 20-30 cm (ave.\pmstd. dev., n=3)</i>	39
Figure 4-14.	<i>Biogas production for (a) biogas rate (mL/gdw/d); and (b) biogas composition rate ($\mu\text{mole/gdw/d}$) as a function of incubation temperature (22oC, 10oC, and 4oC), (□) nitrogen, () methane, (■) carbon dioxide (x\pmst.dev, n=3).</i>	39

Figure 4-15. Biogas production for: (a) biogas rate (mL/gdw/d) and (b) biogas composition rate ($\mu\text{mole/gdw/d}$) as a function of HRC amendment (2%, 1%, 0.5%, and 0.1%) at 22°C, (\square) nitrogen, (\circ) methane, (\blacksquare) carbon dioxide (ave \pm std error, n=3).	40
Figure 4-16. Conceptual sketch of the M-Scale model. Original data are used to evaluate the local mean at different spatial scales. The local means are further attributed different weights and evaluated as the estimates	41
Figure 4-17. Model diagnostics using artificial dataset	43
Figure 4-18. Site-scale sample locations with values indicated in color scales. Left: microbial abundance ($\times 10^7$ microorganisms/g) Right: microbial activity ($\times 10^6$ microorganisms/g). Units in distance: m.	43
Figure 4-19. Micro-scale sample locations with values indicated in color scales. Left: microbial abundance ($\times 10^7$ microorganisms/g) Right: microbial activity ($\times 10^6$ microorganisms/g). Units in distance: m.	44
Figure 4-20. Estimation map of microbial abundance with (left), without (right) measurement error	45
Figure 4-21. Estimation variance map with (left) and without (right) measurement error.	45
Figure 4-22. Likelihood of exceedance of 2.2×10^7 cells/g sediment with (left) and without (right) measurement error.	46
Figure 5-1. Experimental Setup plan and cross-sectional view.	48
Figure 5-2. Left: Soaker hoses before sediment placement. Right: Eroded sediment bed surface after an experiment.	49
Figure 5-3. Air and water injection system.	49
Figure 5-4. Schematic of apparatus to develop gas ebullition through sediments.	52
Figure 5-5. Grain size distributions for “Gudelsky sands” used in sand cap at the Anacostia River site (from App. A of the Cap Completion Report by Horne Engineering Services, 2000) and two samples of the sand used in the current laboratory experiments.	53
Figure 5-6. Grain size distribution determined by Hydrometer analysis of Anacostia sediments.	54
Figure 5-7. Variation in hydraulic conductivity measured for Anacostia River sediments in long duration falling head permeability test.	55
Figure 5-8. Longitudinal velocity profiles at same free stream velocity for experiments with strong injection and no injection conditions.	57
Figure 5-9. x-z velocity fluctuation covariance profiles at same free stream velocity for experiments with strong injection and no injection conditions.	58
Figure 5-10. Longitudinal velocity profiles at same free stream velocity for experiments with strong suction and no suction conditions.	58
Figure 5-11. x-z velocity fluctuation covariance profiles at same free stream velocity for experiments with strong suction and no suction conditions.	58
Figure 5-12. Modified Shields diagram, for the various suction/injection experiments performed.	60
Figure 5-13. Eroded sediment bed surface.	61
Figure 5-14. Concentration vs. time for an advective flow only experiment.	62

Figure 5-15.	<i>A channel formation viewed from the bed surface.</i>	63
Figure 5-16.	<i>Effect of shear versus shear plus ebullition on resuspension rates.</i>	64
Figure 5-17.	<i>Comparison between ebullition and ebullition plus advective flow experiment.</i>	65
Figure 5-18.	<i>Results from 5 ml/min and 50 ml/min seepage experiments with comparison to advective flow experiment</i>	66
Figure 5-19.	<i>Comparison of various Anacostia River sediment experiments</i>	66
Figure 5-20.	<i>Aquablok/ granules</i>	67
Figure 5-21.	<i>Left : Aquablok/ after a day of hydration, Right: Aquablok/ bed after an experiment</i>	67
Figure 5-22.	<i>Concentration measurements for Aquablok/-cap experiment</i>	69
Figure 5-23.	<i>Flexural crack in Aquablok/ formed by air pressure applied beneath</i>	70
Figure 5-24.	<i>Aquablok/ failure by heaving of a block of material.</i>	70
Figure 5-25	<i>Aquablok/ failure by flexing along one side wall.</i>	70
Figure 5-26.	<i>Aquablok/ failure by surface raising in middle of tank.</i>	70
Figure 5-27.	<i>View A of Aquablok/ rupture and air escape through rupture.</i>	71
Figure 5-28.	<i>View B of Aquablok/ rupture and air escape through rupture.</i>	71
Figure 5-29.	<i>Side view of water leakage through rupture in Aquablok/</i>	71
Figure 5-30.	<i>View from above of water leakage through rupture in Aquablok/</i>	71
Figure 6-1.	<i>Laboratory set up of flux chambers for measurement of PAH fluxes from sediments</i>	73
Figure 6-2.	<i>External and internal calibration of phenanthrene concentrations in flux chambers exposed to simulated ebullition.</i>	75
Figure 6-3.	<i>PAH emissions under control conditions in water (A) and air (B).</i>	76
Figure 6-4.	<i>Partitioning behavior of PAH in uncapped sediments (top), and for pyrene from Anacostia River sediments into under three conditions (bottom).</i>	77
Figure 6-5.	<i>Concentration profile of PAH in SPMD over Aquablok-capped Anacostia sediments.</i>	78
Figure 6-6.	<i>Comparison of ebullition-driven fluxes from sediments to the water column with control systems (in mg/m².yr).</i>	79
Figure 6-7.	<i>SPMD results under conditions of advective flow in the absence of a cap (top), and in the presence of a sand (middle) or Aquablok/ (bottom) cap.</i>	80
Figure 6-8.	<i>Flux comparisons for advection-driven uncapped and capped sediments</i>	81
Figure 7-1.	<i>Comparison of Model-Predicted Total Flux for Anthracene, Fluoranthene, Phenanthrene, and Pyrene to Flux Chamber Data (lower and upper error bars for model results represent the 5th and 95th percentiles for predicted flux)</i>	85
Figure 7-2.	<i>Observed Total PAH Sediment Profile for Sand Cap Location “SA-C1” after 30 Months.</i>	86
Figure 7-3.	<i>Model-Predicted Total PAH Sediment Profile for Sand Cap Area after 30 Months</i>	87

Figure 7-4.	<i>Monte Carlo Sensitivity Results for “No Cap” Scenario</i>	92
Figure 7-5.	<i>Monte Carlo Sensitivity Results for Sand Cap Scenario</i>	93
Figure 7-6.	<i>Monte Carlo Sensitivity Results for AquaBlok™ Scenario</i>	93
Figure 7-7.	<i>Monte Carlo Sensitivity Results for Coke Breeze Scenario</i>	94
Figure 7-8.	<i>Cumulative Frequency Distributions for “Uninformed” Monte Carlo Simulations</i>	99
Figure 7-9.	<i>Normalized Histograms for “Uninformed” Monte Carlo Simulations</i>	99

LIST OF TABLES

Table 2-1.	<i>Representative Rates and Attenuation Half-Times</i>	13
Table 2-2.	<i>Overall Assessment of Process Significance</i>	14
Table 3-1.	<i>Distribution of Input Parameters for WASP Model</i>	18
Table 3-2.	<i>WASP model output for strongly sorbing PAH compounds</i>	19
Table 3-3.	<i>WASP model output for mildly sorbing PAH compounds</i>	20
Table 4-1.	<i>Comparison of concepts and parameters for spatial attributes between the M-Scale model and conventional kriging approaches.</i>	42
Table 4-2.	<i>Comparison of spatial covariances between the M-Scale model and conventional kriging approaches.</i>	42
Table 4-3.	<i>Percent area of high microbial abundance (2.2×10^7) classified over the estimation domain under different confidence level of exceedance.</i>	46
Table 5-1.	<i>Discharge, surface velocity and shear stress levels applied to the bed</i>	61
Table 5-2.	<i>Discharge, surface velocity and shear stress levels applied to the Aquablok™ bed.</i>	68
Table 7-1.	<i>Monte Carlo distributions for model confirmation simulations</i>	84
Table 7-2.	<i>Literature-based physical and process input parameter distributions for model sensitivity analysis</i>	88
Table 7-3.	<i>Phenanthrene input parameter distributions</i>	89
Table 7-4.	<i>Benzo(k)fluoranthene input parameter distributions</i>	89
Table 7-5.	<i>Sediment cap thickness distributions (units in cm)</i>	90
Table 7-6.	<i>Constant sediment and cap input parameters</i>	90
Table 7-7.	<i>Total PAH concentration input parameter distributions</i>	95
Table 7-8.	<i>Physical and process input parameter distributions for the Anacostia River</i>	96
Table 7-9.	<i>Summary of ebullition results for Anacostia River sediments as reported by Yuan, et al. (2007)</i>	98
Table 7-10.	<i>“Uninformed” Monte Carlo Simulations: Statistical metrics for predicted 30-year average fluxes (mg/m²/yr)</i>	100
Table 7-11.	<i>Anacostia-specific Monte Carlo simulations: Statistical metrics for predicted 30-year average fluxes (mg/m²/yr)</i>	100

1. PROJECT BACKGROUND

1.1 INTRODUCTION

Dredging of contaminated sediments as a remediation option is associated with high costs, potential ecological risks and limited disposal options. In-place management of sediments, although not well understood, has the potential to provide an important alternative to sediment removal. Despite the development and increasing availability of technologies on the market, their efficient application is hindered by large uncertainties due to a lack of scientifically substantiated causal relationships. While there is a substantial body of reference material on field performance for such technologies, in order to integrate and generalize those lessons in practical decision-making at new sites, basic scientific relationships and uncertainties must be better quantified, i.e. how do pathways and risk end-points change in time and with different technologies; and, how is the system (sediment with monitored natural recovery or cap) response controlled by its biogeochemical and hydrodynamic properties? In other words, what are the impacts of the system on the pathways and risk (mobility, fate, bioavailability and toxicity), and how do these impacts depend on site-characteristics? In addition, the ultimate effects of system characteristics on the pertinent risk end-points are not known in the context of in-place sediment remediation. These questions have not yet been addressed in an integrated fashion, with all components evaluated within the same system, from bench-scale to field scale. Therefore, the propagation of uncertainties associated with transitioning bench-scale measurements to field conditions needs to be quantified.

The critical processes affecting contaminant in sediments are bioturbation, erosion/resuspension, diffusion, advection, and biogeochemical interactions and transformations (NRC, 1997). Overall, knowledge gaps on how to integrate these processes in sediment management remain. As a result, the recommended approach to in-situ remediation has been very conservative, in capping, for example, by discounting multiple functions of individual cap layers and calculating cap thickness by additively combining the thickness necessary for each of the three functions of caps (physical isolation, physical stability and chemical stability) (Palermo et al., 2002). In addition to data gaps in fundamental principles and information applicable to contaminated sediments in general, there is a dearth of site-specific information (Apitz et al., 2002; Palermo et al., 2002). For example, maximum shear stresses, which determine resuspension of sediments, depend not only on climate, or watershed characteristics but also on the specific bed/bottom morphology, and horizontal as well as vertical variations in cohesiveness and shear strength. Further, biogeochemistry/sediment microbiology is variable in time and heterogeneous in space even at the same site. It is thus imperative that scientific inquiries target relevant contaminated sediment sites, capitalizing on existing information and furthering the knowledge base at each.

1.2 OBJECTIVE

The objective of this project is to formulate pertinent relationships and decision criteria with reduced and quantified uncertainty in space and time that will allow improved prediction of decision variables, system integrity, and performance of in-place remedial strategies for PCDD/PAH-contaminated sediments.

This work aims to develop process understanding of seepage and ebullition on PAH fluxes, and integrate these parameters in an uncertainty-based remedial assessment framework (Figure 1-1) for capping strategies, using a combination of experimental work and modeling tools. The specific goals were to:

1. Conduct a comprehensive sediment process review and evaluation to identify data and information needs to help decision-makers most effectively use existing fate and transport frameworks in determining site suitability for *in situ* remedies, and to identify those processes for which the greatest uncertainties exist (Subtask 1)
2. Develop a modeling framework to evaluate the long term impact of advection and ebullition on contaminant fluxes through caps (Subtask 2)
3. Describe the spatial distribution of sediment microbial characteristics (abundance, respiratory competence, microbial ecology, gas ebullition potential) in field and laboratory studies (Subtask 3).
4. Quantify the impact of advection and ebullition on the physical stability of sediments in the presence and absence of caps (Subtask 4)
5. Quantify the impact of advection and ebullition on the chemical stability of PAH in sediments in the presence and absence of caps (Subtask 5)
6. Integrate the flume and field data using scaled uncertainty modeling (Subtask 6)

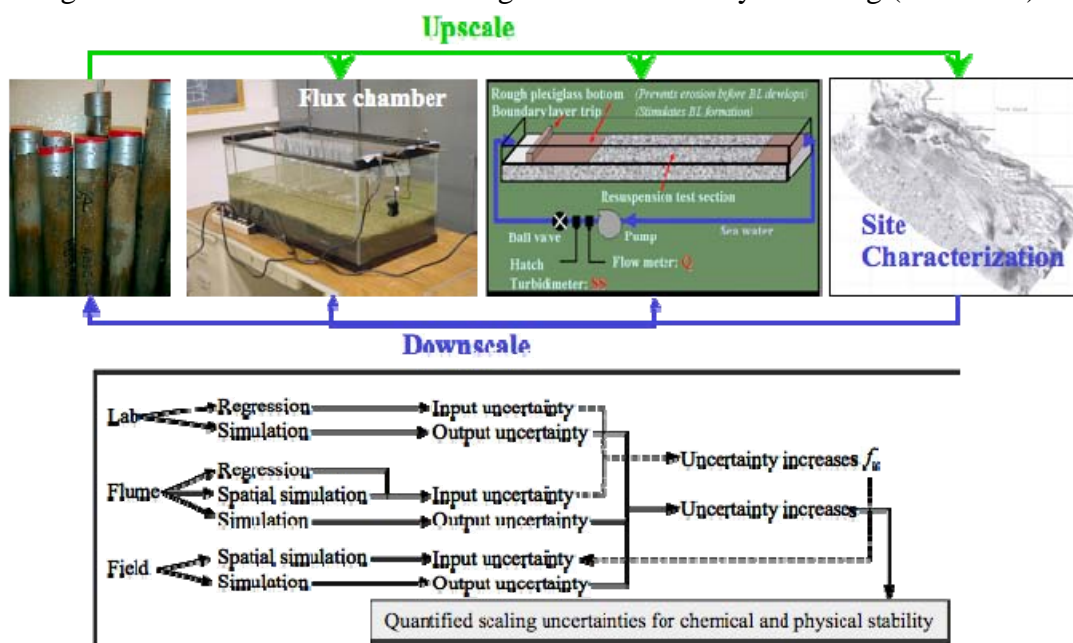


Figure 1-1. Project framework

These goals and subtasks are summarized in Figure 1-2. Also indicated in this figure are the outcomes from experimental and model subtasks that describe the uncertainty based technology evaluation framework. The 'outcome' boxes emphasize the parameter uncertainty quantification and propagation at the system level (WASP and sediment capping model), and extrapolation of the technology indicators from the laboratory to the field scale.

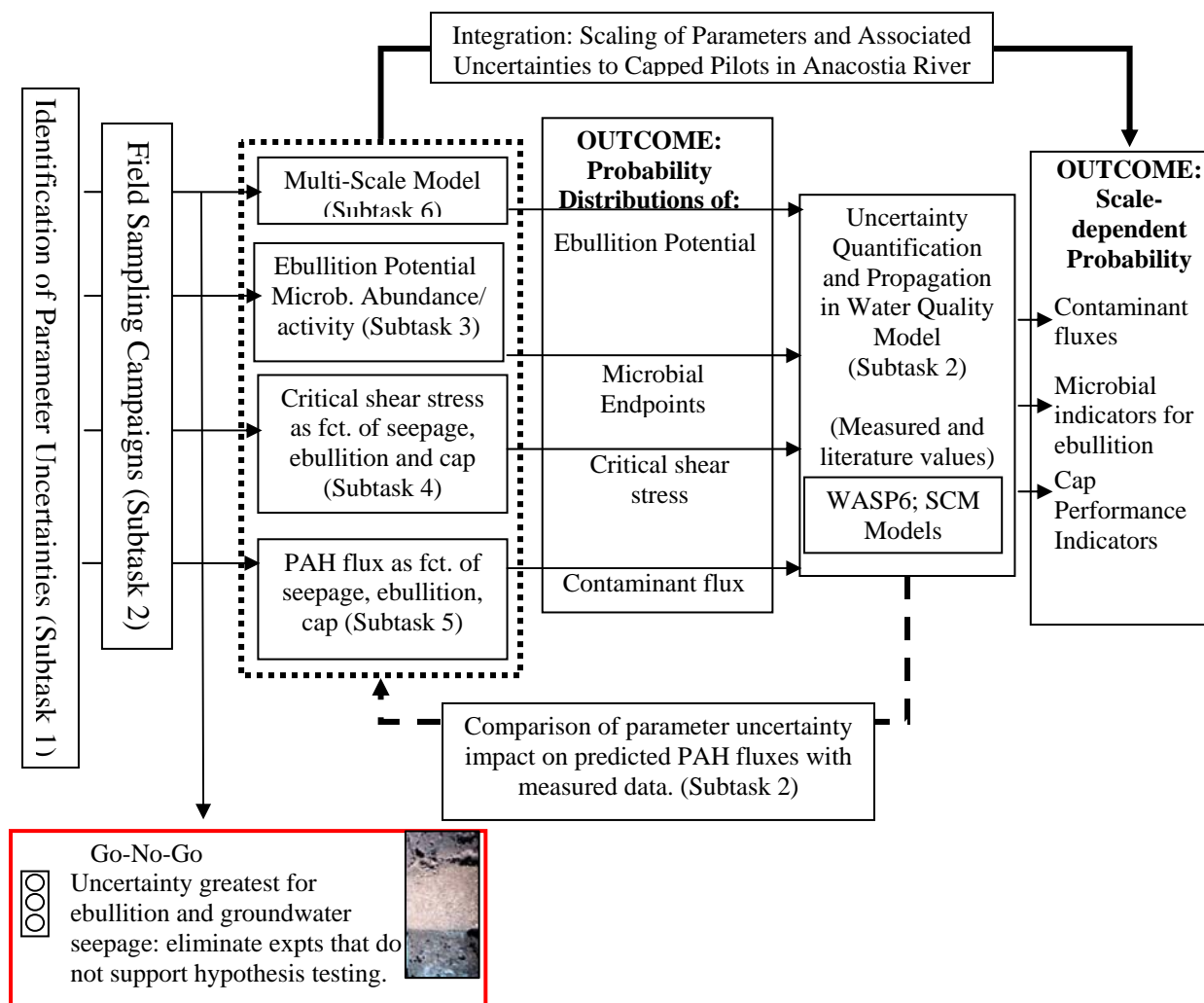


Figure 1-2. Project Flow Chart

2. REVIEW AND EVALUATION OF SIGNIFICANCE AND UNCERTAINTY OF SEDIMENT – WATER EXCHANGE PROCESSES AT CONTAMINATED SEDIMENT SITES

The objective of this sediment process review and evaluation is: *To identify data and information needs to help decision-makers most effectively use existing fate and transport frameworks in determining site suitability for in situ remedies, and to identify those processes for which the greatest uncertainties exist.* Basically, this objective seeks to review:

- What we know about those processes that affect the potential for a site to be remediated by an *in situ* technology;
- How we conceptualize and model those processes;
- What is the relative importance of each process in the decision-making;
- What is the relative importance of each process in site risk reduction; and
- What are the data/information gaps and greatest uncertainties in our ability to quantify the rate and extent of each process in sediment remediation.

In this context, we ask the basic question: *Where would an increase in data and a reduction in uncertainty provide the most utility in making decisions and in successful forecasting of a system's response to in situ remedies?*

In selecting the processes to review, we assume that, for sites being investigated for sediment remediation, risk is controlled by the concentration and bioavailability of the chemicals of concern in the surface sediment layer (upper mixed layer) of the system, or transported to the surface layer. Therefore, we reviewed those processes governing exposures to and losses from surficial sediments. We also have focused on the role of those processes in marine and estuary environments, and we have considered how those processes operate in both natural and capped systems.

Given the above objective, we reviewed the following processes:

- Partitioning of chemicals of concern in surface water and sediments and its effect on bioavailability and fate and transport processes of concern;
- Particle mediated transport by deposition and resuspension (sediment accumulation and scour);
- Gas formation and ebullition in sediments and its effect on sediment and chemical transport and stability;
- Groundwater seepage and its effect on mass transport in surficial sediments and resulting exposure;
- Non-resuspension-mediated chemical mass transfer from surface sediments and the role of bioturbation; and
- Biochemical processes in surface sediments and their role in contaminated sediment natural recovery and *in situ* remediation.

Figure 2-1 provides an illustration of the processes of concern in this review in terms of their potential for increasing or decreasing the exposure of a chemical of concern via the surface sediments of a system.

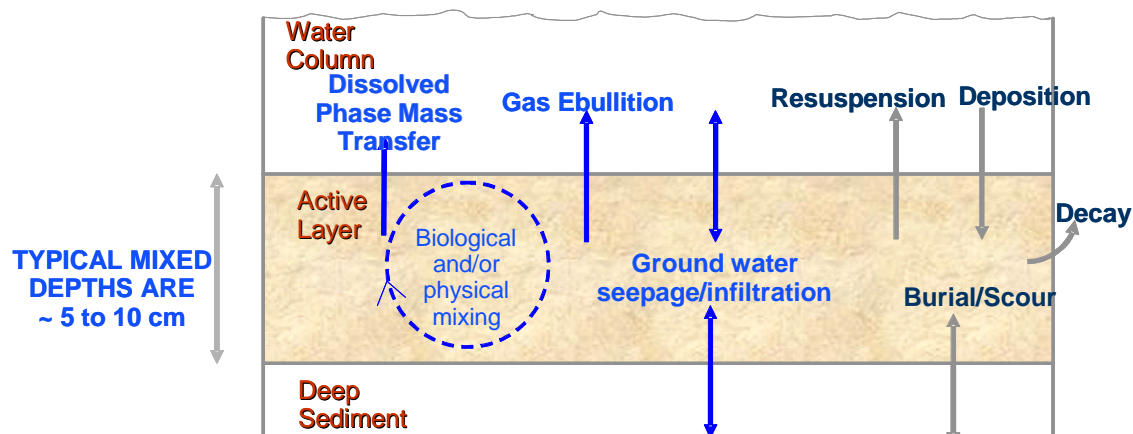


Figure 2-1. Surface sediment processes that affect natural attenuation and in situ remediation.

In conducting the reviews on these six processes, we limited our review of each process to the following topics:

- Provide a statement of the theoretical understanding of the process;
- Make a judgment of the adequacy of site-specific information on the process at a typical contaminated sediment site;
- Determine how the process is mathematically represented in current fate and transport models for contaminated sediments exposure; and
- Present the range of rates for the process that is typically observed and make an assessment of the prediction uncertainty for that process for *in situ* remedial outcomes.

The following section contains a synthesis of the findings of the individual reviews and a comparison of the processes in terms of their significance and overall prediction uncertainty. The individual reviews for each of these processes are presented in Appendices A-E.

2.1 PARTITIONING

Theoretical Process Understanding: Most chemicals of concern in contaminated sediment sites are hydrophobic; therefore, they have a propensity to partition to particulate matter. The degree to which contaminants can desorb from particles determines the mass available for biota exposure, as well as the rate of transport out of the system from other processes. Research shows that the partitioning behavior of the contaminant present can be influenced by a variety of factors, including chemical composition, sediment size and composition, hydraulics and hydrodynamics, and water chemistry. Often, a 3-phase partitioning approach is used, where the fraction in the

dissolved phase is disaggregated between sorbate bound to dissolved organic matter and truly dissolved sorbate. The 3-phase approach has advantages in relating partitioning to bioavailability, but dissolved organic carbon concentrations are often very small and difficult to measure. Most fate and transport models assume adsorption and desorption kinetics to be in instantaneous equilibrium. This assumption may be adequate when exposure times are long and the hydraulics of the system is relatively stable. However, considerable research has shown that desorption kinetics in natural systems are often quite slow (e.g., on the order of weeks to years to reach equilibrium) and significantly differ from theoretical predictions. Therefore, the equilibrium assumption may not always be valid, particularly in cases of high solute turnover and complex biotransformation processes. Applying a non-equilibrium partitioning function will generally result in a significantly reduced estimate of the concentration in the dissolved phase, when compared to the result of an instantaneous equilibrium model.

Adequacy of Typical Site-Specific Information: Adequate estimation of the partitioning behavior of contaminants requires site-specific data, including physiochemical properties of any sorbate present, sediment characteristics, and water chemistry. Although extensive literature exists documenting various theoretical properties of many contaminants, the actual site conditions can vary significantly, and are often more complex. Site-specific desorption analyses of sediment and water column samples are routinely conducted, and can greatly improve the characterization of the partitioning, and therefore, contaminant mass transfer behavior.

Representation in Leading Fate and Transport Models: Either 2- or 3-phased partitioning approaches can be implemented with the WASP, EFDC, and AQUATOX modeling frameworks. Standard applications of WASP and EFDC assume equilibrium partitioning, while AQUATOX assumes non-equilibrium partitioning.

Uncertainty: Accurate modeling of the fate and transport of HOCs depends greatly on appropriate characterization of the site conditions as well as the physiochemical properties of contaminants of concern. Site-specific data are often limited, requiring assumptions regarding the partitioning coefficients. The use of non-site-specific partitioning data can contribute significant uncertainty to fate and transport modeling, and the extent of this uncertainty is rarely evaluated. Laboratory analysis of samples collected from both the water column and sediment bed of the contaminated site is required for accurate representation of the in-situ partitioning, but even when these are available there is uncertainty associated with translation from the laboratory to behavior at field scale. More complex models tend to have more input data requirements. Uncertainty in the necessary model input data will lead to uncertainty in predictions.

2.2 PARTICLE DEPOSITION AND EROSION

Theoretical Process Understanding: Considerable research has been conducted in this area, but much of the theory has been developed using non-cohesive sediments, which are of less relevance than cohesive sediments for understanding contaminant fate and transport. According to Stokes Law, particle settling is dictated by particle diameter and density, but important factors causing non-ideal settling include particle shape and concentration, flow velocity and turbulence, and flocculation. Flocs formed by fluid shear and differential settling differ in time to form,

character, and settling rates: differential settling is slower and forms larger flocs with lower settling velocities. Deposition onto and attachment to the sediment bed have been described as probabilistic processes that are affected by turbulence at the sediment-water interface and by cohesiveness of the solid material. Sediment scour depends on hydraulic shear stress rising above a critical level, sufficient to dislodge particles. Scour and resuspension of non-cohesive sediments are well understood as functions of particle diameter, but widely applicable relationships predicting cohesive sediment scour have not yet been developed, requiring development of site-specific information. Cohesive sediment scour has been observed to depend on sediment bulk density, surface and porewater chemistry, algal colonization, and gas formation, in addition to bottom shear velocity. Estuary resuspension is most often driven by tidally-induced velocities, so that periodic resuspension and deposition cycles occur as a function of tidal cycles. Most often the net deposition is not significant, but is greatest in the region of the maximum salinity gradient, which leads to what is known as a turbidity maximum.

Adequacy of Typical Site-Specific Information: Site-specific distributions of suspended sediment particle sizes can be inexpensively obtained, and are often available for use in fate and transport model development. However, suspended solids calibration data alone will not uniquely constrain the relative settling and resuspension fluxes that determine the water column suspended solid concentrations; and this is important because it is the relative settling and resuspension fluxes that determine the net movement of particle-associated contaminants between bottom sediments and overlying water.

For cohesive sediments, we are still at the point where deposition and resuspension rates must be measured on a site-specific basis in order to adequately constrain particle-associated contaminant fluxes between water and bottom sediments. Actual sediment deposition rates, or the non-ideal factors that affect them, are much less likely to be known, as are data on floc formation and actual deposition rates of particles under varying conditions. Continuous flow records are available to estimate frequencies and magnitudes of high-flow events for most rivers. Site-specific scour measurements have been conducted at numerous sites, using *ex situ* and *in situ* flumes of various designs. A wide range of results has been found with the different flume types, spanning orders of magnitude. Net deposition rates can also be inferred from column studies and dredging records. Suspended solids loads, instream concentrations, and deposition and resuspension rates are often less thoroughly studied and documented than contaminant concentrations, but are necessary to constrain estimates of net solids deposition. Its two components (deposition and erosion) cannot be individually constrained because of their simultaneous nature, and can only be estimated by controlled experimentation.

Representation in Leading Fate and Transport Models: Both deposition and resuspension rates are represented phenomenologically in models, requiring site-specific rate measurements to parameterize the process formulations. In WASP and EFDC applications, multiple particle size categories are typically used to capture deposition variability, with chemical partitioning also varying by particle size. Settling rates can also be varied by water-column segment, reflecting differences in flow regimes. WASP can also be linked to a high-resolution hydrodynamic model. In EFDC, this linkage is built into the modeling framework.

Uncertainty: The main uncertainties in deposition processes are associated with particle size distributions and shapes, the degree of particle aggregation/disaggregation as a function of shear stress and particle properties, and the effects of fluid shear and bottom roughness on deposition. The main uncertainties for erosion (resuspension) process include the effects of depth and

associated consolidation on critical shear stress, and the true resuspension rates of cohesive sediments with a range of compositions, ranging from virtually all clay and fine silt with high organic content to a significant fraction of sand but still enough clay/silt to impart cohesive properties. The literature includes a very wide range of estimates for these parameters, reflecting potential measurement artifacts and the generally unsettled state of measurement technologies. Additional sources of uncertainty include armoring processes and the extent to which erosion rates change over time and amount of material eroded, and quantifying the effect of sediment porosity on resuspension, including the impact of gas bubble formation as it affects sediment column stability.

2.3 NON-RESUSPENSION RELATED MASS TRANSFER PROCESSES

Mass transfer between the sediment bed and the overlying surface water can be attributed to a wide range of processes. Because hydrophobic contaminants adsorb preferentially to sediment solids, resuspension can account for much of the contaminant sediment-water column mass transfer that occurs under ambient conditions. Processes contributing to resuspension include:

- flow event-driven scour;
- particulate transport due to benthic activity; and
- physical disturbance from wind-driven waves, fish activity, or human activity.

However, experience at several large contaminated sediment sites has found that non-resuspension-related processes can contribute significantly to contaminant mass transfer. Contributing processes include:

- direct desorption from surface sediments to the water column;
- molecular diffusion of dissolved phase or colloid-bound porewater PCB;
- gas ebullition;
- groundwater advection through the sediment bed;
- hydrodynamically-induced advective pumping through the near-surface interstices in the sediment bed;
- biologically-enhanced porewater transport within the sediment bed and at the sediment-water interface; and
- emergence and uprooting of macrophytes.

Direct desorption into the water column is a partitioning process, and is covered by the review of partitioning. Three additional processes are extensively reviewed below: gas ebullition, groundwater advection, and diffusive mass transport as enhanced by bioturbation.

2.3.1 Gas Ebullition

Theoretical Process Understanding: - The total flux of contaminants due to gas ebullition across the sediment-water interface reflects the following coupled processes:

- Gas generation and consumption;
- Gas bubble formation and growth;
- Gas bubble migration and escape;
- Three-phase partitioning between solid, gas and aqueous phases in voids, tubes, and the water column, and advection to the atmosphere;

- Physical transport of particles carrying contaminants by microcurrents in the wake of gas bubbles, and
- Resuspension as enhanced by the lower bulk density of gassy sediments.

Research indicates that bubble formation is highly variable on a diurnal and seasonal basis, with the rate ultimately limited by supply of organic matter to sediments. Gas ebullition is promoted by high organic carbon influx, methanogenic activity, high sediment temperature, low atmospheric and hydrostatic pressure, low rates of bioturbation and groundwater seepage, and unconsolidated, fine-grained sediment texture. Gas bubble formation and ebullition tend to strip chemicals from porewater through partitioning to bubbles, to mix surface sediments, and to reduce measured sediment stability by increasing porosity. A study of one contaminated site estimated that a 3-foot-thick sand cap would be necessary to completely suppress gas ebullition.

Adequacy of Typical Site-Specific Information: A wide range of gas ebullition rates has been reported in the literature, spanning at least four orders of magnitude, depending on the physical system investigated. It is not clear which processes and parameters affect this spread. Site-specific rates are not generally available for contaminated sites.

Representation in Leading Fate and Transport Models: The effects of gas ebullition are not simulated in a mechanistic fashion by either WASP or EFDC. Rather, ebullition and other processes are lumped into an enhanced diffusive sediment-water exchange rate that is typically determined from site-specific sediment and water-column data. HEM3D is an extension of EFDC that allows the modeling of methane generation. HEM3D can compute the total gas release from sediments, but without simulating the movement of a separate gas phase. DELWAQ, which was developed by Delft Hydraulics, models sediment diagenesis and explicitly includes ebullition and its effects on contaminant transport and sediment bulk properties. DELWAQ does not compute water movement, requiring a linkage with a model of the water column.

Predictive Uncertainty: Large knowledge gaps exist about the ebullition process, particularly with respect to the mechanistic/ theoretical aspect of processes and empirical measurements of rates and their dependence of environmental factors. The greatest uncertainties surround the process of bubble formation and growth, and the physical transport of contaminants. Bubble sizes and residence times need to be better understood in order to properly estimate the extent of contaminant partitioning into the gas phase. The rate and extent to which migrating bubbles mix sediments is also an important uncertainty. Because gas generation rates are the driving force behind ebullition, it is important to better define the microbial, chemical and physical factors that affect it on all spatial and temporal scales. Diurnal, seasonal and weather related variabilities, as well as spatial variabilities, all contribute to predictive uncertainty. The interaction between groundwater seepage and ebullition is also not well enough understood. Reducing these uncertainties in process understanding and quantitative effects would greatly facilitate the incorporation of ebullition into existing frameworks.

2.3.2 Groundwater Seepage

Theoretical Process Understanding: Contaminant transport through the groundwater-surface water interface (GSI) is governed by a combination of complex hydraulics in and around the sediment bed, and a transport environment in the sediment bed that frequently exhibits sharp

gradients in temperature, salinity, redox chemistry, biological population, and physical disruption. Mechanisms of groundwater flow and exchange with surface water can vary significantly from free-flowing river environments, to lakes and impoundments, to coastal environments, and directionality of exchange can vary across reaches or even at a scale of meters. Where surface water concentrations are significantly lower than porewater concentrations, the bulk exchange coefficient is essentially equal to the Darcy velocity. The porewater concentration may be less than expected based on the solid-phase concentration, where transport through the sediment bed is too rapid to allow equilibrium to be reached.

Adequacy of Typical Site-Specific Information: Estimation of groundwater mediated fluxes requires measurement of groundwater seepage and associated contaminant porewater concentrations, both of which present significant challenges and have not been measured in many systems. Data show a wide range of measured seepage rates, spanning more than four orders of magnitude. In general, it appears that the highest seepage rates are associated with the highest conductivity formations (sands and coarse sands), and lower rates of seepage are associated with lower conductivity silts and silty sands. Methods that integrate seepage estimates over a larger scale tend to show median seepage rates that are lower than those obtained by point measurements, possibly due to the effect of averaging out localized high-rate seeps. The most detailed studies of porewater concentrations also show a very high degree of spatial variability, even on a scale of meters.

Representation in Leading Fate and Transport Models: Models of the GSI are not well developed, and are often lumped into an overall mass transfer flux that includes a variety of mechanisms that cause overall sediment porewater chemical flux to the overlying water column. The level of representation is limited by the level of understanding of processes and the limited data available for most sites. Model developers have typically developed either groundwater or surface water models, with rough linkages through source terms, without representation of the temporally and spatially dynamic nature of the GSI. The groundwater model has recently been linked to surface water models DAFLOW and SFR1, allowing for some dynamic interactions with these limited surface water tools.

Predictive Uncertainty: The high degree of spatial heterogeneity and variability of seepage fluxes and porewater concentrations implies a high degree of uncertainty in local contaminant fluxes, although this uncertainty is reduced at a more integrated spatial scale. An analysis of observed ranges of seepage fluxes and distribution coefficients for PCBs indicates that contaminant fluxes would be significantly reduced by a low permeability cap, and would be further reduced if the cap contained adsorptive materials, and that these conclusions hold across the range of site-specific parameter values.

2.3.3 Diffusive Mass Transfer and Bioturbation

Theoretical Process Understanding: Diffusive mass transport of porewater contaminants across the sediment-water interface is restricted by the thickness of the benthic boundary layer, which is very difficult to either measure or to relate to system properties. Bioturbation, which encompasses a diverse set of mixing processes mediated by benthic organisms, is generally thought to be the most important mechanism for reworking sediments and releasing porewater contaminants in sediments. Bioturbation increases flux by one to two orders of magnitude over molecular diffusion alone. The depths of bioturbation in freshwater and marine sediments are typically less than or equal to 10 cm and 30 cm, respectively, but are highly variable over space

and time. Bioturbation is controlled by a variety of biotic (organism size and seasonal life cycles, population density, deposition of organic matter, and species diversity) and abiotic (temperature, sedimentation and erosion conditions and sediment chemistry) factors. The importance of these multiple factors coupled with the spatial and temporal heterogeneity of benthic communities has made it difficult to determine which factors are most important in driving biological mixing.

Adequacy of Typical Site-Specific Information: Aside from population densities of benthic organisms, process-related parameters are typically unknown for specific sediment sites. Mixing depths can be inferred indirectly from radioisotope core profiles and sediment x-rays and photography. Significant cost can be incurred to characterize a large site, due to the likelihood of spatial heterogeneity and the high cost of radioisotope analysis.

Representation in Leading Fate and Transport Models: Mechanistic representations of bioturbation are absent in WASP and EFDC. Site-specific biodiffusion coefficients are typically included in lumped diffusions terms, with coefficients determined by calibration to water-column data. Mechanistic models of bioturbation have also been developed, reflecting the multiple mechanisms by which various benthic organisms cause vertical mixing of sediment contamination.

Predictive Uncertainty: Chemical transport within the upper layers of bed sediments is a very complex process that will continue to challenge the efforts of environmental chemists, benthic biologists, and engineers. Aside from radionuclide tracer data, the laboratory and field data needed to verify mechanistic models for a specific site are usually very limited. While molecular diffusivity can be predicted with reasonable accuracy based on chemical characteristics and sediment porosity, biodiffusion is much more difficult to predict without extensive knowledge of local benthic populations and processes. Biodiffusion releases to the water column at rates excluding molecular diffusion must therefore be considered unless ruled out by site-specific benthic studies.

2.4 BIOTRANSFORMATION

Theoretical Process Understanding: Biochemical transformation processes can occur due to chemical and biological processes. Biodegradation can occur due to growth metabolism or catabolism. For environmental transformations, redox conditions are particularly important because of their determining role in the microbial ecology and energetics, and sediments tend to be highly anaerobic below about 0.5 cm of depth. Biogenic gas production may also affect contaminant partitioning and sediment stability. For PCBs and other persistent sediment contaminants, rates of degradation are generally very slow, so that biodegradation is not generally a quantitatively important remediation process. However, biotransformations may be important for converting chemical to more labile, mobile forms, and may also decrease or exacerbate toxicity, altering risk without significantly changing total concentration.

Adequacy of Typical Site-Specific Information: There is significant variability in biotransformation potential from site to site, and transformation rates are highly dependent on the bioavailability of contaminants, as well as the site at which data were collected. Data are rarely available over sufficiently long spatial scales and in sufficient spatial-, temporal-, and congener-level resolution to estimate transformation rates.

Representation in Leading Fate and Transport Models: Chemical and biological transformations are generally treated as pseudo-first-order processes in WASP, AQUATOX, and EFDC. Degradation is modeled as loss of the parent product, rather than transformation to a specified daughter product. Differential decay rates may be specified by model segment.

Predictive Uncertainty: The leading models contain simplifications and assumptions of site-specific parameters to facilitate application with limited data, generally represented as 1st-order decay rates. Given the wide range of degradation rates provided in the literature, and the hazards of translating laboratory rates to the field, there is considerable uncertainty in predicting biochemical transformation fluxes at any given site.

2.5 OVERALL SIGNIFICANCE AND RELATIVE UNCERTAINTY

To gain the most benefit from improvement of process representations one should focus on those processes to which the surface sediment response to alternative *in situ* technologies is most sensitive (i.e. where the process plays a significant role in governing the rate of change in surface sediment concentrations over time) and for which there is high degree of uncertainty/variability. For example, it does not pay to reduce process uncertainty for a process that does not significantly affect the change in exposure from surface sediments over time.

The relative significance of processes in a system-level context can best be assessed by comparing their rates on an equivalent basis. To do that we can initially compare the estimated half-time for natural attenuation of a chemical in a surface sediment layer if the process of concern is the only one leading to that attenuation (i.e., a simple washout half-time). This is not a definitive definition of significance because the relative significance of processes and their half-time for exposure change over time may vary as a function of the particular *in situ* technology being applied. Nevertheless, a screening assessment of significance can be obtained by comparing the attenuation half-times with no remediation action. For this comparison, we assume the following common parameter values (minimum, median, maximum): bulk density: 1.0×10^5 , 2.25×10^5 , 5×10^5 g/m³; surface sediment mixed layer depth: 5, 10, 15 cm; particle density 2.0, 2.25, 2.5 g/cm³; porosity 0.8, 0.9, 0.95; equilibrium partition coefficient 10^5 , 10^6 , 10^7 cm³/g.

Estimates of process parameters determining mass transfer in sediment-surface water systems can vary over as many as three orders of magnitude, and for some processes, measurement issues and heterogeneities make it difficult to reduce this uncertainty, even with site-specific data. For this reason, a probabilistic approach is needed to quantify the uncertainty in any process and its impact on prediction. Process prediction uncertainty can be difficult to evaluate on a generic basis, but can be estimated by developing probability distributions from the rates reported in the literature. In doing so, we must recognize that the range of reported rates include both measurement error as well as the influence of all of the factors leading to stochastic variability in the environment. We used a simple Monte Carlo analysis to develop a half-time distribution for the processes of interest using estimated distributions of process-governing parameters based on our review of parameter variability and uncertainty. The characteristics of the resulting half-time distributions are presented in Table 2-1.

Table 2-1. Representative Rates and Attenuation Half-Times

Process	Range of Observed Rates	Median Washout Half-time	Ratio (75%/25%) Washout Half-times
Net Sedimentation	-2 to 5 cm/y	0.5 to 15 yrs [*]	NA ^{**}
Gas Ebullition			
Gas Phase Transport (Stripping)	0 to 47 cm/d (0 to 17000 cm/y)	20,000,000 yrs ^{***}	22 ^{***}
Particle Entrainment	Unknown	Unknown	Unknown
Groundwater Seepage	0 to 125 cm/d (0 to 46000 cm/y)	3,700 yrs	25
Bioturbation	0.001 to 30 cm ² /y ^{****}	500 yrs	20
Molecular Diffusion in Porous Media	0.3 to 30 cm ² /y ^{****}	1,100,000 yrs	9
Biotransformation	Very wide (chemical-dependent) 10 ⁻⁴ to 10 ⁻⁶ /d ^{****}	55 yrs	4

^{*} Applies only when net depositional. Not a median due to unknown distribution shape.

^{**} Unknown distribution shape for the sedimentation/erosion rates

^{***} by partitioning to bubble phase (does not account for particle entrainment and diffusion enhancement)

^{****} Note that units are different from the rest in this column

An overall assessment of the relative magnitude of predictive uncertainty for the transport and transformation processes of interest can be made by combining the knowledge gained from the significance and uncertainty/variability analysis presented above with an evaluation of the other factors leading to prediction uncertainty (theoretical understanding, model representation and process parameterization, and site-specific information). This qualitative information is presented in Table 2-2.

Table 2-2. Overall Assessment of Process Significance

Process	Theoretical Understanding (Mathematical Formulation)	Model Representation (Process Parameterization)	Site-specific Information (Process Variability and Availability of Data)	Overall Predictive Uncertainty	Process Significance
Partitioning	+++	+++	++	+++	****
Net Sedimentation	++	+++	++	++	****
Gas Ebullition	+	+	+	+	**
Groundwater Seepage	+++	++	+	++	**
Diffusive Mass Transfer, including Bioturbation	+++	++	+	++	***
Biotransformation	+++	++	+	++	**

++++ (Low uncertainty) → + (High uncertainty)

**** (High Significance) → * (Low Significance)

3. WATER QUALITY MODEL FRAMEWORK FOR UNCERTAINTY QUANTIFICATION AND PROPAGATION

The objective of the water quality model development effort was to provide a framework capable of assessing the impact of parameter uncertainty on model predictions of PAH releases in water from capped and uncapped sediments in the presence of porewater advection, ebullition, and other processes. Two modeling applications were used: the water quality analysis simulation model (WASP), and the newly developed sediment flux model (SFM).

There is a range of complexity of numerical models used for assessment of time-dependent exposure and risk at a contaminated sediment site under natural attenuation conditions and under alternative remedial actions. Figure 3-1 is a representation of four tiers of model complexity. The Tiers represent successively more mechanistic approaches, supported by higher data resolution and addressing more complex management questions. The process review (from section 2) assumes that a representation of each process is being considered explicitly in the predictive analysis, as in Tiers 2- 4, rather than implicit representation that is assumed in Tier 1. The level of complexity used for a given site will be governed largely by the resources available for site characterization and remedial assessment, which in turn is usually determined by an estimate of the magnitude and complexity of the site and its remediation. It is very important to recognize that as model complexity increases, the level of temporal, spatial, and process resolution of data that must be collected to support (provide model input, calibration, and validation) the model must also increase in a commensurate fashion. However, if there are sufficient data to support an increase in model complexity (as defined by increased spatial, temporal, and process resolution), this will generally increase the utility of the model in terms of the complexity of the management questions that can be addressed and the accuracy with which those questions can be answered (i.e., reduction of uncertainty).

Based on our process review, we were able to obtain insights into what can be gained in terms of increased model predictive confidence by identifying the most significant processes governing a system's response to *in situ* remediation and by

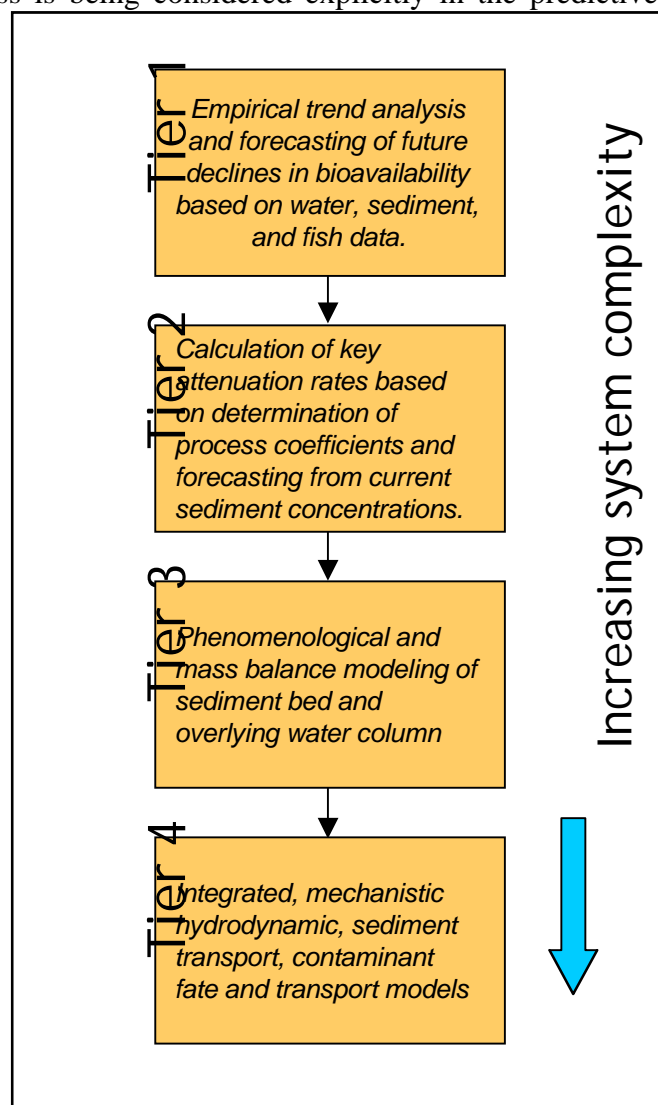


Figure 3-1. Tiered Model Complexity

increasing the understanding and data for those processes.

There are a few general statements that can be made regarding our ability to predict the response of a system to alternative *in situ* remedial technologies.

First and foremost, none of the processes included in our models is well enough theoretically understood to provide a completely mechanistic mathematical formulation and to parameterize that process formulation on the basis of simple characteristics of the system and chemicals of concern within that system. Instead, process representations are in general semi-mechanistic. We formulate the process to be as consistent with our theoretical understanding as possible in terms of how the process rate and extent depends on system parameters. For example, cohesive sediment resuspension is known to be a function of bottom shear stress, sediment porosity, and sediment bulk density; but the coefficients for those determinants of resuspension must in general be determined by site-specific sediment erosion experiments. In other words, we must rely on site-specific process rate measurements and overall model calibration to produce a model that can be effectively used to forecast the response of a contaminated site to alternative remedial options.

In the project, we initially used the water quality analysis simulation program (WASP), and progressed towards a custom designed dynamic sediment flux model (CFM) to assess the impact of uncertainty in the specified processes on capping efficiency.

3.1 WATER QUALITY ANALYSIS SIMULATION PROGRAM (WASP)

3.1.1 Model Description and Parameterization

WASP (and the complementary TOXI module) is probably the most widely used water quality model. The TOXI module can be used to simulate the fate and transport of multiple generalized toxic substances in the water column, as well as the sediment bed. Sorption to multiple sediment classes (both cohesive and non-cohesive) is also accommodated. Spatial and temporal variations in organic carbon content are supported.

The partitioning algorithm may be either a 2- or 3-phase partitioning approach. However, a 3-phase model requires a known distribution of DOC, which is often difficult to measure and thus becomes a calibrated term. Equilibrium partitioning is assumed, and the user is required to enter a partitioning coefficient (either solid distribution or organic carbon normalized) for each modeled contaminant, and may vary the values for either the water column or sediment bed. Although WASP/TOXI assumes linear equilibrium partitioning, it is possible to modify the model source code to accommodate dynamic sorption and desorption kinetics.

3.1.2 Parameterization

The objective of our preliminary exercise was to provide an assessment of the impact of parameter uncertainty on model predictions of PAH emissions in water from capped and uncapped sediments in the presence of advection and microbial ebullition. The water quality simulation was based on a version of WASP customized by Limno-Tech Inc. to capture the processes indicated in Figure 2-1. The code used is very similar to the EPA's WASP5 model with some modifications to the sediment transport mechanics and the implementation of a

framework to make a large number of consecutive simulations possible. With added sediment transport functions - LTI-TOXI has several additional methods for simulating sediment resuspension and deposition, including a cohesive sediment model. WASP was further modified so it can be run from the command line, which is critical for the Monte Carlo simulation. Finally, LTI-TOXI was linked to a custom DYNHYD model – this is necessary for WASP to simulate hydraulics of the estuary.

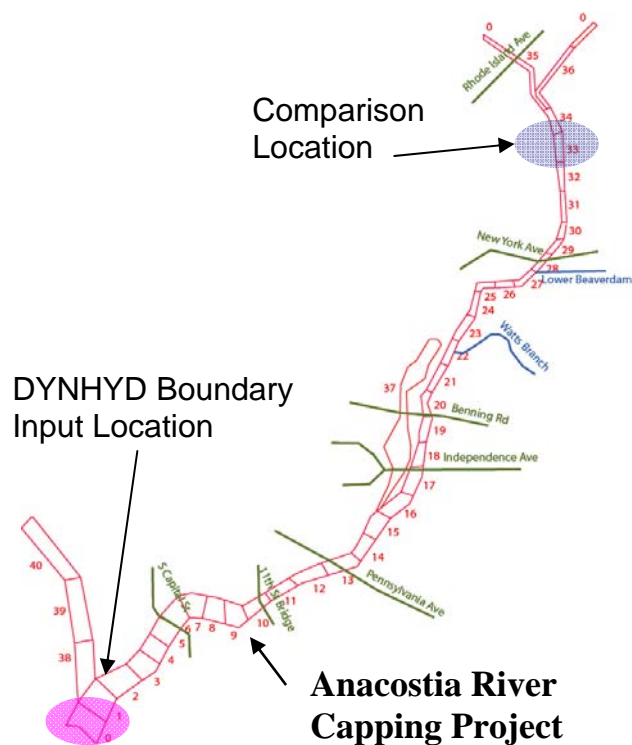


Figure 3-2. Basic model segmentation of WASP for the Anacostia River.

Hence, the physical system the code simulated was based on the hydrodynamics of the Anacostia River, and the capping demonstration site near the naval yard in Washington D.C (Figure 3-2). In an effort to maintain the goal of a general uncertainty analysis of contaminated sediment sites the physical characteristics of the model were occasionally altered from the cap site to represent more typical conditions. The uncertainty analysis focused primarily on PAH's and cohesive sediments in an estuarine setting. The results presented here represent an uncapped scenario. The key model outputs of interest include: Water levels, Flow rates, Suspended solids concentrations, Dissolved contaminant concentrations, Suspended contaminant concentrations, Net sedimentation rates, Contaminant fluxes at sediment-water interface, Contaminant fluxes between sediment layers, and Contaminant fluxes between water-column segments (e.g. downstream boundary).

The distribution of the parameters used as model inputs in a Monte Carlo type simulation constitute a vital part of the analysis and can significantly impact the results. Log-normality is generally accepted as an appropriate distribution for most variables in environmental engineering and was assumed for all the input parameters used in this simulation. Since WASP is a large-scale model there has been no attempt to differentiate parameter uncertainty caused by spatial heterogeneity (within the scale of a WASP segment which is approximately 10,000 m²) or measurement error – they are assumed to equivalently contribute to uncertainty in a large-scale model framework.

Generally the analysis of available data and the expertise of experienced modelers indicate that most parameters vary over approximately an order of magnitude, with a notable exception being biodegradation whose variation spans closer to two orders of magnitude. The following table (Table 3-1) is a summary of the input parameters and the approximate limits that contain 95% of the input distribution.

Table 3-1. Distribution of Input Parameters for WASP Model

	Low	Average	High	Notes:
Partitioning (Log K_{oc})	Average-0.5	Dependant on PAH	Average+0.5	Uncertainty has some dependence on PAH
Anaerobic Biodegradation (half-life)	1 year	10 years	100 years	Some dependance on PAH weight/structure
Net Deposition	0.2 cm/yr	0.6 cm/yr	1.3 cm/yr	Diurnal resuspension pattern in model
Groundwater Advection	0.9 cm/day	2.3 cm/day	5 cm/day	
Porewater Diffusion	1.15E-08 m ² /s	2.33E-08 m ² /s	4.68E-08 m ² /s	A calibrated parameter based on modeling experience
Particle Mixing	2.1E-11 m ² /s	7.4E-11 m ² /s	2.6E-10 m ² /s	

While net deposition in the model ranged from approximately 0.2-1.2 cm/yr, diurnal resuspension and deposition were modeled such that the total resuspension was approximately 2-3 cm/yr and total deposition was approximately 3-4 cm/yr.

3.1.3 Preliminary Assessment of Uncertainty Quantification and Propagation

To determine which parameter caused the most uncertainty in the model output a Monte Carlo analysis was completed with the value of one of the parameters held constant, this was repeated for each parameter leading to 6 independent Monte Carlo simulations. This entire process was done for both a relatively low partition coefficient (Phenanthrene Log K_{oc} approximately = 4.3) and a relatively high partition coefficient (Benzo[k]fluoranthene Log K_{oc} approximately = 5.7). The mass of contaminant lost to the water column divided by the original mass of the contaminant in the sediment was used as the relevant data for comparing model results.

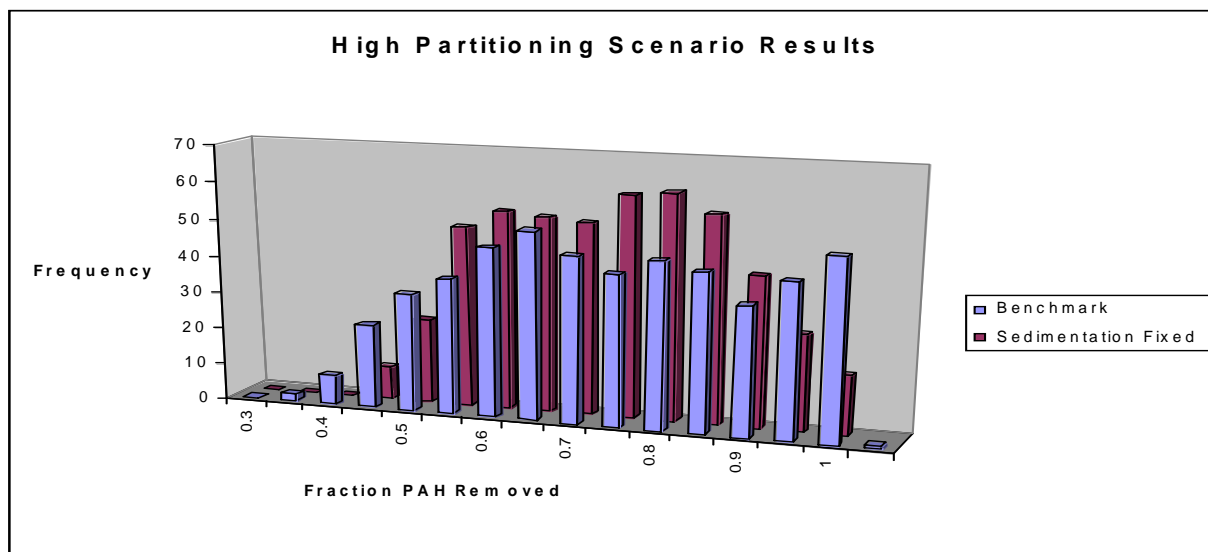
The standard deviations of the results from the Monte Carlo analyses with a parameter held constant were compared to the standard deviation of a benchmark Monte Carlo analysis where no parameter was held constant. The parameter that, when held constant, most reduces the standard deviation of the results is considered to be the parameter causing the greatest uncertainty in the model output. The statistical test used to compare standard deviations was the F test testing the hypothesis $f > F_{1-\alpha/2, m-1, n-1}$ where $f = s_1^2 / s_2^2$ and m and n were always 500 representing the number of runs in the Monte Carlo simulation.

High Partition Coefficient. The model was run for 30 years based on guidance by the EPA that this time frame was appropriate for comparing remediation scenarios at contaminated sites. Using a partition coefficient of approximately 5.7 representing benzo[k]fluoranthene, the following results were obtained (Table 3-2)

Table 3-2. WASP model output for strongly sorbing PAH compounds

	Standard deviation of % original mass lost		
Benchmark No Constants ($=s_1$)	0.171	s_1^2 / s_2^2	P-value
Constant Partitioning ($=s_2$)	0.171	1.000	0.5000
Constant Biodegradation ($=s_2$)	0.115	2.181	0.0000
Constant Sediment Transport ($=s_2$)	0.138	1.524	0.0000
Constant Groundwater Advection ($=s_2$)	0.171	1.000	0.5000
Constant Pore Diffusion ($=s_2$)	0.162	1.102	0.1389
Constant Mixing ($=s_2$)	0.171	1.001	0.4955

The results indicate that biodegradation and sediment transport are essentially the only two processes causing uncertainty in the high partition coefficient scenario, with porewater diffusion coming in a distant 3rd. The P-value for sediment transport and biodegradation is essentially 0 which means there is extremely high confidence that the standard deviation of those cases is less than the benchmark scenario, on the other hand the P-values of approximately 0.5 indicate no reduction in uncertainty. The results of this analysis agree well with the sensitivity analysis performed for the same scenario. The histogram (Figure 3-3) compares the results of the constant sediment transport to the benchmark case. Though the results are not obvious because of the large spread in the data (caused by the large uncertainties in the parameters), it is apparent that the case in which sedimentation is fixed varies less than the benchmark case.

**Figure 3-3. Uncertainty propagation of PAH fluxes for strongly sorbing compounds**

Low Partition Coefficient. In the low partition coefficient scenario the run time was reduced to 5 years to prevent scenarios in which too much contaminant mass was lost to produce useful data (in a 30 year run too large a percent of scenario's lost essentially all chemical mass before the simulation completed – leading to a spike at the right side of the histogram, confusing the results). Using a partition coefficient of approximately 4.3 representing phenanthrene the analysis yielded the following results (Table 3-3):

Table 3-3. WASP model output for mildly sorbing PAH compounds

	Standard deviation of % original mass lost		
Benchmark No Constants ($=s_1$)	0.145	s_1^2 / s_2^2	P-value
Constant Partitioning ($=s_2$)	0.117	1.527	0.0000
Constant Biodegradation ($=s_2$)	0.114	1.611	0.0000
Constant Sediment Transport ($=s_2$)	0.131	1.223	0.0120
Constant Groundwater Advection ($=s_2$)	0.136	1.137	0.0757
Constant Pore Diffusion ($=s_2$)	0.137	1.108	0.1259
Constant Mixing ($=s_2$)	0.136	1.124	0.0958

The results indicate that partitioning and biodegradation are significantly contributing to the uncertainty in this model. Sediment transport is a distant 3rd while the other processes appear to have a much less significant impact.

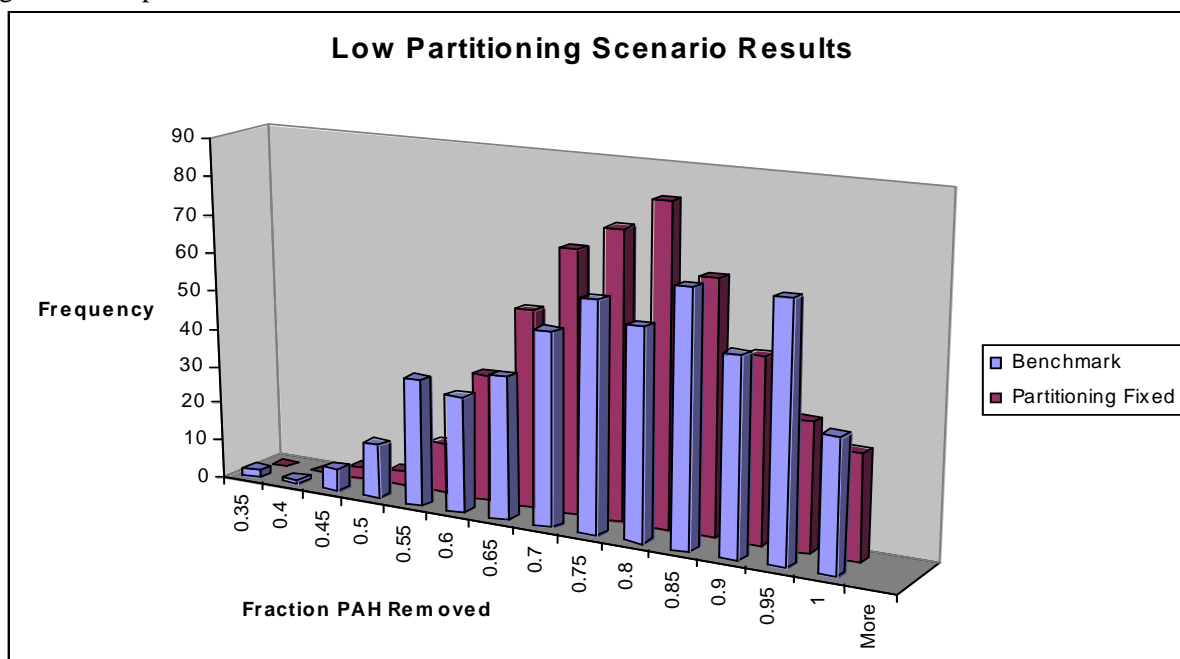


Figure 3-4. Uncertainty propagation of PAH fluxes for mildly sorbing compounds

From the histogram (Figure 3-4) it can be seen that when partitioning is fixed the distribution of results is more centered and less spread out than in the benchmark case. A sensitivity analysis done for this scenario indicates very similar results as to the importance of the uncertainty in each of the processes.

From a modeling perspective the results may be considered intuitive. Referring to Figure 3-5, the high partition scenario in which $\text{Log } K_{oc}=5.7$ is beginning to approach a scenario in which a very small amount of contaminant is available for the porewater processes. The particle resuspension processes are dominant and sediment resuspension and biodegradation control model uncertainty.

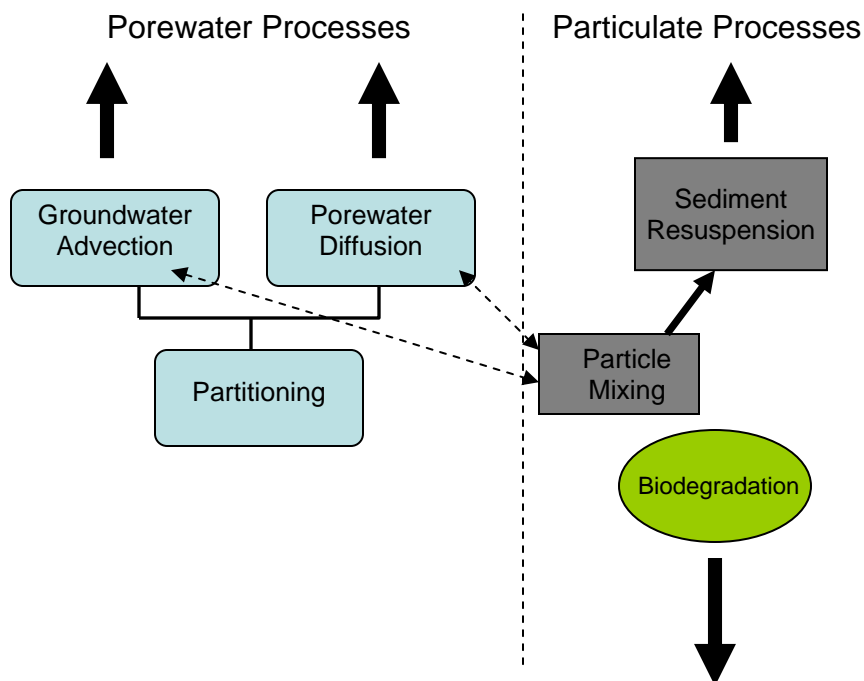


Figure 3-5. Contaminant transport process flow chart

However, in the scenario of a relatively low partition coefficient ($\text{Log } K_{oc}=4.3$) the scenario appears to be dominated by the uncertainties in the partitioning coefficient since it dictates how much contaminant is available in the porewater. Because groundwater advection and porewater diffusion are dependent on the amount of contaminant in the porewater their uncertainties do not impact the model as much as partitioning even though they also vary over approximately an order of magnitude. The impact of biodegradation on even the low partition coefficient case is simply a testament to the large amount of uncertainty associated with the parameter. Although the WASP model cannot directly account for processes such as gas ebullition, the results of the Monte Carlo analysis may still be helpful in determining the uncertainty caused by this process. Ebullition may carry contaminant through sediment through gas bubble-facilitated processes, increase groundwater advection by creating channels in sediment, mix the sediment, and finally it may increase sediment instability (Section 5). Of these processes the Monte Carlo analysis suggests that understanding role of ebullition in sediment instability is a promising area of research.

3.2 SEDIMENT FLUX MODEL (SFM)

The WASP-based model was found to have serious limitations with respect to simulation of cap properties and processes. In order to facilitate additional Monte Carlo evaluations, and capping scenarios in particular, a customized Sediment Flux Model (SFM) was developed using Visual Basic for Applications (VBA) within Microsoft Excel.

3.2.1 Differences Between WASP and SFM

The SFM contains a similar level of sediment process complexity as within the WASP model, but with improved flexibility and efficiency. In general, the processes represented in the SFM are identical to those represented in the WASP model. The SFM is configured as a one-dimensional model of the sediment bed only, and the water column is represented as a set of external boundary conditions instead of being actively simulated within the model. For the current application, the SFM provides several important advantages over the original WASP framework, including:

- While the basic WASP code is inflexible with regard to specifying and tracking sediment layer-variable physical properties, the SFM accommodates layer-variable properties, including sediment organic carbon fraction, bulk density, and hydraulic conductivity. This capability is important to obtaining physically realistic simulations of capped sediments.
- User inputs, including Monte Carlo specifications (i.e., parameter mean and standard deviation values), can be readily manipulated within Excel worksheets.
- Water column boundary conditions can be more easily controlled to fix the desired sediment and PAH settling/deposition fluxes.
- Simulation run-times are generally faster than those for the original WASP model
- Post-processing of model results is more flexible, and key results can be reported directly to worksheets at a user-defined interval. At a minimum, predictions of contaminant flux and vertical concentration profiles are reported on an annual basis.

The SFM framework code has been verified by comparing results to previous WASP simulations and by comparing capping predictions to results calculated using simple analytical models. Although the current application of the SFM is restricted to one dimension, the model could readily be extended to a dynamic simulation of hydraulics and contaminant transport and fate in the water column similar to the WASP model.

3.2.2 Model Conceptual Design

The Sediment Flux Model (SFM) represents key sediment/chemical input parameters and transport and fate processes in similar fashion to the original WASP model. Key processes include the following:

- Equilibrium partitioning of chemical within the sediment and water column;
- Resuspension due to flow/wind-wave action (and/or gas ebullition);
- Deposition of suspended solids and chemical from the water column;
- Porewater exchange at the sediment-water interface and between adjacent sediment layers;
- Particle mixing between adjacent sediment layers;
- Porewater advection due to groundwater seepage; and
- Biodegradation of chemical mass.

The processes outlined above are shown graphically in Figure 3-6. It should be noted that gas ebullition is not explicitly included in the SFM; however, this process can be represented using a combination of processes, including resuspension, and particle/porewater exchange.

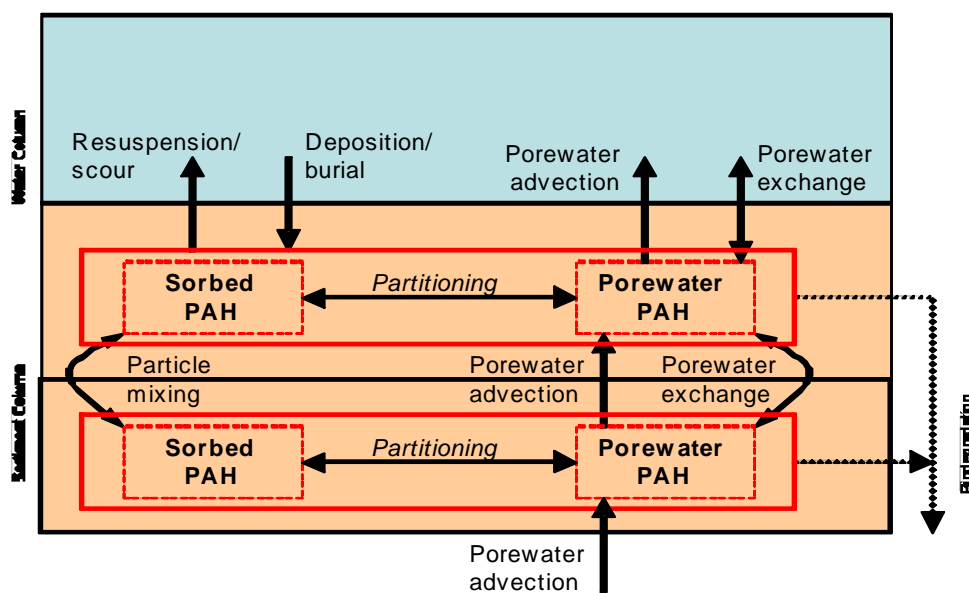


Figure 3-6. Sediment Flux Model Process Diagram

General and chemical-specific user-defined inputs for the SFM include:

- Water column total suspended solids concentration (mg/L), settling rate (m/day), and fraction of organic carbon for the “parent” bed material;
- Resuspension rate related to water column processes (i.e., flow and wind-wave induced resuspension) and microbial-generated gas ebullition within the sediment column (mm/yr);
- Groundwater head gradient (m/m) - assumed to be net positive from the sediment bed to the water column;
- “Mixed depth” of the sediment column, which determines the depth range over which to apply separately specified particle mixing rates due to bioturbation processes, gas ebullition, etc.;
- Chemical carbon-normalized partitioning coefficient (L/kg-C);
- Chemical bulk concentration in the water column through time (ng/l); and
- Chemical biodegradation half-time in sediment column (years).

The sediment bed in the SFM is configured based on a set of “sediment types”. Each sediment type, and its associated physicochemical properties, are defined by the user. For example, sediment types can be added to the model to individually represent parent bed material, sand cap material, and Aquablok™ material. The set of physicochemical constant properties that must be defined specifically for each sediment type includes:

- Fraction of organic carbon;

- Dry bulk density and particle density;
- Hydraulic conductivity; and
- Particle mixing and porewater exchange rates.

The SFM sediment bed is initialized by specifying the number of bed layers, the thickness of each layer, the initial layer-specific chemical concentration, and the initial percentages of each sediment type (totaling 100%) in each layer. The bed physicochemical properties described above are then internally calculated within the SFM as the percentage-weighted average of the values defined for each sediment type in order to initialize each sediment layer in the model. The sediment type percentages are subject to change during the model simulation as the result of simulated mixing and deposition processes. Time-dependent consolidation of the sediment bed is not considered within the current model. Appropriate configuration of the primary sediment “types” (i.e., parent, sand cap, and AquablokTM) permits a representative simulation of internal sediment advection and mixing processes.

3.2.3 Model Process Representation

For most major processes, the SFM incorporates the same core process equations used by the WASP model, with some enhancements. These processes can be parameterized based on available literature and/or site-specific data from field and laboratory studies depending on the nature and objectives of the model application. Each of the major processes is described briefly below, including relevant equations. Model input parameters are highlighted in *italics*.

- Chemical Equilibrium:

The SFM assumes instantaneous chemical equilibrium within each sediment bed layer. The partitioning coefficient (K_d , L/kg-solid) for a given PAH compound is computed as:

$$K_d = foc * K_{oc} \quad (3-1)$$

where foc is the fraction of organic carbon (kg-C/kg-solid) and K_{oc} (L/kg-C) is the organic carbon partitioning coefficient. The foc and K_{oc} parameters are input by the user as constant values. The equilibrium fractions of chemical in the dissolved phase (f_d) and the particulate phase (f_p) are computed internally in the SFM as:

$$f_d = \frac{1}{1 + (K_d * C_{solids})} \quad (3-2)$$

$$f_p = 1 - f_d \quad (3-3)$$

where C_{solids} is the dry bulk density of the sediment bed (kg-solids/L).

- Porewater Exchange:

The porewater exchange processes represented in the model account for the exchange of dissolved chemical mass between adjacent sediment bed layers and between the surface bed layer and the overlying water column.

$$\frac{\Delta M_{i,k}}{\Delta t} = \left(\frac{D_{ij} * A_{ij} * n_{ij}^2}{L_{c,ij}} \right) * \left(\frac{f_{dk,j} * C_{k,j}}{n_j} - \frac{f_{dk,i} * C_{k,i}}{n_i} \right) \quad (3-4)$$

where:

$\Delta M_{i,k}/\Delta t$ is change in mass of chemical k in sediment layer i with respect to time;
 $f_{dk,i}$ and $f_{dk,j}$ are the fraction of chemical dissolved in layers i and j ;
 D_{ij} is the average exchange coefficient (m²/day) for layers i and j ;
 $L_{c,ij}$ is the characteristic mixing length (meters) between layers i and j ;
 $C_{k,i}$ and $C_{k,j}$ are bulk chemical concentrations (g/m³);
 n_i and n_j are the porosities in layers i and j ;
 n_{ij} is the average porosity for layers i and j ; and
 A_{ij} is the average surface area for the layers (m²).

The exchange coefficients (D) and the porosity (n) are specified for each individual sediment type included in the model, and the SFM computes mass-weighted values of these variables by layer based on the simulated mixture of sediment types. The characteristic mixing length (L_c) is generally assumed to extend between the midpoints of adjacent layers. For exchange between the water column and the surficial sediment layer, L_c is assumed to be equal to the thickness of the surficial layer.

The porewater exchange process is intended to account for a range of physicochemical processes occurring in the sediment including molecular diffusion and “enhanced” exchange due to bioturbation and/or gas ebullition.

- Particle Mixing:

Mixing of sediment particles in the bed commonly occurs as the result of bioturbation activity in the bed and/or larger scale physical mixing phenomena. Vertical mixing between adjacent sediment layers can be described as:

$$\frac{\Delta M_{i,k}}{\Delta t} = \left(\frac{E_{ij} * A_{ij}}{L_{c,ij}} \right) * (C_{k,j} - C_{k,i}) \quad (3-5)$$

where:

E_{ij} is the average mixing coefficient (m²/day) for layers i and j ;
 $L_{c,ij}$ is the characteristic mixing length (meters) between layers i and j ;
 $C_{k,i}$ and $C_{k,j}$ are bulk chemical concentrations (g/m³); and
 A_{ij} is the average surface area for the layers (m²).

- Biodegradation:

Biodegradation is represented in the SFM as a simple, first-order decay process:

$$\frac{\Delta M_{i,k}}{\Delta t} = M_{i,k} * e^{-(k_{deg} * dt)} \quad (3-6)$$

where $M_{i,k}$ is the mass of chemical k (kg) in a sediment layer i , k_{deg} is the biodegradation rate (day^{-1}), and dt is the model timestep (days). The biodegradation rate (k_{deg}) is calculated based on a user-specified half-time for biodegradation ($DegHT$, years): $k_{deg} = \ln(2)/DegHT$.

- Deposition and Resuspension:

The SFM calculates gross settling and deposition flux of sediment ($SFlux_{dep}$, $\text{g/m}^2/\text{day}$) as the product of the water column settling rate (V_s , m/day) and the constant total suspended solids concentration (TSS , g/m^3):

$$SFlux_{dep} = V_s * TSS \quad (3-7)$$

The SFM is configured so that the user can specify separate rates for flow-induced resuspension (V_{r2}) and “background” resuspension (V_{r1}). The “background” resuspension rate can be used to represent erosion caused by any non-flow processes, potentially including gas ebullition. The SFM calculates gross sediment resuspension flux ($SFlux_{res}$, $\text{g/m}^2/\text{day}$) based on the total erosion rate ($V_{r1} + V_{r2}$) and the sediment bulk density ($BulkDen$, kg/m^3)

$$SFlux_{res} = (V_{r1} + V_{r2}) * BulkDen * \left(\frac{m}{1,000 mm} * \frac{1,000 g}{kg} * \frac{yr}{365.25 days} \right) \quad (3-8)$$

The net change in mass of chemical k with respect to time in surface sediment layer i can be expressed as:

$$\frac{\Delta M_{i,k}}{\Delta t} = \left[(SFlux_{dep} * A_i) * \left(\frac{C_{w,k} * f_p}{C_{TSS}} \right) \right] - [(SFlux_{res} * A_i) * C_{i,k}] \quad (3-9)$$

where:

- A_i is the surface area of layer i (m^2);
- $C_{w,k}$ is the bulk chemical concentration in the water column (g/m^3);
- f_p is the particulate fraction of the bulk water chemical concentration;
- C_{TSS} is the total suspended solids concentration in the water column (g/m^3); and
- $C_{i,k}$ is the bulk chemical concentration in surficial sediment layer i (g/m^3).

- Groundwater Advection:

The specific groundwater vertical discharge through the bed (V_{gw} , m/s) is calculated as the constant product of the user-specified groundwater gradient ($GWgrad$, m/m) and the minimum hydraulic conductivity ($Kcond$, m/s) of any layer in the active sediment bed:

$$V_{gw} = GWgrad * Kcond \quad (3-10)$$

Multiplying the specific groundwater discharge by the nominal surface area (1 m^2) of the sediment bed gives the volumetric discharge (Q_{gw} , m^3/s). The model is designed to handle either upward or downward vertical porewater advection, although the upward flux is generally of most interest when evaluating cap feasibility and efficacy. Advective transport of dissolved mass of chemical k into segment “i” from segment “j” ($M_{i,k}$ in kg) is calculated as:

$$\frac{\Delta M_{i,k}}{\Delta t} = Q_{gw,ji} * \left(\frac{f_{d,j} * C_{k,j}}{n_j} \right) \quad (3-11)$$

where:

- $Q_{gw,ji}$ is the porewater flow from segment j to segment i (m^3/s);
- $C_{k,j}$ is the bulk chemical concentration in segment j (g/m^3);
- $f_{d,j}$ is the fraction of dissolved fraction of chemical in segment j ; and
- n_j is the porosity of segment j .

- Sediment Bed Handling:

The SFM includes a robust sediment bed handling algorithm that tracks the volume, thickness, sediment and chemical mass, and sediment type composition (and related physical properties) through time for each individual sediment bed layer. The user-specified input parameters *VRatioMin* and *VRatioMax* can be used to instruct the model when to modify the surface bed layer to accommodate deposition or resuspension of sediment:

1. The *VRatioMin* parameter indicates the fraction of the original surface layer volume at which the surface layer will be combined with the adjacent subsurface layer (i.e., “erosion trigger”).
2. The *VRatioMax* parameter indicates the fraction of the original surface layer volume at which the surface layer will be divided into two layers of half the initial thickness (i.e., “deposition trigger”).

For example, if *VRatioMax* is set equal to 2.0 and the initial surface layer thickness is 1.0 cm, then the surface layer will be split into two 1-cm layers if/when the thickness becomes 2.0 cm. When a “deposition trigger” occurs, the two newly formed layers take on the physicochemical characteristics of the original surface layer. When an “erosion trigger” occurs, the physicochemical characteristics of the newly formed layer are

calculated based on volume-weighted averaging of the original layer characteristics. This bed handling protocol was originally developed by LimnoTech in the 1990s for the Lower Fox River (WI) and incorporated into the WASP5 model. Other present-day models that represent sediment bed and transport processes, such as the *Environmental Fluid Dynamics Code* (EFDC), incorporate similar bed handling routines.

- Water Column Boundary Conditions:

The SFM represents the water column overlying the sediment bed essentially as a set of boundary conditions. The following constituents are represented in the boundary conditions:

1. Total suspended solids (TSS, mg/l);
2. Fraction of organic carbon associated with TSS; and
3. Bulk chemical concentration (ng/l).

Water column TSS and the associated organic carbon fraction are specified as constant values. The bulk chemical concentration for year t (C_t , ng/l) is calculated based on an initial concentration (C_0 , ng/l) and a half-time constant for decline ($t_{0.5}$), which are specified by the user:

$$C_t = C_0 * e^{-\left(\frac{0.693 * t}{t_{0.5}}\right)} \quad (3-12)$$

- Porewater Boundary Condition:

In addition to specifying the groundwater gradient in the sediment column, the (constant) porewater chemical concentration associated with porewater entering at the bottom of the bed must be specified.

4. SPATIAL DISTRIBUTION OF SEDIMENT MICROBIAL CHARACTERISTICS IN FIELD AND LABORATORY SETTINGS.

The objective of this task is to develop proxy parameters (microbial abundance and activity) and descriptive functions for microbial ebullition in sediments as input factors for the integrative Sediment Flux Model (Section 7). A secondary objective was to quantify the spatial distribution of microbial abundance and activity in the field and in a laboratory flux chamber to integrate information obtained across various scales in a geostatistical model developed in this study (M-Scale; Section 4.3). For more complete data and discussion of these results, please see the following two doctoral dissertations:

- Li, Meng-Ying (2008). *The M-Scale Model: A Multi-Scale Estimation Model for Decision Support of On-Site Remediation*. Doctoral Dissertation, The University of Michigan.
- Wang, Q. (2008). *The Effect of Capping on the Ebullition Potential and Microbial Ecology of Contaminated Surface Sediments*. Doctoral Dissertation, University of Toledo.

4.1 MICROBIAL ABUNDANCE AND ACTIVITY MEASUREMENT

4.1.1 Materials and Methods

Two types of samples were used in this task: (i) core samples collected from the uncapped control, sand cap and Aquablok™ capped sediments (Figure 4-2, A), and spatially distributed samples collected from the uncapped control used in the flux chamber experiments (Figure 4-2, B; see also Section 5). The sediment reactor tank (18x36x18 in; Figure 4-1), is outfitted with a re-circulating surface water pump to mix the water column overlaying the sediments, and create an erosion/scouring disturbance, and a grid of diffusers placed under the sediments to simulate a gas ebullition or an advection disturbance. The field samples analyzed in this study represented both surficial (5 cm below the cap) and deeper segments from the core. The samples collected

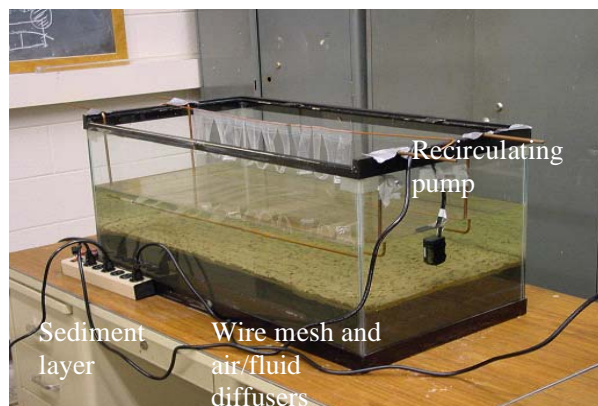


Figure 4-1. Sediment Tank Reactor.

from the flux chamber were randomly distributed to capture both short and long distance correlations in microbial attributes.

The samples were collected from two sites: uncapped sediment (No-cap) and sand capped sediment (Sand-cap) in Anacostia River in October (17-19) of 2006. The caps were placed between March and May of 2004 (Reible et al., 2006). Water depth at the sites ranged from 6.43 to 17.3 m. Cores were divided and samples were processed at 10 cm intervals from the sediment surface. The samples processed were core sections

collected from 0-10 cm (top), 10-20 cm (middle), and 20-30 cm (bottom) below sediment surface. The samples were stored in the dark at 4°C.

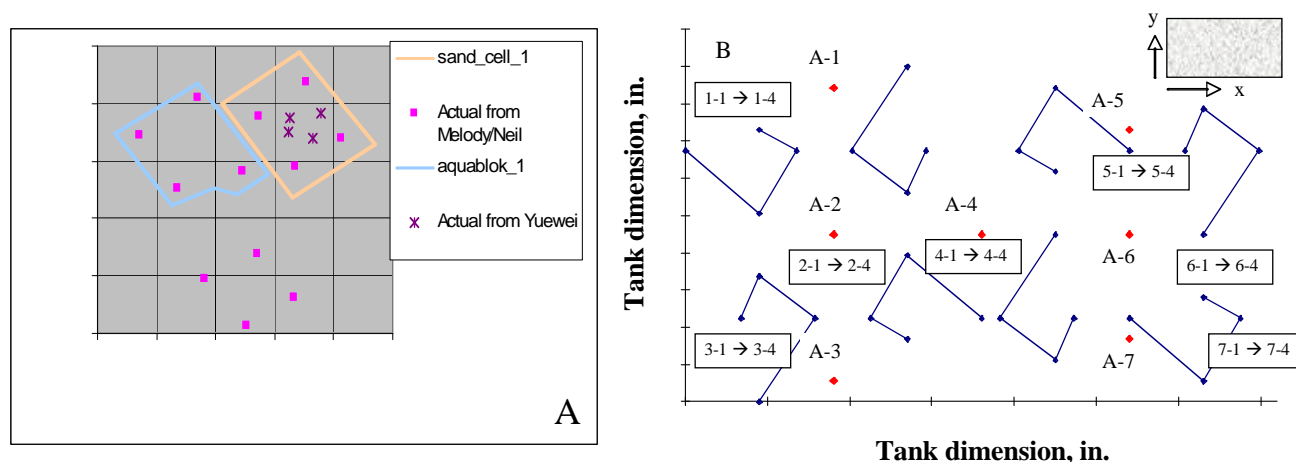


Figure 4-2. Sampling schemes in the field (A) and the laboratory tank reactor (B)

Enumeration of active and total cells. Active bacteria in the samples were stained with the tetrazolium salt CTC (5mM) and incubated at room temperature for 16 h in dark. The samples were then fixed using formaldehyde (2%). Tween 80 (0.1%) was added, followed by sonication for 5 min to separate bacterial cells and solid particles and to decrease background fluorescence. The samples were centrifuged at low speed 50xg for 20 min and supernatant was transferred and stained by non-specific stain PG (PicoGreen) (0.5%) for 5 min for counting total bacteria. The sample was then filtered onto black polycarbonate filters (Poretics, Polycarbonate, Black, 25 mm; Pore Size: 0.2 μ m) under low vacuum pressure. Slides of samples were prepared and counted using fluorescence microscopy ($\times 1000$). A minimum of 10 random fields or 200 bacteria were counted for each slide. Analysis of each sample was replicated ($n=3$).

Community level physiological profiling (anaerobic BIOLOG) In anaerobic chamber, 5g of sediment (wet weight) was added into 45 mL of sterile 10 mM sodium phosphate buffer (1.64g/L $\text{Na}_2\text{PO}_4\text{H}\cdot 7\text{H}_2\text{O}$ and 0.47g/L $\text{NaH}_2\text{PO}_4\cdot \text{H}_2\text{O}$ adding nano pure water to 1 L mark in a 1 L bottle and making pH=7.6 following by sterilization in an autoclave) in milk dilution bottles and shaken for 1 hr at 200 rpm outside anaerobic chamber. The samples were moved back to anaerobic chamber and serially diluted (using anaerobic inoculating fluid) to achieve approximate 10^4 cells per 100 μ l based on active bacterial counts. Each diluted sample was loaded into the wells of an anaerobic BiologPlate (AN-BiologPlate) that included 95 carbon substrates and one control well (100 μ l per well) outside anaerobic chamber. Samples were incubated in Oxoid AnaeroGenTM Compact System that can provide a hydrogen-free anaerobic condition at 30°C for 5 days then analyzed by visual counting of purple wells. AN-BiologPlate analysis provided an estimation of the community metabolic diversity (CMD) of anaerobic heterotrophic bacterial communities.

Data analysis and Statistics. To facilitate comparison across cap-type, data reporting microbial activity and numbers were averaged to represent the parameters under each cap-type. For

comparison of more than two samples, analysis of variance (ANOVA) was performed (A-P). For direct comparison between two samples, a student's t-test was performed (T-P). In both cases, significance was determined at $\alpha \leq 0.05$.

4.1.2 Results and Discussion

Total and active bacterial counts. The total and active numbers of bacteria in different site samples are shown in Figure 4-3. The three site samples indicated a similar number of total bacterial, $2.26 \times 10^7 \pm 5.17 \times 10^6$, $2.34 \times 10^7 \pm 1.26 \times 10^7$, and $2.36 \times 10^7 \pm 6.88 \times 10^6$ cells per gram of dry weight (g^{-1}DW) for no cap, synthetic aggregates cap, and sand cap sediment samples, respectively. Sand cap sediment samples had higher active bacterial numbers that is $7.41 \times 10^6 \pm 1.47 \times 10^6$ cells g^{-1}DW than both no cap and synthetic aggregates cap sediment samples, which have similar active bacterial numbers of $5.92 \times 10^6 \pm 2.03 \times 10^6$ and $6.40 \times 10^6 \pm 3.88 \times 10^6$ cells g^{-1}DW , respectively. Accordingly, sand cap samples also have highest active percentage (32.03%) than no cap sediment samples (25.65%) and synthetic aggregates cap sediment samples (26.30%).

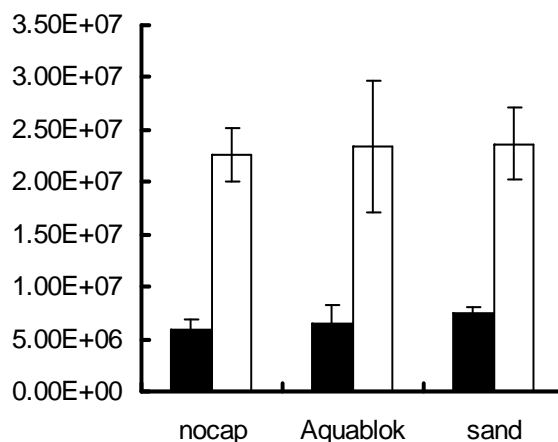


Figure 4-3. The average number of total and active bacteria per gram dry sediment across cap type. (■) active numbers (□) total numbers

Fluorescein diacetate assay. Similar to the results from total and active bacterial counts, the order of fluorescein produced ($\mu\text{g/hr}$) from highest to lowest for three types of samples is: sand, 2.256 ± 0.094 , Aquablok™, 1.927 ± 0.202 , and no cap, 1.763 ± 0.075 sediment samples.

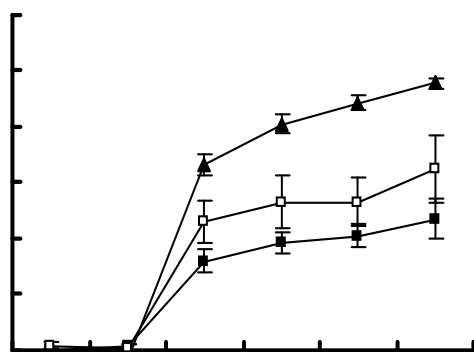


Figure 4-4. Average metabolic response (AMR) across cap type. (▲) No cap, (■) Aquablok™ cap, (□) Sand cap

Community level physiological profiling (BioLog). Both the average metabolic response (AMR) and community metabolic diversity (CMD) show same pattern. The six day data is provided as an example. From Figure 4-4, we found that no cap samples indicated highest AMR and CMD (0.957 OD and using 19 carbon substrates out of 30). Synthetic aggregates cap samples have the lowest AMR and CMD (0.471 OD and 11 substrates out of 30). Comparing total and active bacterial counts and FDA, the synthetic aggregates cap samples always have a lower activity than sand cap samples (AMR and CMD are

0.648 OD and using 14 substrates out of 30).

Community Analysis. DNA fingerprinting revealed that the cap type (No Cap, Sand Cap, Synthetic Aggregate Cap) impacted the structure of the microbial communities based on denaturing gradient gel electrophoresis (DGGE) of PCR amplified DNA using Bacterial and Archaeal primers (Figure 4-5). Unique bands were cut to be sequenced. 16S rDNA bands purified from DGGE were cloned and sent out to MWG (USA) to be sequenced. Phylogenetic analysis was done using Blast and ClustalW. As expected, most of the Bacterial species identified such as *Alteromonas sp.*, *Spirochaeta sp.*, were anaerobic. After cap placement, there was an increased intensity in some of the dominant bands found in uncapped sediments. These were also identified as anaerobic microbial communities. Further, some communities appeared to shift after cap placement. For example, *Rhodoferrix ferrireducens* are aerobic microbes that were clearly present in uncapped samples but became weak or disappeared in capped sediment samples.

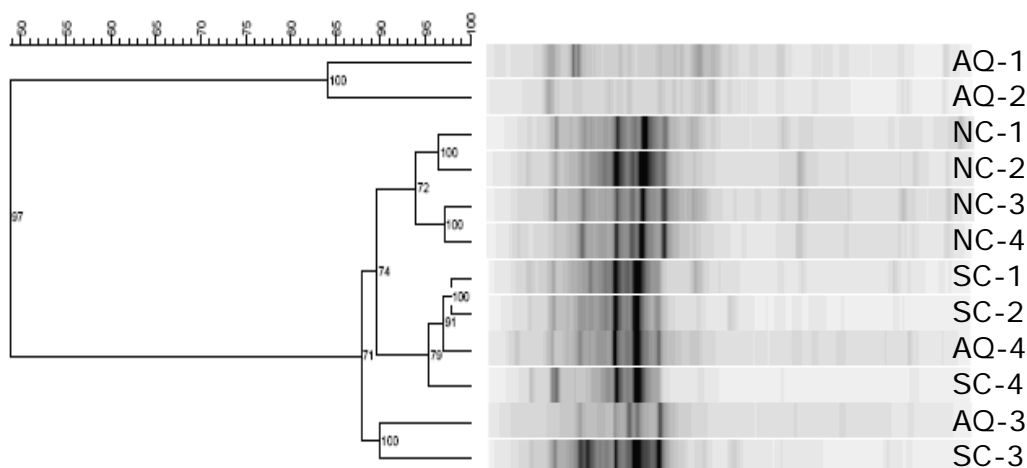


Figure 4-5. Dendrogram for DGGE from bacteria in sediments. Similarity between sample types is shown. (NC-1) No Cap, CNW-3, 0-5 cm*, (NC-2) No Cap, CNE-3, 0-5 cm, (NC-3) No Cap, CSW-4, 0-5 cm, (NC-4)) No Cap, CSE-4, 0-5 cm, (AQ-1) Synthetic aggregate Cap , ABSE-6(4), 20-25cm, (AQ-2) Synthetic aggregate Cap , ABSE-6(5), 25-30cm, (AQ-3) Synthetic aggregate Cap , ABNE-6, 0-5 cm , (AQ-4) Synthetic aggregate Cap, AS_5, 0-5 cm, (SC-1) Sand Cap, SES-5, 0-5 cm, (SC-2) Sand Cap, NWS-5 , 0-5 cm , (SC-3) Sand Cap, NES-4, 0-5 cm, (SC-4) Sand Cap, LT3, 0-5 cm.

In capped samples, there was an emergence of some of the species such as *Sphingomonas sp.*, *Flavobacterium sp.*, *Spirochaeta sp.* that can survive in either aerobic or anaerobic conditions. Surprisingly, the Archaeal bands were not very strong indicating that they were not dominant in the samples processed (mostly top 5 cm). This may be attributed to the fact that some of the species present including *Sphingomonas sp.* and *Flavobacterium sp.* can survive in the anaerobic environment, particularly in the presence of abundant nitrate. http://sunrain.net/cgi-bin/r_ecdict_e.cgi?word=imaginably&output=gb&searchmode=exact Since nitrate reduction is thermodynamically favorable as compared to methanogenesis, competition for nutrients may have limited the ability of Archaeal microbial communities to compete.

Flux Chamber Microbiology. The results from sediment testing for microbial abundance and metabolic competence in the unamended flux chamber are shown in Figure 4-6. The data representing cores A1-A7 indicate that, despite the extensive sediment mixing, there is a great

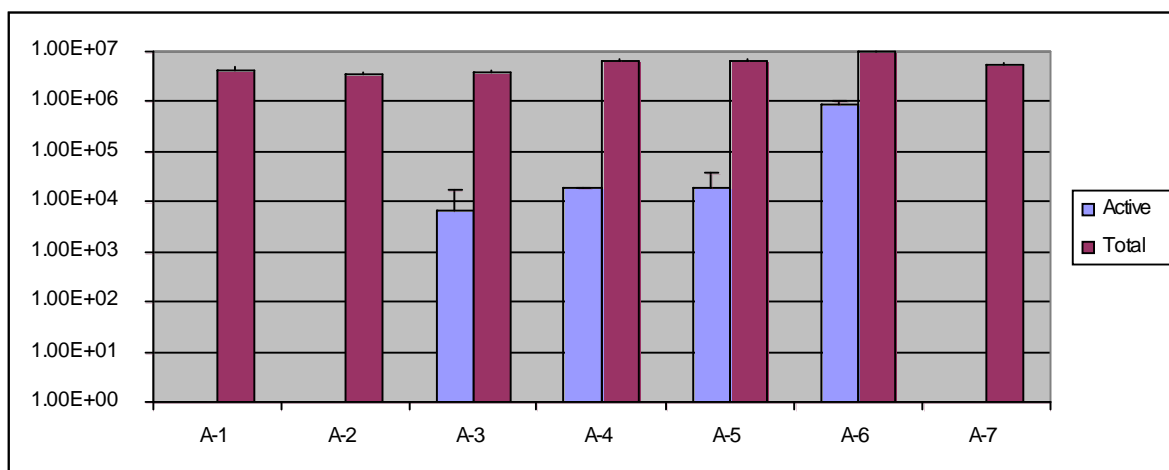


Figure 4-6: Microbial abundance and activity in unamended sediment flux chamber

degree of spatial heterogeneity across the tank in active numbers of microorganisms, ranging from 0 to about 10% of total organisms. The total microbial abundance is similar to that observed in the field cores, but the fraction of respiratory competent organisms is much lower than in the cores (6-45%). This observation may be due to the extensive manipulation of the sediments prior to the laboratory test, including: the sediments were collected with a backhoe and deposited in 55 gal. drums; the sediments were exposed to aerobic conditions for mixing prior to deposition in the tank; and the sediments were exposed to an artificially-induced 'ebullition' flux of air.

At the fine-scale spatial resolution (within sample clusters), much greater homogeneity was observed in active microorganisms, as exemplified for sample clusters 1.1-1.4, 3.1-3.4, 6.1-6.4 and 7.1-7.4 (for location, ref. Figure 4-1, B). Again, the abundance of total microorganisms was on the order of 10^7 microorganisms/g, while active organisms ranged from 10^4 - 10^6 per gram sediment, except for sample 1.2 (Figure 4-7). This represents an active fraction of organisms on the order of 1-16% between these four sample clusters (with a tighter distribution within a cluster), which is lower than in the preserved field cores, but similar to that observed at large spatial resolution. Interestingly, sampling clusters in the neighborhood of samples A-1 and A-7 (which showed no active microorganisms) indicate the presence of 1-10% active microorganisms, suggesting that even at the small scale, inhomogeneities exist.

Field Scale Microbiology. The results from the dual stain microscopy data are shown in Figures 4-8 and 4-9, illustrated for background samples, and those collected from the sand cap and Aquablok cap. Aquablok is a proprietary clay-encapsulated granular material that expands and seals once in contact with water. The difference in spatial distribution of microbial activity can be observed from Figure 4-8, which shows an epifluorescent microscopic photograph for

samples with 0.7 and 65% activity. The total microbial numbers range was $1.4\text{E}5$ to $2.8\text{E}7$ per gram of sediment.

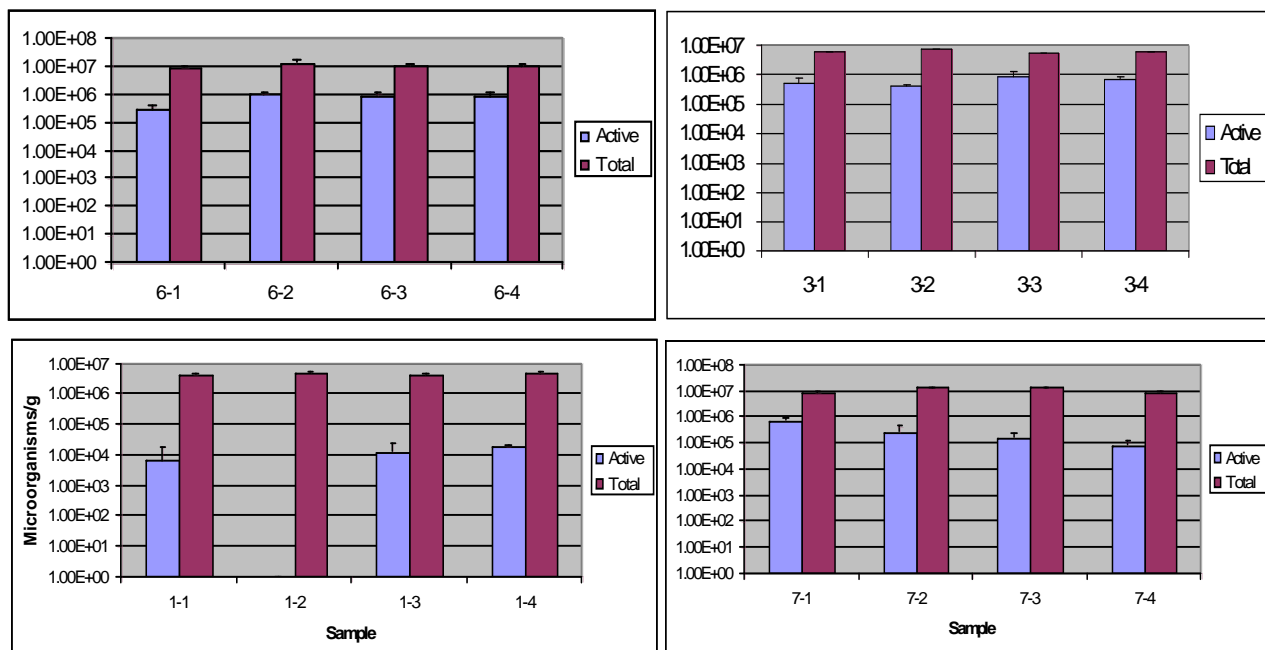


Figure 4-7. Total and active microorganisms at fine scale spatial resolution in the flux tank chamber

The generally high activity numbers are on par with those observed in anaerobic digesters and are well above those measured in other riverine and estuarine sediments, and indicates that there should be an ample supply of labile organic carbon to sustain microbial activity. The values for capped and uncapped sediments are shown in Figure 4-9.

The following trends can be discerned:

- (i) capped sediments exhibit lower total microbial numbers than uncapped sediments, but a higher fraction of the organisms is active;
- (ii) the total bacterial count appears to peak at 15-20 cm under the cap or river bottom; and
- (iii) the active fraction of organisms is fairly constant with depth under caps, but decreases by up to 90% in uncapped sediments.

It is unclear at this time what may have caused this difference as a function of capping scenario. The CTC test presumably primarily measures reduction of the hydrogenase enzyme complex, which would indicate a differential response between archaea and bacteria. Since the community analysis indicated that archaea were not very abundant and that capped samples showed the emergence of bacteria with multiple respiratory pathways, the variable activity was presumable due to the variable community compositions.

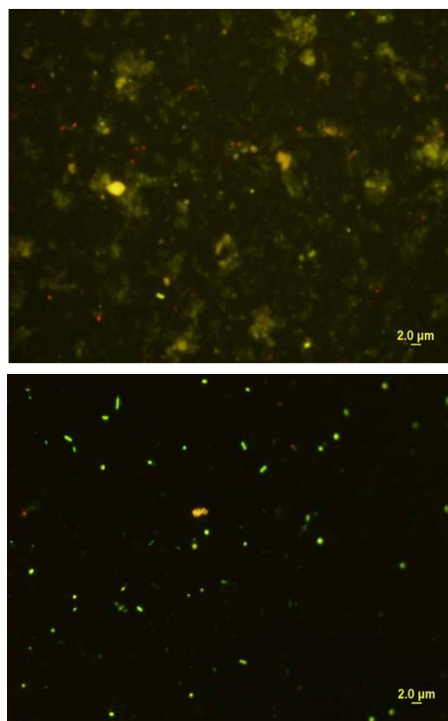


Figure 4-8. Microbial activity as measured using CTC for 65% (top) and 0.7% (bottom) active sediment samples.

4.1.3 Extraction of Data for Integration Modeling

The activity and abundance data indicate substantial variability with depth in all capping scenarios (Figure 4-8). At a spatial level, microbial abundance is constant, but substantial variability is noticeable in activity level (Figure 4-5 and 4-6). We have mapped these data spatially (Section 4.3) at both the lab and the field scale to assess whether the spatial variability was reproducible, and concluded that the variability in the laboratory data could be used to inform microscale variability in the field. With respect to Task 6, we decided to not directly use the microbial abundance and activity data in the integrative SFM, but rather use them to constrain the microbial ebullition fluxes in the model. The ebullition measurements are described in Section 4.2.

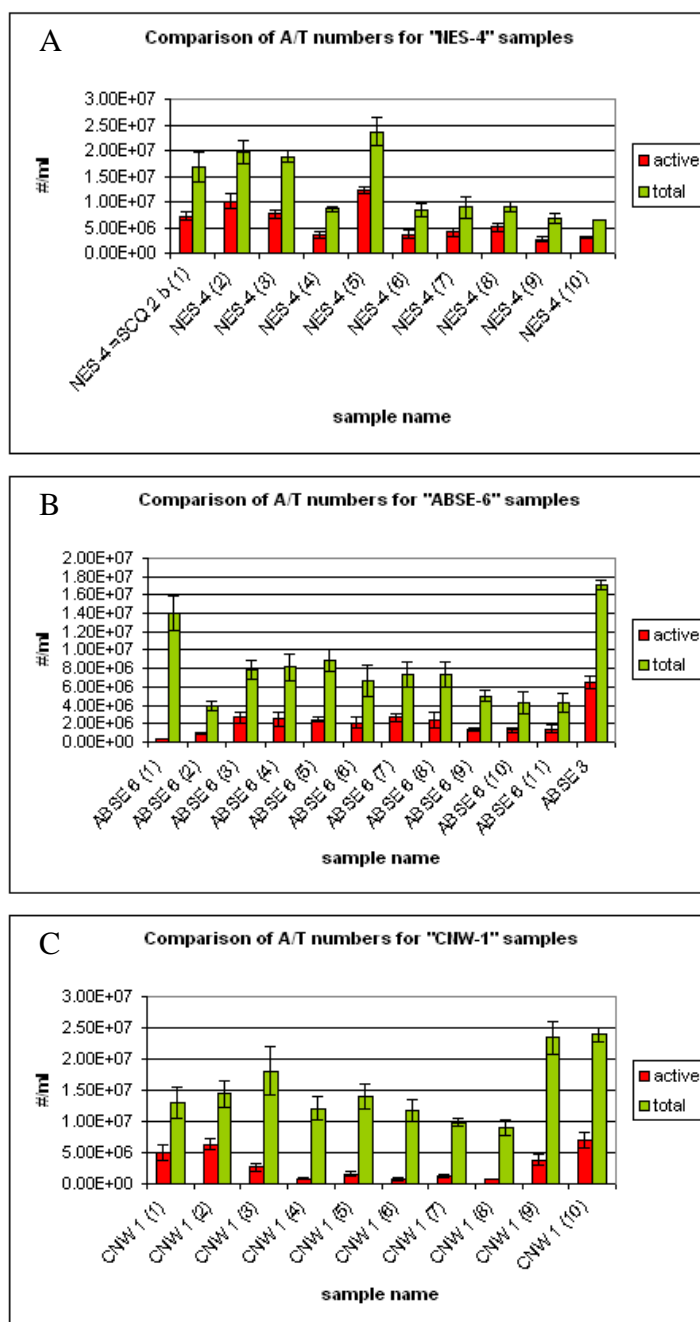


Figure 4-9. Total and active microorganisms in sand (A), Aquablok (B) and uncapped (C) sediments (left to right, 5 cm increments below the cap)

4.2 MICROBIAL EBULLITION MEASUREMENTS

4.2.1 Experimental Approach

Incubation experiment with Hydrogen Release Compound (HRC). Two cores, C-SW4 and S-NE4, were selected and divided into three depths for this work. Triplicates were processed at each depth interval (total 18 samples). 15 grams of sediment and 5 mL pure water were added to each 20 mL serum vial (allowing 40% by volume headspace) with 2% HRC of the sediment weight in the vials to stimulate and accelerate the biogas formation. The vials were incubated for 80 days at ambient temperature (around 22°C).

Biogas characterization and term definition. Biogas composition was measured by a GC (GOW-MAC Series 400 GC/TCD) equipped with 10'x1/8" Haysep DB column. The flow rate of carrier gas (Helium) for the GC was set as 30 mL/. The temperatures of column, detector, and injector were 120°C, 135°C, and 150°C, respectively. The bridge current was set to 105 mA. Volumetric production rate or biogas volume production rate (mL/gdw/d) will be expressed as “biogas rate” hereinafter and biogas production rate of individual components ($\mu\text{mol/gdw/d}$) will be simplified as “composition rate” such as “N₂ rate”, “CH₄ rate”, and “CO₂ rate” hereinafter.

Total organic carbon (TOC). TOC was measured for sediments from both before incubation and after 28 days to approximate biodegradable organic carbon. TOC was extracted from sediment particles: 4 g wet each sediment was added into a 50 mL tube and added to 40 mL with 0.1M NaOH. The tubes were shaken for 2 hours, centrifuged for 30 min at 5000 at 5°C. The supernatant was separated into a 50 mL tube. The process was repeated and supernatants were combined prior to analysis.

Impact of temperature on biogas formation. Uncapped sediments were chosen to study the impact of temperature on ebullition potential. 15 grams of sediment and 5 mL pure water were added to 20 mL serum vial (allowing 40% by volume headspace) with 1% HRC of the sediment weight in the vials to stimulate and accelerate the biogas formation. With this method, the sample was distributed to nine serum vials. The vials were shaken to mix HRC and water with sediment well, and then sealed and incubated for up to 60 days at three different temperatures 4°C, 10°C, and ambient temperature (around 22°C) in three vials (triplicate), respectively. Only one feeding of HRC was used during the incubation.

Impact of biodegradable carbon on biogas formation. Uncapped sediments were chosen to study the impact of nutrient, concentration of HRC, on ebullition potential. The sample was distributed to 12 serum vials. Of the 12 vials, four vials were fed with 0.1%, 0.5%, 1% and 2% HRC of the sediment weight in the vials, and set at ambient temperature (around 22°C). So, this experiment will be called “carbon incubation”, hereinafter. Only one feeding of HRC was used and incubation had lasted 34 days.

4.2.2 Results and Discussion

Gas Production Trends.

In an effort to understand the nature and extent of methane production, flux and microbial activity of Anacostia river sediment samples, gas ebullition experiments were carried out using the sediment cores collected in the 2004 field sampling campaign. A long-term study of samples

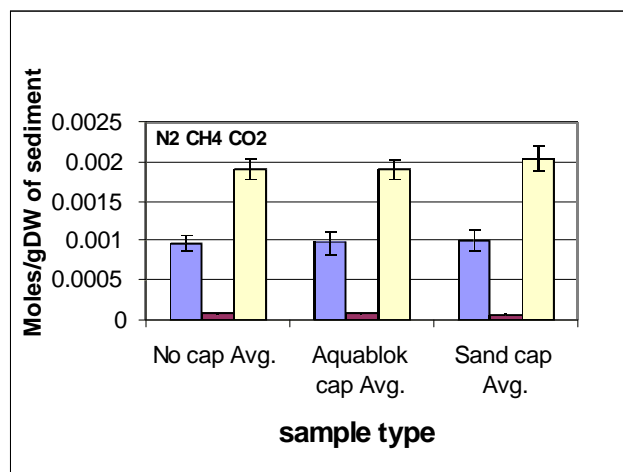


Figure 4-10. Distribution of gas production from Anacostia River sediments

from each capping regime (4 each) has been initiated to monitor gas production and composition with time (Figure 4-10). The sediments were incubated in 20 mL serum vials with fixed amounts of hydrogen release compound (HRC) (2% by volume) under anaerobic conditions, but in the absence of externally amended electron acceptor. After approximately two weeks of incubation, our data indicates that there are temporal differences in the quantity and composition of gas for each sample type. Carbon dioxide gas was the most important constituent of biogas (60-65%), followed by dinitrogen gas (32%), and methane (3-5%). This composition is different from what is observed at many field sites, where methane

is the dominant gas (after carbon dioxide), however, it reflects the low abundance of Archaea observed at the site. There were no statistical differences between the total amount (moles) of methane (approx. 5.5×10^{-4}) or carbon dioxide (approx. 9×10^{-4}) generated or the total volume of gas (approx. 34 mL) generated as a function of sample type over the two-week incubation period.

The kinetics of gas production is illustrated in Figure 4-11 for carbon dioxide (right) and dinitrogen gas (left) over a 5-week incubation period. The time trends differ in that there is fairly sustained production of CO₂ (driven by the available HRCTM compound added to the vials) over this period, whereas the available nitrate/nitrite in the sediment become depleted over time. Differences between samples are difficult to detect due to the small volume of sediments being processed. The next set of experiments will involve larger volumes of sediment to verify these results.

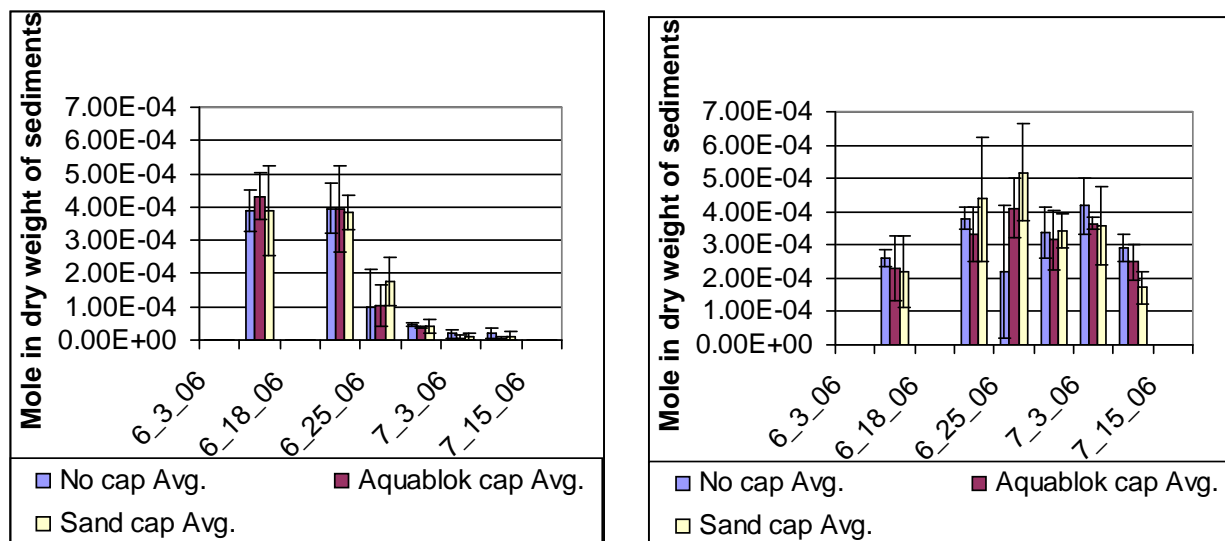
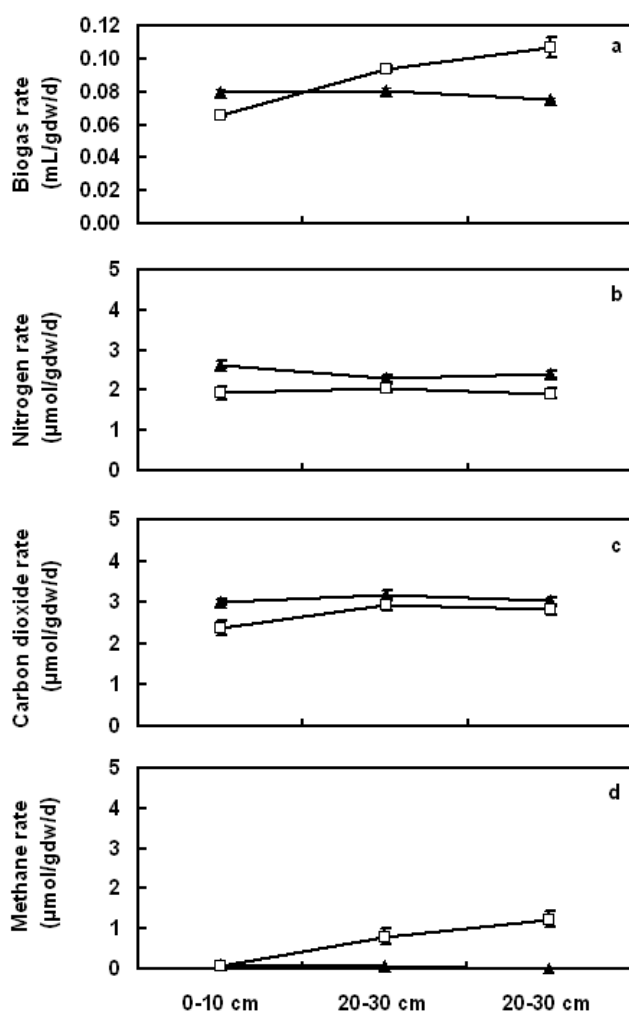


Figure 4-11. Time trends of dinitrogen (left) and carbon dioxide in sediments



After the 80 day incubation, the sand-cap samples in top depth showed a lower biogas rate than No-cap samples (a). However, **Error! Reference source not found.**4-12 indicates that Sand-cap samples had higher number of active cells than No-cap sample in top depth. The comparatively more bioprocesses occurring in the top of sand capped sediments were likely once limited by competition with denitrifiers.

This analysis is also supported by Figure 4-13 where Sand-cap top depth has an obvious shift and lower peak during the first four days. In addition, abundant N_2 was observed in all samples (b). However, Sand-cap samples began to increase the biogas rate from middle to bottom depth (a). The increased biogas rate was mainly contributed by both increased CH_4 rate (d) that was related to increased biodiversity

Figure 4-12: Biogas and composition rate (mL/gdw/d and μmole/gdw/d, respectively) in 80 days incubation experiment with 2% HRC at room temperature in three depths, 1-10 cm (top), 10-20 cm (middle) and 20-30 cm (bottom): (a) biogas rate; (b) nitrogen rate; (c) carbon dioxide rate; (d) methane rate. (▲) No-cap, (□) Sand-cap (average±standard error, n=3).

and decreased N_2 (d) stimulated by relatively active denitrifiers.

That is why No-cap samples kept a much lower CH_4 in three depths where N_2 had a higher value than Sand-cap samples. It also indicates that methanogens are mainly distributed in the range of 10-30 cm depth, with an increased trend with depth.

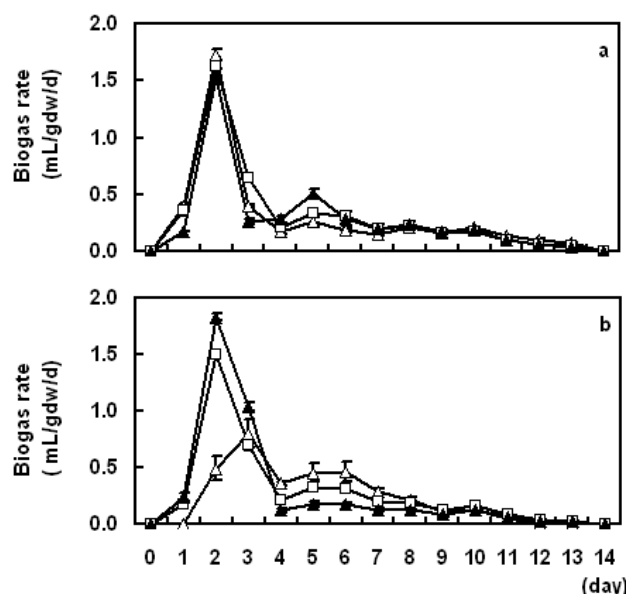


Figure 4-13: Biogas rate (mL/gdw/d) in time distribution for the first 14 day incubation experiment when biogas stopped and no measurable biogas volume for several days in three depths: (a) No-cap; (b) Sand-cap. (Δ) 0-10 cm, (□) 10-20 cm, (▲) 20-30 cm (average±standard error, n=3)

activity due to consumption of substrates. On the other hand, the middle and bottom Sand-cap samples showed an increase in the methane production rate toward the end of the 80 day incubation period, suggesting increased ebullition will occur following capping, particularly in deeper sediments.

Biogas dependence on temperature

The 22°C samples show the highest biogas rate (0.077 mL/gdw/day) and composition rate (Nitrogen 2.07; Carbon dioxide 1.25; and Methane 1.58 in $\mu\text{mol/gdw/d}$) ($P < 0.05$). Only 22°C samples produced methane gas (Figure 4-14). This result demonstrates the consistent observation with literature data in capped areas during summer. Decreased temperature not only reduced methane production rate, but also change the pathway of the degradation process, such as H_2/CO_2 -dependent methanogenesis decreased with decreasing temperature. So, methanogens in sediments were mainly considered as H_2/CO_2 -dependent methanogens that favor higher temperature than acetate-dependent

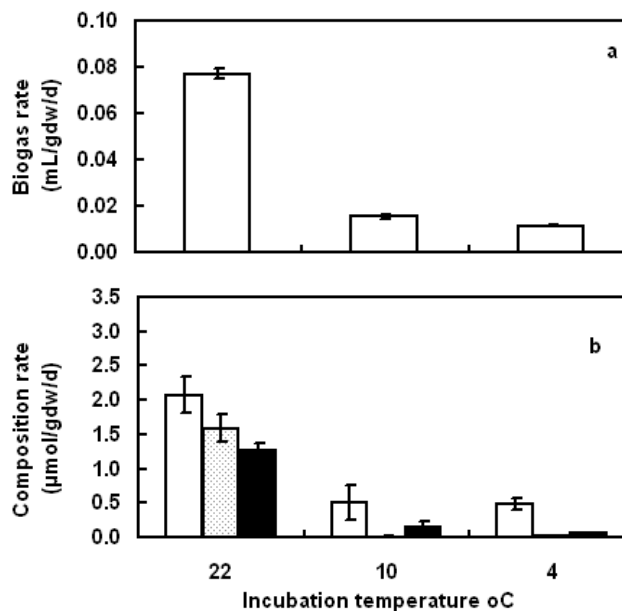


Figure 4-14. Biogas production for (a) biogas rate (mL/gdw/d); and (b) biogas composition rate ($\mu\text{mole/gdw/d}$) as a function of incubation temperature (22°C, 10°C, and 4°C), (□) nitrogen, (■) methane, (▨) carbon dioxide (Error! Reference source not found.)

methanogens.

Biogas dependence on HRC concentration

An obvious decrease in both biogas and composition rate was observed with the decrease of HRC concentration from high to low: 2%, 1%, 0.5%, and 0.1%, for which biogas rate in mL/gdw/d are: 0.129, 0.087, 0.065, and 0.037, respectively ($P < 0.05$). The 2% HRC vials had an obviously higher biogas rate including nitrogen and carbon dioxide (Figure 4-15). However, no methane gas was observed. The reason might be higher H_2 concentration released by 2% HRC selected for denitrifying bacteria, resulting in the production of toxic intermediates from denitrification.

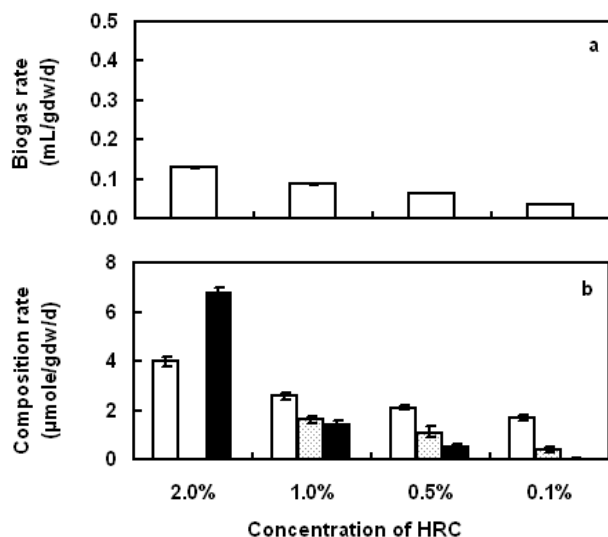


Figure 4-15. Biogas production for: (a) biogas rate (mL/gdw/d) and (b) biogas composition rate (μmole/gdw/d) as a function of HRC amendment (2%, 1%, 0.5%, and 0.1%) at 22°C, (□) nitrogen, (○) methane, (■) carbon dioxide (ave±std error, n=3).

4.2.3 Data Extraction for Integration Modeling

The data from direct ebullition measurements indicated that the methane fluxes in these sediments were very low, due to the low numbers of Archaea in the community composition. The implication of this finding would be that the extent of PAH partitioning to the gas bubbles would be expected to be very low as well. This hypothesis was tested in Task 4 (Section 6), whereby air was forced through the sediment flux tank to simulate the theoretical impact of gas ebullition on PAH fluxes emitted from the sediment. These measurements, along with the process understanding of ebullition from Anacostia River sediments, were used in the SFM.

4.3 SPATIAL MODELING OF SEDIMENT MICROBIAL CHARACTERISTICS

The substantial degree of spatial distribution in microbial activity and abundance (Figure 4-6 and 4-7), necessitated spatial analysis and integration using geostatistics tools. The following sections describes the geostatistics tools, including a newly developed tool that explicitly specifies spatial scales, and compares the results from their analysis. The objective of this task is to enable appropriate scaling of the laboratory data to the field. This task requires that (1) the scale at which the data are collected can be explicitly incorporated in the analysis, and that (2) the spatially-distributed data points can be interpolated while preserving small scale features.

4.3.1 Description of Modeling Tools

In observation of the complexity of contaminant assessment in the sediment environment, spatial estimation approaches have been applied to provide information for decision-making (Englund

and Heravi, 1993; U.S. EPA, 2005). Especially when a conceptual site model including, for example, a contaminant mass transport model is not available or not sufficient to estimate the spatial attributes, statistical models are often used to make estimates of attribute values and evaluate the estimation uncertainty where no sample is taken (Goovaerts, 1998; Adriaens et al., 2006; Chil`es and Delfiner, 1999). Although based on similar principles of spatial estimation, different models have been developed to fit different estimation objectives.

Ordinary kriging (OK) is a parametric approach generally used for local estimation which generates a smooth visual representation of the spatial distribution. The smooth estimation map, however, under-represents the spatial variability, a situation usually called smoothing effect (Isaaks and Srivastava, 1989). The approach yields good estimates locally that minimize estimation variance, while their estimates exhibit a smoothing effect due to their tendency to produce a central value among sample points, thus reducing the variability of the estimate.

Constrained kriging (CK, Cressie, 1993) is a technique used to generate estimations that reproduce global and spatial variability without ad hoc post-processing to reduce the smoothing effect. This technique has the potential to exhibit estimation stability, where estimates may or may not be singular depending on the strength of covariance (the absolute value of the covariance) between sample and estimation locations.

The M-Scale model is a new spatial estimation method that has the ability to produce a single estimation map on the basis of covariance between mean values at different scales. This multi-scale estimation method is capable of using the covariance between means to facilitate both the explanatory needs for the possible causal relations between different spatial scales by the covariances between means, and estimation purposes that depict the spatial variability. The estimation uncertainty of the M-Scale model is reduced using Lagrange optimization, which is the same optimization concept used in OK and CK. The explicit incorporation of scaled information for the M-Scale model further enables the reproduction of spatial variability by an additional constraint attributing the largest weight to the scale that is most related (corresponding to the largest covariance) to the target scale, which is expected to reduce the smoothing effect observed in conventional kriging approaches.

This model is based on two tenets: (i) calculating average values for different scales at each estimation location, and (ii) attributing different weights to these averages to generate the estimates, as shown in Figure 4-16. The M-Scale model applies a constraint to reproduce variability, in addition to the unbiasedness constraint, while avoiding overestimation of the extent of threshold exceedance around

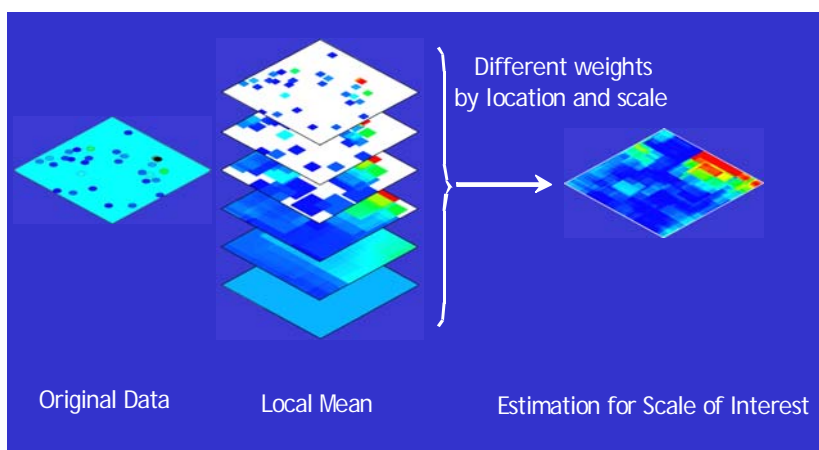


Figure 4-16: Conceptual sketch of the M-Scale model. Original data are used to evaluate the local mean at different spatial scales. The local means are further attributed different weights and evaluated as the estimates

the sample locations. As a linear spatial estimator, the M-Scale model minimizes estimation variance, and the parameters and statistics are analogous to those used in OK and CK. The concepts and parameters described earlier for OK and CK are compared to those in M-Scale in Tables 4-1 and 4-2.

Table 4-1. Comparison of concepts and parameters for spatial attributes between the M-Scale model and conventional kriging approaches.

Spatial Attributes	M-Scale	Kriging
Unknown Value	$Z_{D_t}(x)$	Z_0
Sample Value	$Z_{D_a}^*(x)$	Z_i
Independent Variable	scale a at location x	location x

Table 4-2. Comparison of spatial covariances between the M-Scale model and conventional kriging approaches.

Spatial Attributes	M-Scale	Kriging
Global Variance of Unknown	$C_{D_t D_t}$	$\sigma^2 = C(0)$
Sample-to-Sample Covariance	$C_{D_a D_b}^*(x)$	C_{ij}
Sample-to-Unknown Covariance	$C_{D_a D_t}$	C_{i0}

A complete description of M-Scale is provided in Li (2008).

The M-Scale model was tested using an artificial dataset to validate and generalize the assumptions associated with the features of this model. First, M-Scale assumes second order stationarity (variance and covariance stays the same across the modeled spatial domain) between scales, as opposed to second order stationarity between points in the case of ordinary kriging. Second, the model incorporated one additional constraint for local stationarity (local mean values) as compared to kriging models. A sample application with artificially generated data is presented to demonstrate the improvement over ordinary kriging (OK) using summary statistics that characterizes spatial variability, including variance of estimates, variogram of estimation map, and threshold estimation map. The results indicate that M-Scale model reproduces not only the variance of overall measurements, but also the spatial variability between estimation locations (Figure 4-17). This figure represents the following metrics of variation in its comparison of M-Scale and OK with the target simulation:

- (i) Global variability:
 - a. Standard deviation (std): Reduced standard deviation indicates smoothing
 - b. A-D test statistics (A^2): Larger A^2 indicates worse fit of histogram
- (ii) Spatial variability:
 - a. Variograms: Increased range (rg) of influence and reduced sill (sl) indicate smoothing
 - b. Threshold indicator maps: Reduced area for extreme thresholds indicates smoothing

The results indicate that the M-Scale model reproduces the global standard deviation, the value distribution histogram, and point-to-point spatial variability. Especially for the indicator map,

the M-Scale estimation clearly reflects the possible high/low value boundaries, while for OK the boundary may be misjudged.

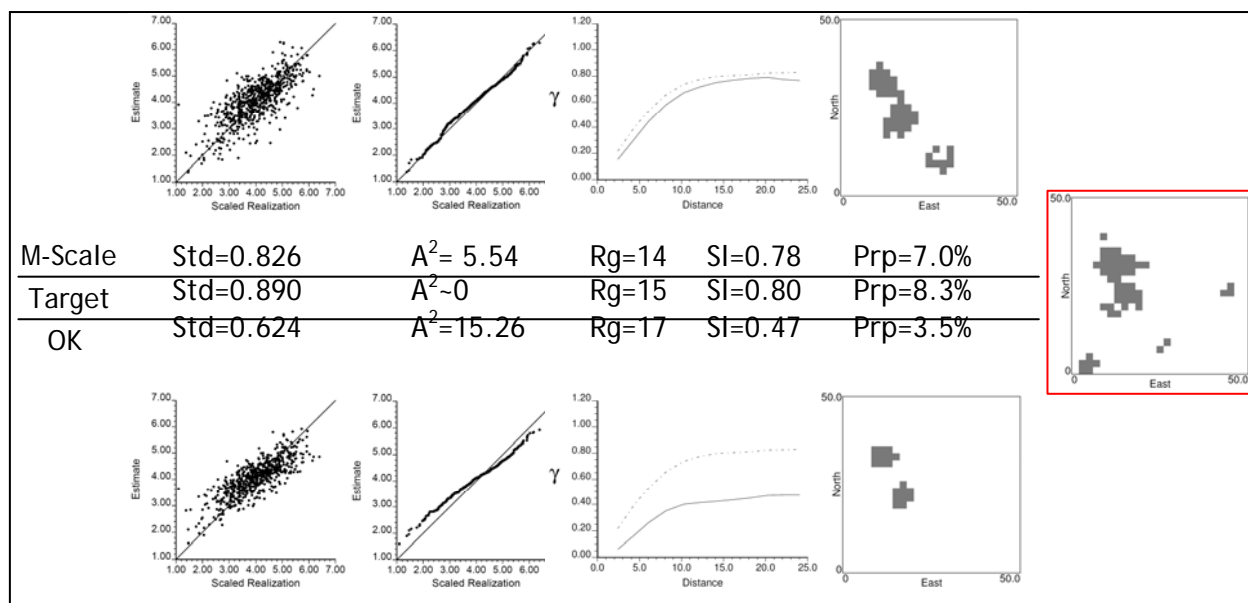


Figure 4-17. Model diagnostics using artificial dataset

4.3.2 Data Treatment and Variogram Development

To test the M-Scale model in its capacity to propagate uncertainty across scales, we have spatially sampled the control flux chamber for microbial abundance and activity (CTC-competence). The results will allow us to compare the results obtained from paired field samples with those from a more homogenized system in the laboratory. The results indicate that the total numbers of microorganisms does not change significantly in space, ranging from $3E6$ - $1E7$ /g sediment, which is similar to that observed in the field ($5E6$ - $2E7$ /g sediment). Surprisingly, the distribution of microbial activity (expressed as % of total) was substantially different from that observed in field samples: 3-15% (laboratory); 5-50%. The spatial distribution of site and flux tank microbial abundance and activity is shown in Figures 4-18 and 4-19.

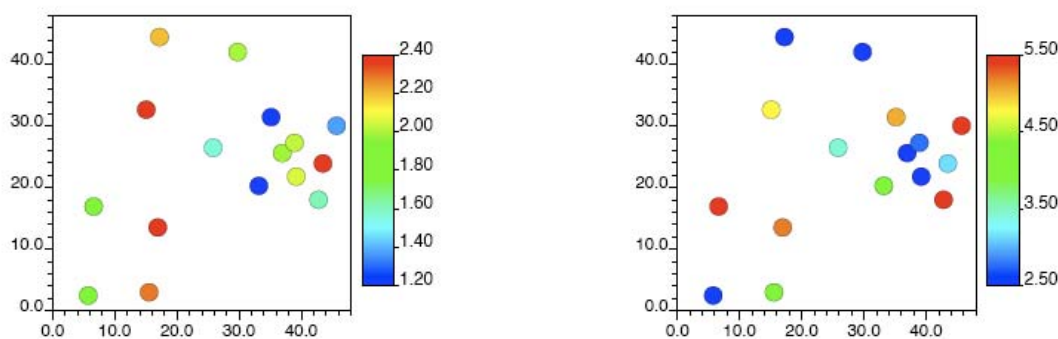


Figure 4-18: Site-scale sample locations with values indicated in color scales. Left: microbial abundance ($\times 10E7$ microorganisms/g) Right: microbial activity ($\times 10E6$ microorganisms/g). Units in distance: m.

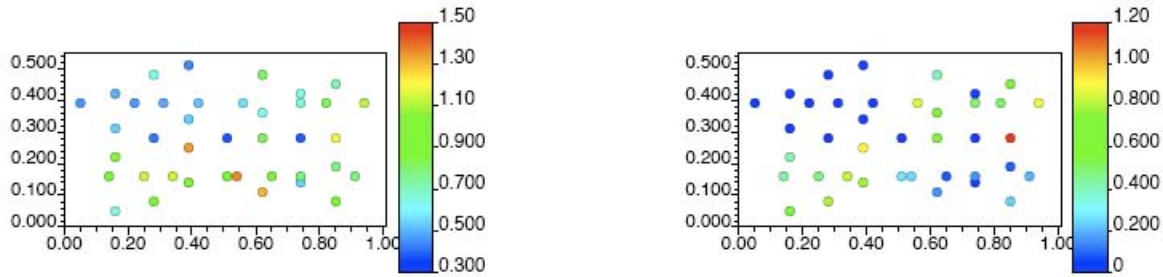


Figure 4-19: Micro-scale sample locations with values indicated in color scales. Left: microbial abundance ($\times 10^7$ microorganisms/g) Right: microbial activity ($\times 10^6$ microorganisms/g). Units in distance: m.

The modeling approach included the following steps:

- Fitting of variogram models using datasets of both the site scale and the micro-scale;
- Evaluate the micro-scale variability by the micro-scale variogram. Calculate the measurement error by subtracting the micro-scale variability from the nugget effect;
- With the site scale variogram excluding or including the measurement error, generate the likelihood map of exceedance for the threshold of interest;
- Under different confidence levels, explore the impact of excluding measurement error by calculating the difference in areas of the contamination zone.

In this study, samples taken at the tank scale are assumed to be representative of the micro-scale samples taken on-site. The micro-scale variability of the site-scale measurement, consequently, is evaluated using the variogram of the tank-scale measurements, subsequently the measurement error variance is evaluated and extracted from the nugget effect of the site-scale variogram. The resulting variogram of the site-scale variability is used to generate estimates and estimation variance for the three estimation models.

Variograms for microbial abundance:

$$\text{site-scale: } \gamma(h) = 0.176 + 0.244 \cdot \text{Exp} \left(\frac{h}{25.00^m} \right)$$

$$\text{micro-scale: } \gamma(h) = 0.020 + 0.080 \cdot \text{Exp} \left(\frac{h}{0.38^m} \right)$$

Variograms for microbial activity:

$$\text{site-scale: } \gamma(h) = 1.980 + 3.800 \cdot \text{Exp} \left(\frac{h}{9.00^m} \right)$$

$$\text{micro-scale: } \gamma(h) = 0.020 + 0.150 \cdot \text{Exp} \left(\frac{h}{0.38^m} \right)$$

Exp () denotes the exponential variogram model. The nugget effect for the site-scale variogram is calculated directly using the 1'-apart collocated core sample pairs and averaged over all sample locations. Although the variogram of the flux chamber data also feature a nugget effect, the amount of this part relative to that of the core sample is found to be negligible, and thus the nugget effect from the field data was used. The nugget effect for

microbial abundance is 0.976 and for microbial activity is 1.980. For microbial abundance data the micro-scale variability (true information) is 0.068 as calculated using the tank variogram model, and for microbial activity using the same approach the value is 0.102. Subsequently, the measurement error is found by subtracting the amount of micro-scale variability from the value of the nugget effect, or 0.108 and 1.85 for microbial abundance and activity, respectively.

4.3.3 Results and Discussion

The M-Scale model, OK and CK are used as estimation models to observe the impact of excluding measurement error. Six maps of three sets are generated for each estimation model, with two maps of each set representing the results for retaining and excluding the measurement error, respectively. This is illustrated for microbial abundance estimates. The three sets of maps are respectively the estimation map (Figure 4-20), the estimation variance map (Figure 4-21), and the likelihood map for exceeding a certain threshold (Figure 4-22). The threshold was chosen based on the numbers of organisms in the ebullition experiment that were capable of generating gases. This report will illustrate the findings for microbial abundance and compares M-scale to ordinary and constrained kriging (Table 4-3).

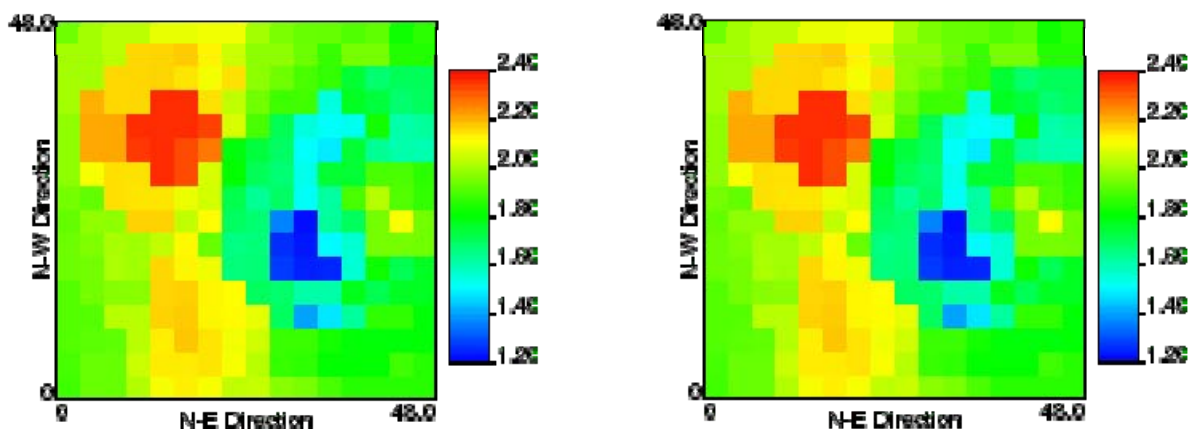


Figure 4-20. Estimation map of microbial abundance with (left), without (right) measurement error

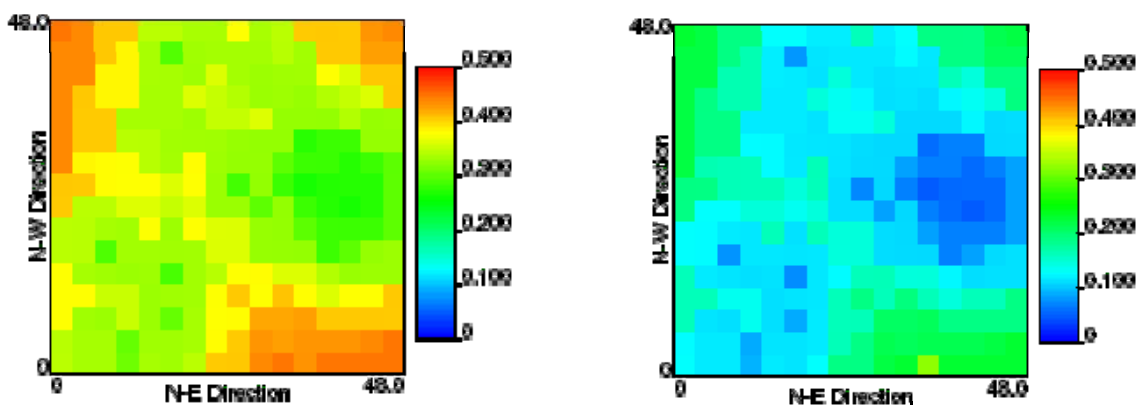


Figure 4-21. Estimation variance map with (left) and without (right) measurement error.

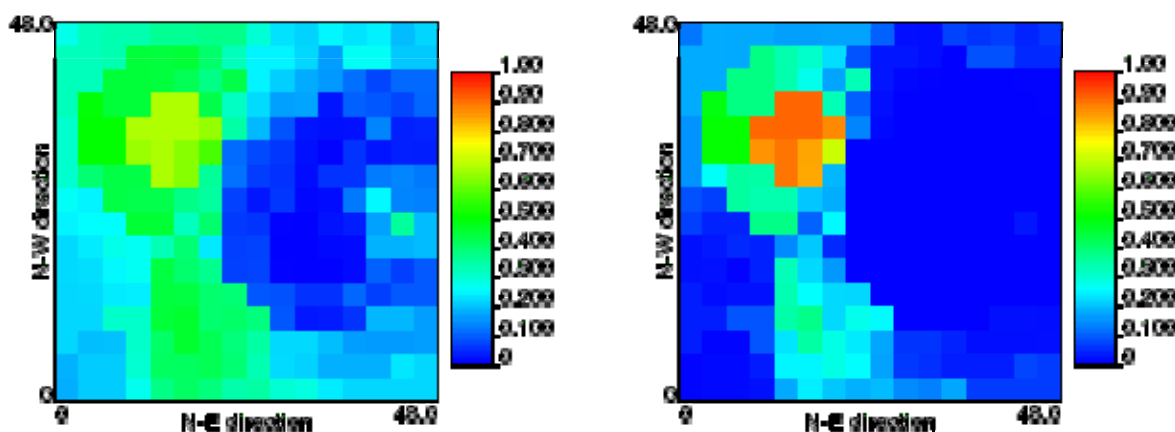


Figure 4-22. Likelihood of exceedance of 2.2×10^7 cells/g sediment with (left) and without (right) measurement error.

This result is consistent with published results on the impact of the nugget effect on estimation maps. The impact of the nugget effect on the estimation map is negligible. However, in all estimation models the estimation variance is lower when measurement error is excluded, which can be explained by the fact that the estimation variance is essentially the weighted mean of covariances between sample and estimate pairs, and variance/covariance between samples. The likelihood of exceedance of the target value visually show more contrast, with higher estimates to be more likely to exceed the threshold, and lower estimates to be less likely to exceed the threshold.

Table 4-3: Percent area of high microbial abundance (2.2×10^7) classified over the estimation domain under different confidence level of exceedance

	M-Scale		OK		CK	
% conf.	Measurement Error		Measurement Error		Measurement Error	
level	included	excluded	included	excluded	included	excluded
20	60.55	14.84	59.77	39.45	59.77	48.05
40	10.94	8.20	19.92	13.28	41.41	36.33
60	4.69	6.64	3.12	3.52	25.00	23.83
80	0.00	3.52	0.00	0.39	7.81	10.16

It is observed in Table 4-3 that to achieve a high confidence level of exceedance (high willingness of analyst to accept an incorrect decision), a larger contamination zone is delineated after nugget-effect reduction. However, a reduction of area is observed with the exclusion of measurement error for the classification of microbial abundance by CK estimation using a 60% confidence level. This could be explained by the fact that CK estimates are sensitive against the nugget effect, consequently the nugget effect impacts the ccdf evaluated by CK for the

likelihood-based classifications not only on the variance of the ccdf (reduces the size of distribution), but also on the expected value of the ccdf (shifts the position of the distribution). Because CK uses local variability of the samples to reproduce variability of the estimates, the benefit of nugget-effect reduction is not only the reduction for estimation variance, but also the adjustment of relevant impacted areas.

4.4 OVERALL SIGNIFICANCE AND IMPACT ON UNCERTAINTY

The impact of conducting measurements are variable scales (field and tank) was mainly observed by way of the fact that the tank helps to extract the true microscale variability component of the nugget effect observed for samples in the field. Hence, exclusion of measurement error by taking into account micro-scale variability based on small-scale experiments helps in an improved delineation of sediment microbial characteristics that may bear relevance on long-term applicability of capping scenarios. In this set of experiments, the M-Scale tool (and other geospatial statistical tools) was applied to microbial characteristics relevant to ebullition only. It was observed in Sections 5 and 6 that ebullition forcings were substantially less significant than advective forcings, and hence the impact of microbial parameters on the overall uncertainty of PAH flux estimates was limited.

5. IMPACT OF ADVECTION AND EBULLITION ON THE PHYSICAL STABILITY OF SEDIMENTS

The objective of this task is to experimentally derive a quantitative descriptor for sediment stability dependence on ebullition and advection under various capping conditions as an input for the integrative SFM model described in Section 7. For more complete information on the experimental procedures, data and discussion, please see:

- Cakir (2008), *Stability of Cohesive Sediments Subject To Pore Water and Gas Ebullition Fluxes and Effectiveness of Sand and Aquablok® Caps in Reducing the Resuspension Rates*, Doctoral Dissertation, The University of Michigan

5.1 EXPERIMENTAL APPROACH

5.1.1 Description of Environmental Apparatus

The stability of Anacostia River sediment and capped beds under a combination of conditions including hydrodynamic shear stresses as well as vertical pore water transport and gas flux were investigated in a recirculating flume. The flow rate is varied to create conditions below and above the critical shear stress required to initiate sediment transport. The test section is a depressed section within a false floor that is to be filled with the sediment and/or capping material. It is approximately 2.00m long, with a 0.3m wide cavity installed in a false floor in the bottom of the flume of twice the width in order to avoid wall effects (Figure 5-1). The sediment bed thickness is around 10cm. If the experiment involves Aquablok cap or sand cap on top of a sediment layer, the cap is adjusted to be around 10cm in thickness.

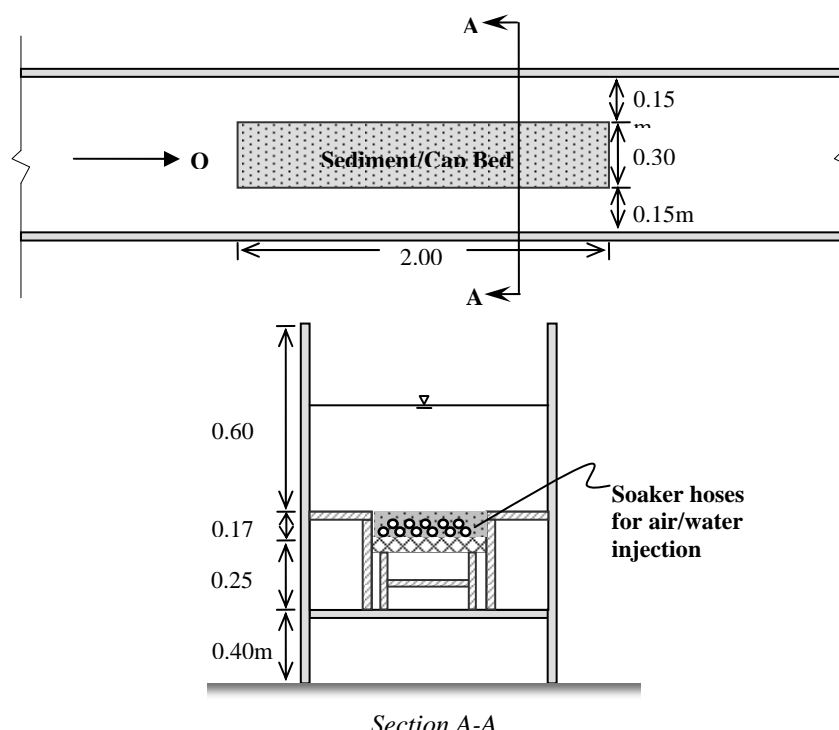


Figure 5-1. Experimental Setup plan and cross-sectional view

For the gas flux and pore water flow experiments, in order to be able provide flow distribution as uniform as possible through the bed, a set of perforated pipes (soaker hoses) is employed beneath the sediment layer (Figure 5-2). Air is used to simulate gas flux resulting from microbial activity and the rates for both air and water recharges were selected so that they are representative of values suggested from the literature. However, the lowest injection rates were adjusted to be able to see effects within the duration of a typical experiment, which was approximately six hours



Figure 5-2. Left: Soaker hoses before sediment placement. Right: Eroded sediment bed surface after an experiment

Flow rates through the soaker hoses were measured with flowmeters for water injection. A special setup was arranged to measure the air injection rates. This setup consists of two bottles connected to each other and then to the soaker hoses (Figure 5-3). An amount of water consistent with the desired air injection rate is added to the first bottle so that the air in the second bottle becomes pressurized. If, for example, 10ml/min of air injection rate is required, 100ml of water was added at every 10min. to maintain a regular injection rate. At the beginning of each experiment a predetermined amount of water was added to bring the air in the soaker hoses to a pressurized state after which additional water resulted in air bubbling through the sediment bed.



Figure 5-3. Air and water injection system

Ebullition fluxes were reported in the literature as 0.01 cm/d – 47.45 cm/d. 1-10-50 cm/d were the initial selected rates for the experiments. Smaller values were not tested since it was assumed that these would not exhibit any effect on the sediment stability. Pore water seepage rates were reported as 0.01 cm/d – 124.38 cm/d. 0.1-1-12 cm/d were the selected rates for the experiments. Adjustments to these rates were made after preliminary experimental findings were reviewed.

Sediment concentration levels in the water column are measured with the use of a turbidimeter and are used to compute re-suspension rates. This turbidimeter is connected

to the return pipeline in the recirculating flume system downstream from then recirculation pump. A flow-through cell is used to take continuous turbidity measurements. It is presumed that the flow through the recirculation pump homogenizes the flow providing for a uniform sediment concentration that is subsequently sampled by the turbidimeter. The turbidimeter is connected to a data acquisition system through which the readings are collected in terms of voltages to give the total suspended sediment concentrations from a calibration of turbidity vs. concentration that had been performed for this sediment.

Discharges are measured with a pressure transducer connected to the two sides of an orifice plate in the pipeline. An initial study was performed to relate the bed shear stress to the local turbulence characteristics and the local velocity in the flume. In order to calculate the shear stress values, surface velocities for each discharge increment were measured. An acoustic Doppler velocimeter (ADV) was installed in the flume at the downstream end of the sediment bed. The depth of the flow was set at 25 cm.

5.1.2 Experimental Procedures

Considering the possible uncertainties involved in the experimental procedures to be followed, reproducibility of the measurements was very important. Experimental procedures were improved at the early stages of the investigation by repeating the experiments several times. Once the procedures for different types of experiments were developed, each experiment was repeated at least two times to confirm the results.

Preliminary experiments were conducted to determine the shear stress levels leading to re-suspension in the flow. Based on these observations, a range of different discharge rates were chosen for the experiments creating shear stresses below and above critical shear stress values. Initially for the re-suspension experiments with only advective flow, a five-step discharge increase was taken as the experimental protocol, starting from a low shear stress level and incrementally increasing the shear stress. In most of the experiments no significant erosion was observed during the first three discharge rates. However to make sure that the effect of ebullition and/or seepage was captured in the results effectively, all the experiments were carried with this 5-step discharge scheme. At each discharge step, the flow was run for one hour. Although it may be possible that this time interval has some effect on the results, this parameter was not investigated in the experiments. one hour long discharge steps also enabled us to complete the experiments in a reasonable time frame adding up to 5 hours as the total duration of one experiment.

The bed preparation procedure was particularly important. It was observed that the homogeneity of the sample had some impact on the results. Therefore, it was necessary to mix the sample thoroughly before placing into the test cavity in the flume. In order to obtain a consistent sample density, a small sample of sediment was collected and weighed prior to each experiment. Results showed that the specific gravity of the small sediment samples was about 1.2 and among the experiments, this number varied less than one percent, minimizing the effect of density variation on the results. While it is also known from literature that consolidation degree has a significant impact on erosion rates, this phenomenon was not considered as a parameter in our experiments. For each experiment, the sediment was placed and left to settle overnight. Four separate experiments were conducted consecutively over a four-day period for each placement of the

sediment. It was determined that after about four days of experiments, the sediment was consolidating, creating a denser layer at the bottom of the cavity. This occurred even though prior to each individual experiment, the sample was remixed thoroughly in the cavity. After each four experiment set, all the bed material was removed from the container and remixed in an external tank and placed back into the test cavity. It was possible to obtain consistent test results in our experiments following this procedure

Another important aspect that attention had to be paid to was to ensure that the bed surface was flush and undisturbed as much as possible. Every bed sample had to be prepared extremely carefully. The optimal bed preparation procedure was developed after many trials and the test procedure was carefully followed for each subsequent experiment.

Description of Ebullition/Pore Water Injection Procedures. This section describes the methodology developed during the course of the investigation to allow for the production of a specified water or gas flux. Several issues had to be resolved. Initial observations indicated that vertical water or gas flow would tend to occur through well-defined channels. The methodology for the uniform application of pore water or gas flux was relatively straightforward to resolve. Initial investigation indicated that a major problem would be associated with the tendency for flow to preferentially occur along container walls, potentially impacting the experiments. The solution to this problem was to supply the fluid away from the container walls and then to allow the vertical channel flow to develop within the interior of the sediment bed. Injection was made through one of two devices; bubble bars or soaker hoses. Bubble bars are devices used to introduce small diameter bubbles into fish aquariums. These are constructed from fused sand particles. Applied air would need to acquire an initial pressure of approximately 43 cm of head (meaning that an initial air pressure of 43 cm is required in order to force air through the bubble bars) in order to be forced through the small diameter openings due to capillary pressure effects. Applied water would effectively require no pressure to be forced through the opening. The bubble bars were used in the fish tank experiments due to concern of contamination from the soaker hoses impacting the chemical measurements. Six individual bubble bars were used in each experimental setup to distribute the injected fluid broadly across the bottom of the fish tank. With air injection, it was observed in preliminary experiments that air tended to exit through a few larger pores in each bubble bar. A similar situation occurred with the soaker hoses, which were used in the flume experiments. Soaker hoses are used for low rate irrigation applications and are constructed with a large number of small diameter openings. Five individual soaker hoses with center-to-center spacing of approximately 5 cm were connected to a common source and ran the length of the test bed.

Water was applied through the bubble bars by one of two methods. In the flume experiments, the inflow was simply metered in at the desired rate. This was not possible to accomplish in the fish tank experiments where the need was to keep a fixed amount of water in the apparatus for the duration of an experiment. The procedure in this situation was to remove a daily volume of water (determined by the desired average daily flux rate) from the liquid above the top of the sediment/cap system and return that water to a bottle at a small positive head relative to the water in the fish tank so that it would leak through the sediment layer on a time approximately equal to one day. If the water did not leak through at the desired rate, the next day's addition resulted in an increased head in the supply bottle, increasing the flow rate through the sediment layer. In

this way, an approximately constant daily flux through the sediment could be maintained for the ten week duration of the experiment. It was found that the head required to maintain the desired flux increased slowly over the duration of the experiment.

Attempts to supply air at a constant rate met with more difficulties. If the air inflow was metered with a standard flow meter, an initial inflow rate would decline slowly with time due to the buildup in pressure within the sediment. Therefore, it became necessary to gradually increase the supply pressure in order to maintain a gas flow rate. Once the gas bubbles eventually formed a channel through the sediment layer and began to escape into the overlying water, the pressure required to maintain a gas flow rate dropped dramatically making it difficult to maintain a constant gas pressure.

QuickTime™ and a
decompressor
are needed to see this picture.

Figure 5-4. Schematic of apparatus to develop gas ebullition through sediments.

This situation was eventually resolved by adopting a novel methodology to ensure that a long term average gas flux was maintained through the sediment. The procedure was implemented with the idea in mind that gas release was presumed to be through a series of discrete release events. The apparatus indicated schematically in Figure 5-4 indicated how this was accomplished. Water was supplied to Bottle A at the desired rate of the gas flux although in a series of discrete additions at time intervals that depended on the particular experiment (daily for the fish tank experiments versus time intervals as short as ten minutes in the flume experiments). The water source was supplied through a trap so that air could not escape back through the water injection hose. This water addition tended to compress the air in Bottle A, increasing the pressure which was then transmitted directly to Bottle B. When the air pressure in Bottle B increased to a level required to initiate bubbling through the sediment, the bubbling event would relieve pressure in the bottles and eventually the bubbling would cease until the addition of more water increased the pressure again to a level required to initiate a new event. If Bottle A became full during the experiment, it was isolated from Bottle B and emptied and the pressure level within the bottles re-established before continuing the experiments.

It was observed that the initial bubbling event in each experiment required more pressure to cause gas release compared to subsequent experiments. Also the bubble sizes associated with the first gas release event were generally much larger than in subsequent events after the gas flow channels became more well formed. If the applied water flux was sufficiently large, gas release could become continuous and not comprised of a series of discrete events; it is not clear that this condition is representative of natural systems.

The specification for the sand cap. The sand cap to be applied to the demonstration sites in the Anacostia River called for the use of sand commonly referred to as *concrete sand*. There is a specification for the size distribution of concrete sand. A grain size analysis for the actual sand

placed in the sand cap at the Anacostia site is provided in Appendix A of the report *Cap Completion Report for Comparative Validation of Innovative Active Capping Technologies Anacostia River, Washington DC* (Horne, 2004).

For the experiments in the laboratory experiments, sand that was classified as concrete sand was purchased locally and used to create the caps in the various experiments. A sieve analysis was performed on two samples of this sand and is included in Figure 5-5. It appears to be slightly finer than the sand used in the actual Anacostia River sand cap but has a similar grain size distribution at the small grain sizes and deviates somewhat at the larger sizes. A sand cap thickness of 10 cm was implemented in all experiments. The sand was applied carefully to the surface of the sediment layer in order to minimize mixing of the sand and the sediment. A small layer of water was added above the sediment prior to the sand placement in order to minimize any compression of the sediment due to the sand placement

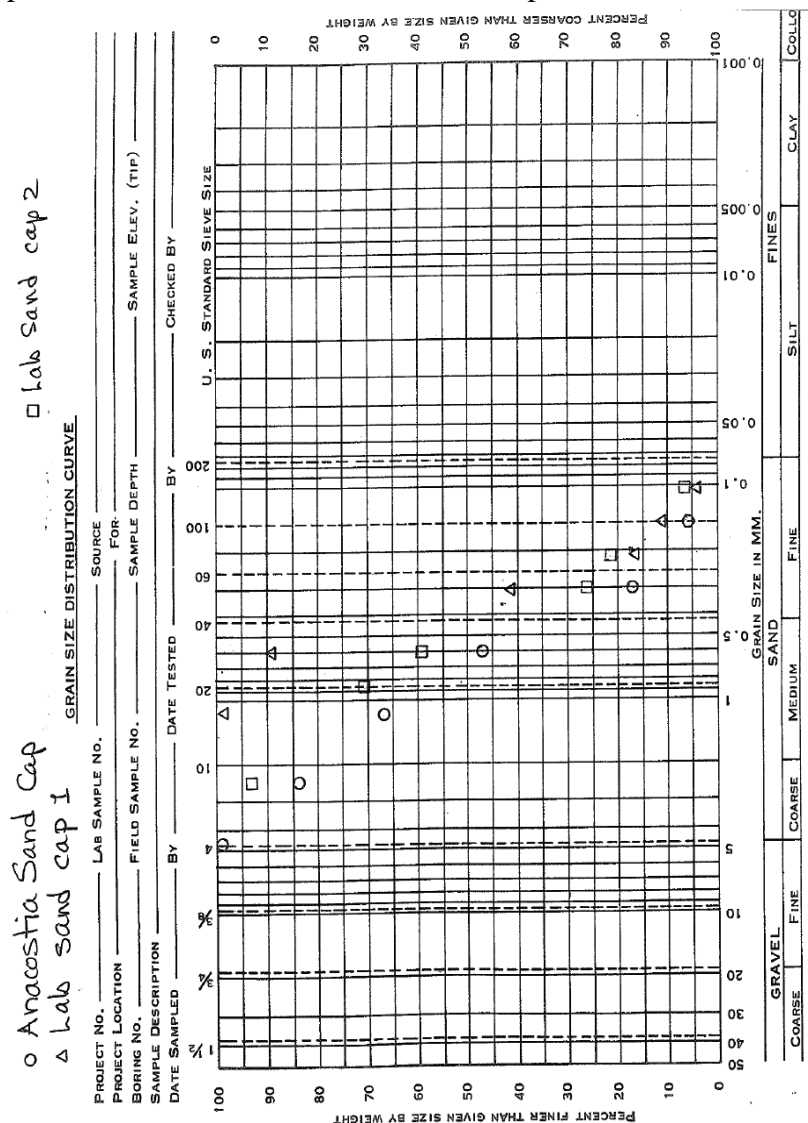


Figure 5-5. Grain size distributions for “Gudelsky sands” used in sand cap at the Anacostia River site (from App. A of the *Cap Completion Report* by Horne Engineering Services, 2000) and two samples of the sand used in the current laboratory experiments.

Grain size analyses were performed with hydrometer tests. Standard procedures were followed in the performance of these tests. Sediment samples were obtained from two of the drums to check for consistency. Results are presented in Figure 5-6. The median sedimentation diameter d_{50} is approximately 10 μm , placing the material well into the clay-size particle range.

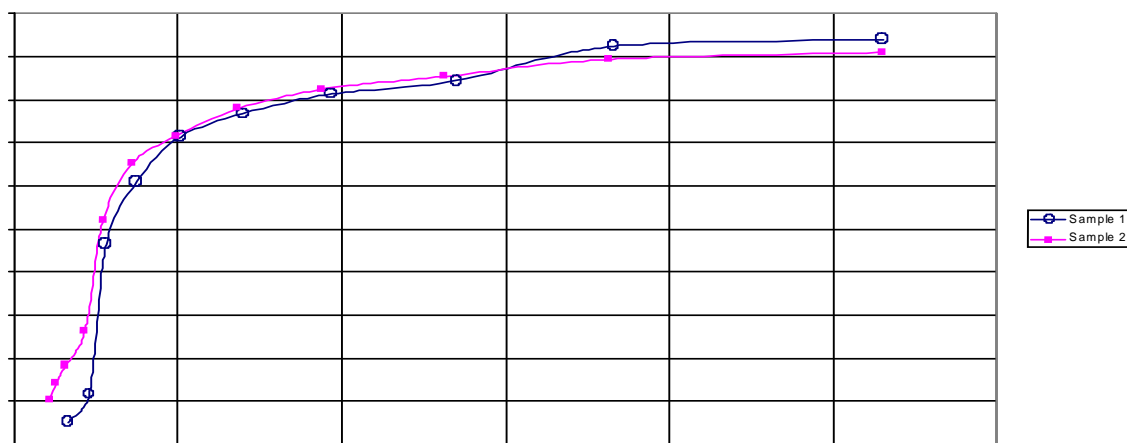


Figure 5-6. Grain size distribution determined by Hydrometer analysis of Anacostia sediments.

Atterburg limit tests were performed on representative samples of the sediment. The plastic limit for the samples tested averaged to 43.4 percent while the liquid limit was 77.7 percent. As discussed above, the sediment was mixed to achieve a desired bulk density prior to placement. The selection of the target bulk density was somewhat arbitrary but was based on a decision to achieve a desired level of sediment consistency in order to be able to place the sediment conveniently in the test setups and generally required the addition of some water to the sediment sample. The selected value of the bulk density was 1.2 gm/cm^3 .

Several attempts were made to measure the matric permeability of the sediment. Preliminary measurements were made from sediment cores collected by pushing an 8-cm diameter acrylic tube into the sediment in one of the drums. A core length on the order of 15-20 cm was obtained by this procedure. The core was then subjected to a falling head permeability test. The initial test was performed by applying the water head to the top of the core. Results of the testing as presented in Figure 5-7 indicated a permeability that decreased with time as the measurement proceeded. It is presumed that this decline in permeability could have been associated with consolidation in the sediment core due to the pressure gradient applied across it or else small leaks along the sidewalls of the cylinder being closed; the testing converged to a hydraulic conductivity of $7.8 \times 10^{-6} \text{ cm/s}$. A second experiment was performed by applying the water pressure to the bottom of the sediment core.

In this state, the water pressure gradient would oppose the tendency of the sediment to consolidate and substantially larger permeabilities were measured on the order of 2.6×10^{-4} cm/s. It is possible that leakage at the side walls of the cylinder contributed to this larger value. Finally, an attempt was made to measure the permeability of the disturbed sediment at the placement density. Given the results of the initial measurements discussed above, the measurement was performed by applying the water pressure from below to avoid the consolidation of the sediment due to the applied pressure. However, only very small water pressure heads could be applied without flow being initiated through a well-defined channel in the sediment. Once that condition developed, much larger water fluxes could be forced through the sediment without a significant increase in pressure head. Consequently, only very small pressure heads could be applied to the sediment in order to perform the permeability measurement. Consequently, it was difficult to perform accurate measurements. The estimated sediment permeability from this measurement was 4.4×10^{-6} cm/s or much closer to the initial experiment performed in a downflow mode.

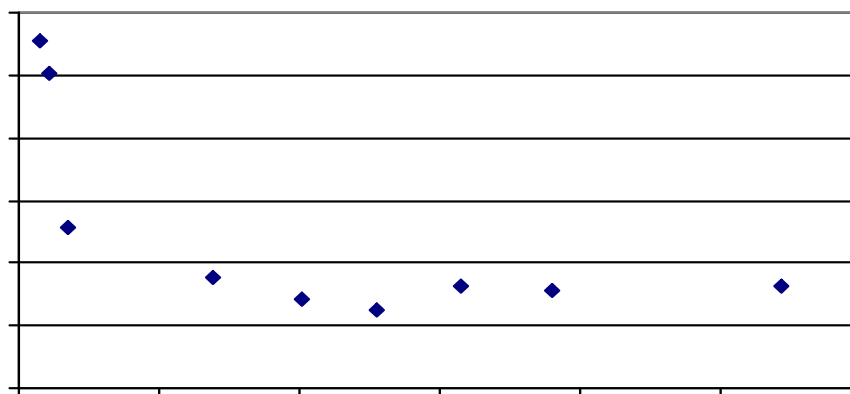


Figure 5-7. Variation in hydraulic conductivity measured for Anacostia River sediments in long duration falling head permeability test.

A prior comment from the IPR related to the fact that: “The standard practice for evaluating critical shear on field-collected sediments is to fix the field-collected core in the base of the chambers, with a controlled piston fixed at the bottom of the core pushing the material into the flume at a known/controlled rate. The description of your flume system appears to require the material to be taken out of the core, in order to then be pressed into an elongated bed.” We acknowledge that some testing on cohesive sediments in the past has involved the mentioned procedure (e.g. McNeil, et al., 1996). It is also noted that results from previous experiments also indicate considerable variability among different experimental techniques in the measured rates of sediment re-suspension and there is no consensus on the “correct” method to apply. Indeed, this ambiguity has led to attempts to measure sediment re-suspension rates in-situ (Ravens and Gschwend, 1999; Ravens, 2007) in spite of the attendant difficulties in performing that type of experiment. The results of the second paper listed above indicate considerable variability among different measurement methods.

We have attempted to understand the reasons for these conflicting conclusions and have come to some understanding of the probable causes. It now appears that one of the major issues is that it is essentially impossible to make direct measurements of bed shear stress, especially in experiments with pore water flux such that a load cell measurement is not feasible. Therefore the bed shear stress needs to be inferred by indirect measurements and the results are dependent on the specific assumptions employed in the analyses. It appears that some of the previous studies do not estimate the bed shear stresses accurately, potentially leading to incorrect conclusions. We had recognized the issue of bed shear stress determination in our earlier research and concluded that it would be necessary to develop a better procedure for determination of the bed shear stress in our own experiments. It is noted however, that we can conclusively state that we have verified what seems to be the only logical conclusion which is that a vertically upward pore water flux serves to de-stabilize the bed sediments while the opposite conclusion holds for a downward pore water flux.

5.1.3 Modeling Considerations

Measurements of bed stability subjected to vertical pore water flux. One specific issue that may impact interpretation of results is that in a straight flume, there is a region of boundary layer growth starting from the channel inlet and, dependent on the flume length and the water depth, the boundary layer will not be fully developed at the test section. In order to get around this issue, some researchers have performed studies with water depths as low as 2-3 cm. Although we recognized this issue in the design of our experiments, it did not seem realistic to conduct experiments with water depths this small and we therefore elected to perform experiments in which there is a developing boundary layer. According to standard boundary layer theory, the bed shear stress decreases with downstream distance. However, if the test section is sufficiently far downstream from the channel inlet, the variation of the bed shear stress even over the 2 m long test bed over which our experiments were performed should be sufficiently small to not significantly impact our experimental results. This is consistent with our experimental observations; if the longitudinal variation of shear stress were important, the observation of initiation of sediment transport should be confined to the upstream end of the test bed. However, the visual observations of initiation of motion indicated that the locations where sediment transport began to occur could be anywhere along the test bed and perhaps more related to minute imperfections of the bed surface.

After considerable review of our experimental results and considerations of the underlying theory, we ultimately elected to determine bed shear stresses based on measurements of Reynolds Stresses with an Acoustic Doppler Velocimeter (ADV). To state the process simply, we measure the vertical velocity profile above the center of the sediments bed. The ADV probe is capable of measuring the instantaneous velocity components in all three dimensions. From a statistical analysis of the velocity fluctuations, we can compute the Reynolds Stress term associated with the vertical/longitudinal velocity components which is proportional to the turbulent shear stress. However, there are some limitations to this technique. One of these is that the ADV probe can only measure down to about 0.5 cm above the bed so that the quantity measured cannot be the true bed shear stress. A second, related issue is that the turbulence diminishes close to the bed so that the Reynolds Stress term is only a component of the total shear stress. We chose to resolve both of these dilemmas by making a series of measurements

over a rigid boundary that we could compare to other historical turbulence measurements in a developing boundary layer and determine how to interpret the measurements to determine the bed shear stress.

We have therefore obtained a series of velocity profiles for flows with and without vertical flux through the sand bed. The results of some typical experiments are provided in Figs. 5-8 and 5-10 and demonstrate the intuitive result that when the pore water is upwards into the flow, the lower velocities near the bed are pushed further out into the flow and, similarly, when there is suction into the bed, higher velocities persist closer to the bed surface. The two sets of measurements contain velocity profiles where the free stream velocity is similar in case without suction or injection and in similar experiments with high injection or suction rates. What it means is that if one used the surface velocity or the discharge to characterize the flow, injection into the flow will actually serve to reduce the bed shear stress at a common surface velocity or discharge compared to a zero injection condition. We believe that this situation has led to confusion in the past in discussions on the influence of bed injection or suction on sediment stability.

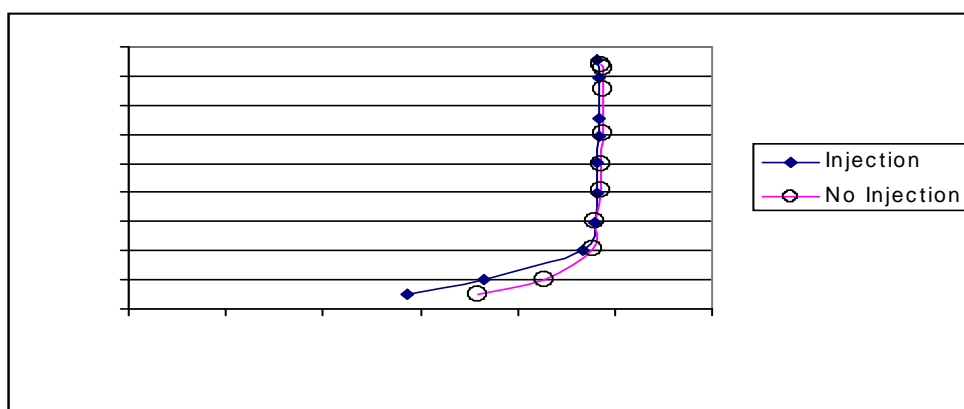


Figure 5-8. Longitudinal velocity profiles at same free stream velocity for experiments with strong injection and no injection conditions.

Since most accepted bed stability criteria are shear stress based, it is irrelevant how the velocity or discharge required to initiate sediment transport varies with injection or suction; the only thing that is important is how the shear stress varied. Thus we can observe in our experiments that a greater discharge might be required to initiate sediment motion but at the same time, a lower shear stress is experienced and therefore by shear stress-based criteria, the bed is less stable. We doubt that anyone would contest that a vertically upwards pore water flux results in an upwards piezometric pressure gradient since this is a key aspect of elementary theory of flow in porous media. Figures 5-9 and 5-11 provide partial support for this argument. In these figures, plots of the profiles of the covariance of the vertical-longitudinal velocity fluctuation correlations are presented for the same experimental conditions as in Figures 5-8 and 5-10, respectively. This covariance is proportional to the Reynolds stress, which is the turbulent shear stress (although the ADV cannot measure down to the bed level) and the results clearly show that at the same free stream velocity injection increases the local shear stress while suction decreases it. Therefore, consideration of the flow velocity required to initiate sediment motion is not a well-defined

concept is situation with strong suction or injection and it only leads to confusion in understanding of basic flow processes.

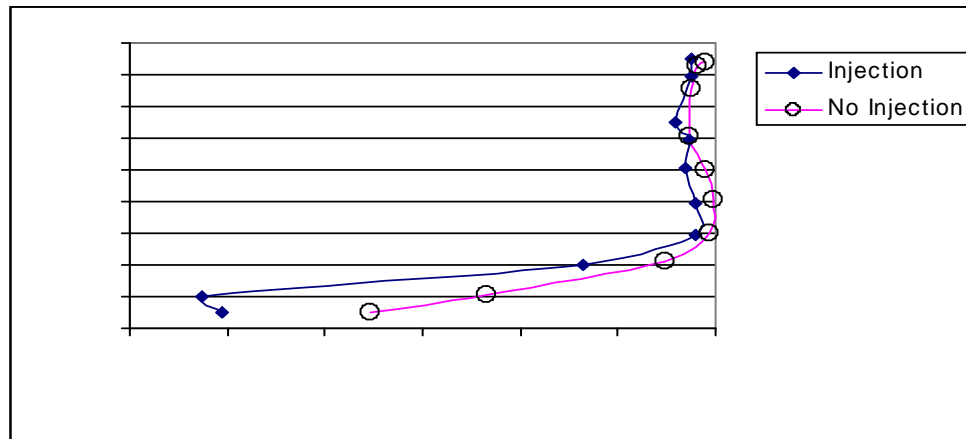


Figure 5-9. x - z velocity fluctuation covariance profiles at same free stream velocity for experiments with strong injection and no injection conditions.

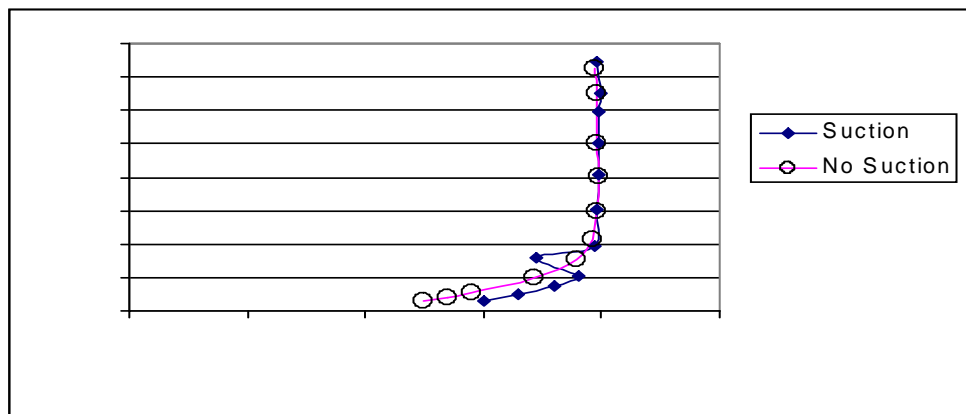


Figure 5-10. Longitudinal velocity profiles at same free stream velocity for experiments with strong suction and no suction conditions.

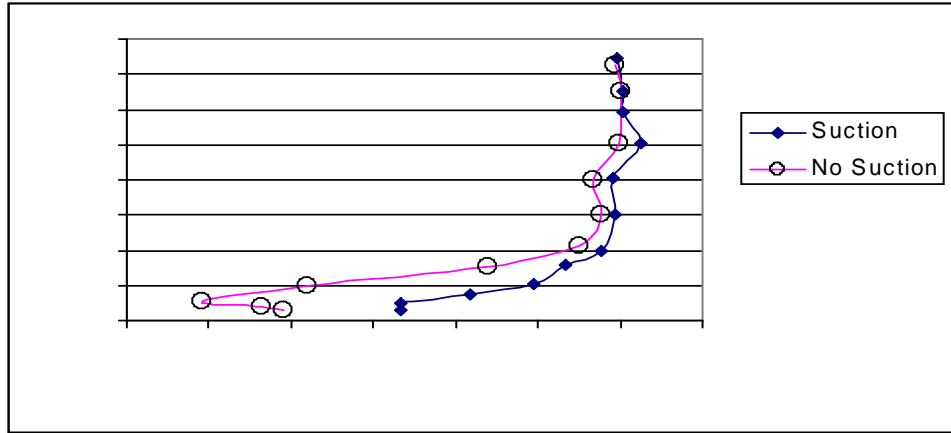


Figure 5-11. *x-z velocity fluctuation covariance profiles at same free stream velocity for experiments with strong suction and no suction conditions.*

Bed armoring processes. Bed armoring is definitely an issue that can control subsequent bed stability. The process referred to in the comments is generally considered to be what is called “static armoring” in which finer materials that are not stable to an applied shear stress are washed out of the bed, leaving behind the coarser material present in the original bed. It has been observed that there must be a significant grain size distribution in order for this effect to be observed. One traditional measure of the grain size distribution is the geometric standard deviation, s_g . Previous studies suggest that the geometric standard deviation needs to be in excess of approximately 3 in order for static armoring to be a relevant process. While we don’t discount this process in specific applications, it will not be relevant to the relatively uniform sands that we have performed investigations on to date in order to develop our theory. Based on the sand specified for the sand cap representative of the Anacostia site, it also is the case that the geometric standard deviation is less than 3 and it is therefore expected that static armoring will not be a significant issue in cap stability

Applicability of Model for Seepage Effects on Bed Stability. We have developed a scaling law to include the effect of the seepage pressure into the formulation of the dimensionless critical shear stress that is traditionally used to define the stability of noncohesive sediments, as detailed in “*Stability of Non-Cohesive Sediments under Conditions of Pore Water Flux* (Cakir and Wright, 2006). The basic premise of the development is presented in the manuscript. The so-called Shields parameters:

$$R_* = \frac{(\tau_0 / \rho)^{1/2} d_s}{\nu} \quad \tau_* = \frac{\tau_0}{(\rho_s - \rho) g d_s} \quad (5-1)$$

are used to prepare a plot (called Shields diagram) of experimental data describing the conditions for initiation of motion for non-cohesive sediments with no bed seepage. In the above expressions, τ_0 is the bed shear stress, d_s is the sediment grain diameter, ρ_s and ρ are the mass densities of the sediment and fluids, respectively, ν is the kinematic viscosity of the fluid and g is

gravity. What is presented in the paper is a rationalization of the parameter t^* by consideration of elementary forces on a single sediment particle located on the sediment surface. Then the seepage force due to flow through the sediment bed is added to the formulation to derive a modified dimensionless shear stress t_m^* . At the time the manuscript was prepared, we have not finalized the measurements for bed shear stress and simplified estimates were required for that parameter. In spite of that, the formulation was demonstrated in the manuscript to adequately account for the effects of seepage on bed stability for the two smallest sediment sizes studied. Since that time, we have formalized a procedure for determination of the bed shear stress as discussed above. This procedure has been implemented in the modified Shields diagram as presented in Figure 5-12. The three relatively uniform sands used in the study are presented on the plot as well as experiments performed with sand material with the same specifications as the sand cap at the Anacostia site. It is suspected that there is still some uncertainty in the computation of bed shear stress but the data with relatively large piezometric gradients through the sediment bed tend to collapse to the traditional relationship sediment beds with no seepage. We conclude that this approach is useful for characterizing the effects of bed seepage on sediment stability to applied shear stresses and that we can use the results of this portion of the study to assess the effect of pore water flux on sand cap stability.

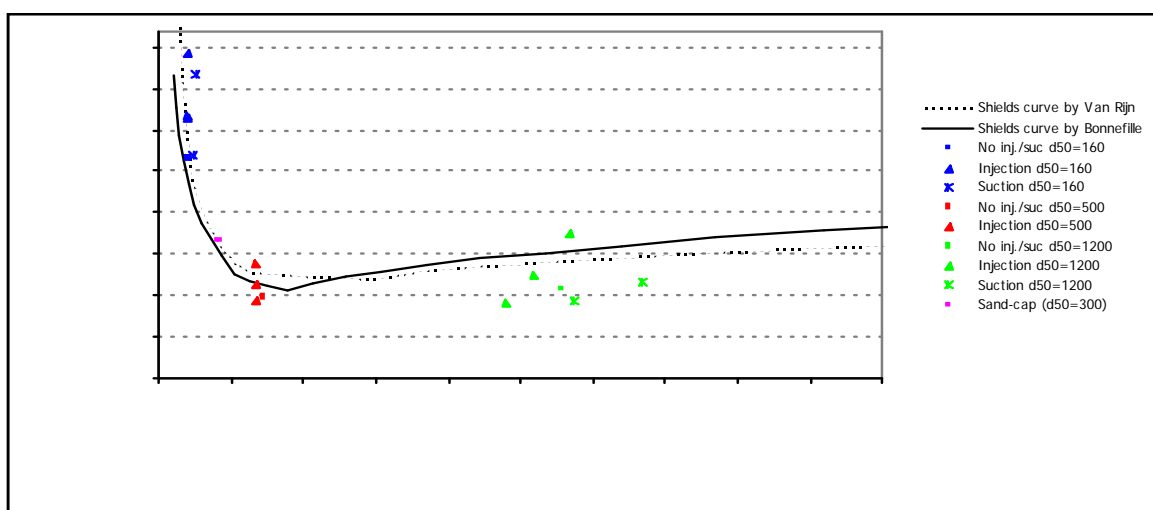


Figure 5-12. Modified Shields diagram, for the various suction/injection experiments performed.

Experiments on Cohesive Sediments. From the time that this research was initially conceived, it was understood that a likely outcome of the research would be that either pore water or gas migration through cohesive sediment beds would likely occur through isolated channels; migration rates suggested from field measurements are simply too large to be consistent with Darcy-based flow through the fine-grained sediments typical of the Anacostia site. Therefore, it was planned from the outset to conduct experiments in relatively large sediment beds in order to ensure that the evolution of the imagined flow channels would be independent of container side-wall effects that might dominate the experiment if 5-cm diameter sediment cores were studied. The “flux chamber experiments” (where we measure mass transport of contaminants into the semi-permeable membrane devices) for example, are conducted in containers that are approximately 0.45 by 0.90 meters in plan dimensions. Similarly, the flume experiments were conducted in test beds that were 0.3 by 2.0 meters in plan dimension. The large number of

experiments planned for both of these sets of experiments thus requires large volumes of sediment to perform. Towards this end, we had a total of four 55-gallon drums of Anacostia River sediment obtained for conducting these experiments. This sediment was disturbed during the collection process and it is simply not feasible to obtain and place undisturbed sediment beds at this scale.

Considerable preliminary effort was expended to understand the nature of the processes associated with gas and pore water migration through the sediments; results of these efforts have been described in previous annual reports. A key outcome was that it was possible to confirm that both gas and pore water migration is through channels that form in the cohesive sediments. A decision was required to establish a consistent procedure for sediment bed preparation for both the fish tank and the flume experiments. After some initial investigation, it was concluded that the best procedure would be to extract sediment from the drums, clean it of debris such as plastic, clam shells, sticks, etc., mix to a density to be maintained consistently among all experiments, and to allow the sediment to settle for a period of time prior to commencing the experiment. The settling time was taken as 12-24 hours. It is noted that longer settling times would result in densification of the sediment through the consolidation process. However, there were practical limits on the amount of time required in order to conduct the large number of projected experiments. In addition, if the processes of pore water flux and gas ebullition were to be studied, it is not consistent with a natural system to allow the sediment to settle for 30 or 60 days, for example, without these processes being present and then to suddenly impose the process on a partially consolidated sediment. It is noted that although the term “settling” is applied above to the resting period between the placement of the sediment and the initiation of an experiment, the sediment density was sufficiently high that a clear water layer did not form above the sediment during the settling period. However, it is acknowledged that the sediments were tested at a lower density that would be expected in-situ. Based on previous studies by others, we expect that the shear strength of the tested sediment will be less than what would have been associated with the sediment at the time it was collected. Since the primary objectives of the experiments were 1.) to example the effects of pore water and gas flow on sediment stability and 2.) to investigate the effects of various capping technologies, we believe that the procedure described above still allowed these objectives to be met.

5.2 RESULTS AND DISCUSSION

In order to get a base set of resuspension data, advective flow experiments were conducted with Anacostia River sediment. In this context, *advective flow* implies that only the re-circulating flow creating a bed shear stress without pore water or ebullition flux was examined. Average discharge rates applied to the bed during an experiment are given below in Table 5-1 together



Figure 5-13. Eroded sediment bed surface

with the corresponding shear stresses. Shear stresses were calculated using surface velocities (V_x) measured with the ADV but are correlated to the maximum value of the Reynolds stress in the vertical profile as described in a previous section of this report.

It was observed that as the shear stress applied to the sediment bed surface was increased, chunks of sediment particles were torn from the surface layer, creating stripe-like formations on the

sample surface (Figure 5-13). Only that portion of the sediment that was removed from the bed and carried in suspension in the flow was measured with the turbidimeter. This was considered to be the most relevant quantity in the consideration of contaminant mass transfer to the water column since mass transfer from sediment carried in suspension would more readily facilitate mass transfer compared to chunks of sediment sliding along the bed and potentially subsequently deposited in lower energy zones downstream from the point they were scoured. Large scale scour holes did not form in the sediment bed over the duration of the experiment at the levels of shear stress applied.

Table 5-1. Discharge, surface velocity and shear stress levels applied to the bed

Q(m³/s)	V_x(cm/s)	Bottom shear stress (N/m²)
0.028	25.264	0.1257
0.032	27.865	0.1486
0.037	31.126	0.1796
0.041	34.337	0.2125
0.047	37.865	0.2512

Sediment concentrations measured by the turbidimeter due to increased shear stress levels induced by advective flow are given below in Figure 5-14. The time versus concentration graph shows that there is not significant erosion on the bed during the first 3 hours of the experiment. During the fourth and fifth hour, resuspension is evident with increasing rates as the shear stress level is increased. The raw data exhibits short term fluctuations because of the measurement techniques and moving averages for the concentration values have been computed. Data trends are revealed much more clearly in the concentrations computed from the moving averages.

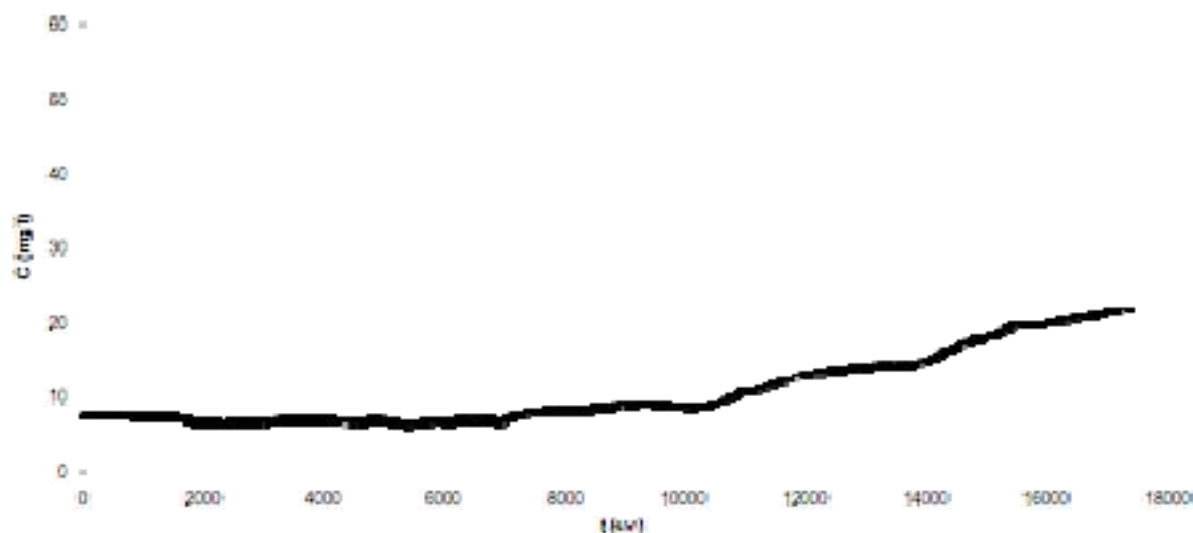


Figure 5-14. Concentration vs. time for an advective flow only experiment

The qualitative trends are consistent with the results of previous studies on sediment resuspension that have been conducted in a similar experimental framework. Since the flume water is being recirculated in the experiment, a constant slope to the concentration versus time plot would imply a constant resuspension rate. The trend observed in nearly all experiments is that the slope of the line is initially greater after the elevated shear stress is applied and then the slope gradually decreases with time (e.g. see Piedra-Cueva, I. and Mory, M. 2000 *Erosion of a Deposited Layer of Cohesive Sediment*, in Dynamics of Estuarine Muds, Thomas Telford Publishing and Ravens, T.R. 2007 *Comparison of Two Techniques to Measure Sediment Erodibility in the Fox River, Wisconsin*, Journal of Hydraulic Engineering, 133(1) 111-115.

It is assumed that this behavior may be due to the removal of the least stable areas of the sediment bed at any applied shear stress and therefore, there is a time dependence to the resuspension process. Although this finding is widely reported in the literature, there is no generally accepted process for analyzing the data and erosion rates reported in the literature are computed in a variety of different ways. Most previous studies have used shorter time intervals for measurement at a given shear stress level and that will exacerbate the difficulty of comparing to their findings. Consequently, we are trying to find the most effective way to compute resuspension rates from the measurements, but a key aspect of the final approach implemented will be to apply a consistent and well-defined approach, something that is not always clear in previous studies reported in the literature. Resuspension rates may be calculated in several different ways. At the current time, we are working with the concentrations computed from moving averages for each time interval to calculate resuspension rates. During each hour with a constant shear stress, resuspension rates can be calculated over smaller time increments, for example 5-10 minutes. In this fashion, the variation in resuspension rate over the one hour interval can be estimated. We observe a smaller variation in the rate towards the end of the one hour interval and while we are exploring the data to determine the most effective way to compare the data, it appears that resuspension rates will be taken from the later stages of the one hour time interval. This is generally consistent with other approaches implemented in previous studies, although as discussed above, there is no consistent procedure that has been implemented in previous studies, and in some cases, the data analysis procedures have been insufficiently documented to be able to determine the data analysis procedures.

5.2.1 Ebullition Forcings

Considering the ebullition experiments, the observations from the fish tank experiments and from the flume experiments are very similar regarding the physical processes associated with transport of sediment into the water column. Air migration tends to occur as a series of discrete “bubbling events” associated with a cyclical buildup of gas pressure within the sediment and a release of that pressure following bubble release. This is consistent with discussions in the previous literature as well as personal observations of gas release from natural sediments. This process is likely to be exacerbated in the tidally influenced Anacostia River as the tidal fluctuations in water level will create a cyclical variation in overlying pressure that should have a strong influence on the release of gas from the sediments. It is noted that this effect was noted studied in the laboratory experiments. As the air bubbles emerge from the sediment bed, they carry a significant amount of sediment in their wakes. The amount of sediment resuspended depends on several factors such as bubble size, bubbling frequency and time of bubbling through the experiment. Once a channel (Figure 5-15) is well-established in the sediment bed, there

appears to be a reduction in the resuspension rate. This observation is based on both visual observations as well as turbidity measurements. If a bubbling event stops at some point from a



Figure 5-15. A channel formation viewed from the bed surface

channel and restarts at a later time then the channel may find the time to heal itself. Consequently, the resuspension rates due to ebullition appear to be correlated to two time dependent processes, how long a bubbling event lasts and the time interval between successive events. It appears to be quite random where the channels form and at how many discrete points bubbling occurs at a given air discharge rate. Therefore, we observe considerable variation among repeated experiments involving gas ebullition. Our observations showed that there were multiple different bubbling locations formed over the surface of the entire sediment bed during the experiments suggesting that the results can be considered to be an aggregate of the effects averaged

over the sediment bed surface area.

The initially selected ebullition rates were 1-10-50 cm/d in terms of fluxes. Applying these rates to our sediment bed surface area, air discharge rates were calculated at 200 ml/min. Several experiments were conducted to investigate the effect of each ebullition rate. Our investigations showed that 50 ml/min was a very high rate creating continuous air bubbling and this is felt to not be representative of occurrences in natural systems. 200 ml/min ebullition experiments were eliminated from further consideration because of this reason. On the other hand, 5 ml/min injection rates may end up with a situation where no air bubbling events occurred during some one hour measurement periods. One or two bubbling events lasting 20 minutes during the whole 5 hours of a single experiment was not definitive for the purpose of determining the added effect of ebullition on resuspension rate. An additional ebullition rate of 10 ml/min was chosen to be investigated in more detail. This rate also created fairly sustained bubbling in many of the experiments, effectively limiting the ebullition rates that could be investigated with our experimental setup. The results from several ebullition experiments at different injection rates are given in Figure 5-16.

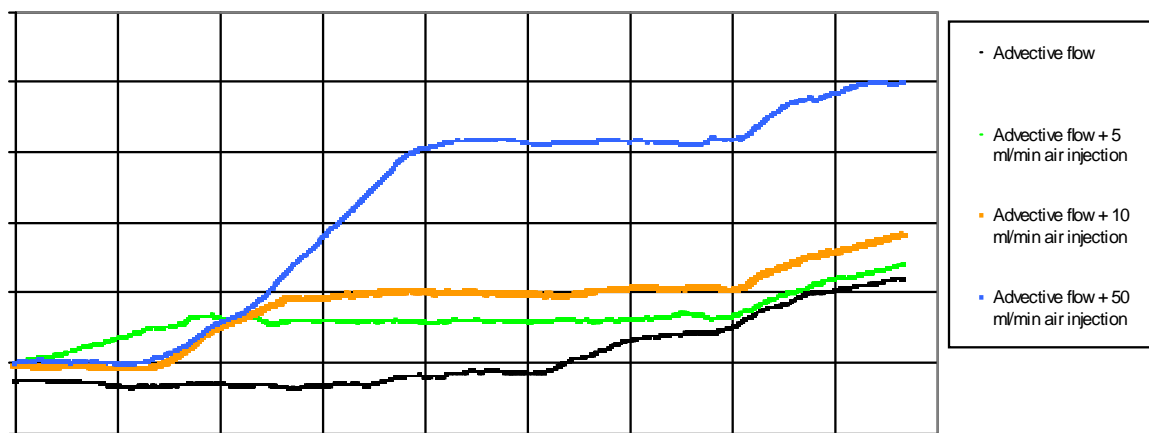


Figure 5-16. Effect of shear versus shear plus ebullition on resuspension rates

As can be seen from the data, ebullition results in higher concentration sediment resuspension compared to advective flow only experiments. This effect increases with the ebullition rate. However, the data also suggests that once bubbling channels are formed in the sediment bed, contribution of ebullition to the resuspension rates is minimal. Note that the final slopes in all experiments are nearly the same suggesting that in the last hour of the experiment, the resuspension is dominated by the effect of the applied shear stress and independent of the ebullition rate.

Additional experiments were conducted in order to observe the impact of ebullition on the resuspension rates in the presence of low shear stresses that are not anticipated to cause any erosion of the sediment surface. Figure 5-17 presents the results of these measurements. In the first experiment at a very low shear stress level without causing any erosion, a 10 ml/min ebullition rate was applied on the bed and resulted in resuspension early in the experiment. As the bubbling channels were formed, there was no additional resuspension occurring; in fact the data suggests a decrease in suspended sediment concentration, presumably due to deposition in quiescent areas within the flume. In the second experiment, the same ebullition rate was applied together with increasing shear stresses. As can be seen from Figure 5-17, increasing shear stress induced by advective flow becomes effective only at about the highest shear stress level.

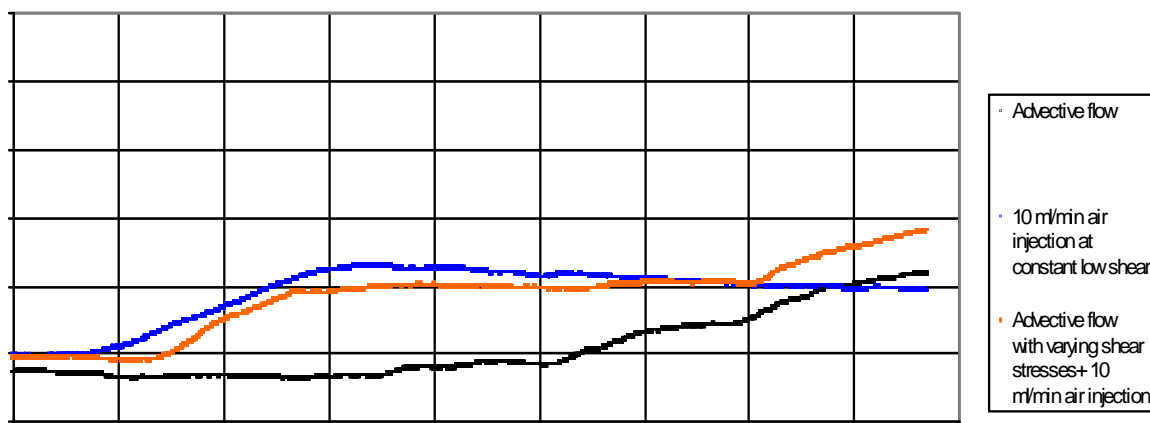


Figure 5-17. Comparison between ebullition and ebullition plus advective flow experiment

5.2.2 Advective Forcings

The selected fluxes for the seepage experiments were 0.1-1-12 cm/d. These fluxes would be converted to water injection rates as 0.5-5-50 ml /min. Examination of the results at the 5 ml/min injection rate, it was recognized that 0.5 ml/min does not exhibit a discernable effect on resuspension rates. Even 5 ml/min had a minimal effect on the suspended sediment concentrations. On the other hand, the 50 ml/min seepage rate significantly changed the resuspension rates (Figure 5-18). When the 50 ml/min injection rate was applied to the bed, there was no visible vertical flow into the water column but visual observations were hampered by the turbidity in the recirculating water. It was observed that at such high water injection rates, the density of the sediment bed was lowered during the course of the experiment reducing the overall stability of the sediment and resulting in higher resuspension. This density drop was confirmed with the measurements on sediment samples taken from the bed following completion of the experiments.

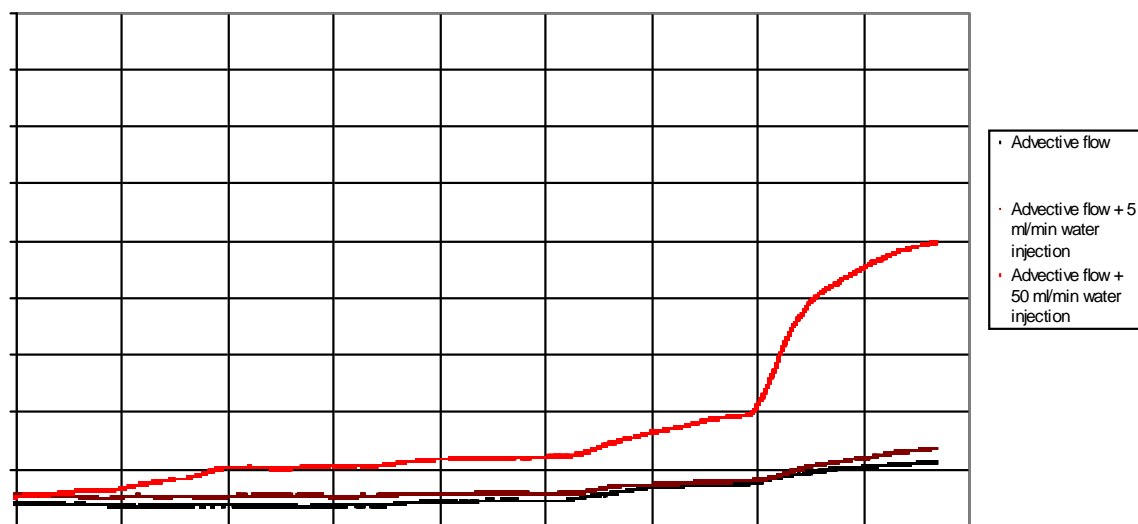


Figure 5-18. Results from 5 ml/min and 50 ml/min seepage experiments with comparison to advective flow experiment

Investigating the combined effect of shear, ebullition and seepage constitutes the last part of the Anacostia River sediment experiments. As 50 ml/min was decided to be too high and 5 ml/min as too low regarding the ebullition rates, the rest of the experiments were conducted with the 10 ml/min ebullition rate. A comparison of all the experimental results is given in Figure 5-19.

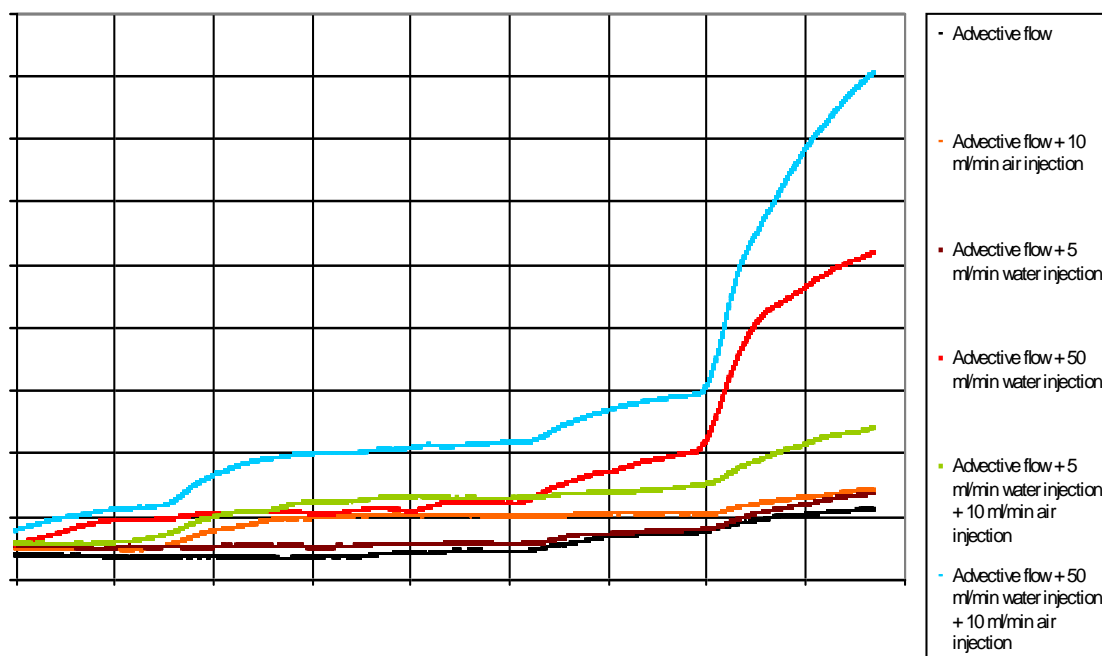


Figure 5-19. Comparison of various Anacostia River sediment experiments

It can be seen from the graphical representation that the highest concentration levels and resuspension rates were reached with the combined effect of shear, 10 ml/min ebullition and 50 ml/min seepage. Further mathematical analyses will be performed on the data to compare individual and combined effects of these parameters.

5.2.3 Aquablok™ Cap Experiments

Aquablok™ is a patented technology used to minimize the resuspension of contaminated sediments into the water flow once placed on the sediment bed. This material consists of small sized aggregates covered with bentonite which hydrates under water creating a relatively low conductivity layer (Figures 5-20 and 5-21).

The effectiveness of Aquablok™ caps to prevent the resuspension of contaminated sediments into the water flow was intended to be studied within the scope of this investigation. Nevertheless, fish tank experiments discussed in another section of this report revealed that there are limitations to what can be investigated in the flume studies. In regards to the seepage experiments, applied water injection would either leak along the side walls or accumulate



Figure 5-20. Aquablok™ granules

beneath the Aquablok™ until the cap ruptured because of very low conductivity of the Aquablok™ material when hydrated. Similarly, in the ebullition experiments, it was observed that pressure build up under the Aquablok™ cap was released only with a large rupture which would make the flow dynamics over the cap very complicated and strongly dependent on the geometry of the ruptured surface. Since the formation of the rupture is quite random in time and space, obtaining reproducible results in a laboratory experiment even with the relatively significant test bed surface area seems to be impossible and side wall effects would dominate the behavior of the experiment. In light of the experimental observations from the fish tank experiments, it was decided to investigate the stability of Aquablok™ cap considering only the effect of shear stress induced by advective flow. The cap thickness was set at 10 cm to be consistent with the fish tank experiments, but this should not have any impact on the observed results.



Figure 5-21. Left : Aquablok™ after a day of hydration, Right: Aquablok™ bed after an experiment

Other test conditions were similar to the other experiments, except that much higher shear stresses were necessary to erode the Aquablok™ surface. Our investigations showed that Aquablok™ was extremely stable without failure under even very high shear stresses. The Aquablok™ experiment was initiated with the shear stress values applied during the Anacostia River sediment experiments. There was no indication of significant destabilization of the bed for any of these shear stress levels. Therefore, shear stress values were increased further to observe the limitation to the stability of the Aquablok bed. Shear stress values are given in Table 5-2 together with discharges and surface velocities. It should be noted that not every shear stress level was applied for a entire hour to limit the total duration of the experiment. Looking at the surface of the bed after the experiment, it was observed that some bentonite was eroded from the surface and some small aggregate particles were carried downstream by bed load transport. However, the majority of the aggregate seemed to adhere to the bentonite layer underneath creating an armoring layer (Figure 5-21).

Concentration measurements in the water also confirmed the stability of the Aquablok bed. There was no change in the turbidity values until very high discharge rates were reached at around $Q = 0.076 \text{ m}^3/\text{s}$. At this point the turbulence downstream of the flume led to resuspension of some bentonite covering the aggregate material that had been previously eroded and transported downstream and deposited just upstream from the pump intake. This resuspension is due to a strong inlet vortex at the pump intake and cannot be related to the general flow conditions over the Aquablok™ surface. Concentration measurements are presented in Figure 5-22. The rise in turbidity late in the experiment is due to this resuspension of previously eroded bentonite material as opposed to a catastrophic failure of the Aquablok™ cap.

Table 5-2. Discharge, surface velocity and shear stress levels applied to the bed

Q(m³/s)	V_x(cm/s)	Bottom shear stress (N/m²)
0.028	26.494	0.1363
0.031	29.538	0.1642
0.037	32.374	0.1921
0.043	35.883	0.2291
0.048	39.515	0.2702
0.053	42.685	0.3083
0.055	45.220	0.3403
0.067	53.921	0.4599
0.076	60.454	0.5594
0.100	79.276	0.8895
0.125	108.935	1.5324
0.141	115.488	1.6935
0.142	132.324	2.1377

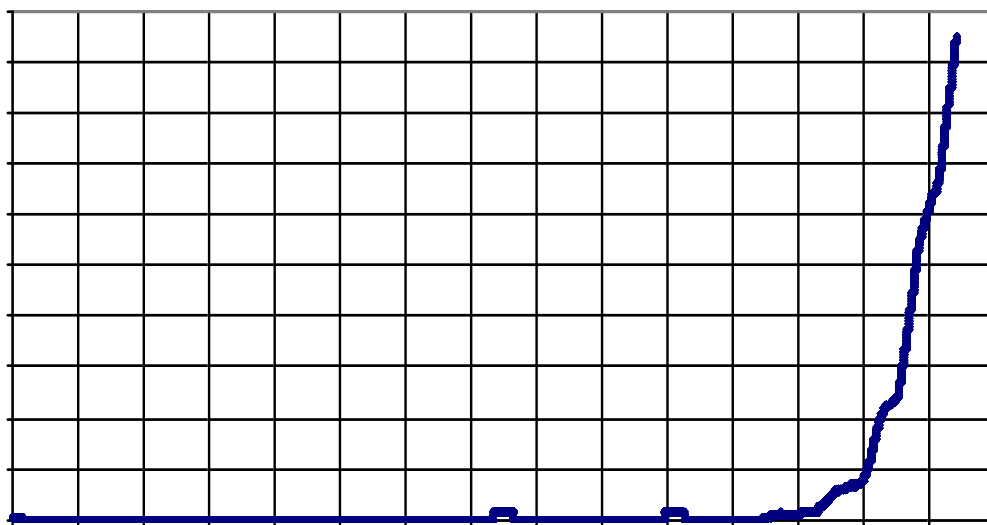


Figure 5-22. Concentration measurements for Aquablok™ cap experiment

Note on Failure of Aquablok™ caps. The Aquablok™ materials were applied in a similar fashion to the sand cap placement. A small water layer was carefully applied to the top of the sediment. Initially, individual Aquablok™ pellets were carefully dropped onto the top of the sediment and the cap layer gradually built up. Initial experiments were performed to determine the swelling of the Aquablok™ so that the final thickness of the Aquablok™ cap after full hydration would be the desired thickness, typically 10 cm.

In general, the Aquablok™ cap that was formed was basically impervious to either water or gas flow. This any attempt to force a fixed rate of gas or water through the cap would result in a rapid buildup in pressure beneath the Aquablok™. This pressure buildup would result in a subsequent buckling of the Aquablok™ until the cap ruptured and then water or gas could flow readily through the rupture.

Initial experiments were performed in a small tank six inches wide. In this experiment, the walls of the tank provided a sliding surface for the Aquablok™ and it deformed more or less as a flexible beam as indicated in Figure 5-23. When the same experiments were performed in the wider (0.45 m or three times wider) fish tanks, the failure mechanisms were more variable. In some instances, failure would occur by buckling along one side wall in a fashion similar to that noted above. In other instances, a block of Aquablok™ could be more or less uniformly heaved up until a failure occurred. In still other experiments, failure occurred away from the side walls of the tank and resembled a growing volcano until the surface raised sufficiently for air or water escape through the ruptures formed in the surface. No fundamental difference in the failure mode was observed between gas or water addition so it is felt that the differences in failures are due at least partially to random effects and the proximity to the wall where the buckling process was initiated. A series of test experiments were performed in tanks with plan dimensions of 0.45

by 0.45 m. Different thicknesses of Aquablok™ layers ranging from about 7-15 cm were produced and pressure gradually increased beneath them until failure of the cap was observed. Several photos of failed Aquablok™ layers are provided in Figures 5-24 to 5-26. Failure tended to occur at a fairly constant pressure regardless of the Aquablok™ thickness or whether air or water was used to produce the pressure. The required pressure head differential in order to initiate cap failure was consistently in the range of 25-30 cm. It is interesting to note that this failure pressure was also independent of whether the cap failure occurred along a tank wall or internally within the tank. We conclude from these findings that the performance of Aquablok™ caps will be regulated primarily by the process of cap failure and the ability for underlying gas or water to leak through the ruptures. Figures 5-27 and 5-28 show an Aquablok™ cap that has failed internally within the tank and developed rupture cracks. In this experiment, air was supplied beneath the cap and air bubbles are seen escaping through the crack and rising to the surface. In order to visualize the same occurrence when water was applied beneath the cap, red dye was added to the injected water. The red dye appeared rapidly after injection into the fish tank and showed up in discrete and well-defined locations as indicated in Figures 5-29 and 5-30.

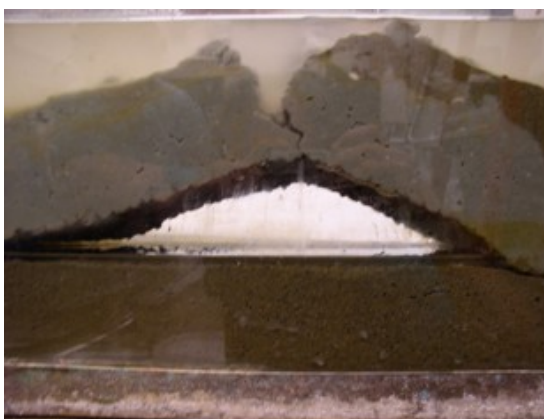


Figure 5-23. Flexural crack in Aquablok™ formed by air pressure applied beneath

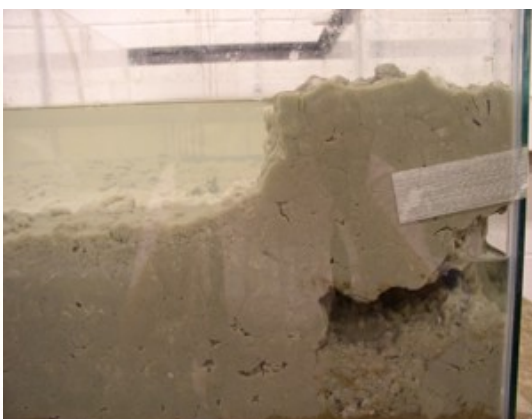


Figure 5-24. Aquablok™ failure by heaving of a block of material.

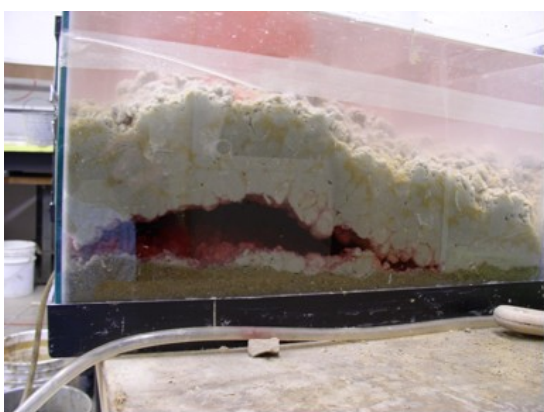


Figure 5-25 Aquablok™ failure by flexing along one side wall

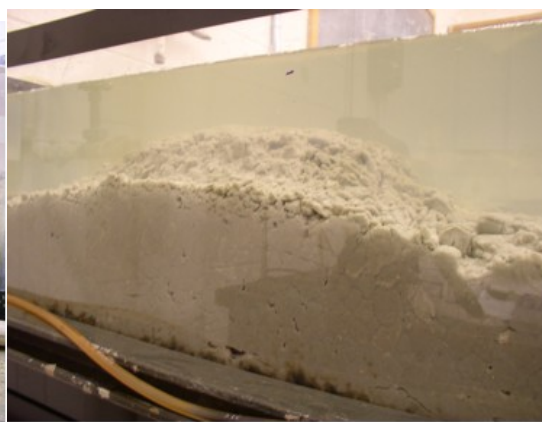


Figure 5-26. Aquablok™ failure by surface raising in middle of tank.

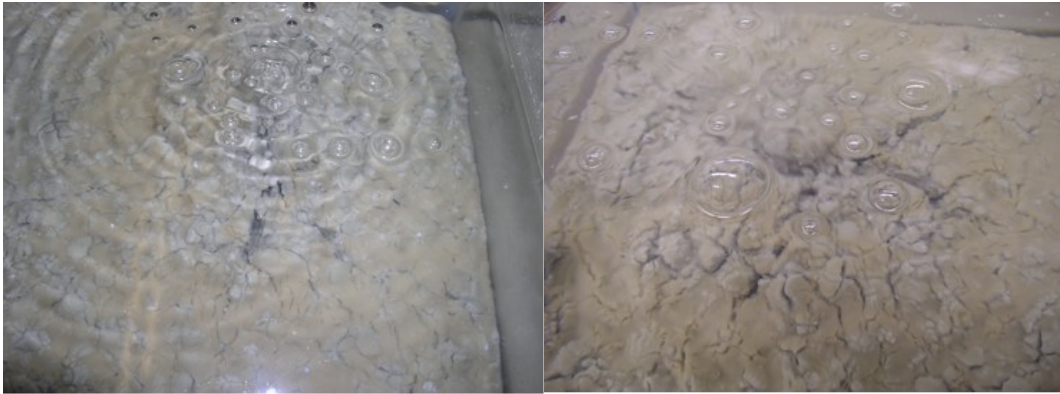


Figure 5-27. View A of Aquablok™ rupture and air escape through rupture.

Figure 5-28. View B of Aquablok™ rupture and air escape through rupture



Figure 5-29. Side view of water leakage through rupture in Aquablok™

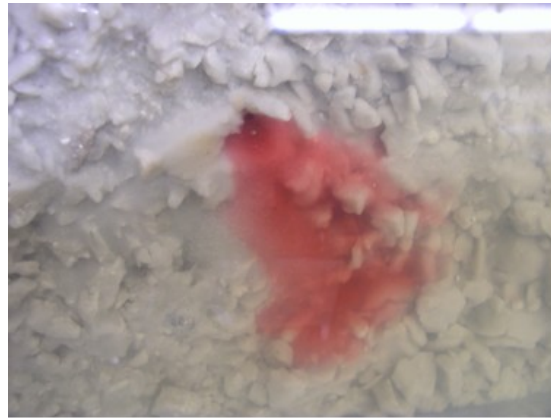


Figure 5-30. View from above of water leakage through rupture in Aquablok™

5.3 OVERALL SIGNIFICANCE AND IMPACT ON UNCERTAINTY

Investigations with regards to non-cohesive sediment bed stability were performed aiming to validate a proposed framework to modify the conventional Shields parameters to account for the effects of bed seepage on stability. This framework suggests that hydraulic gradient through the bed is a key parameter while many previous studies suggest that the velocity through the bed surface is the key parameter.

Experiments were conducted on sand beds subject to pore water flux and visual incipient motion observations were made to determine the threshold for movement. Experiments were performed with relatively high suction and injection hydraulic gradients ranging from -0.84-0.71. Even though these may not always be representative of field conditions, the framework suggests that gradients this high will clearly show the effect of seepage on bed stability and illustrate the

validity of the formulation. Since estimation of bed shear stress for the beds subject to seepage appears to be a major issue influencing the interpretation of the findings leading to contradictory results such as reported in the literature, detailed studies were performed for the determination of the critical bed shear stresses from turbulence measurements in the vicinity of the bed surface.

The bed stability was examined by evaluating the critical bed shear stress (resultant bed shear stress experienced by the individual grains at the threshold condition) in a way that all the different effects of seepage either on the flow or on the sediment bed particles were considered together. For example, injection reduces the effective weight of the individual grains while decreasing the local velocity and increasing the thickness of the boundary layer; at the same time, the Reynolds shear stress increases near a bed subject to injection relative to a condition without injection at the same free stream velocity. After including all the possible different effects of injection and suction in the data analysis framework, it was concluded by the interpretation of the findings from the sand beds studied ($d_{50}=160 \mu\text{m}$, $d_{50}=500 \mu\text{m}$ and $d_{50}=1200 \mu\text{m}$) that injection destabilizes the bed and suction does the reverse. Although a number of assumptions were made for the determination of the bed shear stress used in the determination of the modified dimensionless shear stress and the grain Reynolds number used in the modified Shields curve, the data agree fairly well with the modified Shields curve.

Computation of the modified Shields parameters eliminates much of the scatter in the data but even more importantly, the data for individual grain sizes tend to follow the general trends of the Shields curve much better than the un-modified data especially for the 160 and 1200 μm . Furthermore, a methodology has been developed to start with data or predictions that would be commonly available (e.g. from models of sediment beds without seepage) and extend that information to apply for application with higher rates of suction or injection.

The results of advective flow experiments performed on the Anacostia River sediment showed a critical shear stress value of approximately 0.19 N/m² which is larger than the critical shear stress determined for the smallest non-cohesive grain size bed ($d_{50}=160 \mu\text{m}$) indicating that cohesiveness of the sediment plays an important role in bed stability. Dependence of resuspension rates to the excess shear stress was determined to follow a quadratic relationship. With regards to the pore water and ebullition experiments, we used ranges of fluxes that between 1.2 cm/d and 12 cm/d. Data analysis for advection experiments did not show any apparent change in critical shear stresses and a similar quadratic relationship was found to be valid for the results of both 1.2 cm/d and 12 cm/d pore water experiments. A linear relationship was obtained, relating the erosion rate constant, M to the pore water flux, I . Although ebullition events increased the resuspension rates significantly, it was also observed that once a bubbling channel in the sediment was established, the contribution of the ebullition events to the resuspension rates was negligible.

6. IMPACT OF ADVECTION AND EBULLITION ON THE CHEMICAL STABILITY OF PAH IN SEDIMENTS

The overall objective of this subtask is to assess the degree to which ebullition and advection affect the elimination of PAH from sediments, and the extent to which different capping strategies influence the PAH fluxes.

6.1 EXPERIMENTAL APPROACH

6.1.1 Description of Experimental Apparatus

The test bed consists of a tank (Figure 6-1), outfitted with a diffusion chamber for gas and water amendments on the bottom, a dedicated recirculating pump to mix the water column in each of the capped systems (uncapped, sand cap, Aquablok™ cap). The ebullition simulation method is based on controlled air displacement by water (420 ml/d) to achieve an air flux on the low end of reported values for the natural system; the advective flow simulation method is based on communicating vessels whereby a fixed volume of water (1,200 ml/day) is pushed through the diffusion bars at the bottom of the tank. The advective fluxes were similar to those observed in the Anacostia River as reported in Horne (2006).

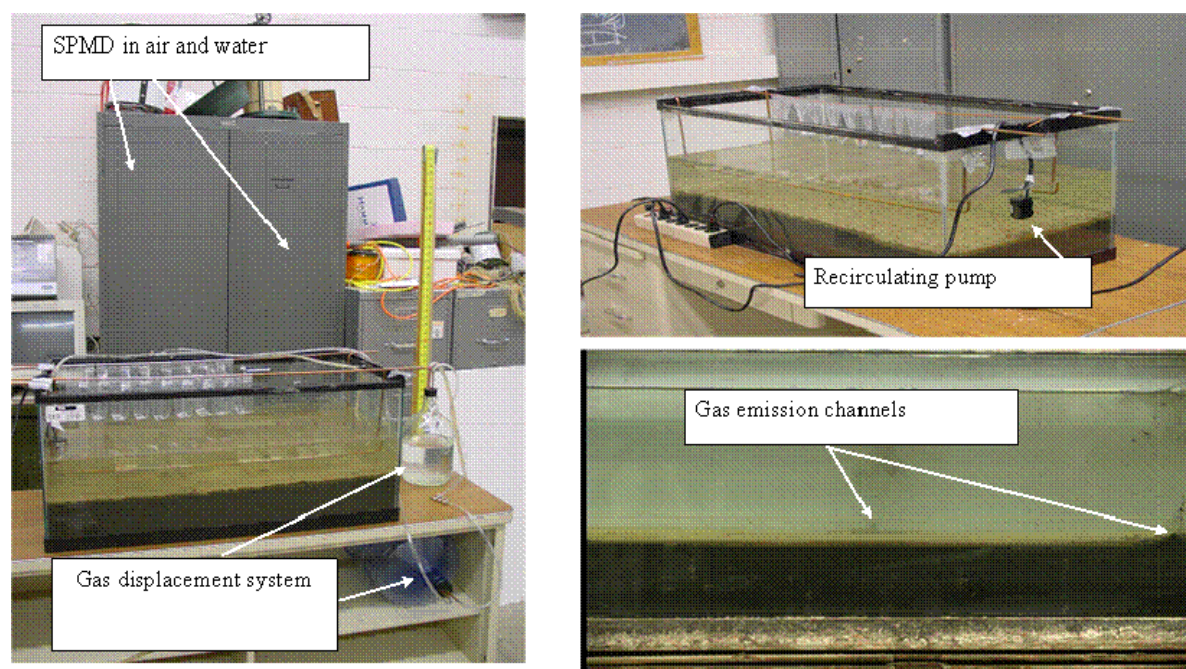


Figure 6-1. Laboratory set up of flux chambers for measurement of PAH fluxes from sediments

Semi-permeable membrane devices (SPMD) were deployed to capture the spatial heterogeneity in PAH fluxes at the sediment bed/surface water interface (but not in contact with the sediment), and in air (above the water column and below the cover of the flux chamber). SPMD were chosen for their effective entrainment of PAH and other hydrophobic chemicals in the triolein matrix. Sufficient SPMDs were deployed for triplicate measurements in air and water spanning

a ten-week timeframe, to capture the onset and saturation (if any) of PAH release in the system. Triplicate SPMD were sacrificed after 0, 2, 3, 4, 8, and 10 weeks, extracted with hexane, concentrated and analyzed using GC-MS (see method described below). Based on the SPMD literature, at least 4 weeks (28 days) are required for the system to reach equilibrium within the context of a natural environment. Considering the external forcings applied to the enclosed system used here, the objective was to evaluate the relative trends as a function of capping scenario and advection/ebullition rates applied.

6.1.2 Experimental Conditions and Preliminary Analysis

We developed an approach to use SPMDs as a measure of PAH accumulation from sediments. SPMDs (filled with 4.4-4.6 g of treolein) spiked with C¹³-labeled phenanthrene, anthracene, fluoranthene and pyrene were purchased from Environmental Sampling Technologies, Inc. The SPMDs were prepared, dialyzed, and then concentrated to 1 ml in hexane. The SPMD concentrated dialysate was then analyzed by gas chromatography/mass spectroscopy (GC/MS) for each of the polycyclic aromatic hydrocarbons (PAHs).

Preparation: The SPMDs were cleaned and prepared for dialysis following the standard operating procedure provided by the SPMD manufacturer (SOP E-14). After cleaning and preparation the SPMDs were dialyzed according to SOP E-15. This procedure calls for an initial dialysis time of 24 hours and a second dialysis for 8 hours. Because of timing issues the initial and second dialysis ran for 24 each, for a total of 48 dialysis time. The dialysate was very clean and was not filtered prior to the concentration step (SOP E-21). Standards and method blanks were also placed in the same containers as the SPMD samples, and they were brought to the same volume as the other SPMDs ~350 mls. The manufacturer recommends following SOP E-44 for concentrating the dialysate. This is a concentrating procedure using a Kuderna-Danish concentrator. Instead, a Zymark turbovap concentrator was used for this experiment. The turbovap heats the dialysate to 55C while simultaneously blowing nitrogen gas over the sample. The nitrogen was set to 12 psi on the turbovap. Standards and method blanks were also concentrated to 1 ml hexane in the same manner.

Problems were encountered with water accumulating (0.5-1 ml) during concentrating step in some of the samples. It is unclear how the water got into the dialysate. The water could have been from the clean up of SPMDs (SOP E-14), or it may have come from the turbovap during the concentration step. The turbovap uses a water bath to heat the samples. The samples that had water were brought to volume with isopropanol, or with hexane (in this case, the solvent fraction was separated from the water phase). The mass spectrometer results showed a much lower PAH response for the samples brought to volume with isopropanol. The low GC/MS response is probably do to the loss of PAHs in the sample, because of the low solubility of the PAHs in a water/isopropanol mix.

Mass Spectrometer Analysis: The resulting samples were analyzed on a Hewlet Packard 5890 GC/5972 MSD using HPs mass spectrometer software for system control, and data collection and processing. Samples were injected at a volume of 2 µl using the HP 7673 autoinjector. The column used in the analysis was a J&W DB-5, 60 meters x 0.25 mm, with a 1 µm film thickness. The mass spectrometer was operated in the single ion monitoring mode. The ions (m/z) that were selected include; 178, 188, 202, and 212. The concentrations of each PAH in the dialysate

were calculated based on both external and internal standardization. This procedure is illustrated for phenanthrene in Figure 6-2: A. the concentration of PAH vs. time, B. the concentration of C-13 labeled PAH vs. time, and C. concentration of PAH normalized to internal standard (C-13) vs. time.

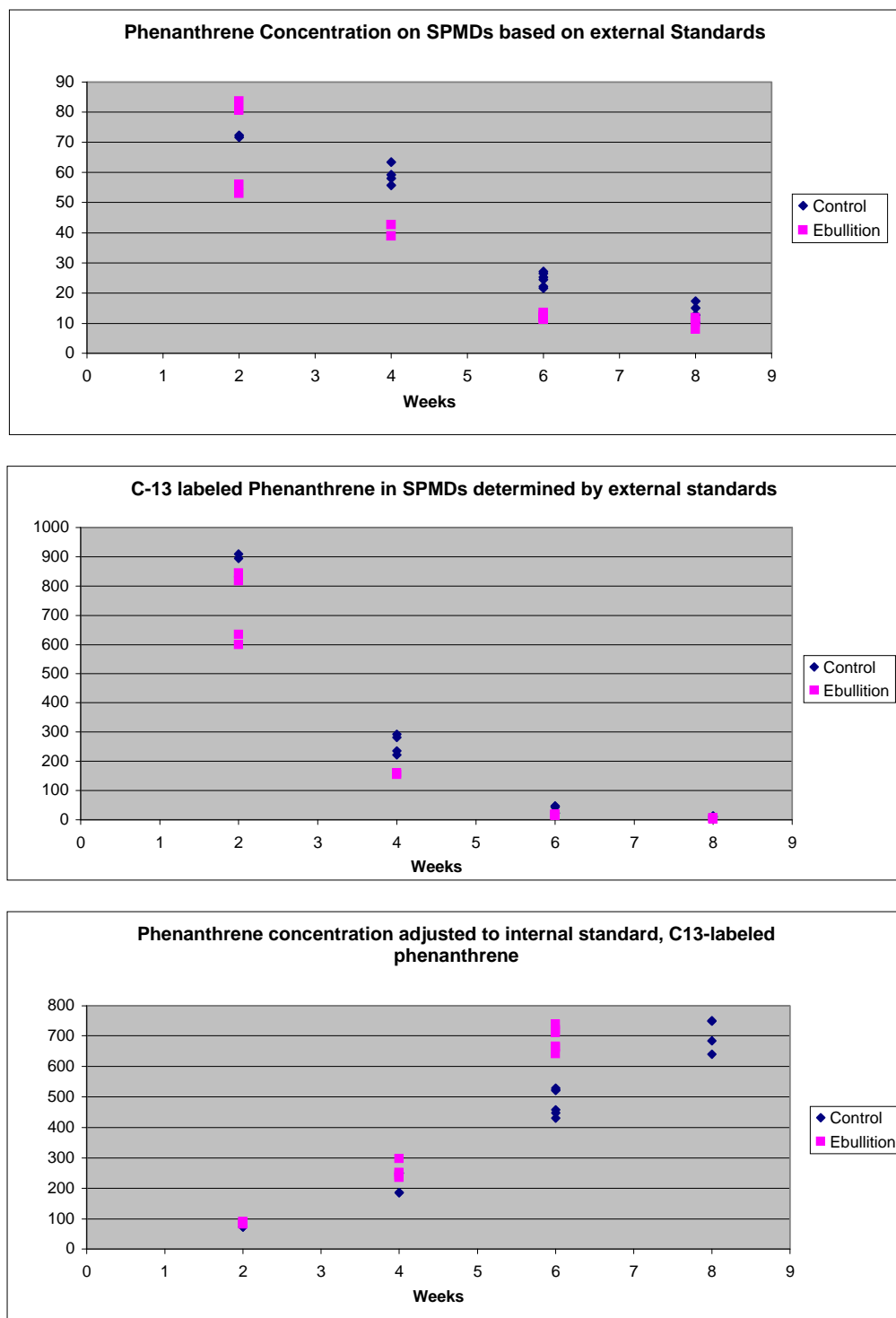


Figure 6-2. External and internal calibration of phenanthrene concentrations in flux chambers exposed to simulated ebullition

It should be noted that when we started this work, we did not have C-13 labeled SPMD, and the calculations for all those plots (mainly advection-driven fluxes and control systems) were based on external standard calibrations only. From Figure 6-2, it can be noted that internal calibration has a major impact on the concentrations in the SPMD due to 'leakage' of the PAH out of the treolein during the 6-10 week incubation period. Where possible, we applied the internal calibration of the control and advection samples to adjust these concentrations.

6.2 RESULTS AND DISCUSSION

The work focused on applying the SPMDs to uncapped and capped sediments in the presence of simulated ebullition and advection. The following data will be presented: (i) PAH Emissions under control conditions; (ii) PAH Emissions in the presence of ebullition; (iii) PAH Emissions in the presence of advection; (iv) Estimated PAH fluxes under all conditions.

6.2.1 SPMD-PAH Concentrations under Control Conditions

The SPMD test conditions included a set of control flux chambers, to allow for computation of PAH emissions from sediments in the absence of ebullition and advection, and in the absence of a cap. Unfortunately, these SPMDs did not have internal calibration standards, and were corrected for calibration curves developed later. The only sediment disturbance and potential driving force in these systems was the recirculating surface water column, and thus the fluxes are mainly diffusion driven. As in all systems, SPMD were deployed in the overlaying water (Figure 6-3, A), as well as in the air directly above the flux chamber (Figure 6-3, B).

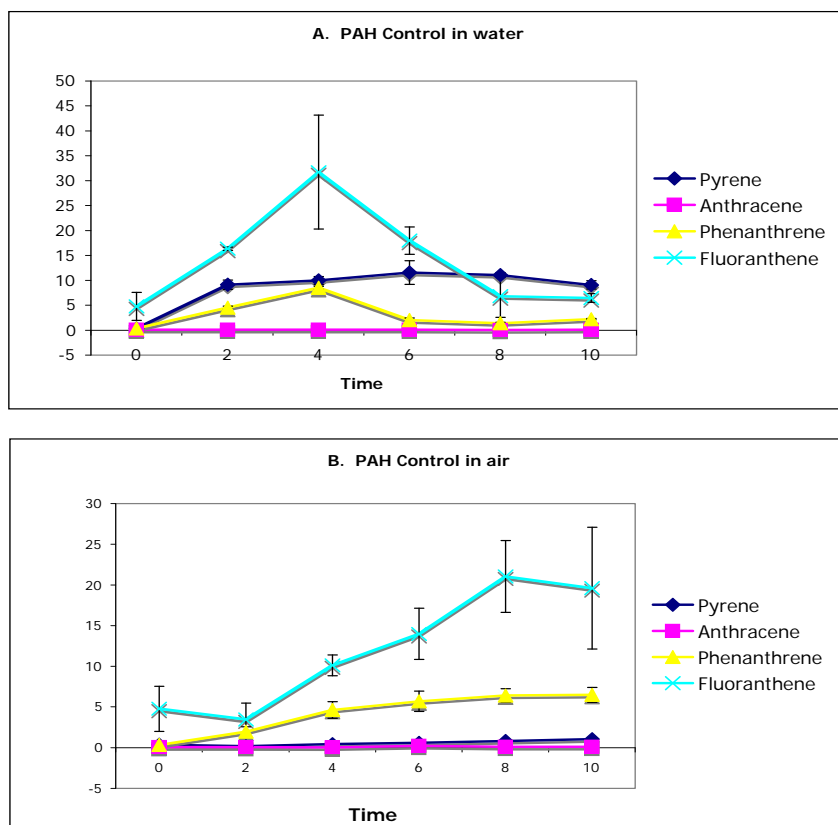


Figure 6-3. PAH emissions under control conditions in water (A) and air (B).

The results indicate that even under control conditions PAH emissions from the sediments can be observed, but the total cumulative concentration of any individual PAH does not exceed 25 ppb. Fluoranthene is the most prevalent and rapidly accumulating compound, and anthracene is consistently the least prevalent PAH extracted from the SPMD. The trends in water and air are similar for the various PAH compounds measured. Pyrene, the most soluble compound, is surprisingly not the most accumulative PAH. This can possibly be explained by incomplete removal of the sediment fines from the SPMD, despite multiple washings. Hence, the trends do not necessarily reflect solubility trends but represent a combination of PAH attached to sediment fines, and those solubilized in water. Based on a total sediment flux chamber area of 0.4 m^2 , the total fluxes (extrapolated from the 10-week accumulation concentration) range from $0.7 \text{ } \mu\text{g}/\text{m}^2\cdot\text{year}$ for anthracene to $83 \text{ } \mu\text{g}/\text{m}^2\cdot\text{year}$ for pyrene.

6.2.2 PAH Fluxes in the Presence of Ebullition

The SPMD accumulation of PAH in the water phase is exemplified for all compounds in uncapped sediments in Figure 6-4 (top). The results indicate the following trends: 1. The cumulative concentration is one order of magnitude higher than in the control sediments; 2. Fluoranthene exhibits the highest rates, followed by phenanthrene, pyrene and anthracene; 3. The emissions appear to increase linearly after week 2, with no sign of SPMD saturation after 6 weeks.

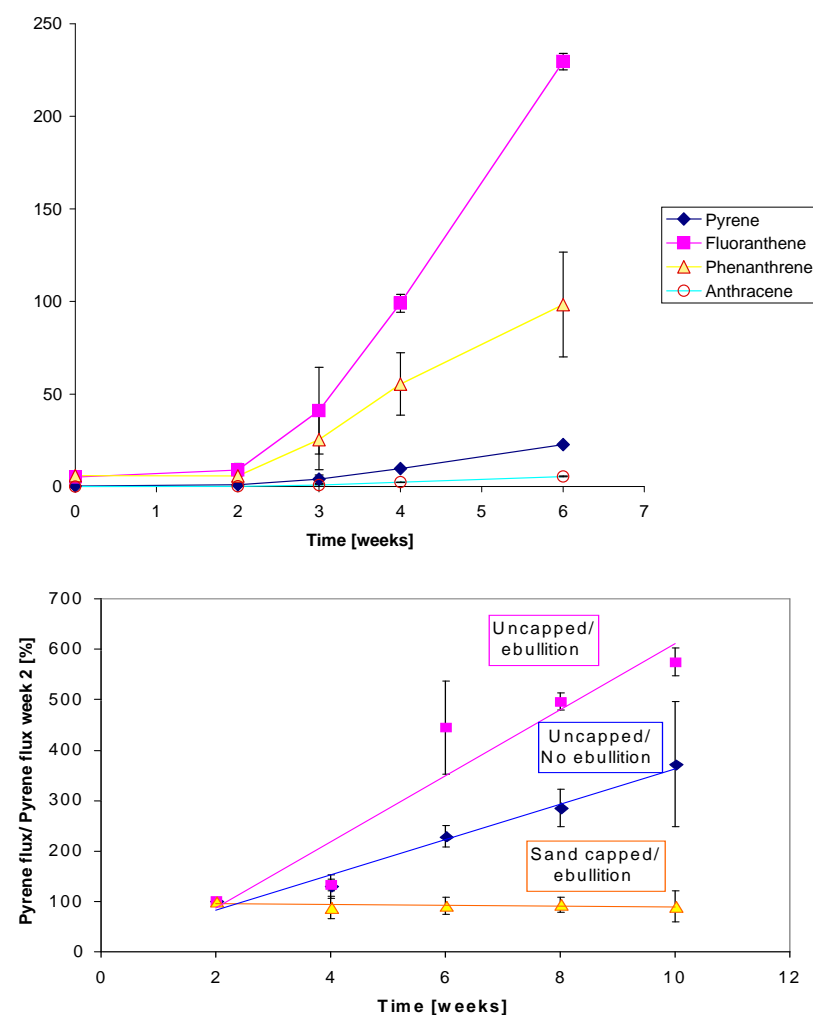


Figure 6-4. Partitioning behavior of PAH in uncapped sediments (top), and for pyrene from Anacostia River sediments into under three conditions (bottom).

uncapped sediments in Figure 6-4 (top). The results indicate the following trends: 1. The cumulative concentration is one order of magnitude higher than in the control sediments; 2. Fluoranthene exhibits the highest rates, followed by phenanthrene, pyrene and anthracene; 3. The emissions appear to increase linearly after week 2, with no sign of SPMD saturation after 6 weeks. Taking into account the total surface area in the flux chamber (0.4 m^2), the calculated fluxes (in $\mu\text{g}/\text{m}^2\cdot\text{year}$) range from 50 (anthracene) to 2,000 (phenanthrene), or two orders of magnitude higher than control systems.

The impact of capping strategy and ebullition on PAH fluxes is illustrated for pyrene in Figure 6-4 (bottom) in uncapped sediments (with and without ebullition) and sand-capped sediments with ebullition. The actual SPMD concentrations ranged from 80 ppb in

uncapped control sediments, to 140 ppb in uncapped sediments with ebullition, to nondetect in sand-capped systems. As expected, the rate of accumulation increases when ebullition is present, and is reduced in the presence of a sand cap. The values on the Y-axis indicate the percent accumulation relative to time 2 weeks, at which time the first data point was collected. The data suggest that the sand cap is protective over a 10-week time frame in the presence of ebullition rates similar to those observed at a number of field sites. Similar results were obtained for other PAH.

In the presence of a clay (Aquablok™) cap, the situation is different (Figure 6-5). As indicated in Section 5 (physical stability of sediments), the clay caps are subject to catastrophic events (particularly in confined systems such as the flux chambers), resulting in a breach of the protective layer (see also Figure 5-25 to 5-30). During the first two weeks, the concentrations of the measured PAH increased dramatically, after which they decreased (phenanthrene) or stabilized (pyrene, fluoranthene) for the next 6 weeks. Anthracene was not observed in the SPMD collected from these systems. Hence, it shows that once the system reaches equilibrium following breaching, no further accumulation occurs.

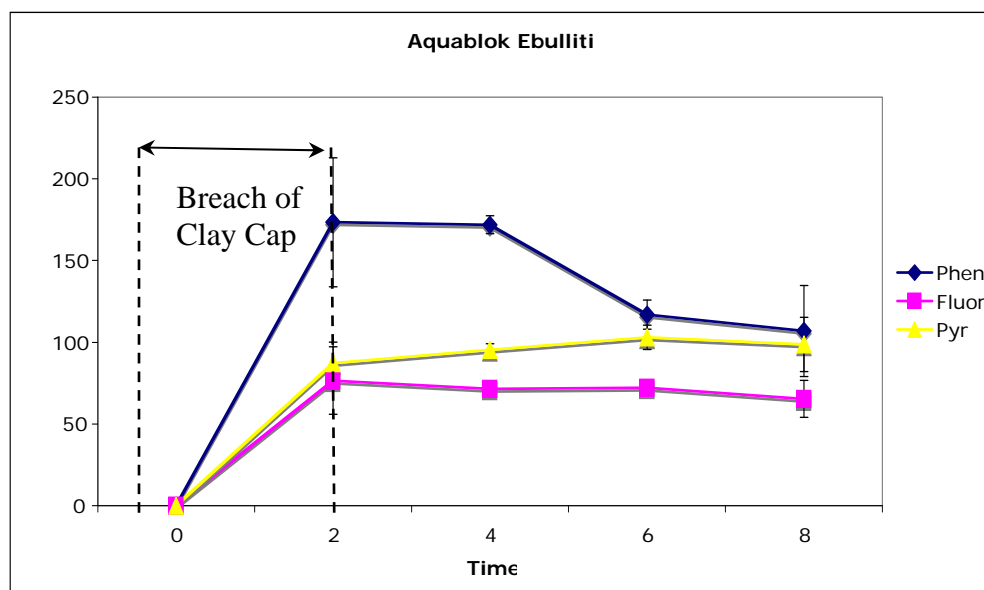


Figure 6-5. Concentration profile of PAH in SPMD over Aquablok-capped Anacostia sediments.

Since our early work on SPMDs (particularly controls and ebullition systems shown in figures 6-3 to 6-5) did not have internal standards, and needed to be adjusted using calibration curves established later, it was decided to repeat a subset of the flux chamber experiments. The objective was to compare ebullition- and advection-driven fluxes against control systems. The concentrations of PAH in water-deployed SPMD were translated into estimated PAH fluxes from the sediment, by first converting concentration to mass, and dividing it by the surface area in the tank.

All ebullition-driven fluxes are plotted against control fluxes, and are exemplified for uncapped sediments in Figure 6-6. It can be observed from these experiments and plots that ebullition does

not significantly increase the PAH fluxes from sediments, even at ebullition rates that were on the high end of those reported in the literature. As indicated in the discussion on the impact of ebullition on the physical stability of sediments (Section 5), ebullition results in the formation of preferential paths that consist of a limited surface area of the total tank. Ebullition is composed of discrete events, and did not appear to have a measurable impact on the shear stress of the sediment bed. It is therefore not surprising that ebullition did not significantly impact the PAH flux over and above the control fluxes driven by diffusion only.

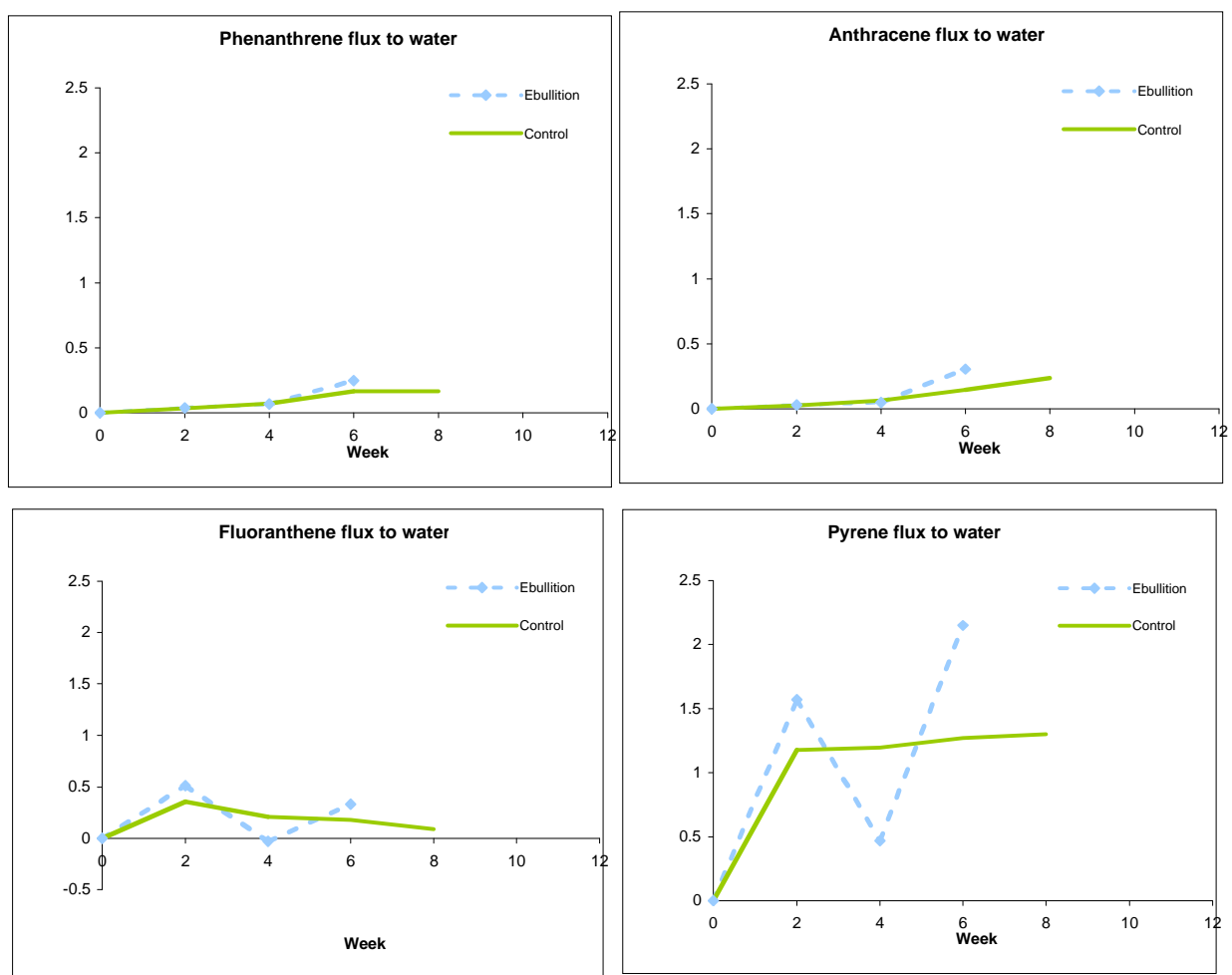


Figure 6-6. Comparison of ebullition-driven fluxes from sediments to the water column with control systems (in mg/m².yr).

6.2.3 PAH Fluxes in the Presence of Advection

Separate systems were developed to test the impact of advection on SPMD concentrations; these values are shown in Figure 6-7. The imposed advection rates were similar to those observed using seepage meters in the Anacostia River. It is clear from the results presented in these figures that in the absence of caps (and after breaching of the Aquablok cap), the cumulative concentrations are one order of magnitude higher (> 3,000 ppb) than in the ebullition-driven systems (< 200 ppb).

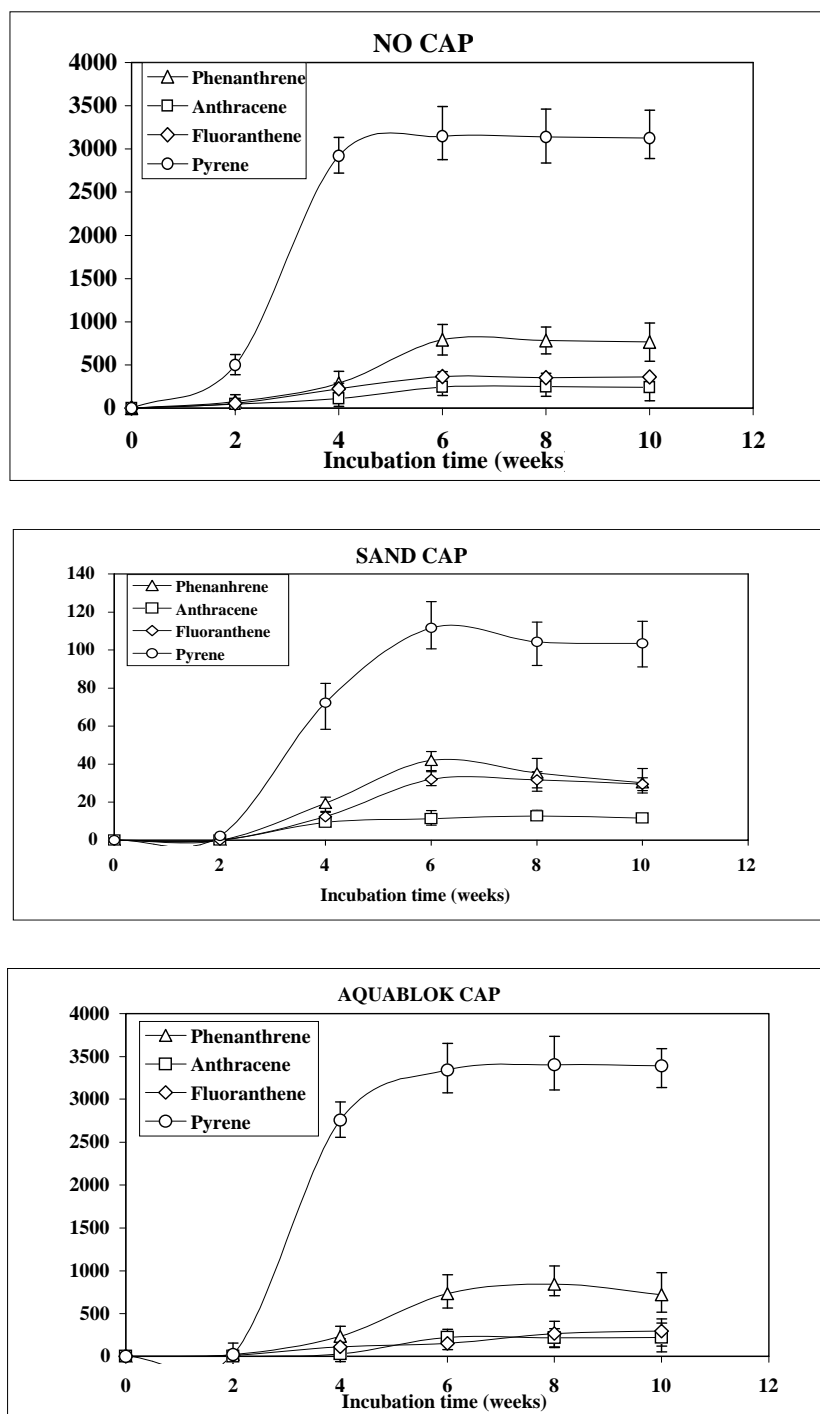


Figure 6-7. SPMD results under conditions of advective flow in the absence of a cap (top), and in the presence of a sand (middle) or Aquablok™ (bottom) cap

In the presence of a sand cap, the cumulative concentrations after 10 weeks are similar to those observed in the presence of ebullition-driven concentrations in uncapped sediments, showing again that the sand cap is protective under advective conditions. In all cases, the trends show that pyrene fluxes are highest and anthracene fluxes lowest, indicating that under advective conditions PAH solubility may be a better descriptor for fluxes than in the presence of ebullition.

In all capping scenarios and for all compounds it appears that bioaccumulation reaches a maximum level after six weeks. This may indicate that either an equilibrium has been reached beyond which no further net transport occurs (i.e. sediment fluxes equal partitioning of PAH out of the SPMD), or that the available or soluble PAH in the sediment porewater channels are largely depleted.

These trends are reflected in the flux calculations conducted for porewater advection-driven systems. (Figure 6-8), which clearly demonstrate the protective impact of sand caps, whereas the Aquablok cap (because of breaching) results in similar fluxes relative to uncapped sediments. When compared to the data from the control system in Figure 6-6, it is observed that fluxes under control conditions exceed those resulting from advection in the case of anthracene, fluoranthene and pyrene. Since the control and advection driven system used different sediment batches, we suspect that these fluxes are not directly comparable, as are uncapped, sand-capped and Aquablok-capped systems (which all used the same batch). For this analysis, we therefore assumed that the control systems exhibited fluxes that were similar or below those calculated for sand capped sediment systems.

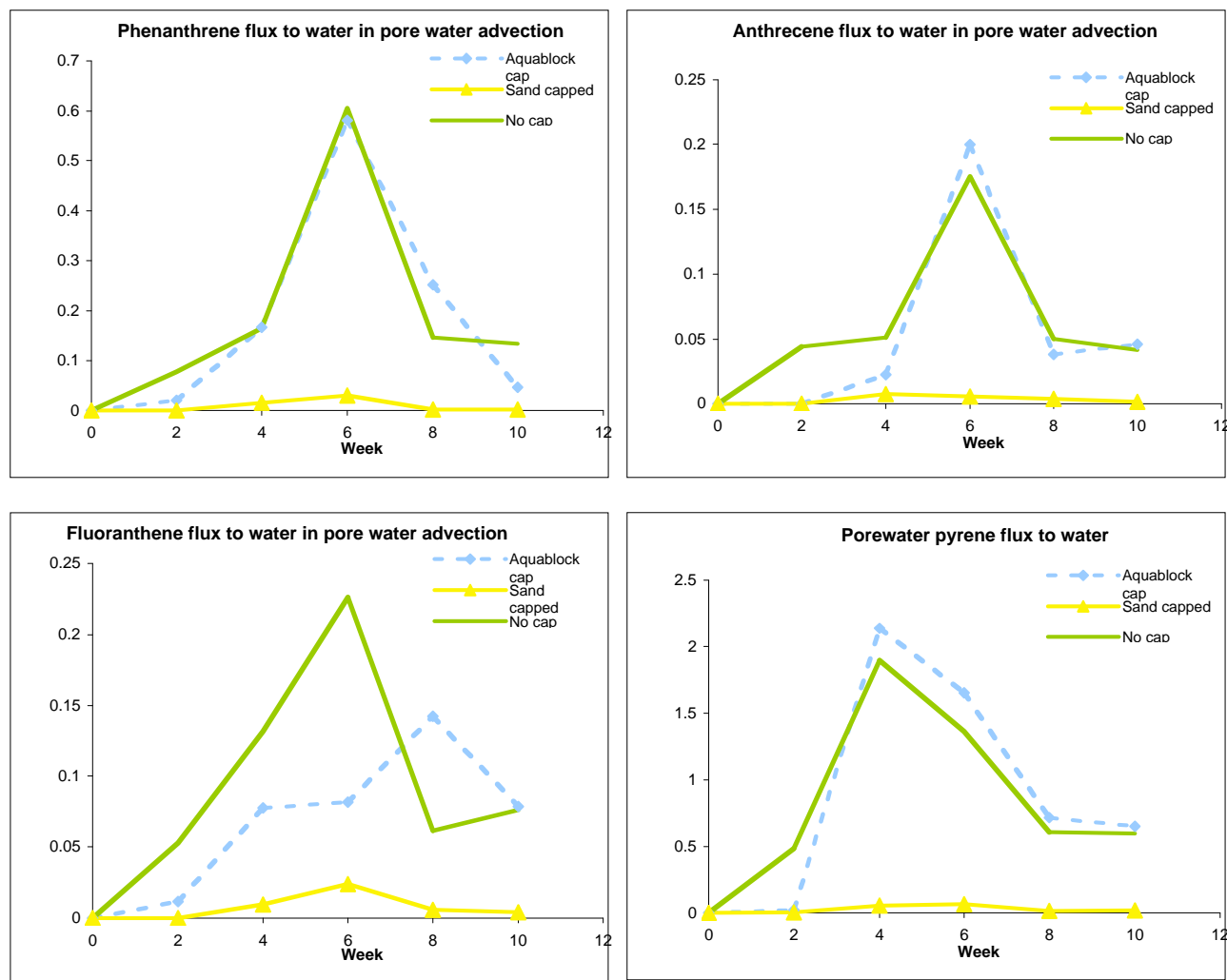


Figure 6-8. Flux comparisons for advection-driven uncapped and capped sediments

6.3 OVERALL SIGNIFICANCE AND IMPACT ON UNCERTAINTY

The results of diffusion-driven (no ebullition or advection, only water column mixing) PAH emissions in uncapped sediments resulted in annualized fluxes ranging from 0.1-1.2 mg/m².yr, depending on the PAH considered. The impact of ebullition on PAH fluxes ranged from 0.3-2.2 mg/m².yr in uncapped systems, while sand caps reduce the annualized fluxes to 0.01-0.05 mg/m².yr. Similarly, advective flow experiments performed on uncapped Anacostia River sediments resulted in annualized fluxes on the order of 0.05-2.0 mg/m².yr, with sand caps decreasing the flux to 0.01-0.02 mg/m².yr. Whereas sand caps are clearly protective over the 10-week experiments, Aquablok caps were not in the systems we evaluated because of breaching issues. No clear correlations could be observed between fluxes and PAH properties, except for that the anthracene fluxes tended to be the lowest; the most soluble PAH (pyrene) did not exhibit the highest fluxes. The trends of fluxes were non-linear, but highly variable in time; this variability was similar between advection and ebullition, unlike what was observed in the sediment resuspension experiments. In part because of these uncertainties, the integrative modeling of the experimental data aggregated all PAH observations, rather than modeling all individual PAH. The approach to data integration and SCM validation is described in Section 7.

7. INTEGRATION OF FLUME AND FIELD DATA USING UNCERTAINTY MODELING

7.1 SEDIMENT FLUX MODEL CONFIRMATION

As with any model, it is important to verify the accuracy of the Sediment Flux Model (SFM) process representation and to confirm the ability of the model framework to reproduce observations available from field and/or laboratory studies. Model verification consisted of thorough review and testing of the Excel-based Visual Basic for Applications code. Model confirmation involved comparisons to 1) experimental results for PAH flux from laboratory studies, and 2) sediment core profiles obtained from post-cap monitoring work conducted for the Anacostia River test capping site.

7.1.1 Flux Chamber Experiments

A series of experiments was conducted using Anacostia River sediments, including flume studies, studies of microbial abundance and activity, and flux chamber experiments. As discussed previously in this report, the flux chamber experiments specifically investigated the role of porewater advection and ebullition in facilitating flux of PAHs from the sediment bed to the overlying water column. The flux chamber experiments were conducted for both an uncapped and a sand-capped sediment bed configuration. The results of these experiments were used to support the SFM model development and application in two important ways:

- *Porewater advection*: the porewater advection experiments can be used to confirm the SFM's ability to predict comparable contaminant fluxes under similar conditions.
- *Ebullition*: the results of the ebullition experiments can be used to inform the parameterization of porewater exchange rates within the SFM. This aspect of the model application is discussed further in Section 7.2.

The SFM was designed as a flexible framework for simulating contaminant flux rates for a wide variety of conditions and bed configurations. Therefore, it was feasible to configure the model to emulate the sediment bed configuration and boundary conditions used in the flux chamber experiments. Model simulations were designed as follows:

- For both the uncapped and sand cap cases, 10 1-cm bed layers were specified to represent the 10 cm of native sediment used in the flux chamber experiments.
- For the sand cap case only, the native sediment layers were overlain with 10 1-cm layers of sand cap.
- A porewater advection rate of 0.3 cm/day was specified consistent with the rate used in the experiments.
- A porewater exchange rate of $1\text{e-}9\text{ m}^2/\text{s}$ was used to represent molecular diffusion.
- Particle mixing rates were set to zero based on the assumption that bioturbation processes were a negligible factor during the flux chamber experiments.

- For sand cap simulations, the initial PAH concentration in the cap was assumed to be 0.1% of the median initial concentration in the native sediment layers.

A set of 100 Monte Carlo simulations were conducted (separately) for the uncapped and capped bed configurations for the four (4) PAH compounds investigated in the flux experiments: anthracene ($\log K_{oc} = 4.4$), fluoranthene (5.0), phenanthrene (4.3), and pyrene (4.9) (Mackay, et al., 1992). Initial sediment concentrations of these compounds were varied based on a log-normal distribution developed from sediment cores for the capping site (Horne, 2003b). Organic carbon fractions in the sediment bed were also varied based on data available from the site characterization report. Table 7-1 provides a summary of the distribution inputs for the Monte Carlo simulations.

Table 7-1. Monte Carlo Distributions for Model Confirmation Simulations

Model Input Parameter	Distribution Type	Mean	Standard Deviation	Units
Initial concentration (anthracene)	Log-normal	-0.750	0.630	ln(ppb)
Initial concentration (fluoranthene)	Log-normal	0.944	0.470	ln(ppb)
Initial concentration (phenanthrene)	Log-normal	0.504	0.508	ln(ppb)
Initial concentration (pyrene)	Log-normal	0.643	0.481	ln(ppm)
Fraction organic carbon	Normal	0.070	0.028	g/g

In order to maintain consistency with the flux chamber experiments, flux estimates were calculated based on model predictions for cumulative mass transfer of PAH between weeks 2 and 4 of the simulations. Monte Carlo results for the 4 PAH compounds presented in Table 7-1 were summed to provide overall median and upper/lower confidence intervals (i.e., 5th/95th percentiles). Flux estimates based on the flux chamber observations were summed in similar fashion.

Model-predicted fluxes are compared to flux chamber estimates in Figure 7-1 for the uncapped and sand cap cases. Error bars shown for the model results represent the interval between the 5th and 95th percentiles. Note that for the sand cap scenario, error bars are difficult to distinguish because the distribution of predicted fluxes is very tight. Based on Figure 7-1, the model reproduces the flux chamber results quite well, especially considering the potential uncertainties in the flux chamber measurements and the initial PAH concentrations in the sediment used for the experiments. Perhaps most importantly the model accurately represents the change in flux that occurs as a result of overlaying the native sediment with a 10-cm sand cap layer. These results suggest that the mass transport processes represented in the model are accurate and that the parameterization for the flux chamber simulations is reasonable. These observations provide confidence that the SFM can be used as a reliable tool for quantifying the reduction in flux that can be expected from various capping technologies and the associated uncertainty.

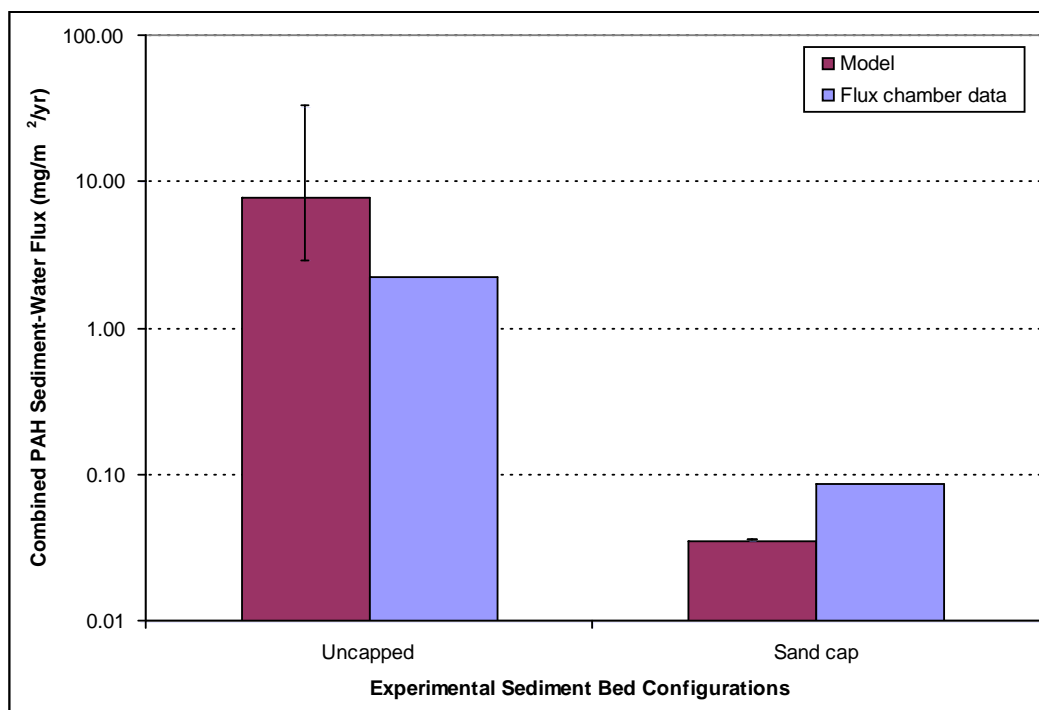


Figure 7-1. Comparison of Model-Predicted Total Flux for Anthracene, Fluoranthene, Phenanthrene, and Pyrene to Flux Chamber Data (lower and upper error bars for model results represent the 5th and 95th percentiles for predicted flux)

7.1.2 Anacostia River Pilot Capping Study

In addition to testing the SFM predictions against experimental results for PAH flux, model predictions for sediment PAH profile were compared to profiles estimated from cores taken from the Anacostia River pilot capping area. Following construction and placement of a series of reactive caps in March/April 2004 (Horne, 2003a), follow-up monitoring activities were conducted by Horne Engineering at 1-month, 6-month, 18-month, and 30-month intervals to verify the overall integrity and performance of each pilot area. Post-cap monitoring for all pilot areas included coring and measurement of vertical PAH profiles at the specified intervals (Horne, 2007b). The results of this study provide datasets that can be used to confirm the ability of the SFM to predict the evolution of the vertical sediment PAH profile for a 2-3 year period following cap placement.

Results from coring and subsequent measurement of the total PAH profile suggest that the cap layer(s) maintain their integrity with PAH levels below detection limits. A distinct surface sediment layer appears to be developed on top of the cap over the 30-month period, which suggests that net deposition of suspended sediment from the water column results in a low level of recontamination in the cap test areas. The SFM was configured to represent the initial conditions for the sand cap case in order to illustrate the ability of the model to simulate the evolution of the PAH profile over the 30-month period of observation. A SFM Monte Carlo simulation was configured as described below:

- A 9.4-inch layer of sand material overlying a parent bed was specified (consistent with the mean sand layer thickness measured at the site). The initial total PAH concentration in the sand cap layers was assumed to be zero.
- The total PAH concentration in the parent bed was specified as a distribution based on available core data (refer to Table 7-6).
- Physicochemical parameters and process rates were configured based on data available from the Anacostia River site characterization report (Horne, 2003b), radiochemistry analyses (Chan and Bentley, 2004), and other supporting literature. Refer to Tables 7-7 and 7-8 for the input distributions for total PAH partitioning coefficients, net sediment burial rates, porewater advection rates, porewater exchange rates, particle mixing rates, and sediment organic carbon content.
- A constant total PAH concentration of 100 ng/l was assumed for the water column boundary condition. (This is consistent with observed concentrations in the surface sediment layers and with water column data collected following capping.)

A Monte Carlo simulation consisting of 100 model runs was conducted for a 3-year period. A measured PAH profile for the sand cap area (Figure 7-2) was compared to the model-predicted total PAH profile (Figure 7-3) at the 30-month point.

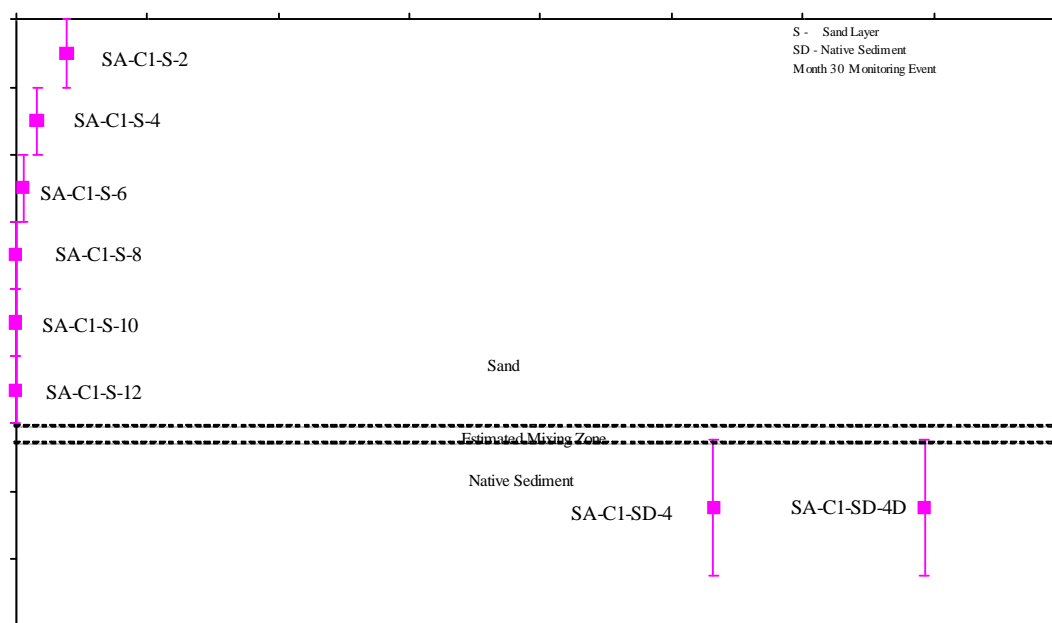


Figure 7-2. Observed Total PAH Sediment Profile for Sand Cap Location “SA-C1” after 30 Months

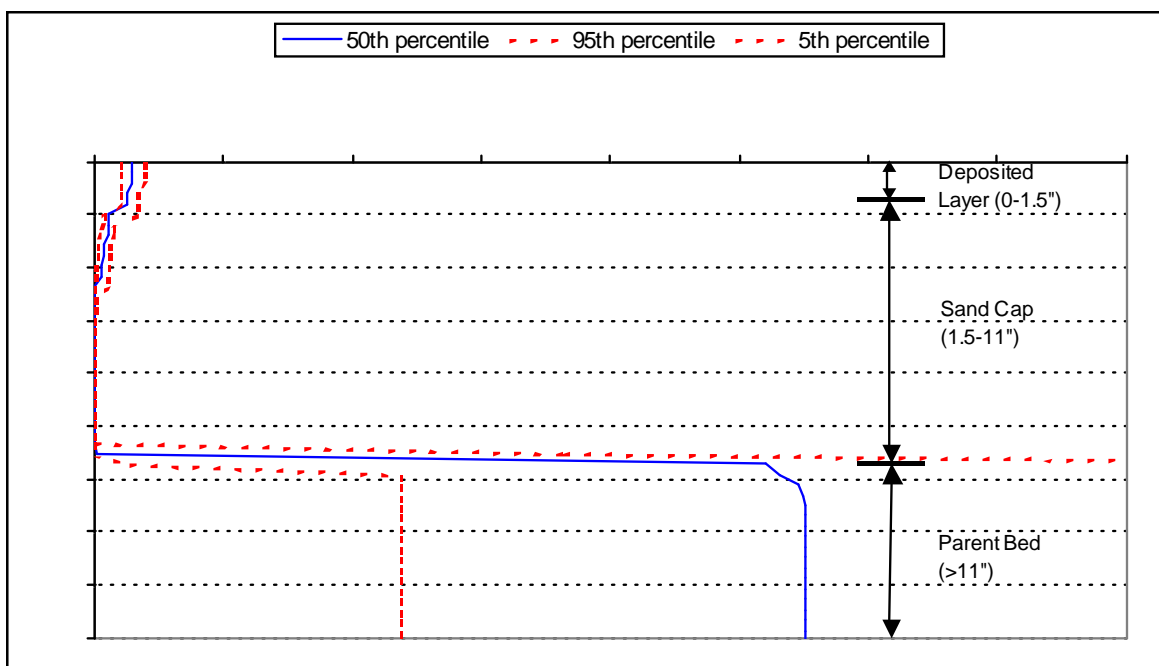


Figure 7-3. Model-Predicted Total PAH Sediment Profile for Sand Cap Area after 30 Months

Based on this comparison, the following observations were made:

- The model predicts a similar depth and total PAH concentration for the surficial layer formed by deposition of suspended sediment relative to the observed profile. This indicates that the model is properly representing deposition and burial of suspended sediment and associated PAH mass;
- The SFM maintains the integrity of the sand cap throughout the 30-month period, consistent with the observed profile; and
- Model-predicted total PAH concentrations in the parent bed layers (> 11") are similar to observed concentrations;

The strong similarities between the model-predicted PAH profile and the observed profile provide confidence that the SFM can be configured to accurately represent the major chemical transport processes and associated parameterization for the Anacostia River capping site.

7.2 MODEL UNCERTAINTY ANALYSIS

An integrated Monte Carlo tool was constructed as part of the Sediment Flux Model (SFM) development effort. This tool provides the option of including any of the SFM inputs described in the previous section in a Monte Carlo evaluation. To include an input parameter, the user specifies a mean and standard deviation value, and also indicates whether the parameter is assumed to be normally or log-normally distributed. Minimum and maximum values can be specified to keep input parameter estimations within a bounding range.

The Monte Carlo simulation tool was applied to 1) investigate the sensitivity of model predictions to key input parameters, and 2) evaluate the uncertainty in model-predicted PAH flux based on "uninformed" and Anacostia-specific parameter input distributions. This chapter presents and summarizes key results from the SFM applications in order to demonstrate 1) the

necessity of collecting site-specific data via field and laboratory studies, and 2) the value of developing a site-specific, integrated model of the physicochemical processes for evaluating PAH flux in uncapped and capped areas.

7.2.1 Monte Carlo Sensitivity Analysis

As an initial step in evaluating parameter uncertainty, the SFM Monte Carlo tool was applied to evaluate the sensitivity of the key process and physicochemical parameters represented in the model. This section discusses the design and outcome of the sensitivity simulations.

Simulation Design. Constructing the SFM sensitivity analysis involved two major steps: 1) identifying a subset of model input parameters to which the model is likely to be sensitive, and 2) developing a representative input distribution for each parameter. The following parameters were identified as being important to include in the sensitivity analysis:

- Porewater advection (i.e., groundwater seepage) rate;
- Porewater exchange rate;
- Particle mixing rate;
- Sediment net burial rate;
- Carbon content of sediment bed;
- Coefficient for chemical partitioning to organic carbon (K_{oc});
- Chemical concentration in sediment bed; and
- Cap thickness.

The goal of the sensitivity analysis was to rely primarily on existing literature to define the input distributions, in order to illustrate the importance of collecting site-specific data for key parameters. Therefore, literature-based estimates of parameter value ranges were obtained from the project literature review report (LimnoTech, 2006) or supplemental literature sources whenever possible. Estimated ranges of porewater exchange, particle mixing, and sediment burial rates were obtained from the literature report. Ranges for porewater advection rates were determined from a review of seepage data presented in Thibodeaux and Mackay (2009). Ranges for organic carbon fraction in sediment were estimated based on general literature and professional judgment. The ranges and estimated distributions for all of these parameters are summarized in Table 7-2.

Table 7-2. Literature-Based Physical and Process Input Parameter Distributions for Model Sensitivity Analysis

Model Input Parameter	Units	Range	Distribution Type	Mean ¹	Standard Deviation ¹
Porewater advection rate ²	cm/day	0.1 – 79	Log-normal	0.48	1.45
Porewater exchange rate	m ² /s	(5e-10) – (5e-7)	Log-normal	-7.8	0.8
Particle mixing rate	m ² /s	(1e-12) – (5e-9)	Log-normal	-10.2	0.9
Carbon content	%	0.1 – 15	Log-normal	0.09	0.54
Burial rate	cm/yr	0.0 – 5.0	Normal	2.5	1.25

¹Values are log-normalized for all parameters except burial rate.

²For actual model simulations, a normal distribution was assumed with a mean of 3 cm/day (st.dev. 1.5 cm/day).

It should be noted that the distribution shown in this table for porewater advection rate was ultimately narrowed for practical considerations. All of the literature based distributions were assumed to be log-normal with the exception of burial rate, which has a much tighter range and is better characterized by a normal distribution.

Phenanthrene (median log K_{oc} = 4.3) and benzo(k)fluoranthene (median log K_{oc} = 5.7) were identified as the PAH compounds to represent in the sensitivity analysis because their respective partitioning coefficients (K_{oc}) are representative of the range of PAH compounds found at the Anacostia River pilot capping site. The inclusion of two compounds with disparate partitioning coefficients also provided an opportunity to evaluate the effect of partitioning behavior on the chemical flux predicted for different process rate sensitivity simulations. Distributions of partitioning coefficients for phenanthrene and benzo(k)fluoranthene were developed based on Mackay, et al. (1992) and are presented in Tables 7-3 and 7-4.

Table 7-3. Phenanthrene Input Parameter Distributions

Model Input Parameter	Units	Range	Distribution Type	Mean	Standard Deviation
K_{oc}	log(L/kg-C)	3.6 – 6.1	Log-normal	4.3	0.5
Initial sediment concentration	log(ppb)	2.79 – 4.04	Log-normal	3.32	0.30

Table 7-4. Benzo(k)fluoranthene Input Parameter Distributions

Model Input Parameter	Units	Range	Distribution Type	Mean	Standard Deviation
K_{oc}	log(L/kg-C)	4.0 – 7.0	Log-normal	5.7	1.1
Initial sediment concentration	log(ppb)	2.52 – 3.81	Log-normal	3.12	0.31

Specifying chemical concentrations or cap thicknesses via literature-based sources was not feasible, as these parameters are very specific to site sediment conditions and cap implementation approach. Therefore, Anacostia-specific distributions were used to represent these parameters in the overall sensitivity analysis. Anacostia-specific distributions for phenanthrene and benzo(k)fluoranthene concentrations were developed based on core data from the site characterization (Horne, 2003b) and are shown in Tables 7-3 and 7-4, respectively.

Cap thicknesses for the Anacostia River pilot capping site were measured as part of the post-cap monitoring effort. Three cap configurations were evaluated as part of the sensitivity and uncertainty modeling evaluation: sand cap, AquaBlok™ (with sand overcap), and coke breeze (with sand overcap). Distributions of cap and overcap thicknesses are provided in the cap completion report (Horne, 2004) and are presented in Table 7-5. Other cap-specific properties that were assumed to be constant are summarized in Table 7-6.

Table 7-5. Sediment Cap Thickness Distributions (units in cm)

Bed Configuration Scenario	Sand Overcap		Reactive Cap	
	Mean	Std Dev	Mean	Std Dev
No cap	n/a	n/a	n/a	n/a
Sand cap	23.6	8.1	n/a	n/a
AquaBlok™ + sand cap	13.5	4.6	14.7	4.8
Coke breeze + sand cap	16.3	3.6	2.5	n/a

Table 7-6. Constant Sediment and Cap Input Parameters

Model Input Parameter	Units	Sediment/Cap Type			
		Parent Bed	Sand Cap ²	AquaBlok™	Coke Breeze ²
Hydraulic conductivity	m/s	1.0e-8 ¹	1.19e-6	4.59e-11 ³	1.19e-6
Organic carbon content (for sediment)	(%)	n/a	0.03%	0.14%	100%
Dry bulk density ⁴	kg/m ³	630 ²	1,650	940	940

Notes:¹Estimated value based on a typical clay/silt mixture for an estuarine system.²Values obtained from Anacostia River site characterization report (Horne, 2003b).³Obtained from AquaBlok, Ltd. (2004).⁴A particle density of 2,500 kg/m³ was assumed for all sediment/cap types.

A total of 64 Monte Carlo simulations were conducted using a combination of 8 different parameters, 4 cap scenarios, and 2 PAH compounds (phenanthrene and benzo(k)fluoranthene). The following section summarizes the results of these simulations and associated findings. Mean values were used for parameters in simulations where those parameters were not included in the Monte Carlo. For example, a constant sediment burial rate of 2.5 cm/yr was used in all simulations except for the Monte Carlo run addressing burial rate sensitivity.

The initial Monte Carlo simulations were based on the porewater advection rate distribution defined in Table 5.1. However, using this log-normal distribution was found to be problematic for two reasons: 1) using a median advection rate of 3.0 cm/day resulted in groundwater seepage being the dominant process in nearly all sensitivity evaluations, and 2) consideration of advection rates greater than ~10 cm/day required severe reductions in model time step, which made the groundwater sensitivity run impractical. To address these issues, the distribution for porewater advection rates used in the seepage sensitivity was modified to be normal with the same mean value (3.0 cm/day) and a standard deviation of 1.5 cm/day. In addition, a constant advection rate of 0.3 cm/day was used to support the non-seepage sensitivity runs so that the sensitivity of other parameters could be adequately assessed. This rate was selected because it is consistent with mean observed rates for the Anacostia River pilot capping site.

Simulation Results. Box and whisker plots are shown in Figures 7-4 through 7-7 for the four cap scenarios. Each chart shows results for phenanthrene and benzo(k)fluoranthene for the 8 input parameters for which sensitivity runs were conducted. All flux predictions are expressed as average fluxes based on the 30-year period simulated. The box in these charts represents the

interquartile range (i.e., 25th and 75th percentile) of the predicted flux distribution, and the horizontal dash within the box represents the median (50th percentile) value. The lower and upper whiskers represent the 5th and 95th percentile values, respectively.

Relative to phenanthrene ($\log K_{oc} = 4.3$), predicted benzo(k)fluoranthene ($\log K_{oc} = 5.7$) flux is less sensitive to the input parameters evaluated. The stronger partitioning to organic carbon exhibited by benzo(k)fluoranthene makes this compound less mobile and, therefore, less susceptible to removal from the bed via porewater advection or exchange processes. Predicted fluxes for the “no cap” scenario are most sensitive to contaminant concentration, sediment organic carbon content, partitioning coefficient, and porewater exchange rates. Predicted fluxes for the “sand cap” scenario exhibit a similar degree of sensitivity to contaminant concentration, organic carbon content, and partitioning coefficient as the “no cap” case does, albeit at lower average flux rates. Results of the porewater advection sensitivity suggest that groundwater seepage can generate high contaminant fluxes, but indicate relatively low sensitivity based on the set of 100 simulations conducted. In reality, sensitivity to porewater advection should be high because the literature-based rates range from zero advection to very high rates. Therefore, a larger range of results at the lower end of the distribution would be expected for a larger number of Monte Carlo simulations (e.g., 1000 runs).

In comparing the results of the two synthetic cap scenarios, the AquaBlok™ scenario demonstrates higher sensitivity to contaminant concentration, organic carbon fraction, partitioning coefficient, and porewater exchange rate. The coke breeze scenario demonstrates a higher sensitivity to porewater advection. These results highlight the differences in how these respective caps function to limit the upward migration of contaminant within the sediment bed. AquaBlok™ is specifically designed to have a very low hydraulic conductivity in order to serve as a barrier to groundwater seepage. Coke breeze, on the other hand, has very high carbon content and sorptive capacity and is designed to sequester contaminant mass as it migrates toward the sediment-water interface. High porewater advection rates can limit the long-term effectiveness of this technology by facilitating a high contaminant flux that eventually results in exhaustion of the available sorptive capacity.

Overall, the results of the sensitivity analysis suggest that the “no cap” and sand cap scenarios are sensitive to most of the input parameters tested, with phenanthrene generally demonstrating higher sensitivity due to its greater mobility. For the “no cap” scenario, predicted fluxes appear to be less sensitive to burial rate and particle mixing for the literature-based ranges. Fluxes predicted for the sand cap scenario tend to be less sensitive to porewater exchange, particle mixing rates, as well as cap thickness. Similarly, the AquaBlok™ and coke breeze scenarios demonstrate lowest sensitivity to burial rate, particle mixing rate, and cap thickness. As discussed above, the coke breeze results demonstrate much greater sensitivity to porewater advection rates than those for AquaBlok™.

The relative lack of sensitivity to cap thickness is of particular note. In general, the presence of a sand cap alone may be effective in limiting contaminant flux in the short-term; however, the long-term performance of this capping technology is compromised to a large degree by the lack of sorptive capacity (i.e., organic carbon) available in the sand layer. Low organic carbon content (i.e., < 0.1%) results in relatively high dissolved fractions of contaminant, thus permitting porewater advective and diffusive processes to effectively transport contaminant mass to the sediment-water interface. In addition, the hydraulic conductivity of sand material is typically higher than that of the clay/silt sediment mixtures that tend to dominate bottom sediments at

contaminated sediment sites, such as the Anacostia River pilot capping site. As a result, the placement of a sand cap does not provide an effective barrier to groundwater seepage. The combination of these factors limits the importance of the sand cap and overcap thickness in terms of long-term mean flux predictions.

The outcome of the sensitivity analyses establishes that predicted fluxes are sensitive to multiple model input parameters for all four capping scenarios. This finding suggests that there is a need to understand how the *combined* uncertainty (and, in the case of cap thickness, spatial variability) of these parameters ultimately translates to uncertainties in flux predictions and overall cap performance. The SFM provides an integrated modeling framework that can be used to make this translation and quantify cap performance.

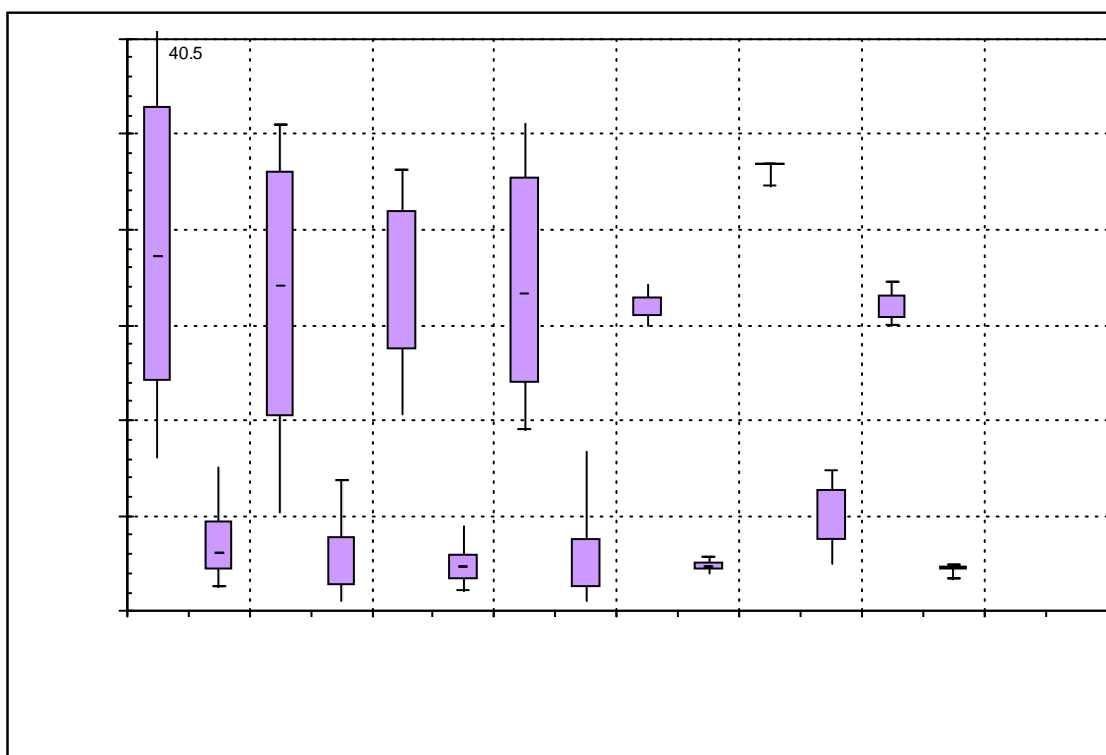


Figure 7-4. Monte Carlo Sensitivity Results for "No Cap" Scenario

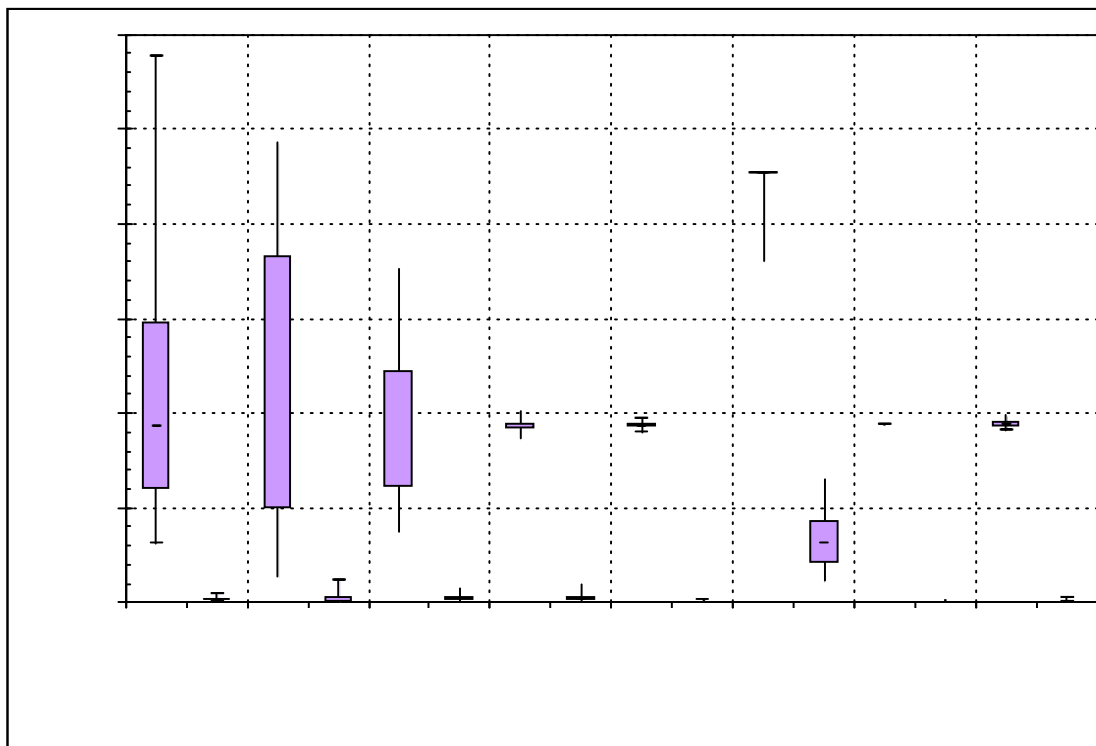


Figure 7-5. Monte Carlo Sensitivity Results for Sand Cap Scenario

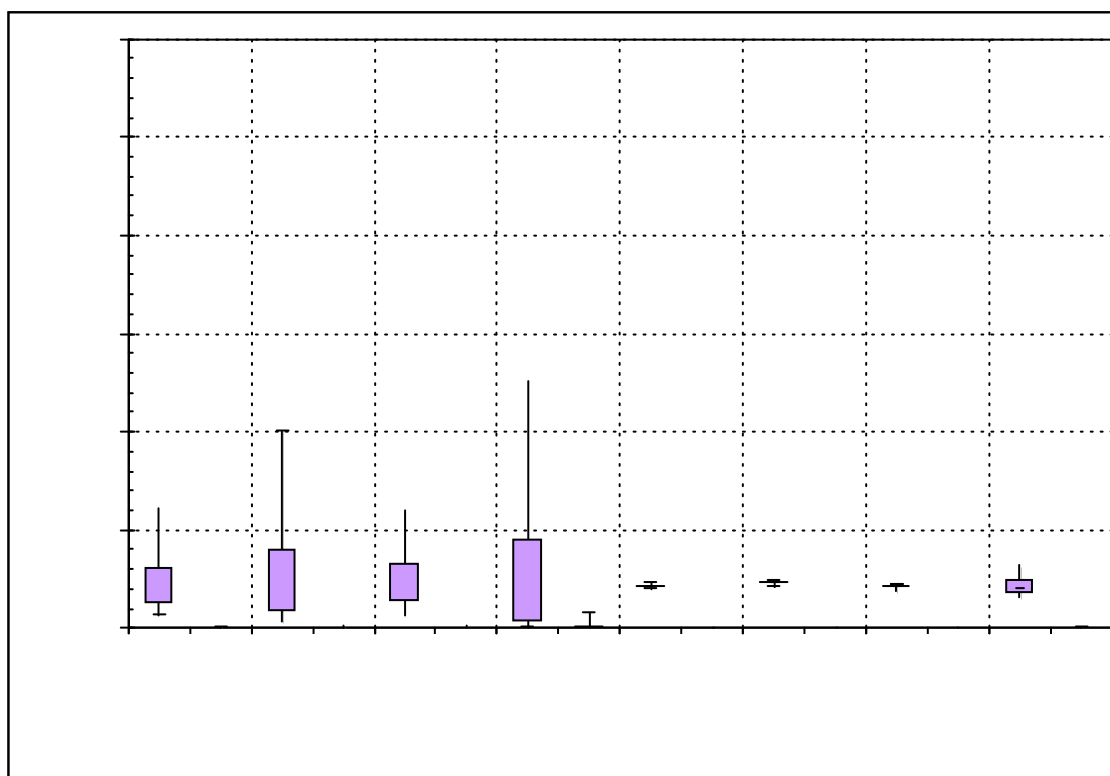


Figure 7-6. Monte Carlo Sensitivity Results for AquaBlok™ Scenario

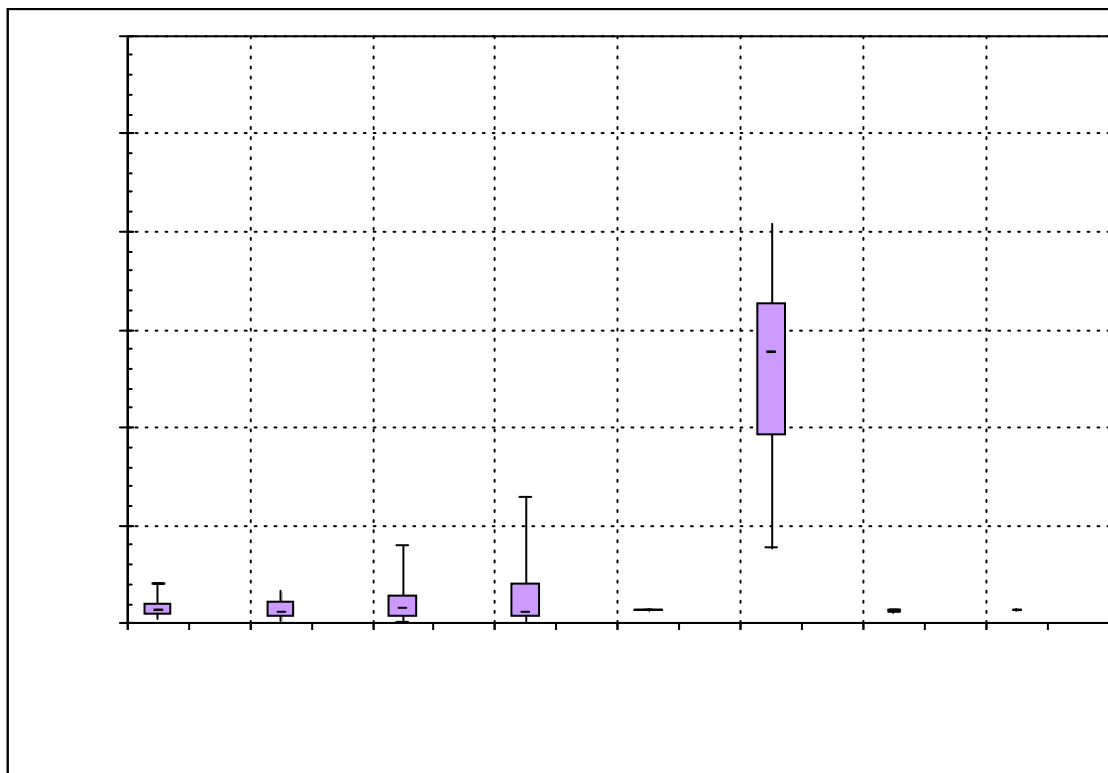


Figure 7-7. Monte Carlo Sensitivity Results for Coke Breeze Scenario

7.2.2 Monte Carlo Uncertainty Analysis

A primary objective of the project is to demonstrate the benefits of collecting field data, conducting laboratory experiments, and applying models on a site-specific basis in terms of reducing uncertainty in the anticipated contaminant flux resulting from various capping actions. This section describes the application of the SFM to provide a quantitative demonstration of uncertainty reduction for total PAH flux using site-specific data and experiments for the Anacostia River pilot capping area. The results of the application underscore the importance of 1) collecting site-specific data, and 2) integrating those site-specific data into a well-conceived mathematical model for quantifying contaminant transport and fate for the management (i.e., capping) scenarios of interest.

Simulation Design. The Monte Carlo uncertainty analysis required consideration of both the “uninformed” distributions presented in Table 7-2, as well as a refined set of input parameter distributions developed based on site-specific field studies and laboratory experiments conducted for Anacostia River sediments.

The sensitivity analyses presented in Section 7.2.1 included simulations for both phenanthrene ($\log K_{oc} = 4.3$) and benzo(k)fluoranthene ($\log K_{oc} = 5.7$) so that the effect of partitioning characteristics could be directly investigated. Ultimately, management questions for the Anacostia River (and other sites with PAH contamination) will be focused on the flux of “total PAH” from the sediment bed to the water column. Therefore, “total PAH” was represented in all of the Monte Carlo simulations conducted to support the uncertainty investigation. Log-normal distributions for K_{oc} and total PAH concentration were developed based on Mackay, et. al.

(1992) and coring data from the Anacostia River site characterization (Horne, 2003b), respectively (Table 7-7).

Table 7-7. Total PAH Concentration Input Parameter Distributions

Model Input Parameter	Units	Range	Distribution Type	Mean	Standard Deviation
Koc	log(L/kg)	n/a	Log-normal	5.7	0.5
Initial sediment concentration	log(ppb)	3.96 – 4.92	Log-normal	4.35	0.23

The sensitivity analyses presented in Section 7.2.1.2 were conducted primarily based on the use of parameter distributions that are supported by the body of literature across study sites located in multiple regions and comprised of a variety of water body characteristics (e.g., marine, estuarine, lacustrine, and riverine systems). Monte Carlo simulations were developed to represent an uncapped scenario and three capping scenarios for the set of “uninformed” distributions presented in Table 7-2 to demonstrate the range of flux predictions that can be expected in the absence of site-specific data for a contaminated sediments site.

Developing a “site-specific” uncertainty analysis for the Anacostia River pilot capping site required compiling all of the available data produced by 1) the suite of site characterization studies (Horne, 2003b), and 2) site-specific laboratory studies of the effect of ebullition and porewater advection processes on contaminant fluxes for uncapped and capped sediments.

Anacostia River: Site Characterization Study

A considerable amount of detailed chemical, biological, geophysical, and geotechnical data were collected as part of the Anacostia River site characterization effort conducted by Horne Engineering (2003b). Field measurements that were directly used in developing input parameter distributions for the SFM uncertainty analysis included:

- Groundwater seepage rates measured for six locations in the pilot capping area (Horne, 2003b);
- Sediment cores (9 samples for 0-6”, 17 samples for > 6”) collected and analyzed for PAH concentrations and total organic carbon content (Horne, 2003b);
- Sediment burial and mixing rates quantified based on geochronological analysis of Anacostia River sediment cores (Chan and Bentley, 2004);
- Cap thicknesses measured as part of the cap completion study and presented as normal distributions in the cap completion report (Horne, 2004).

The input parameter ranges and distributions developed based on these studies for porewater advection rates, particle mixing rates, total organic carbon content, and sediment burial rates are presented in Table 7-8. The development of the input distribution for porewater exchange rates is detailed in the next section pertaining to the ebullition studies. Normal distributions were assumed for all process rates and physical parameters shown in Table 7-8 because the number of data points available was relatively small and because the associated value ranges generally spanned less than an order of magnitude.

Table 7-8. Physical and Process Input Parameter Distributions for the Anacostia River

Model Input Parameter	Units	Range	Distribution Type	Mean ¹	Standard Deviation ¹
Porewater advection rate ¹	cm/day	0 – 4.2	Normal	0.86	0.87
Porewater exchange rate	m ² /s	(5e-10) – (1.6e-9)	Normal	1.05e-9	2.75e-10
Particle mixing rate ²	m ² /s	(7.6e-11) – (1.1e-10)	Normal	9.2e-11	2.3e-11
TOC content ¹	%	0.013 – 0.143	Normal	0.070	0.028
Burial rate ²	cm/yr	0.61 – 1.00	Normal	0.76	0.21

¹Source: Horne, 2003b²Source: Chan and Bentley, 2004

Anacostia River: Cap Distribution Study

Placement of innovative capping technologies in the Anacostia River pilot capping area was carried out in 2004 (Horne, 2003a). For a sand cap, design thickness was approximately 10 inches (25 cm). For a synthetic AquaBlok™ cap, a 4-inch (10-cm) AquaBlok™ layer is covered with a 6-inch (15-cm) sand over cap. Data collected as part of the 18-month survey of capped areas indicated that total cap thicknesses (including cap and overcap) varied from 3 to 19 inches for sand caps, 3 to 21 inches for AquaBlok™ caps, and 6 to 12 inches for the coke breeze areas (Horne, 2007a). Minimum cap thicknesses were generally observed near the edges of the capping areas.

Characterization of cap thickness variability is an important component of the overall uncertainty analysis because, as demonstrated in Section 7.2.1, model predictions of PAH fluxes can be sensitive to cap thicknesses under some circumstances. Normal distributions of cap and overcap (where applicable) thicknesses were developed and reported by Horne Engineering (Horne, 2007). These distributions, which are reproduced in Table 7-5, were incorporated into both the “uninformed” and the “site-specific” Monte Carlo simulations.

Anacostia River: Ebullition Studies

The literature review conducted by LimnoTech (2006) addressed each of the key processes that have the potential to effect the rate of contaminant transfer (i.e., flux) from the sediment bed to the water column for an area contaminated by hydrophobic organic compounds. One of the findings of the literature review was that both gas ebullition and porewater advection are potentially significant processes affecting contaminant flux at a given site. The influence of porewater advection on contaminant transport is generally well-understood and can be faithfully represented in mathematical models of the sediment bed. However, ebullition represents a much more complex processes by which gas bubbles generated by microbial activity in the sediment bed potentially enhance contaminant transport by multiple pathways.

Ebullition rates reported in the literature range from 0.1-100 L/m²/day (0.01-10 cm/day) for marine and coastal sites. The SFM does not explicitly represent the physicochemical process of

gas ebullition or its direct influence on the transport of contaminants. However, the model is well-suited to *indirectly* represent the effects of gas ebullition on contaminant flux in three ways:

- Enhanced mixing of sediment particles and porewater within the sediment bed can be simulated via increased rates of particle mixing or porewater exchange between sediment layers.
- Enhanced exchange of contaminant from the sediment bed to the water column can be simulated via increased rates of porewater exchange at the sediment-water interface.
- Increases in erosion rates and/or reductions in critical shear stresses resulting from gas ebullition can be factored into the two resuspension rates input to the model.

The use of the flux chamber results for porewater experiments to confirm the model's ability to simulate this key transport mechanism was discussed in Section 7.1. The results of the ebullition experiments, on the other hand, were used to directly support the development of process rates for the model application. The SFM was configured to represent the sediment conditions in the flux chamber, including an input distribution of PAH compound concentrations based on cores collected and analyzed as part of the site characterization study (Horne, 2003b). Based on this simulation design, porewater exchange coefficients were calibrated to obtain contaminant fluxes consistent with those measured in the flux chamber experiments. The underlying assumption in this analysis was that any enhancement in PAH mass transfer resulting from ebullition could be reasonably represented through the use of the porewater exchange coefficients, which move dissolved chemical mass between adjacent sediment layers and between the surficial sediment layer and the water column.

The gas introduction rates used in the flux chamber experiments (approximately 0.1 cm/day, or 1.0 L/m²/day) were similar to gas generation rates measured by Himmelheber and Hughes (2005) and reported by Hughes (2004) for Anacostia River sediments (0.03-0.09 cm/day). Therefore, conditions used in the flux chamber setup were representative of gas generation rates expected in the field. The ebullition "calibration" simulations with the SFM yielded a range of porewater exchange rates (5e-10 – 1.6e-9 m²/s) that are generally similar to those corresponding to molecular diffusion, as represented by the lower end of the range in Table 7-2 (5e-10 m²/s). The combination of these independent site-specific measurements (i.e., flux and ebullition rates) suggests that ebullition is not a significant factor influencing the movement of contaminants from the sediment bed to the water column in the Anacostia River.

Yuan, et al. (2007) produced an independent set of flux measurements for phenanthrene using Anacostia sediments and a range of ebullition rates. Gas introduction rates of 0.1, 0.29, 30.7, and 196.3 cm/day were used in these experiments, with the minimum rate being representative of measured ebullition rates for the Anacostia River. Phenanthrene flux results from this study are summarized in Table 7-9. Also included in this table is the estimated porewater exchange coefficient that would be required to generate the measured flux for initial phenanthrene concentrations used in the experiments. The exchange coefficient calculated for the 0.1 cm/day ebullition case is approximately 6e-10 m²/s. This coefficient falls within the calibrated range of coefficients (5e-10 – 1.6e-9 m²/s) based on the flux chamber results described above. Therefore, the ebullition study conducted by Yuan, et al. provides corroborating support for the flux chamber results and the conclusions drawn from those results.

Table 7-9. Summary of Ebullition Results for Anacostia River Sediments as Reported by Yuan, et al. (2007)

Gas Flux (cm/day)	Phenanthrene Flux (g/m ² /s)	Porewater Exchange Coefficient (m ² /s)	Notes
196.3	1.96E-06	2.8E-05	
30.7	2.44E-07	3.5E-06	
0.29	1.17E-10	1.7E-09	
0.1	4.17E-11	6.0E-10	Maximum ebullition rate for Anacostia capping site based on Himmelheber and Hughes (2005)

As discussed above, it was assumed that porewater exchange coefficients could be reasonably used to represent the effects of ebullition on contaminant movement both within the sediment bed and between the surficial sediment layer and the water column. Implicit in this assumption is the assumption that the ebullition rates of interest for the experiments and the Anacostia River have no discernable impact on rates of erosion for surficial sediments. This assertion is supported by the series of flume experiments that were conducted as part of this project. As described in this document and previous annual reports, the flume experiments were designed to investigate whether gas introduction to the sediment bed affected erosion rates by 1) lowering the critical shear stress for erosion of surficial sediments, and/or 2) increasing rates of erosion once the critical shear stress is exceeded. Multiple experiments were run with ebullition rates ranging from 1-50 cm/day. Overall, the findings from the flume study suggest that high rates of ebullition can result in a noticeable lowering of critical shear stress, as well as an increase in erosion rates. However, the critical shear stress for erosion exceeded 1 dyne/cm² even for the maximum ebullition rate used in the flume experiments (50 cm/day). Even this reduction in critical shear stress would be insufficient to induce resuspension of sediments in the Anacostia River capping area because DYNHYD/WASP modeling of this area indicated that maximum hourly shear stresses do not exceed 0.6 dyne/cm² during a full year of simulation. Although ebullition is very unlikely to have any effect on resuspension in the Anacostia River, the results of the flume study suggest that ebullition may play a role in enhancing resuspension for sites that are susceptible to higher rates of gas generation and periodic elevated shear stresses in excess of critical shear stresses.

Simulation Results & Discussion The input parameter distributions presented in Tables 7-5 through 7-8 were used to develop Monte Carlo simulations consisting of 100 individual runs for four cap-related scenarios: uncapped, sand cap, AquaBlok™ (with sand overcap), and coke breeze (with sand overcap). Separate Monte Carlo simulations were run for the “uninformed” and “Anacostia-specific” distributions. Figures 7-8 and 7-9 present cumulative frequency distributions (CFDs) and idealized normalized density distributions of model-predicted total PAH flux for the four cap scenarios for the “uninformed” case (note that the x-axis is based on a logarithmic scale).

As expected, the model predicts that the “no cap” case has the highest flux values. The lowest predicted fluxes are for the coke breeze and AquaBlok™ scenarios, while the sand cap scenario falls in the middle of the range. Overall, these results suggest that significant reductions in total

PAH could be expected due to implementation of the AquaBlok™ or coke breeze caps. Placement of a sand cap provides a modest reduction in flux and a tighter distribution than the other capping options.

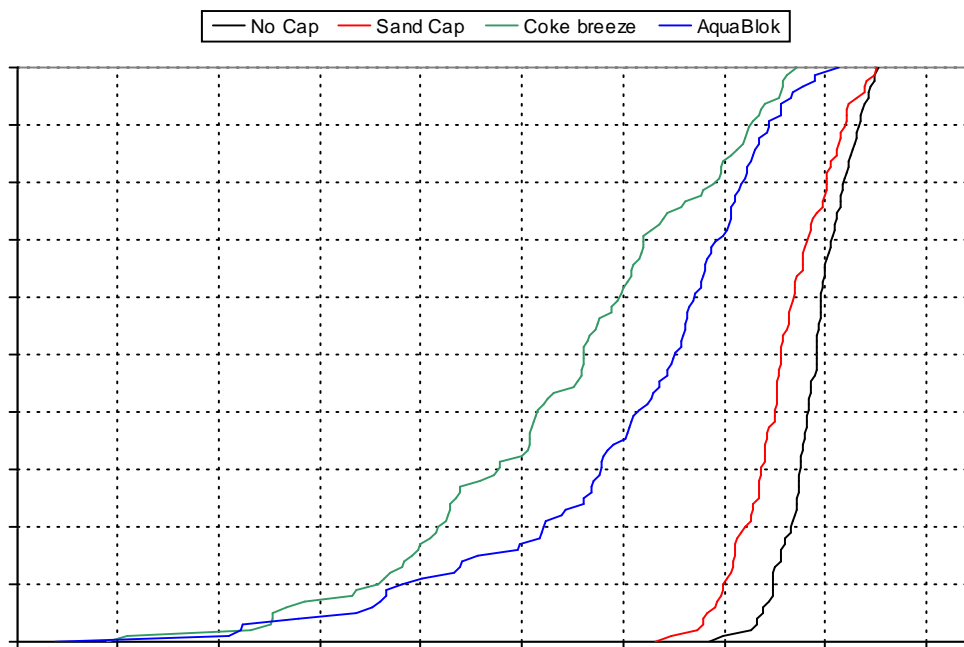


Figure 7-8. Cumulative Frequency Distributions for “Uninformed” Monte Carlo Simulations

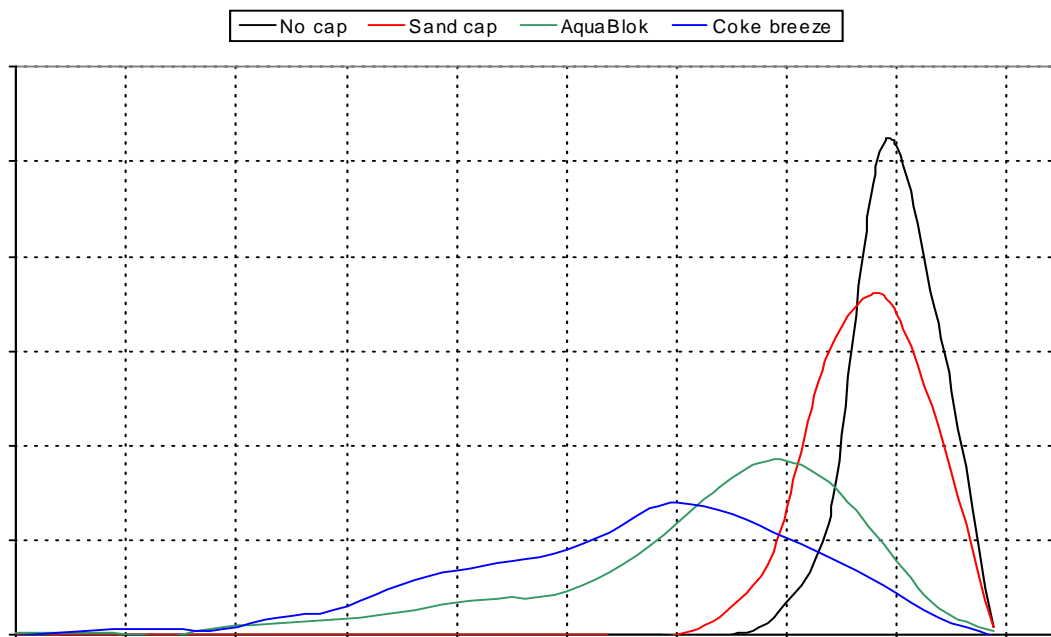


Figure 7-9. Normalized Histograms for “Uninformed” Monte Carlo Simulations

Key statistical metrics including mean, median, and interquartile range are compiled for the “uninformed” and Anacostia-specific cases in Tables 7-10 and 7-11, respectively. The final row in Table 7-11 presents the percent reduction in the interquartile range (IQR) for the Anacostia-specific case relative to the uninformed case. A comparison of Tables 7-2 and 7-8 suggests that the input distributions are considerably tighter for the Anacostia-specific case for many parameters. In addition, the mean/median values of the distributions are significantly lower for most parameters. The comparison of results in Tables 7-10 and 7-11 confirm that these differences in the input distributions result in a significant reduction in both the mean/median values and the range of the predicted total PAH flux distributions. In fact, the interquartile range, which serves as an indicator of the “width” of the distribution, is reduced by more than 98% for the four cap scenarios.

Table 7-10. “Uninformed” Monte Carlo Simulations: Statistical Metrics for Predicted 30-Year Average Fluxes ($\text{mg}/\text{m}^2/\text{yr}$)

Metric	No Cap	Sand Cap	AquaBlok™	Coke Breeze
Mean	158	85	5.0	1.4
Median	68	13	0.10	0.0017
25th Percentile	28	4.5	0.0016	4.46E-06
75th Percentile	179	74	1.33	0.092
Interquartile Range (IQR)	151	69	1.33	0.092

The Anacostia-specific results indicate that the presence of an AquaBlok™ or coke breeze cap (with a sand overcap) in the model reduces the predicted mean/median flux and the interquartile range by 5 to 9 orders of magnitude relative to the “no cap” and sand cap scenarios. These results suggest that implementation of AquaBlok™ or coke breeze capping technologies in the field should result in much improved long-term cap performance relative to a sand cap alone.

Table 7-11. Anacostia-specific Monte Carlo Simulations: Statistical Metrics for Predicted 30-Year Average Fluxes ($\text{mg}/\text{m}^2/\text{yr}$)

Metric	No Cap	Sand Cap	AquaBlok™	Coke Breeze
Mean	2.7	0.40	2.40E-06	6.47E-05
Median	1.3	0.05	1.31E-12	3.94E-12
25th Percentile	0.62	0.0027	1.57E-16	4.84E-14
75th Percentile	3.2	0.20	2.07E-09	1.11E-09
Interquartile Range (IQR)	2.6	0.20	2.07E-09	1.11E-09
Reduction in IQR	98.3%	99.7%	~100.0%	~100.0%

7.3 SUMMARY OF FINDINGS

Monte Carlo-based predictions of PAH flux obtained for the sensitivity and uncertainty analyses provide valuable insight into the relative importance and sensitivity of model input parameters and the impact of the basis for value distributions. The outcome of these modeling analyses demonstrates that:

- As illustrated by the sensitivity analyses, model-predicted fluxes are strongly dependent on multiple process rates and physical parameters. Therefore, there is a clear need to evaluate the combined effect of input parameter uncertainties on uncertainties in expected fluxes and cap performance.
- Partitioning and other chemical-specific characteristics of a particular contaminant play a critical role in determining the extent to which that contaminant can be mobilized and transported to the sediment-water interface.
- Significant reductions in input parameter uncertainties can be expected by incorporating site-specific field studies and in-situ/laboratory experiments, as opposed to relying exclusively on ranges available in literature for key process parameters;
- Significant (i.e., orders of magnitude) reductions in mean/median and interquartile range (IQR) for predicted total PAH flux can be obtained when relying on site-specific datasets to reduce parameter uncertainty for the Anacostia River; and
- An integrated capping model framework, such as the SFM, can be used to effectively compare relative performance across multiple capping technologies, as well as to evaluate the effect of combined parameter uncertainties on predicted contaminant flux from the sediment bed to the water column.

For the Anacostia River, findings from site-specific field and laboratory studies and the uncertainty analysis conducted with the SFM have shown that microbial gas-generated ebullition is likely not a significant process affecting contaminant flux through cap layers at the site, while groundwater seepage is likely to be an important long-term process in areas where there is a net advective flux of water from the sediment bed to the overlying water column. The current findings suggest that additional site characterization of the Anacostia River capping site should consider studies aimed at reducing the uncertainty and spatial variability in groundwater seepage rates.

7.4 “SEDIMENT FLUX MODEL” – FUTURE IMPROVEMENTS

The development of the “Sediment Flux Model” (SFM) for the project represents a step forward in terms of mathematical and modeling tools available for evaluating the performance of various capping technologies. The SFM contains a similar level of sediment process complexity embodied within other available models. However, the SFM is a user-friendly tool that is specifically designed to simulate the effect of capping actions on contaminant flux. Particularly important and unique to the model structure is the ability to simulate multiple “sediment” materials, which allows for an explicit representation of the physical properties not only of the parent bed material, but also sand cap, AquaBlok, coke breeze, and potentially other cap materials.

There are a number of potential enhancements that could be made to the SFM framework to further increase the utility and flexibility of the model with regard to simulation of cap performance. Possible improvements to the SFM's representation of ebullition processes, resuspension processes, and spatial complexity are discussed below.

- Ebullition Process: The ability of the SFM to represent microbial-generated gas ebullition could be improved by allowing the user to specify a constant or time-variable ebullition rate that would then affect 1) resuspension rates and/or critical shear stress of surficial sediments, and/or 2) adsorption and absorption of contaminant mass to individual gas bubbles and subsequent transport to the overlying water column. These enhancements to the model structure would require that results of site-specific experiments be available to parameterize the ebullition rate and associated effects on other process rates.
- Resuspension: In addition to directly representing the effects of ebullition on resuspension rates, a more detailed resuspension algorithm could be incorporated into the model to represent flow-induced resuspension that includes armoring and is dependent on cap material characteristics. This improvement, along with explicit simulation of water column processes (see below), would provide a fully dynamic simulation of sediment transport processes affecting the sediment bed in different locations.
- Spatial Complexity: The current application of the SFM was configured as a one-dimensional model of the sediment bed, with water column conditions considered as a set of boundary conditions. However, the model could readily be extended to couple a dynamic simulation of hydraulics and contaminant transport and fate in the water column to the existing sediment bed model. This improvement would be particularly useful for applications to sites where flow-induced resuspension events are important and/or recontamination from the water column is a key concern. In addition, incorporating the SFM into a spatially discrete, whole system model would allow the framework to represent spatial variability in process rates, such as groundwater seepage and ebullition rates.

Although the model capabilities described above were not critical for the Anacostia River application developed for this project, they could be potentially important for other sites where capping technologies are under consideration. For example, the presence of significant ebullition or resuspension rates could necessitate the need for a more direct and detailed accounting of the effects of these processes on contaminant flux. Incorporating additional spatial complexity in the model would allow for a more comprehensive simulation of contaminant transport and fate for sites with complex hydraulics and/or contaminant loading conditions. A more spatially-resolved model would also permit evaluation of cap stability for extreme events, such as a 100-year flood event.

8. REFERENCES

- Adriaens, P., M.-Y. Li, and A. M. Michalak. 2006. Scaling methods of sediment bioremediation processes and applications. *Eng. Life Sci.*, 6(3): 217–227.
- Apitz, S.E., Davis, J.W., Finkelstein, K., Hohreiter, D.L., Hoke, R., Jensen, R.H., Jersak, J., Kirtay, V.J., Mack, E.E., Magar, V., Moore, D., Reible, D., Stahl, R. (2002) Critical Issues for Contaminated Sediment Management, MESO-02-TM-01.
<http://meso.spawar.navy.mil/docs/MESO-02-TM-01.pdf>
- AquaBlok, Ltd. 2004. “Test Report #3: Bench-Scale Hydraulic Conductivity of Typical FW AquaBlok™ Formulations in Fresh Water.”
- Chan, K.S. and Bentley, S.J. 2004. “Result of Geochronological Analyses of Anacostia River Multicores”, Louisiana State University Coastal Studies Institute.
- Chil`es, J.P. and P. Delfiner. 1999. *Geostatistics: Modeling Spatial Uncertainty*. Wiley Series in Probability and Statistics- Applied. John Wiley & Sons, Inc.
- Cressie, N. 1993. Aggregation in geostatistical problems. In A. Soares, editor, *Geostatistics Tr´oia ’92*, volume 1, pages 25–36, Dordrecht, the Netherlands. Kluwer Academic Publishers.
- Englund, E.J. and N. Heravi. 1994. Phased sampling for soil remediation. *Environ. Ecol. Stat.*, 1:247–263.
- Goovaerts, P. 1998. Geostatistical tools for characterizing the spatial variability of microbiological and physico-chemical soil properties. *Biol. Fertil. Soils*, 27 (4):315–334.
- Himmelheber, D. and Hughes, J. 2005. “Complete tetrachloroethene dechlorination in Anacostia River Sediment”, SETAC 26th Annual Meeting in North America, Baltimore, Maryland, USA, November 13-17, 2005.
- Horne Engineering Services, LLC (Horne). 2003a. “Basis of Design for Comparative Validation of Innovative ‘Active Capping’ Technologies, Anacostia River.” Revised draft report prepared for the Hazardous Substance Research Center. Washington, DC. November.
- Horne Engineering Services, LLC (Horne). 2003b. “Site Characterization Report for Comparative Validation of Innovative ‘Active Capping’ Technologies, Anacostia River.” Revised draft report prepared for the Hazardous Substance Research Center. Washington, DC. December.
- Horne Engineering Services, LLC (Horne). 2004. “Cap Completion Report for Comparative Validation of Innovative ‘Active Capping’ Technologies, Anacostia River.” Revised draft report prepared for the Hazardous Substance Research Center. Washington, DC. December.
- Horne Engineering Services, LLC (Horne). 2007a. “Final Month 18 Monitoring Report Comparative Validation of Innovative ‘Active Capping’ Technologies.” Report prepared for the Hazardous Substance Research Center. Washington, DC. May.

- Horne Engineering Services, LLC (Horne). 2007b. "Final Month 30 Monitoring Report Comparative Validation of Innovative 'Active Capping' Technologies." Report prepared for the Hazardous Substance Research Center. Washington, DC. September.
- Hughes, J.B., Valsaraj, K.T., and C.S. Wilson. 2004. "In-Situ Containment and Treatment: Engineering Cap Integrity and Reactivity." Proposal to EPA for Grant #R819165-01-0.
- Isaaks, E.H. and M. M. Srivastava. 1989. An Introduction to Applied Geostatistics. Oxford University Press.
- LimnoTech. 2006. "Review and Evaluation of Significance and Uncertainty of Sediment – Water Exchange Processes at Contaminated Sediment Sites." Report developed for the University of Michigan. February.
- Mackay, D., W.Y. Shiu, and K.-C. Ma. 1992. "Illustrated Handbook of Physical-Chemical Properties and Environmental Fate for Organic Chemicals: Volume II – Polynuclear Aromatic Hydrocarbons, Polychlorinated Dioxins, and Dibenzofurans." Lewis Publishers. Chelsea, MI.
- McNeil, J., Taylor C., and Lick, W.J. 1996. Measurements of Erosion of Undisturbed Bottom Sediments, *Journal of Hydraulic Engineering*, 122(6) 316-324
- National Research Council. (NRC). 1997. Contaminated Sediments in Ports and Waterways: Cleanup Strategies and Technologies. National Academy Press, Washington DC, 295 p.
- Palermo, M.R., Thompson, T.A., Swed, F. 2002. White Paper No. 6B – In-Situ capping as a remedy component for the lower Fox River. Response to a document by the Johnson Company: Ecosystem-based rehabilitation plan – An integrated plan for habitat enhancement and expedited exposure reduction in the lower Fox River and Green Bay. December 2002.
- Ravens, T.R. and Gschwend, P.M. 1999. Flume Measurements of Sediment Erodibility in Boston Harbor, *J. Hydr. Eng.*, 125(10), 998-1005.
- Ravens, T.R. 2007. Comparison of Two Techniques to Measure Sediment Erodibility in the Fox River, Wisconsin, *J. Hydr. Eng.*, 133(1) 111-115)
- Thibodeaux, L.J. and D. Mackay. 2009. "Chapter 11: Advective Pore Water Flux and Chemical Transport in Bed-Sediment" in "Handbook of Environmental Chemodynamics Mass Transport Coefficients." Draft manuscript.
- USEPA. 1993. "The Water Quality Simulation Program, WASP5 – Part A: Model Documentation." Athens, GA. September.
- USEPA. 2005. Contaminated Sediment Remediation Guidance for Hazardous Waste Sites. Washington, DC.
- Yuan, Q., K.T. Valsaraj, D.D. Reible, and C.S. Willson. 2007. "A Laboratory Study of Sediment and Contaminant Release during Gas Ebullition." *J. Air and Waste Management* 57(9), 1103-1111.

APPENDICES

- A. Literature Review “Review and Evaluation of Significance and Uncertainty of Sediment – Water Exchange Processes at Contaminated Sediment Sites”.
- B. Excel Spreadsheets of Flux Calculations
- C. List of Publications and Presentations

Review and Evaluation of Significance and Uncertainty of Sediment – Water Exchange Processes at Contaminated Sediment Sites



Prepared for:

University of Michigan

September 23, 2005

DRAFT



Limno-Tech, Inc.

Excellence in Environmental Solutions Since 1975
Ann Arbor, MI

TABLE OF CONTENTS

1. Introduction	1
1.1 Objective.....	1
1.2 Scope of Review	1
2. Summary of Review and Evaluation	3
2.1 Major Findings.....	3
2.1.1 Partitioning.....	4
2.1.2 Particle Deposition and Erosion.....	5
2.1.3 Processes Affecting Non-Resuspension Related Mass Transfer from Sediments to Water	6
2.1.4 Biotransformation.....	10
2.2 Overall Significance and Relative Uncertainty.....	10
Appendix A: Partitioning	12
Appendix B: Solids Deposition and Erosion.....	26
Appendix C: Ebullition	42
Appendix D: Groundwater Seepage	60
Appendix E: Non-resuspension Mediated Sediment Mass Transfer and the Role of Bioturbation	78
Appendix F: Biochemical Transformations	114

LIST OF FIGURES

Figure 1. Surface sediment processes that affect natural attenuation and <i>in situ</i> remediation.....	2
Figure 2. Increasing complexity of numerical models.....	3
Figure A1: Conceptual fate and transport model for hydrophobic organic compounds.....	14
Figure C1. Gas bubble generation processes and the impact of gas bubbles on sediment and contaminant stability	45
Figure C2. Ebullition rates reported in the literature.	50
Figure C3. Ebullition fluxes as measured by Strayer and Tiedje, 1978 in a Michigan freshwater lake.	53
Figure C4. Distribution of hourly ebullition rates over the course of 1-2 days. (data from Joyce and Jewell, 2003).	55
Figure D1: Distribution of Seepage Rate Measurements.....	73
Figure D2: Groundwater Seepage Flux: Chemical Stability Map for PCB.	74

LIST OF TABLES

Table 1. Representative Rates and Attenuation Half-Times	12
Table 2. Overall Assessment of Process Significance.....	13
Table A1: Estimated Partition Coefficient Values for Several Compounds.....	19
Table C1. Ebullition rates reported in the literature.	50
Table D1: Reported Measurements of Seepage Rate	72
Table E1: Estimated Molecular Diffusivities for Selected Contaminants	86
Table E2 Biodiffusion Coefficients and Depths.....	100

1. INTRODUCTION

This document contains a report of the literature review and evaluation performed to address the first objective of the University of Michigan project supported by the Department of Defense/USEPA/Department of Energy Strategic Environmental Research and Development Program (SERDP). The project is entitled “Integrating Uncertainty Analysis in the Risk Characterization of In-place Remedial Strategies for Contaminated Sediments.” Limno-Tech, Inc. is a sub-contractor to the University of Michigan and is tasked with conducting this review and assessment.

1.1 OBJECTIVE

The objective of this sediment process review and evaluation is:

To identify data and information needs to help decision-makers most effectively use existing fate and transport frameworks in determining site suitability for in situ remedies, and to identify those processes for which the greatest uncertainties exist.

Basically, this objective seeks to review:

- What we know about those processes that affect the potential for a site to be remediated by an *in situ* technology;
- How we conceptualize and model those processes;
- What is the relative importance of each process in the decision-making;
- What is the relative importance of each process in site risk reduction; and
- What are the data/information gaps and greatest uncertainties in our ability to quantify the rate and extent of each process in sediment remediation.

In this context, we ask the basic question: *Where would an increase in data and a reduction in uncertainty provide the most utility in making decisions and in successful forecasting of a system's response to in situ remedies?*

In selecting the processes to review, we assume that, for sites being investigated for sediment remediation, risk is controlled by the concentration and bioavailability of the chemicals of concern in the surface sediment layer (upper mixed layer) of the system, or transported to the surface layer. Therefore, we reviewed those processes governing exposures to and losses from surficial sediments. We also have focused on the role of those processes in marine and estuary environments, and we have considered how those processes operate in both natural and capped systems.

1.2 SCOPE OF REVIEW

Given the above objective, we reviewed the following processes:

- Partitioning of chemicals of concern in surface water and sediments and its effect on bioavailability and fate and transport processes of concern;
- Particle mediated transport by deposition and resuspension (sediment accumulation and scour);

- Gas formation and ebullition in sediments and its effect on sediment and chemical transport and stability;
- Groundwater seepage and its effect on mass transport in surficial sediments and resulting exposure;
- Non-resuspension-mediated chemical mass transfer from surface sediments and the role of bioturbation; and
- Biochemical processes in surface sediments and their role in contaminated sediment natural recovery and *in situ* remediation.

Figure 1 provides an illustration of the processes of concern in this review in terms of their potential for increasing or decreasing the exposure of a chemical of concern via the surface sediments of a system.

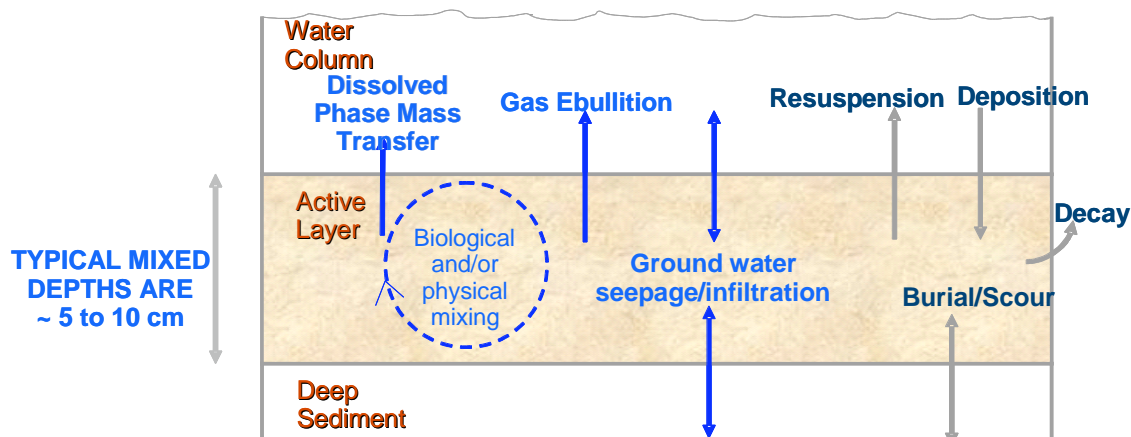


Figure 1. Surface sediment processes that affect natural attenuation and *in situ* remediation.

In conducting the reviews on these six processes, we limited our review of each process to the following topics:

- Provide a statement of the theoretical understanding of the process;
- Make a judgment of the adequacy of site-specific information on the process at a typical contaminated sediment site;
- Determine how the process is mathematically represented in current fate and transport models for contaminated sediments exposure; and
- Present the range of rates for the process that is typically observed and make an assessment of the prediction uncertainty for that process for *in situ* remedial outcomes.

The following section contains a synthesis of the findings of the individual reviews and a comparison of the processes in terms of their significance and overall prediction uncertainty. The individual reviews for each of these processes are presented in Appendices A-E.

2. SUMMARY OF REVIEW AND EVALUATION

2.1 MAJOR FINDINGS

There is a range of complexity of numerical models used for assessment of time-dependent exposure and risk at a contaminated sediment site under natural attenuation conditions and under alternative remedial actions. Figure 2 is a representation of four tiers of model complexity. The Tiers represent successively more mechanistic approaches, supported by higher data resolution and addressing more complex management questions. The process review in this report assumes that a representation of each process is being considered explicitly in the predictive analysis, as in Tiers 2- 4, rather than implicit representation that is assumed in Tier 1. The level of complexity used for a given site will be governed largely by the resources available for site characterization and remedial assessment, which in turn is usually determined by an estimate of the magnitude and complexity of the site and its remediation. It is very important to recognize that as model complexity increases, the level of temporal, spatial, and process resolution of data that must be collected to support (provide model input, calibration, and validation) the model must also increase in a commensurate fashion. However, if there are sufficient data to support an increase in model complexity (as defined by increased spatial, temporal, and process resolution), this will generally increase the utility of the model in terms of the complexity of the management questions that can be addressed and the accuracy with which those questions can be answered (i.e., reduction of uncertainty). Our desire in conducting this process review was to obtain insights into what can be gained in terms of increased model predictive confidence by identifying the most significant processes governing a system's response to *in situ* remediation and by increasing the understanding and data for those processes.

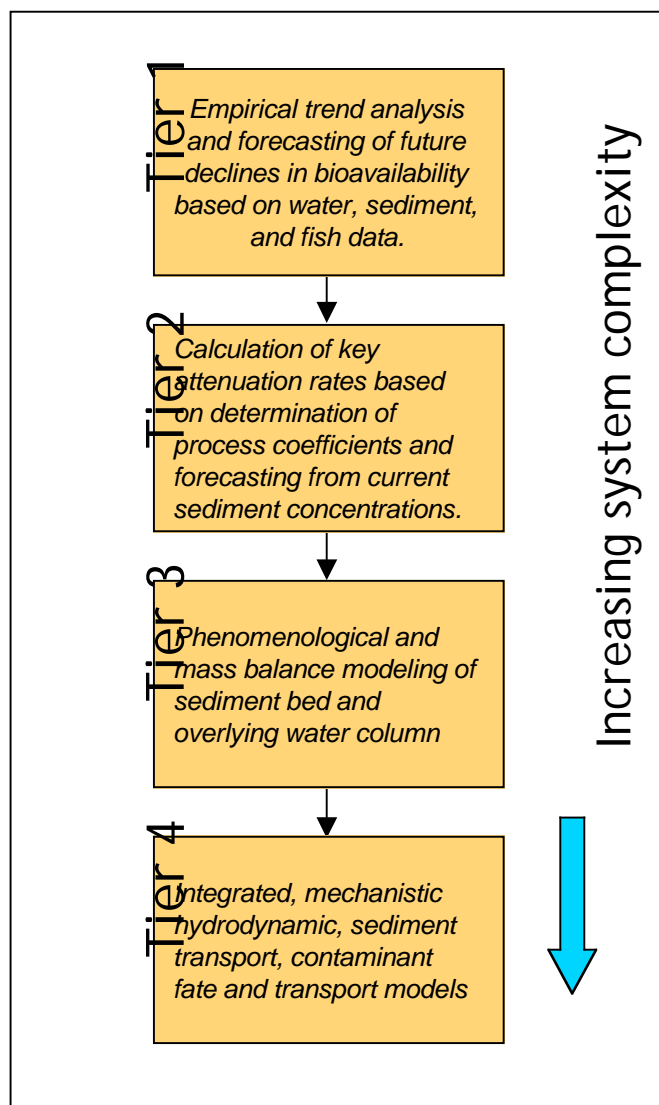


Figure 2. Increasing complexity of numerical models.

There are a few general statements that can be made regarding our ability to predict the response of a system to alternative *in situ* remedial technologies. First and foremost, none of the processes included in our models is well enough theoretically understood to provide a completely mechanistic mathematical formulation and to parameterize that process formulation on the basis

of simple characteristics of the system and chemicals of concern within that system. Instead, process representations are in general semi-mechanistic. We formulate the process to be as consistent with our theoretical understanding as possible in terms of how the process rate and extent depends on system parameters. For example, cohesive sediment resuspension is known to be a function of bottom shear stress, sediment porosity, and sediment bulk density; but the coefficients for those determinants of resuspension must in general be determined by site-specific sediment erosion experiments. In other words, we must rely on site-specific process rate measurements and overall model calibration to produce a model that can be effectively used to forecast the response of a contaminated site to alternative remedial options.

The following is a summary of findings for each process of concern, with respect to their relative importance and uncertainty in determining suitability for *in situ* remedies.

2.1.1 Partitioning

Theoretical Process Understanding: Most chemicals of concern in contaminated sediment sites are hydrophobic; therefore, they have a propensity to partition to particulate matter. The degree to which contaminants can desorb from particles determines the mass available for biota exposure, as well as the rate of transport out of the system from other processes. Research shows that the partitioning behavior of the contaminant present can be influenced by a variety of factors, including chemical composition, sediment size and composition, hydraulics and hydrodynamics, and water chemistry. Often, a 3-phase partitioning approach is used, where the fraction in the dissolved phase is disaggregated between sorbate bound to dissolved organic matter and truly dissolved sorbate. The 3-phase approach has advantages in relating partitioning to bioavailability, but dissolved organic carbon concentrations are often very small and difficult to measure. Most fate and transport models assume adsorption and desorption kinetics to be in instantaneous equilibrium. This assumption may be adequate when exposure times are long and the hydraulics of the system is relatively stable. However, considerable research has shown that desorption kinetics in natural systems are often quite slow (e.g., on the order of weeks to years to reach equilibrium) and significantly differ from theoretical predictions. Therefore, the equilibrium assumption may not always be valid, particularly in cases of high solute turnover and complex biotransformation processes. Applying a non-equilibrium partitioning function will generally result in a significantly reduced estimate of the concentration in the dissolved phase, when compared to the result of an instantaneous equilibrium model.

Adequacy of Typical Site-Specific Information: Adequate estimation of the partitioning behavior of contaminants requires site-specific data, including physiochemical properties of any sorbate present, sediment characteristics, and water chemistry. Although extensive literature exists documenting various theoretical properties of many contaminants, the actual site conditions can vary significantly, and are often more complex. Site-specific desorption analyses of sediment and water column samples are routinely conducted, and can greatly improve the characterization of the partitioning, and therefore, contaminant mass transfer behavior.

Representation in Leading Fate and Transport Models: Either 2- or 3-phased partitioning approaches can be implemented with the WASP, EFDC, and AQUATOX modeling frameworks. Standard applications of WASP and EFDC assume equilibrium partitioning, while AQUATOX assumes non-equilibrium partitioning.

Uncertainty: Accurate modeling of the fate and transport of HOCs depends greatly on appropriate characterization of the site conditions as well as the physiochemical properties of contaminants of concern. Site-specific data are often limited, requiring assumptions regarding the partitioning coefficients. The use of non-site-specific partitioning data can contribute significant uncertainty to fate and transport modeling, and the extent of this uncertainty is rarely evaluated. Laboratory analysis of samples collected from both the water column and sediment bed of the contaminated site is required for accurate representation of the in-situ partitioning, but even when these are available there is uncertainty associated with translation from the laboratory to behavior at field scale. More complex models tend to have more input data requirements. Uncertainty in the necessary model input data will lead to uncertainty in predictions.

2.1.2 Particle Deposition and Erosion

Theoretical Process Understanding: Considerable research has been conducted in this area, but much of the theory has been developed using non-cohesive sediments, which are of less relevance than cohesive sediments for understanding contaminant fate and transport. According to Stokes Law, particle settling is dictated by particle diameter and density, but important factors causing non-ideal settling include particle shape and concentration, flow velocity and turbulence, and flocculation. Flocs formed by fluid shear and differential settling differ in time to form, character, and settling rates: differential settling is slower and forms larger flocs with lower settling velocities. Deposition onto and attachment to the sediment bed have been described as probabilistic processes that are affected by turbulence at the sediment-water interface and by cohesiveness of the solid material. Sediment scour depends on hydraulic shear stress rising above a critical level, sufficient to dislodge particles. Scour and resuspension of non-cohesive sediments are well understood as functions of particle diameter, but widely applicable relationships predicting cohesive sediment scour have not yet been developed, requiring development of site-specific information. Cohesive sediment scour has been observed to depend on sediment bulk density, surface and porewater chemistry, algal colonization, and gas formation, in addition to bottom shear velocity. Estuary resuspension is most often driven by tidally-induced velocities, so that periodic resuspension and deposition cycles occur as a function of tidal cycles. Most often the net deposition is not significant, but is greatest in the region of the maximum salinity gradient, which leads to what is known as a turbidity maximum.

Adequacy of Typical Site-Specific Information: Site-specific distributions of suspended sediment particle sizes can be inexpensively obtained, and are often available for use in fate and transport model development. However, suspended solids calibration data alone will not uniquely constrain the relative settling and resuspension fluxes that determine the water column suspended solid concentrations; and this is important because it is the relative settling and resuspension fluxes that determine the net movement of particle-associated contaminants between bottom sediments and overlying water.

For cohesive sediments, we are still at the point where deposition and resuspension rates must be measured on a site-specific basis in order to adequately constrain particle-associated contaminant fluxes between water and bottom sediments. Actual sediment deposition rates, or the non-ideal factors that affect them, are much less likely to be known, as are data on floc formation and actual deposition rates of particles under varying conditions. Continuous flow records are

available to estimate frequencies and magnitudes of high-flow events for most rivers. Site-specific scour measurements have been conducted at numerous sites, using *ex situ* and *in situ* flumes of various designs. A wide range of results has been found with the different flume types, spanning orders of magnitude. Net deposition rates can also be inferred from column studies and dredging records. Suspended solids loads, instream concentrations, and deposition and resuspension rates are often less thoroughly studied and documented than contaminant concentrations, but are necessary to constrain estimates of net solids deposition. Its two components (deposition and erosion) cannot be individually constrained because of their simultaneous nature, and can only be estimated by controlled experimentation.

Representation in Leading Fate and Transport Models: Both deposition and resuspension rates are represented phenomenologically in models, requiring site-specific rate measurements to parameterize the process formulations. In WASP and EFDC applications, multiple particle size categories are typically used to capture deposition variability, with chemical partitioning also varying by particle size. Settling rates can also be varied by water-column segment, reflecting differences in flow regimes. WASP can also be linked to a high-resolution hydrodynamic model. In EFDC, this linkage is built into the modeling framework.

Uncertainty: The main uncertainties in deposition processes are associated with particle size distributions and shapes, the degree of particle aggregation/disaggregation as a function of shear stress and particle properties, and the effects of fluid shear and bottom roughness on deposition. The main uncertainties for erosion (resuspension) process include the effects of depth and associated consolidation on critical shear stress, and the true resuspension rates of cohesive sediments with a range of compositions, ranging from virtually all clay and fine silt with high organic content to a significant fraction of sand but still enough clay/silt to impart cohesive properties. The literature includes a very wide range of estimates for these parameters, reflecting potential measurement artifacts and the generally unsettled state of measurement technologies. Additional sources of uncertainty include armoring processes and the extent to which erosion rates change over time and amount of material eroded, and quantifying the effect of sediment porosity on resuspension, including the impact of gas bubble formation as it affects sediment column stability.

2.1.3 Processes Affecting Non-Resuspension Related Mass Transfer from Sediments to Water

Mass transfer between the sediment bed and the overlying surface water can be attributed to a wide range of processes. Because hydrophobic contaminants adsorb preferentially to sediment solids, resuspension can account for much of the contaminant sediment-water column mass transfer that occurs under ambient conditions. Processes contributing to resuspension include:

- flow event-driven scour;
- particulate transport due to benthic activity; and
- physical disturbance from wind-driven waves, fish activity, or human activity.

However, experience at several large contaminated sediment sites has found that non-resuspension-related processes can contribute significantly to contaminant mass transfer. Contributing processes include:

- direct desorption from surface sediments to the water column;
- molecular diffusion of dissolved phase or colloid-bound porewater PCB;
- gas ebullition;
- groundwater advection through the sediment bed;
- hydrodynamically-induced advective pumping through the near-surface interstices in the sediment bed;
- biologically-enhanced porewater transport within the sediment bed and at the sediment-water interface; and
- emergence and uprooting of macrophytes.

Direct desorption into the water column is a partitioning process, and is covered by the review of partitioning. Three additional processes are extensively reviewed below: gas ebullition, groundwater advection, and diffusive mass transport as enhanced by bioturbation.

2.1.3.a Gas Ebullition

Theoretical Process Understanding: - The total flux of contaminants due to gas ebullition across the sediment-water interface reflects the following coupled processes:

- Gas generation and consumption;
- Gas bubble formation and growth;
- Gas bubble migration and escape;
- Three-phase partitioning between solid, gas and aqueous phases in voids, tubes, and the water column, and advection to the atmosphere;
- Physical transport of particles carrying contaminants by microcurrents in the wake of gas bubbles, and
- Resuspension as enhanced by the lower bulk density of gassy sediments.

Research indicates that bubble formation is highly variable on a diurnal and seasonal basis, with the rate ultimately limited by supply of organic matter to sediments. Gas ebullition is promoted by high organic carbon influx, methanogenic activity, high sediment temperature, low atmospheric and hydrostatic pressure, low rates of bioturbation and groundwater seepage, and unconsolidated, fine-grained sediment texture. Gas bubble formation and ebullition tend to strip chemicals from porewater through partitioning to bubbles, to mix surface sediments, and to reduce measured sediment stability by increasing porosity. A study of one contaminated site estimated that a 3-foot-thick sand cap would be necessary to completely suppress gas ebullition.

Adequacy of Typical Site-Specific Information: A wide range of gas ebullition rates has been reported in the literature, spanning at least four orders of magnitude, depending on the physical system investigated. It is not clear which processes and parameters affect this spread. Site-specific rates are not generally available for contaminated sites.

Representation in Leading Fate and Transport Models: The effects of gas ebullition are not simulated in a mechanistic fashion by either WASP or EFDC. Rather, ebullition and other processes are lumped into an enhanced diffusive sediment-water exchange rate that is typically determined from site-specific sediment and water-column data. HEM3D is an extension of EFDC that allows the modeling of methane generation. HEM3D can compute the total gas release from sediments, but without simulating the movement of a separate gas phase. DELWAQ, which was developed by Delft Hydraulics, models sediment diagenesis and

explicitly includes ebullition and its effects on contaminant transport and sediment bulk properties. DELWAQ does not compute water movement, requiring a linkage with a model of the water column.

Predictive Uncertainty: Large knowledge gaps exist about the ebullition process, particularly with respect to the mechanistic/ theoretical aspect of processes and empirical measurements of rates and their dependence of environmental factors. The greatest uncertainties surround the process of bubble formation and growth, and the physical transport of contaminants. Bubble sizes and residence times need to be better understood in order to properly estimate the extent of contaminant partitioning into the gas phase. The rate and extent to which migrating bubbles mix sediments is also an important uncertainty. Because gas generation rates are the driving force behind ebullition, it is important to better define the microbial, chemical and physical factors that affect it on all spatial and temporal scales. Diurnal, seasonal and weather related variabilities, as well as spatial variabilities, all contribute to predictive uncertainty. The interaction between groundwater seepage and ebullition is also not well enough understood. Reducing these uncertainties in process understanding and quantitative effects would greatly facilitate the incorporation of ebullition into existing frameworks.

2.1.3.b Groundwater Seepage

Theoretical Process Understanding: Contaminant transport through the groundwater-surface water interface (GSI) is governed by a combination of complex hydraulics in and around the sediment bed, and a transport environment in the sediment bed that frequently exhibits sharp gradients in temperature, salinity, redox chemistry, biological population, and physical disruption. Mechanisms of groundwater flow and exchange with surface water can vary significantly from free-flowing river environments, to lakes and impoundments, to coastal environments, and directionality of exchange can vary across reaches or even at a scale of meters. Where surface water concentrations are significantly lower than porewater concentrations, the bulk exchange coefficient is essentially equal to the Darcy velocity. The porewater concentration may be less than expected based on the solid-phase concentration, where transport through the sediment bed is too rapid to allow equilibrium to be reached.

Adequacy of Typical Site-Specific Information: Estimation of groundwater mediated fluxes requires measurement of groundwater seepage and associated contaminant porewater concentrations, both of which present significant challenges as have not been measured in many systems. Data show a wide range of measured seepage rates, spanning more than four orders of magnitude. In general, it appears that the highest seepage rates are associated with the highest conductivity formations (sands and coarse sands), and lower rates of seepage are associated with lower conductivity silts and silty sands. Methods that integrate seepage estimates over a larger scale tend to show median seepage rates that are lower than those obtained by point measurements, possibly due to the effect of averaging out localized high-rate seeps. The most detailed studies of porewater concentrations also show a very high degree of spatial variability, even on a scale of meters.

Representation in Leading Fate and Transport Models: Models of the GSI are not well developed, and are often lumped into an overall mass transfer flux that includes a variety of mechanisms that cause overall sediment porewater chemical flux to the overlying water column.

The level of representation is limited by the level of understanding of processes and the limited data available for most sites. Model developers have typically developed either groundwater or surface water models, with rough linkages through source terms, without representation of the temporally and spatially dynamic nature of the GSI. The groundwater model has recently been linked to surface water models DAFLOW and SFR1, allowing for some dynamic interactions with these limited surface water tools.

Predictive Uncertainty: The high degree of spatial heterogeneity and variability of seepage fluxes and porewater concentrations implies a high degree of uncertainty in local contaminant fluxes, although this uncertainty is reduced at a more integrated spatial scale. An analysis of observed ranges of seepage fluxes and distribution coefficients for PCBs indicates that contaminant fluxes would be significantly reduced by a low permeability cap, and would be further reduced if the cap contained adsorptive materials, and that these conclusions hold across the range of site-specific parameter values.

2.1.3.c Diffusive Mass Transfer and Bioturbation

Theoretical Process Understanding: Diffusive mass transport of porewater contaminants across the sediment-water interface is restricted by the thickness of the benthic boundary layer, which is very difficult to either measure or to relate to system properties. Bioturbation, which encompasses a diverse set of mixing processes mediated by benthic organisms, is generally thought to be the most important mechanism for reworking sediments and releasing porewater contaminants in sediments. Bioturbation increases flux by one to two orders of magnitude over molecular diffusion alone. The depths of bioturbation in freshwater and marine sediments are typically less than or equal to 10 cm and 30 cm, respectively, but are highly variable over space and time. Bioturbation is controlled by a variety of biotic (organism size and seasonal life cycles, population density, deposition of organic matter, and species diversity) and abiotic (temperature, sedimentation and erosion conditions and sediment chemistry) factors. The importance of these multiple factors coupled with the spatial and temporal heterogeneity of benthic communities has made it difficult to determine which factors are most important in driving biological mixing.

Adequacy of Typical Site-Specific Information: Aside from population densities of benthic organisms, process-related parameters are typically unknown for specific sediment sites. Mixing depths can be inferred indirectly from radioisotope core profiles and sediment x-rays and photography. Significant cost can be incurred to characterize a large site, due to the likelihood of spatial heterogeneity and the high cost of radioisotope analysis.

Representation in Leading Fate and Transport Models: Mechanistic representations of bioturbation are absent in WASP and EFDC. Site-specific biodiffusion coefficients are typically included in lumped diffusions terms, with coefficients determined by calibration to water-column data. Mechanistic models of bioturbation have also been developed, reflecting the multiple mechanisms by which various benthic organisms cause vertical mixing of sediment contamination.

Predictive Uncertainty: Chemical transport within the upper layers of bed sediments is a very complex process that will continue to challenge the efforts of environmental chemists, benthic biologists, and engineers. Aside from radionuclide tracer data, the laboratory and field data needed to verify mechanistic models for a specific site are usually very limited. While molecular diffusivity can be predicted with reasonable accuracy based on chemical characteristics and

sediment porosity, biodiffusion is much more difficult to predict without extensive knowledge of local benthic populations and processes. Biodiffusion releases to the water column at rates excluding molecular diffusion must therefore be considered unless ruled out by site-specific benthic studies.

2.1.4 Biotransformation

Theoretical Process Understanding: Biochemical transformation processes can occur due to chemical and biological processes. Biodegradation can occur due to growth metabolism or catabolism. For environmental transformations, redox conditions are particularly important because of their determining role in the microbial ecology and energetics, and sediments tend to be highly anaerobic below about 0.5 cm of depth. Biogenic gas production may also affect contaminant partitioning and sediment stability. For PCBs and other persistent sediment contaminants, rates of degradation are generally very slow, so that biodegradation is not generally a quantitatively important remediation process. However, biotransformations may be important for converting chemical to more labile, mobile forms, and may also decrease or exacerbate toxicity, altering risk without significantly changing total concentration.

Adequacy of Typical Site-Specific Information: There is significant variability in biotransformation potential from site to site, and transformation rates are highly dependent on the bioavailability of contaminants, as well as the site at which data were collected. Data are rarely available over sufficiently long spatial scales and in sufficient spatial-, temporal-, and congener-level resolution to estimate transformation rates.

Representation in Leading Fate and Transport Models: Chemical and biological transformations are generally treated as pseudo-first-order processes in WASP, AQUATOX, and EFDC. Degradation is modeled as loss of the parent product, rather than transformation to a specified daughter product. Differential decay rates may be specified by model segment.

Predictive Uncertainty: The leading models contain simplifications and assumptions of site-specific parameters to facilitate application with limited data, generally represented as 1st-order decay rates. Given the wide range of degradation rates provided in the literature, and the hazards of translating laboratory rates to the field, there is considerable uncertainty in predicting biochemical transformation fluxes at any given site.

2.2 OVERALL SIGNIFICANCE AND RELATIVE UNCERTAINTY

To gain the most benefit from improvement of process representations one should focus on those processes to which the surface sediment response to alternative *in situ* technologies is most sensitive (i.e. where the process plays a significant role in governing the rate of change in surface sediment concentrations over time) and for which there is high degree of uncertainty/variability. For example, it does not pay to reduce process uncertainty for a process that does not significantly affect the change in exposure from surface sediments over time.

The relative significance of processes in a system-level context can best be assessed by comparing their rates on an equivalent basis. To do that we can initially compare the estimated half-time for natural attenuation of a chemical in a surface sediment layer if the process of concern is the only one leading to that attenuation (i.e., a simple washout half-time). This is not

a definitive definition of significance because the relative significance of processes and their half-time for exposure change over time may vary as a function of the particular *in situ* technology being applied. Nevertheless, a screening assessment of significance can be obtained by comparing the attenuation half-times with no remediation action. For this comparison, we assume the following common parameter values (minimum, median, maximum): bulk density: 1.0×10^5 , 2.25×10^5 , 5×10^5 g/m³; surface sediment mixed layer depth: 5, 10, 15 cm; particle density 2.0, 2.25, 2.5 g/cm³; porosity 0.8, 0.9, 0.95; equilibrium partition coefficient 10^5 , 10^6 , 10^7 cm³/g.

Estimates of process parameters determining mass transfer in sediment-surface water systems can vary over as many as three orders of magnitude, and for some processes, measurement issues and heterogeneities make it difficult to reduce this uncertainty, even with site-specific data. For this reason, a probabilistic approach is needed to quantify the uncertainty in any process and its impact on prediction. Process prediction uncertainty can be difficult to evaluate on a generic basis, but can be estimated by developing probability distributions from the rates reported in the literature. In doing so, we must recognize that the range of reported rates include both measurement error as well as the influence of all of the factors leading to stochastic variability in the environment. We used a simple Monte Carlo analysis to develop a half-time distribution for the processes of interest using estimated distributions of process-governing parameters based on our review of parameter variability and uncertainty. The characteristics of the resulting half-time distributions are presented in the table below.

Table 1. Representative Rates and Attenuation Half-Times

Process	Range of Observed Rates	Median Washout Half-time	Ratio (75%/25%) Washout Half-times
Net Sedimentation	-2 to 5 cm/y	0.5 to 15 yrs [*]	NA ^{**}
Gas Ebullition			
Gas Phase Transport (Stripping)	0 to 47 cm/d (0 to 17000 cm/y)	20,000,000 yrs ^{***}	22 ^{***}
Particle Entrainment	Unknown	Unknown	Unknown
Groundwater Seepage	0 to 125 cm/d (0 to 46000 cm/y)	3,700 yrs	25
Bioturbation	0.001 to 30 cm ² /y ^{****}	500 yrs	20
Molecular Diffusion in Porous Media	0.3 to 30 cm ² /y ^{****}	1,100,000 yrs	9
Biotransformation	Very wide (chemical-dependent) 10 ⁻⁴ to 10 ⁻⁶ /d ^{****}	55 yrs	4

^{*} Applies only when net depositional. Not a median due to unknown distribution shape.

^{**} Unknown distribution shape for the sedimentation/erosion rates

^{***} by partitioning to bubble phase (does not account for particle entrainment and diffusion enhancement)

^{****} Note that units are different from the rest in this column

An overall assessment of the relative magnitude of predictive uncertainty for the transport and transformation processes of interest can be made by combining the knowledge gained from the significance and uncertainty/variability analysis presented above with an evaluation of the other factors leading to prediction uncertainty (theoretical understanding, model representation and process parameterization, and site-specific information).

Table 2. Overall Assessment of Process Significance

Process	Theoretical Understanding (Mathematical Formulation)	Model Representation (Process Parameterization)	Site-specific Information (Process Variability and Availability of Data)	Overall Predictive Uncertainty	Process Significance
Partitioning	+++	+++	++	+++	****
Net Sedimentation	++	+++	++	++	****
Gas Ebullition	+	+	+	+	**
Groundwater Seepage	+++	++	+	++	**
Diffusive Mass Transfer, including Bioturbation	+++	++	+	++	***
Biotransformation	+++	++	+	++	**

++++ (Low uncertainty) → + (High uncertainty)

**** (High Significance) → * (Low Significance)

APPENDIX A: PARTITIONING

A1. INTRODUCTION

Contaminated sites containing hydrophobic organic compounds (HOCs) represent an exposure risk to biota in both bottom sediments and the overlying water column due to partitioning between solid and aqueous phases. Water quality managers and decision makers often use fate and transport models to assess the potential load from the contaminated sediments, and the mass transfer throughout the system. The current theoretical understanding of partitioning behavior is briefly reviewed in this section, and data needs for accurate simulation of toxic fate and transport processes in leading water quality models are discussed.

A2. THEORETICAL PROCESS UNDERSTANDING

The fate and transport of HOCs (e.g., PCBs, PAHs, heavy metals, dioxins, etc.) in aquatic environments is driven largely by partitioning between the dissolved and sorbed (solid bound) phases. The degree to which contaminants can desorb from particles determines the mass available for biota exposure, as well as the rate of transport out of the system from other processes (e.g., groundwater seepage, settling and resuspension, diffusion, etc.). Research shows that the partitioning behavior of the contaminant present can be influenced by a variety of factors, including chemical composition (Means et al. 1980, Karickhoff et al. 1979), sediment size and composition (Rutherford et al. 1992, Huang et al. 2003), hydraulics and hydrodynamics (Wu and Gschwend 1986), and water chemistry (Elzerman and Coates 1987).

Conceptual Model

In aquatic environments, HOCs can partition between the sorbed and dissolved phases at the bottom sediments and within the water column. A simple schematic of these processes is shown in Figure A1, which also includes other major source and sink terms for the compartments (e.g., settling, resuspension, diffusion, etc.). In this framework, only the fraction in the dissolved phase is transported through diffusion, while only the sorbed fraction is subject to settling. Mechanisms such as burial and resuspension act on both the dissolved and particulate fractions.

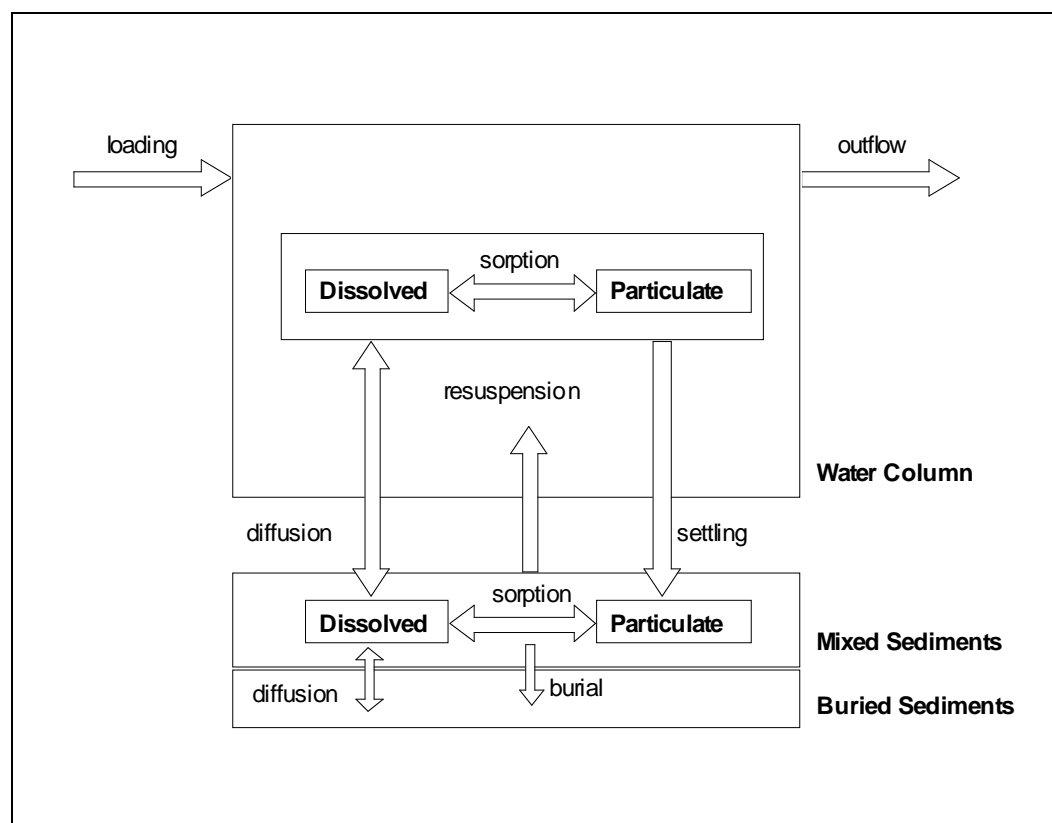


Figure A1: Conceptual fate and transport model for hydrophobic organic compounds.

In general, water quality management with regard to HOCs is focused on limiting exposure due to historically contaminated sediments (i.e., capping, dredging). As pollutant loading to aquatic ecosystems has decreased in the past decades, contaminated sediments have shifted from a sink to a potential source of HOCs. Therefore, remobilization of solids (e.g., resuspension, bioturbation) as well as partitioning at the mixed sediment layer (i.e., between bed and porewater) become increasingly important in risk assessments to benthic biota (Moermond et al. 2004). Desorption to the aqueous, and more bioavailable, phase can increase biota exposure, as can consumption of particle bound contaminants. A net flux out of the mixed sediment layer can lead to similar risks higher in the food web within the water column.

Role of Dissolved Organic Carbon

Many researchers represent the distribution of HOCs as two operationally defined phases, the sorbed fraction (the fraction retained by a filter in a laboratory analysis) and the dissolved fraction (passing through a filter). This 2-phase approach has limitations, such as the inability to differentiate between sorbate bound to dissolved organic carbon (DOC) and that in a truly dissolved phase. This approach may be particularly inappropriate for compounds known to sorb to colloidal matter, such as DOC (Sigleo and Means 1990).

Often, a 3-phase approach is used, where the fraction in the dissolved phase is further categorized between sorbate bound to dissolved organic matter and truly dissolved sorbate. Similar to the 2-phase framework, only sorbate in the particulate phase settles, while the dissolved phases are subject to diffusion. The 3-phase approach has advantages in defining bioavailability, however DOC concentrations are often very small and difficult to measure.

A2.1 EQUILIBRIUM AND DYNAMIC PARTITIONING

Most fate and transport models assume adsorption and desorption kinetics to be at equilibrium with each other (i.e., instantaneous equilibrium). This assumption may be adequate, particularly when exposure times are long and the hydraulics of the system are relatively stable (Wu and Gschwend 1986). However, considerable research has shown that desorption kinetics in natural systems are often quite slow (e.g., on the order of weeks to years to reach equilibrium) and significantly differ from theoretical predictions (Gong et al. 1998, Pignatello et al. 1993). Therefore, the equilibrium assumption may not always be valid, particularly in cases of high solute turnover (i.e., storm events, etc; Wu and Gshwend 1986). In such cases, a dynamic partitioning approach should be considered, where sorption kinetics are dependant on time and/or other system parameters. Examples of empirical representations for both equilibrium and dynamic partitioning behavior are described below.

Equilibrium partitioning is often described by empirical relationships, relating the fractions in the dissolved and sorbed phases. The simplest relationships assume linear partitioning (Karickhoff 1984), and thus the partitioning coefficient is the ratio of the concentrations in the sorbed phase to the dissolved phase (1).

$$K_p = \frac{C_s}{C_w} \quad (1)$$

where: K_p = partitioning coefficient (L^3/M);
 C_s = concentration in sorbed phase (M/M);
 C_w = concentration in dissolved phase (M/L^3);

Often, concentrations in the above equation are normalized to total suspended solids (TSS), or particulate organic carbon (POC).

Several researchers have also found relationships between the partitioning distribution and other properties of the contaminant or the environment of the system. Numerous relationships have been developed based on chemical specific properties, such as the octanol-water partition coefficient (e.g., Means et al. 1980, Karickhoff et al. 1979) and water solubility (Karickhoff et al. 1984). However, the field measurements often deviate from these theoretical predictions. In fact, in-situ concentrations have been found that differ from 1-5 orders of magnitude of those predicted by the equilibrium partitioning models (Zhou et al. 1999, Readman et al. 1987, Cullen 2002).

As previously noted, the assumption of instantaneous equilibrium between the dissolved and sorbed phases may be inappropriate, particularly in hydrodynamically unstable environments (Wu and Gschwend 1986, Gong et al. 1998). Additionally, complex biotransformation processes may preclude equilibrium partitioning even over long time periods (Bertelsen et al. 1998). In fact, even large systems such as Lake Ontario have been shown to exhibit significant disequilibrium in PCB partitioning (Cook and Burkhard 1998). Therefore, a dynamic representation of the partitioning behavior is often more mechanistically valid and may improve model performance and/or reduce predictive uncertainty. For example, applying a non-equilibrium partitioning function will generally result in a significantly reduced estimate of the concentration in the dissolved phase, when compared to the result of an instantaneous equilibrium model.

Gong and Depinto (1998) noted that desorption from contaminated sediments acts in two parts: initial fast desorption to approximately 50% equilibrium, followed by slow desorption that takes on the order of months to equilibrate. Other researchers have noted slow desorption kinetics due to diffusion from porous aggregates (Kleineidam et al. 2004). Thomann and Mueller (1987) developed kinetic relationships for sorption (2) and desorption (3) rates, with provisions for ionization.

$$Sorption = k_{sor} \cdot C_w \cdot (f_n + 0.01) \cdot a_{oc} \cdot C_m \cdot (1 \times 10^{-6}) \quad (2)$$

where: $Sorption$ = sorption rate ($M/L^3 \cdot T$);
 k_{sor} = sorption rate constant ($L^3/M \cdot T$);
 C_w = dissolved concentration (M/L^3);
 f_n = non-ionized fraction;
 a_{oc} = organic matter to carbon conversion factor;

C_m = solids concentration (M/L³);

$$Desorption = k_{des} \cdot C_s \quad (3)$$

where: *Desorption* = desorption rate (M/L³·T);

k_{des} = desorption rate constant (1/T);

C_s = solid-sorbed contaminant concentration (M/L³);

These relationships are the primary partitioning algorithms in AQUATOX (described subsequently).

A3. ADEQUACY OF TYPICAL SITE-SPECIFIC INFORMATION

Adequate estimation of the partitioning behavior of contaminants requires site-specific data, including physiochemical properties of any sorbate present, sediment characteristics, and water chemistry (Elzerman and Coates 1987). Although extensive literature exists documenting various theoretical properties of many contaminants (e.g., PCB congeners, dioxins, metals, etc.), the actual site conditions can vary significantly, and are often more complex (Pignatello et al 1993). Therefore, analysis of sediment and water column samples taken from the site can greatly improve the characterization of the partitioning, and therefore, contaminant mass transfer behavior.

Several analytical methods are available to quantify the partitioning distribution of HOCs. Most of the methods involve, in some manner, exposing sediment samples to a solute for various time periods. Samples are generally prepared with known sediment size class distributions (e.g., sieved samples), and known fractions of organic carbon (f_{oc}). After filtration, measurements of the contaminant of interest are made for both the sorbed (retained by the filter) and dissolved (passing through the filter) phases. It is important to note that the measured concentration in the filtrate may represent the fraction in both the truly dissolved phase and that which is bound to DOC (Butcher et al. 1998). Quantification of the fraction bound to DOC may require more specialized analytical methods; often concentrations in the dissolved phase are below the detection limit of some equipment. Some studies have used isotopic (^{14}C) labeling to improve sensitivity (Gong et al. 1998, Jepsen and Lick, 1999). The phase distribution measurements can be made repeatedly over time to estimate desorption rates (i.e., desorption as a function of time), or after a predetermined length of time (typically months) representing the estimated equilibrium exposure time.

The analytical methods used to assess partitioning of HOCs are generally designed to allow in-situ estimation of the phase distribution of the relevant sorbate. For example, experimentally varying the f_{oc} could create a dependant partitioning relationship allowing for an estimate of the dissolved fraction based on measured f_{oc} . Variations on other system parameters, (e.g., sediment size class distributions, temperature, pH, salinity, etc.) can lead to understanding of their relative influences. However, it is important to note that these dependencies are site-specific and may not be applicable to all situations.

Table A-1 lists the range of equilibrium partitioning coefficients for several HOCs estimated by various researchers. General notes are also included for each study, indicating the variability in site conditions and analytical methods. In most cases, a range of partition coefficient estimates is shown. Because each study is dependent on site-specific conditions, additional variation should be expected when translating these relationships to other sites.

Table A1: Estimated Partition Coefficient Values for Several Compounds.

Compounds	Kp(L/kg)	Comments	Source
Methanol	0.44	Normalized to organic carbon content	Meylen et al 1992
Napthalene	1×10^2	Water column	Thomann and Mueller 1987
Octanol	8.1×10^4	Normalized to organic carbon content	Jepsen and Lick 1999
Hexachlorobiphenyl	$7.9 \times 10^2 - 8.9 \times 10^2$	Detroit River	Jepsen and Lick 1999
Tetrachlorobiphenyl	$1.3 \times 10^4 - 2.2 \times 10^4$	Detroit River	Jepsen and Lick 1999
PCB	$2.2 \times 10^4 - 3.7 \times 10^6$	90 congeners, normalized to POC, Hudson River	Butcher et al. 1998
PCB	$1 \times 10^5 - 1 \times 10^6$	Congeners not specified, water column	Thomann and Mueller 1987
PCB	$8.5 \times 10^1 - 2.4 \times 10^5$	6 congeners, Housatonic River, jar experiments	Alkhatib and Weigand 2002
PCB	$1 \times 10^3 - 6.9 \times 10^5$	6 congeners, Housatonic River, entrainment experiments	Alkhatib and Weigand 2002
Heavy Metals	$6.3 \times 10^5 - 1.6 \times 10^6$	Cadmium, lead zinc	Boyle and Birks 1999
Heavy Metals	$1 \times 10^4 - 1 \times 10^5$	Water column	Thomann and Mueller 1987

Such laboratory studies are intended to help understand the fate and transport mechanisms at contaminated sediment sites. The partitioning coefficients and rates of adsorption and desorption kinetics can be used to drive models to predict and assess potential exposure pathways. The most robust of these models incorporate the partitioning behavior of the relevant contaminants into a hydrodynamic and hydraulic framework. However, several models are available for toxic fate and transport simulation, and they can vary widely with respect to the accommodated processes and data requirements. The validity, and ultimately the usefulness, of such models depends on the adequacy of site specific data, as well as the mechanistic representations in the model framework.

A4. REPRESENTATION IN LEADING FATE AND TRANSPORT MODELS

Several widely used modeling packages employ similar frameworks as shown in Figure 1 to predict the fate and transport of HOCs. In order to be applicable and adaptable for multiple systems, certain assumptions regarding the partitioning mechanisms are made for each modeling package. The assumed partitioning behavior and any possible implications are summarized for several modeling packages below.

- **Water Quality Analysis Simulation Program (WASP):**

WASP (and the complementary TOXI module) is probably the most widely used water quality model. The TOXI module can be used to simulate the fate and transport of multiple generalized toxic substances in the water column, as well as the sediment bed. Sorption to multiple sediment classes (both cohesive and non-cohesive) is also accommodated. Spatial and temporal variations in organic carbon content are supported.

The partitioning algorithm may be either a 2- or 3-phase partitioning approach. However, a 3-phase model requires a known distribution of DOC, which is often difficult to measure and thus becomes a calibrated term. Equilibrium partitioning is assumed, and the user is required to enter a partitioning coefficient (either solid distribution or organic carbon normalized) for each modeled contaminant, and may vary the values for either the water column or sediment bed.

Although WASP/TOXI assumes linear equilibrium partitioning, it is possible to modify the model source code to accommodate dynamic sorption and desorption kinetics. No examples of such modification were discovered in the literature review for this study.

- **Environmental Fluid Dynamics Code (EFDC):**

The toxic fate and transport routines within EFDC are very similar to those of WASP/TOXI. Multiple sediment classes are supported, and either a 2- or 3-phase partitioning model can be used. EFDC also assumes equilibrium partitioning, requiring a partitioning coefficient (either solid distribution or organic carbon normalized) for each modeled contaminant. Spatial and temporal variations in organic carbon content are also supported by EFDC.

EFDC has potentially more complex sediment transport mechanisms than WASP, being able to internally simulate settling and resuspension rates. However, it is important to note that very few toxic modeling applications have been published using EFDC. While the model is widely accepted, it is fairly new to the industry and not fully documented. The majority of published EFDC applications have been related to hydrodynamic cycling, particularly in systems with tidal influences (Ji et al. 1998). Few applications have been published utilizing

the sediment transport algorithms. In fact, LTI has noted multiple programming bugs and errors in some of the more complex sediment transport routines.

Although EFDC is relatively new and there are questions about the validity of some of the routines, it is still one of the most advanced water quality modeling tools. The framework allows 1-, 2-, or 3-dimensional hydrodynamic simulation, and the toxic and sediment transport routines are all dynamically linked.

- **AQUATOX**

AQUATOX is a general ecological risk model with the ability to simulate the fate and transport of toxic chemicals, eutrophication impacts, sediment transport, and food-web linkages. The model is limited in its hydrodynamic ability, but has the potential to link to an external hydrodynamic model, such as EFDC or the Hydrodynamic Simulation Program FORTRAN (HSPF). AQUATOX has been successfully implemented for streams, small rivers, ponds, lakes, and reservoirs.

Most applications of AQUATOX have been for simple lake or reservoir systems due to the hydrodynamic limitations. AQUATOX is limited in both spatial (single completely mixed compartment with seasonal stratification) and temporal (daily average) resolution. Although the model lacks an integrated hydrodynamic framework, it can accommodate complex chemical and biological mechanisms. The chemical fate module of AQUATOX simulates partitioning between water, sediment, and biota for up to 20 organic compounds and can accommodate several degradation processes including biodegradation, photolysis, hydrolysis, and volatilization.

AQUATOX uses a 3-phase approach for sediment-water partitioning, and is based on the organic carbon content. The limited spatial resolution of the model precludes a spatially varying organic carbon fraction; however, both particulate and dissolved organic carbon are simulated internally based on biological mechanisms.

The partitioning is always assumed to be non-equilibrium, utilizing kinetic formulations for sorption (2) and desorption (3) developed by Thomann and Mueller (1987). The partitioning algorithms also account for slow desorption into and out of organic matter and porous aggregates.

Although AQUATOX lacks a true hydrodynamic framework, it is by far the most advanced of the models reviewed here, with respect to toxic chemical fate and transport. The ability to internally simulate organic carbon cycling along with the non-equilibrium partitioning approach offers significant benefit in modeling and risk assessment of contaminated sites. However, few applications have been published using the model, the vast majority of which are simple lake/reservoir or small stream systems.

A5. PREDICTIVE UNCERTAINTY

Considerable strides have been made in the level of understanding of contaminant partitioning between sorbed and dissolved phases. There is general agreement in the literature that a 3-phase (sorbed, dissolved, and bound to dissolved organic matter) approach is the most valid representation of partitioning behavior, particularly where organic carbon content is significant. Use of a 2-phase approach may over-emphasize bioavailability due to an artificially high fraction in the dissolved phase (i.e., no differentiation between fraction bound to DOC). Additionally, an increasing number of studies are showing slow desorption rates and indicating that the instantaneous equilibrium assumption is inappropriate. Equilibrium partitioning will generally result in an over-estimation of the dissolved phase contaminant. However, representation of non-equilibrium partitioning in the fate and transport models used for site management is still rare.

Accurate modeling of the fate and transport of HOCs depends greatly on appropriate characterization of the site conditions as well as the physiochemical properties of contaminants of concern. Site-specific data (e.g., organic carbon content) are often limited, requiring assumptions regarding the partitioning coefficients. Use of estimates from other sites, such as those presented in Table A1, introduces errors due to site-specific differences in sediment and chemical characteristics. Laboratory analysis of samples collected from both the water column and sediment bed of the contaminated site is required for accurate representation of the in-situ partitioning. Organic carbon content (both particulate and dissolved) has been shown to influence partitioning at many sites, and can be simulated in some models (e.g., AQUATOX). However, more complex models tend to have more input data requirements. Uncertainty in the necessary model input data will lead to uncertainty in predictions.

A6. REFERENCES

- Alkhatib, E., and Weigand, C. 2002. "Parameters affecting partitioning of 6 PCB congeners in natural sediments." *Environmental Monitoring and Assessment*, 78:1-17.
- Bertelsen, S.L., Hoffman, A.D., Galliant, C.A., Elonen, C.M., and Nichols, J.W. 1998. "Evaluation of log K_{OW} and tissue lipid content as predictors of chemical partitioning to fish tissues. *Environ. Tox. Chem.*, 17:1447-1455.
- Butcher, J.B., Garvey, E.A., and Bierman, V.J. 1998. "Equilibrium partitioning of PCB congeners in the water column: field measurements from the Hudson River." *Chemosphere*, 36(15):3149-3166.
- Coates, J.A., and Delfino, J.J. 1993. "Sources of uncertainty in the application of the equilibrium partitioning approach to sediment quality assessment." *Water Science and Technology*, 28(8-9):317-328.
- Cook, P.M., and Burkhard, L.P. 1998. "Development of bioaccumulation factors for protection of fish and wildlife in the Great Lakes." *National Sediment Bioaccumulation Conference Proceedings*
- Cullen, A. 2002. "Comparison of measured and predicted environmental PCB concentrations using simple compartmental models." *Environ. Sci. Technol.*, 36:2033-2038.
- Elzerman, A.W., and Coates, J.T. 1987. "Hydrophobic organic compounds: Equilibria and kinetics of sorption. In *Sources and Fate of Aquatic Pollutants* (Edited by Hites, R.A., and Eisenreich, S.J.)" Am. Chem. Soc., Washington, D.C.
- Gong, Y., Depinto, J.V., Rhee, G., and Liu, X. 1998. "Desorption rates of two PCB congeners from suspended sediments – 1. Experimental results." *Wat. Res.*, 32:2507-2517.
- Gong, Y., and Depinto, J.V. 1998. "Desorption rates of two PCB congeners from suspended sediments – 2. Model simulation." *Wat. Res.*, 32:2518-2532.
- Hinton, S.W., Brunck, R., and Walbridge, L. 1993. "Mass-transfer of TCDD/F from suspended sediment particles." *Water Science and Technology*, 28(8-9):181-190.
- Huang, W., Peng, P., Yu, Z. and Fu, J. 2003. "Effects of organic matter heterogeneity on sorption and desorption of organic contaminants by soils and sediments." *Applied Geochemistry*, 18:955-972.
- Hwang, B.G., Jun, K.S., Lee, Y.D., and Lung, W.S. 1998. "Importance of DOC in sediments for contaminant transport modelling." *Water Science and Technology*, 38(11):193-199.

- Jepsen, R., and Lick, W. 1999 "Nonlinear and interactive effects in the sorption of hydrophobic organic chemicals by sediments." *Environmental Toxicology and Chemistry*, 18:1627-1636.
- Ji, Z.-G., Hamrick, J.H., and Pagenkopf, J. 2002: Sediment and metals modeling in shallow river, *Journal of Environmental Engineering*, 128, 105-119.
- Karickhoff, S.W., Brown, D.S., and Scott, T.A. 1979. "Sorption of hydrophobic pollutants on natural sediments." *Water Research*, 13:241-248.
- Karickhoff, S.W. 1984. "Organic pollutant sorption in aquatic systems." *Journal of Hydraulic Engineering*, 110:707-735.
- Kleineidam, S., Rugner, H., and Grathwohl, P. 2004. "Desorption kinetics of phenanthrene in aquifer material lacks hysteresis." *Environ. Sci. Technol.*, 38:4169-41750
- Means, J.C., Wood, S.G., Hassett, J.J., and Banwart, W.L. 1980. "Sorption of polynuclear aromatic hydrocarbons by sediment and soils." *Environ. Sci. Technol.*, 14:1524-1528.
- Meylan, W., Howard, P.H., and Biethling, R.S., 1992. "Molecular topology/fragment contribution method for predicting soil sorption coefficients." *Environ. Sci. Technol.*, 26:1560-1567.
- Moermond, C.T.A., Roozen, F.C.J.M., Zwolsman, J.J.G., and Koelmans, A.A. 2004. "Uptake of sediment-bound bioavailable polychlorobiphenyls by benthivorous Carp (*Cyprinus carpio*)."
Environ. Sci. Technol., 38:4503-4509.
- Pignatello, J.J., Ferrandino, F.J., and Huang, L.Q. 1993. "Elution of aged and freshly added herbicides from a soil." *Environ. Sci. Technol.*, 27:1563-1571.
- Readman, J.W., Mantoura, R.F.C., Rhead, M.M. 1987. "A record of polycyclic aromatic hydrocarbon (PAH) pollution obtained from accreting sediments of Tamar Estuary, UK: evidence for nonequilibrium behavior of PAH." *Science of the Total Environment*, 66:73-94.
- Rutherford, D.W., Chiou, C.T., and Kile, D.E. 1992. "Influence of soil organic matter composition on the partition of organic compounds." *Environ. Sci. Technol.*, 26:336-340.
- Sigleo, A.C., and Means, J.C., 1990. "Organic and inorganic components in estuarine colloids: Implications for sorption and transport of pollutants." *Rev Environ Contam Tox*, 112:123-147.
- Sobek, A., Gustafsson, O., Hajdu, S., and Larsson, U. 2004. "Particle-water partitioning of PCBs in the Photic Zone: a 25-month study in the open Baltic Sea." *Environ. Sci. Technol.*, 38:1375-1382.
- Thomann, R.V., and Mueller, J.A. 1987. *Principles of Surface Water Quality Modeling and Control*, Harper Collins: New York, N.Y.

- Wu, S., and Gschwend, P.M. 1986. "Sorption kinetics of hydrophobic organic compounds to natural sediments and soils." *Environ. Sci. Technol.*, 20:717-725.
- Zhou, J.L., Fileman, T.W., Evans, S., Donkin, P., Readman, J.W., Mantoura, R.F.C., Rowland, S. 1999. "The partitioning between flouranthrene and pyrene between suspended particles and dissolved phase in the Humber Estuary: a study of the controlling factors." *Science of the Total Environment*, 243/244:305-321.

APPENDIX B: SOLIDS DEPOSITION AND EROSION

B1. INTRODUCTION

Sediment settling and resuspension are sediment-water exchange processes that play an important role in determining contaminant exposures at contaminated sites, under uncontrolled conditions and after remediation. Contaminant burial is the result of particle settling at rates exceeding resuspension, typically attenuated by mixing of surficial sediments. Watershed erosion and internal biological production contribute solids for possible sedimentation, and settling is preferentially higher for the largest particles and the lowest ambient flows. At higher flows, resuspension can be initiated, resulting in sediment scour and downstream transport of solids, sorbed contaminants, and porewater. While deposition of solids may occur at downstream locations under conditions of lower energy, sorbed contaminant is subject to phase partitioning during the time that the particle is suspended in the water column, including transfer to truly dissolved and vapor phases, as well as adsorption to dissolved and colloidal carbon.

An objective of capping is to reduce contaminant exposures by minimizing resuspension of contaminated solids. This is accomplished by increasing surficial grain size, covering cohesive sediments with sand or gravel. In net depositional areas, effective upstream source control can augment the effectiveness of engineered caps by facilitating the build-up of a natural cohesive sediment cap. To estimate the reduction in potential exposures due to capping, it is important to have accurate site-specific estimates of deposition and resuspension rates under the expected range of flows and other ambient conditions, for both unremediated and capped sediments. This appendix provides an overview of our theoretical understanding of sediment settling and resuspension processes, the typical availability of site-specific information on these processes, their specification in leading fate and transport models, and the sources and magnitudes of uncertainty in model simulations of settling and resuspension.

B2. THEORETICAL PROCESS UNDERSTANDING

B2.1 SETTLING AND DEPOSITION

Solids deposition is a complex process by which particulate materials, including both individual and aggregate solids, settle from the water column and adhere to the sediment bed.

The mechanisms which describe settling and deposition are controlled by physical and chemical properties of the water column suspended solids, as well as the hydraulic conditions over the depth of the water column. Significant research has been conducted on these influencing factors and mechanics of settling. Mathematical models describing sediment transport in receiving waters have incorporated aspects of these mechanisms to varying degrees of complexity in order to describe the deposition of solids.

Physical properties which factor into the process of solids settling and deposition include:

- ❑ particle diameter, or fractal dimension for aggregate (flocculated) material;
- ❑ particle density;
- ❑ fluid (water) density;
- ❑ particle shape;
- ❑ particle concentration;
- ❑ water velocity, and turbulence; and
- ❑ sediment bed roughness.

Of these factors, the size, density, and shape of a particle all are important determinants of settling velocity, and solids concentration and turbulence indirectly affect settling velocity by influencing formation of flocs. Floc formation is also strongly influenced by particle and surface chemistry. Chemical properties which factor into the process of solids deposition include:

- ❑ particle surface chemistry;
- ❑ particle mineralogy (e.g., silt and clay content); and
- ❑ water chemistry (e.g., marine versus fresh water environments, potential for formation of precipitates, etc.)

In the simplest case, uniformly spherical particles of known diameter and density settle at highly predictable rates (or settling speeds) in accordance with Stoke's Law (Henderson, 1996), which balances drag and acceleration, namely:

$$V_s = \frac{2r^2 g(\rho_p - \rho_w)}{9\eta}, \quad \text{where} \quad (1)$$

V_s = settling velocity;
 g = acceleration of gravity;
 ρ_p = particle density;
 ρ_w = fluid density; and
 η = kinematic fluid viscosity.

Experiments show Stoke's Law to be valid for particles up to about 100 μm in diameter (d), with lower settling velocities than predicted by Stoke's Law for particles with larger Reynolds numbers ($\rho_w V_s d / \eta$). However, suspended solids in natural systems are generally neither uniform nor spherical, so their drag and therefore their settling behavior may deviate significantly from this ideal.

Generally measurable (directly or indirectly) physical properties of the solids and the water in which these are suspended effectively determine the rate at which particles settle and whether, or not, hydraulic shear forces are sufficient to keep the particles suspended in the water column. The chemical properties of the solids and the water can also influence the deposition process through particle aggregation (flocculation) and the effect this has on the effective size, density, and shape of the suspended material.

The mechanics of settling are complex and are influenced by many factors. The studies that have investigated these factors reveal that flocculated or aggregate solids and individual particles have distinct behaviors with regard to settling behavior. Therefore, the research regarding the mechanics of settling is examined within each of these two categories.

B2.1.1 Settling of Individual Particles

Although much of the suspended solids mass transported in natural aquatic systems likely exists in a flocculated state, there are still particles that are not flocculated. Examination of the settling of these particles is a necessary aspect for understanding overall solids settling behavior in aquatic systems. Some research has also been done on the settling of these individual particles. Also, in many existing models of sediment transport, an assumption of no flocculation is made in order to simplify the computational requirements of the model.

Based on experimental data obtained with real particles, Cheng (1997a) developed an empirical formula for settling velocities over a range of diameters, temperatures, and Reynolds numbers. The same calculations were also done using five previously proposed equations (Sha, 1956; Ibad-zade, 1992; Zhang, 1989; Van Rijn, 1989; and Zhu and Cheng, 1993). The proposed equation had the highest degree of predictive accuracy when each of these equations was compared to measured data. It is also applicable to a wide range of Reynolds numbers, and

predicts slightly lower settling velocities than Stoke's Law. Using the simplified equation presented in Cheng (1997a), Cheng (1997b) also developed a method to estimate "the effect of sediment concentration on the settling velocity of uniform, cohesionless particles." This hindered settling formulation allows for the lowering of settling velocity for closely spaced particles in a fluid as compared to an identical isolated particle in a clear fluid. Comparisons of the resulting method for evaluating settling velocity to experimental data from Mints and Shubert (1957) showed good agreement.

B.2.1.2 Formation of Aggregates

Although real settling velocities of discrete particles differ slightly from the predictions of Stoke's Law, the most important deviation is due to particle aggregation, or flocculation. Much of the research on mechanisms of settling examines flocculated particles and the process of flocculation, or aggregation of particles, due to the relatively greater abundance of these types of solids in natural systems, and the important effect of flocculation on settling velocity. In contrast to individual particles, flocs have much lower densities, larger specific surface areas, and fluids may flow through as well as around the aggregated particles. This section provides a brief summary of the flocculation process and reviews the research related to how the conditions under which flocs form impact floc characteristics such as size and rate of formation.

In order for flocs to form, particles must come into contact and there must be a sufficient attraction to hold them together. Clay and other very fine particles in suspension can be subject to mutual attraction, due to van der Waals forces, and repulsion, due to exposure of surface cations. The presence of anions in solution near the particle surface tends to lessen the repulsive force, promoting particle aggregation. The greater the likelihood of collisions due to mixing of the fluid, and the higher ionic strength of the fluid, the greater is the tendency for particles to combine into flocs.

Three processes can be distinguished as causes of particle collisions: Brownian motion, fluid shear, and differential settling (Ives, 1978). In theory, fluid shear is the dominant process for forming flocs of particles having similar sizes, and differential settling predominates as a process by which smaller particles aggregate with larger particles (more than about 50 μm in diameter.) Brownian motion is predominant only for the very smallest particles and is therefore of less importance. Lick et al. (1992) have developed a numerical model of floc formation that encompasses flocculation due to both fluid shear and differential settling, which provides a time-dependent expression for median floc size as a function of solids concentration and velocity gradient, or shear.

Flocs formed by fluid shear and by differential settling differ in time to form and in character. Differential settling is a slower process, due to a lower rate of particle collisions, and forms larger and more fragile flocs, with lower settling velocities. Lick et al. (1993) discuss the flocculation of fine-grained sediments due to differential settling speeds for suspended particles. Hydraulic shear effects dominate in high-turbulence areas; differential settling dominates in open waters, away from shore, and transition areas between these two situations are examined and discussed. Fine-grained, primarily inorganic sediments from the Detroit River inlet to Lake Erie were used in fresh and saltwater experiments, which showed that median particle diameters and time of formation were much greater in differential settling tests than when fluid shear was

applied. In the fluid shear tests, higher solids concentration and ionic strength were associated with more rapid floc formation and smaller steady state floc size.

Droppo and Ongley (1994) discuss flocculation in freshwater rivers with fine-grained suspended sediment. They collected suspended matter from six rivers. Big Otter Creek, Big Creek and the Grand River and its tributary the Nith River all feed into Lake Erie. Sixteen Mile Creek feeds into Lake Ontario. The final site was the St. Lawrence River at Sorel, Quebec. They found that at least 92% of the total suspended material was flocculated in these rivers. No relationship was found between either flocculation and pH or ion concentration, but bacteria and floc size was related during the spring melt.

Milligan and Hill (1998) discuss the results of a laboratory study of the significance of turbulence, composition, and concentration on maximum floc size and settling velocity for materials commonly discharged during offshore hydrocarbon development. An inverting column flocculator was used. Results indicated that turbulence and composition in tandem seem to dominate the maximal floc size.

Stolzenbach (1993) examines differential settling in the marine environment. Findings similar to those determined by the Lick et al. (1993) were found in this investigation. Scavenging efficiencies were “sufficiently large to make scavenging of small particles by aggregates an important component of particle transport throughout the oceanic water column.”

Estuary resuspension is most often driven by shear due to tidally-induced velocities, so that periodic resuspension and deposition cycles occur as a function of tidal cycles. Because of the importance of ionic strength in promoting flocculation, net deposition is greatest in the region of the maximum salinity gradient, which leads to what is known as a turbidity maximum.

In Dyer and Manning (1998), the INSSEV instrument (IN Situ SEtTLing Velocity) was used to determine settling velocity and floc size in several different estuaries. Size and dimension were affected by turbulent shear (more shear causing lower dimension and smaller size), and concentration (higher concentration causing higher dimension and larger size). However, higher concentrations were also shown to promote floc breakdown.

Grossart and Simon (1997) discuss the role of transparent exopolymer particles (TEP) in the formation of organic aggregates, referred to as “lake snow.” This paper discusses particles of a very specific type in a specific environment. Multiple mechanisms of formation were observed throughout seasons due to variations in source particles and physical conditions.

B2.1.3 Settling Speeds of Aggregates

The formation of flocs in natural systems impacts the rate at which particles settle to the sediment bed. Drag forces on a floc differ from those exerted on an individual spherical particle. Researchers have also found that, in addition to floc characteristics such as size and density, how a floc was formed (e.g. differential settling or fluid shear) influences the settling speed of the aggregates.

Wu and Lee (1998) studied the hydrodynamic drag force exerted on a moving floc and its implementation to free-settling tests. This paper described modeling efforts to determine drag coefficients on a permeable floc. Numeric evaluation was done of the hydrodynamic drag force exerted on an individual floc in a quiescent Newtonian fluid for a range of Reynolds numbers. It

was assumed that the interior fluid viscosity is the same as that for the surrounding fluid phase (Neale et al., 1973). The fluid velocity within the porous sphere was calculated using the Darcy-Brinkman law, and the surrounding Newtonian field was calculated using the Navier-Stokes equations. Permeability was parameterized using a constant β , which equals the floc diameter divided by two times the square root of the permeability. It should be noted that permeability is difficult to measure but is usually estimated from porosity values, which are determined from fall velocity measurements. Key findings of the Wu and Lee study are as follows. Floc porosity delays boundary layer separation, reducing drag. For a highly porous sphere, the drag force can be only one fifth of that for a nonporous sphere. On a log-log plot, a linear relationship exists between the settling velocity and the floc diameter. The authors state that there are some drawbacks in applying the present model to real flocs, but it is believed that the results can be used to at least qualitatively give further understanding of the free-settling process.

Johnson et al. (1996) discuss settling velocities of fractal aggregates, stating that natural flocs are fractal in nature and therefore have different scaling properties than are assumed when using Stokes' law to calculate settling velocities. The flocs in the study were generated from dyed latex microspheres in paddle mixers. They found that settling velocities were 4 to 8.3 times higher than predicted with Stokes' law for permeable or impermeable spheres. The paper also discusses using fractal dimensions to predict power law relationships between aggregate size and settling velocity based on Stokes' law. Empirical drag coefficients are determined based on study results. One drawback is that the derived settling velocity equation has constants that are likely to be not truly constant. In the end, despite possible restrictions due to assumptions, the authors state, "there is strong evidence for wide applicability of our observations."

Burban et al. (1990) measured settling speeds of flocs in fresh water and seawater, formed of natural bottom sediments from the Detroit River inlet of Lake Erie, under varying experimental fluid shears. For a given diameter, flocs formed at higher shears and sediment concentrations had higher settling speeds. The effect of sea water was to slightly increase settling speed, relative to flocs formed in fresh water. Because the experimental effect of salinity was small, they concluded that turbulence and solids concentration gradients were probably important causes of the turbidity maximum typically observed in estuaries.

As previously discussed, Lick, Huang, and Jepsen (1993) examined not only the effect of the formation of aggregates on settling, but also the relationships between floc diameter, fluid shear and settling speeds. They found that settling speeds of flocs are much larger when produced by differential settling than when fluid shear is dominant. This is primarily due to larger floc size. They also found that the settling speed increases more rapidly as a function of floc diameter when produced by differential settling.

Burd and Jackson (1997) discuss sedimentation in the presence of aggregation in oceanic surface waters. The fractal nature, structure and dimension of aggregate solids, as well as hydrodynamic interactions between them were evaluated. Expressions for sedimentation rate (or settling speed) were developed based on observed results in this study. The work done here was also based heavily upon work done previously by Farley and Morel (1986). While there are still uncertainties associated with the formulations, the results presented "extend the aggregation models used by [Farley and Morel] to include more complete coagulation kernels and the fractal nature of the aggregates."

B2.1.4 Deposition onto the Sediment Bed

The actual deposition of solids onto the sediment bed is somewhat more complex than what may be described by the settling speed of the suspended material. Turbulence at the sediment-water interface may act as a barrier to the attachment of settling materials. Suspended solids in natural aquatic systems can exhibit a wide range of properties (e.g., size, density, shape, porosity, etc.), so a portion of the material which settles through the water column may remain in suspension or become associated with bed load transport instead of depositing onto the surface of the sediment bed. Because of high fluid shear and solids concentration gradients near the sediment water interface, flocculation may be an important process affecting cohesive sediment deposition.

Krone (1962) developed the empirical concept of “probability of deposition” in order to describe the observed depositional behavior of fine-grained (cohesive) solids. Ariathuri and Krone (1976) used this concept to account for various factors (hydraulic shear and particle variability) that determine what fraction of a particulate class of solids is truly depositional. This concept has been applied in transport models for fine-grained sediments that may exist in suspension as both aggregate and individual particles (STUDH by Ariathurai and Krone 1976, SEDZL by Ziegler and Lick 1986) and has also been extended to coarser-grained (non-cohesive) sediments (Ziegler and Nisbet 1986, Gailani 1991, Jones and Lick 2001).

It is an unresolved question whether deposition and erosion of can occur simultaneously for a given cohesive particle size. Lau and Krishnappan (1994) pose the question “Does reentrainment occur during cohesive sediment settling?” Two previously proposed concepts were presented in the paper. The first is by Lick (1982), postulating that larger particles settle out while fines stay in suspension, and intermediates are both deposited and resuspended at some equilibrium rate depending on shear stress. The second is by Partheniades et al. (1968) and Mehta and Partheniades (1975). In this second view, there is no simultaneous erosion and deposition. Rather, particles settle as flocs and bond to the bed if they are strong enough, or are broken up and returned to flow without depositing. In this study, an annular flume was used with distilled water and kaolin. The results showed, contrary to Lick (1982), that particles from all size classes were deposited and simultaneous erosion and deposition did not take place. The results were consistent with Partheniades et al. (1968) and Mehta and Partheniades (1975), that there is no reentrainment after settling until shear stress increases. This second view is consistent with the “probability of deposition” approach used in many sediment transport models.

B2.2 EROSION

Sediment erosion is a process by which hydraulic shear forces at the sediment-water interface become sufficient to dislodge particles from the bed. Once this material is scoured, it may either become fully resuspended into water column or move along the bottom as bed load (material that is not fully suspended, but can move along the bed surface due to hydraulic forces). With regard to the transport of sorbed pollutants, bed load transport has typically been neglected in contaminant sediment transport models because the bulk of the material transported by this process is coarse-grained and has a limited direct influence on the transport and fate of these contaminants.

As with settling and deposition, sediment scour may be influenced by a variety of physical and chemical properties within the bed and the overlying water column. Physical properties that impact the degree to which the sediment bed may be subject to scour include:

- ❑ bulk properties of the sediment bed (soil strength, plastic limit, bulk density, wet density, etc.);
- ❑ particle sizes and their distribution within the bed;
- ❑ water velocity; and
- ❑ bed roughness.

Bulk sediment properties and particle sizes affect the resistance to shear, which depends on velocity and bed roughness. Chemical properties that influence the likelihood of scour include those that determine interparticle attraction, so the list is similar to those that affect deposition. These include:

- ❑ sediment mineralogy;
- ❑ clay content;
- ❑ surface chemistry; and
- ❑ pore water chemistry.

Perhaps the most important determinant of erodibility is sediment grain size. Because of larger grain size and lesser interparticle forces, the erosion of coarse sediments is qualitatively quite different than erosion of cohesive sediments. It is also much better understood and empirically characterized. Because contaminated sediments are predominantly fine-grained, the process of scour within fine-grained cohesive areas of the sediment bed is of particular interest, and is the focus of this section.

There are two distinct erodibility attributes for a given fine-grained sediment. These are critical shear stress, i.e. the critical level of hydraulic shear stress that is sufficient to dislodge the solid particles, and the erosion rate, i.e. the flux rate of sediment into the water column, as a function of shear stress. In practice, critical shear stress is operationally defined as the point of initiation of measureable erosion, which is currently possible at or above a rate of about 10^{-4} cm/s. For settling and deposition, mechanistic theories based on discrete particle interactions have been developed and fit to experimental data. For erosion, however, which involves the disintegration of a cohesive sediment matrix into discrete suspended particles, mechanistic modeling is less well developed and reliance has been placed instead on site-specific erosion studies. The quantitative effects of bulk properties of sediments on erosion have been inferred from these experiments, rather than from well-established general principles.

Multiple techniques exist to measure sediment erodibility, with advantages, disadvantages, and potential artifacts. The devices that have been used include annular flumes, Sedflume, and straight flumes. Annular flumes, which can be employed either *in-* or *ex situ*, apply rotation of an overlying water column to a bed of in-place or reconstituted sediments, in a closed circular system. Because they are closed systems, potential entrance and entry effects are avoided. Prior to the development of Sedflume, the annular flume was the leading method of erodibility and critical shear stress measurement for sediment transport studies (Lick et al., 1995). At each

velocity and associated shear stress, an experiment was run to establish a steady state suspended solids concentration in the water column, from which net erosion could be inferred. This erosion was interpreted as an event total to steady state, and no time rate of erosion was estimated. Subsequent analyses of these experiments have identified artifacts, such as sediment accumulation along the walls of the annulus, which may understate event net erosion (Jones and Lick, 2000).

Sedflume estimates a time rate of erosion by subjecting a sediment core to a controlled flow in a straight channel. The channel has a false bottom at the center, where a sediment core sample is extruded into the flume. The core is moved upward by an operator such that the sediment surface (i.e., the sediment/water interface) remains approximately level with the bottom of the flume channel. As the core is extruded upward into the flume, the water flowrate through the flume is adjusted. Critical shear stress is associated with the lowest flow at which erosion is observed. For each experimental flow rate, and associated shear stress, sediment erosion is measured by a decrease in the surface elevation, accompanied by a matching increase in the suspended load at the exit of the flume. An advantage of *Sedflume* is that it can estimate changes in critical shear stress and sediment erodibility with depth, limited only by the length of the sample core (McNeil et al., 1996).

Ex situ estimates made with Sedflume generally indicate much greater event depths of scour than annular flume estimates for the same site and same assumed event. The validity of Sedflume measurements depends in part on the operator's ability to keep the top of the eroding sample core level with the bottom of the channel as the experiment proceeds, which may be complicated by erosion of the core into an irregular surface. Much of the material eroded by Sedflume has been observed to be in the form of cohesive chunks, interpreted as "bedload" (Roberts et al., 2001), and a refined version of Sedflume called the Adjustable Shear Stress Erosion and Transport flume (ASSET) incorporates sediment traps to capture and quantify this portion of the eroded mass. Bedload is normally a negligible process for cohesive sediments, and its prominence in Sedflume experiments may account in part for the high apparent erosion rates generated with that device.

Straight flumes subject a rectangular patch of sediment to a straight flow at a known velocity, and estimate the resulting erosion rate by measuring the mass of sediment suspended and exiting the flume. These flumes have been employed in *ex situ* (Butman and Chapman, 1989 and Lee and Mehta, 1994) and *in situ* (Young, 1975, Gust and Morris, 1989) settings. To avoid entry effects and provide a fully developed bottom boundary layer, a floor of sufficient length should be provided between the flume entrance and the exposed sediment (Ravens and Geschwend, 1999). An advantage of the straight flume over Sedflume is that eroding sediment is completely contained within a sediment matrix, which more faithfully reproduces natural conditions than the projection of a core into the water column, as is done with Sedflume. A limitation of the straight flume is that the shape of the experimental bed necessarily changes as material is eroded away, creating a depression, so that this technique best measures erodibility at the sediment surface, at the beginning of the experiment. For one site where measurements of surficial erodibility were made by both Sedflume and an *in-situ* straight flume, Sedflume produced estimates that were higher by a factor of five than the straight flume (Ravens, 2004).

Measured erosion rates using these various techniques range as widely as 10^{-1} to 10^{-4} cm/sec. Because of potential artifacts in all of these methods, it is important to validate site-specific estimates made with either method by incorporating them into sediment mass balances and validating against water column data and net burial rates inferred from the full range of available site evidence. The challenge of measuring and verifying erodibility measurements remains a major source of uncertainty in contaminated sediment management.

The bulk properties that have been correlated with critical shear stresses and erosion rates in experimental flume studies include bulk density, ionic strength, particle size, mineralogy, gas, and benthic and bacterial colonization. Sediment stability has been found to increase with increasing clay content and porewater ionic strength (Lee and Mehta, 1994) and bulk density (Jepsen et al. 1997). The latter finding also translates into a tendency for stability to increase with sediment depth (McNeil et al., 1996 and Ravens and Geschwend, 1999), because compression by sediment overburden tends to reduce water content, increasing bulk density. Young (1975) found that bioturbating organisms tend to reduce critical shear stress, while Tsai and Lick (1987) observed that benthic clams can mitigate against sediment compaction, shorting to a few days the transient time during which stability of new sediment increases due to consolidation. Ravens and Geschwend (1999) found that algal mats can significantly increase sediment stability, and Jepsen et al. (2000) found very substantial reductions in stability, in terms of both critical shear stress and erodibility, when gas was generated in sediment pores by increasing temperature.

The erosion event itself can alter the grain size distribution by selectively eroding lighter particles or delivering particles from upstream. When these processes result in coarser surficial sediments, the result is bed armoring, which can increase critical shear stress and reduce erodibility.

B3. ADEQUACY OF TYPICAL SITE-SPECIFIC INFORMATION

B3.1 SETTLING AND DEPOSITION

At contaminated sediment sites, contaminant concentrations are often the most thoroughly measured parameters, because of their importance in identifying the site as contaminated and for evaluating current risks. Suspended solids loads and instream concentrations, and their covariation with flow and season, are often less thoroughly measured, but are necessary to constrain estimates of net deposition. The two components of this net quantity (namely deposition and erosion) cannot be individually constrained by ambient water column data because of their simultaneous nature, and can only be estimated by controlled experimentation.

Despite the importance of particle size distributions in determining settling rates, these may not be available, especially for a range of flow rates. Similarly, site-specific information on floc formation and floc settling speeds is usually lacking.

B3.2 EROSION

Most important rivers are gaged by the US Geological Survey, so that continuous flow records are available for use in estimating magnitudes and frequencies of high-flow events. However, as discussed above, the lack of a general theory of sediment resuspension makes it impossible to predict scour depths on the basis of relatively inexpensive site-specific measurements of sediment bulk properties. Instead, local measurements of critical shear stress and erodibility are obtained by experimental measurements with site cores, using *ex situ* flumes, or *in situ* flume measurements at multiple locations. Because sediment sites can be spatially heterogeneous, the adequacy of these experimental results for modeling of scour at the desired spatial scale is limited by the resources available for the flume studies. In addition, the magnitudes of the estimated scour can depend profoundly on the measurement technique employed, as discussed in the previous section.

B4. REPRESENTATION IN LEADING FATE AND TRANSPORT MODELS

While state of the art, research-oriented, models may contain many of the detailed mechanisms by which solids deposition and scour may occur, the current widely distributed (i.e., public domain) engineering-oriented models for these processes necessarily employ simplifications of some mechanisms due to constraints in computational time, model development time, and data availability. These models represent the bulk behavior of solids or groups of solids, rather than modeling the forces acting on each individual particle.

The U.S. EPA currently supports two widely available water quality models that can simulate both solids as well as particulate- and dissolved-phase chemicals. These are the Water Quality Analysis Simulation Program (WASP – various versions from 4 through 7) and the Environmental Fluid Dynamics Code (EFDC).

The U.S. EPA WASP model (Wool, et al., 2001; and Ambrose, et al., 1993 and 1988) has origins dating back to models developed to address eutrophication and PCB contamination in the Great Lakes (Thomann, 1975; Thomann et al., 1976; Thomann et al., 1979; Di Toro and Connolly, 1980). The first EPA public domain WASP applications to examine toxic chemicals in receiving waters (and sediments) date back to late 1980s with evaluations of volatile organics in the Delaware Estuary (Ambrose, 1987) and heavy metals in the Deep River, North Carolina (JRB, 1987).

As a public domain model, various enhancements of the WASP model have been made over the years in order to address site-specific needs and improve on the standard transport and kinetic formulations to simulate a variety of toxics, especially hydrophobic organic chemicals (HOCs) and metals. Several modified versions of the WASP model incorporate settling and resuspension functions that are not available in the EPA-supported model. The WASP model discussion below focuses on settling and resuspension representation in the standard EPA-supported model. Many of the sediment transport modifications to WASP are contained within the more recent EFDC model.

The EFDC model is a public domain surface water modeling system capable of one-, two-, or three-dimensional simulations of rivers, lakes, estuaries, coastal seas, and wetlands. The EFDC hydrodynamic model is directly coupled to its sediment and contaminant transport and fate model. EFDC can simulate wetting and drying of flood plains, mud flats, and tidal marshes. John Hamrick (1996) developed EFDC at the Virginia Institute of Marine Science with primary support from the State of Virginia. Since 1996, Tetra Tech, Inc. has maintained EFDC with primary support from the U.S. EPA.

B4.1 SETTLING AND DEPOSITION IN WASP

WASP is a widely used and adaptable model for simulating chemical constituents in the water column and sediments, but it has fairly limited capability, in its standard form, with regard to simulating solids settling and deposition to the sediment bed. In WASP, settling is a completely user-specified value, so there is no inherent mechanistic aspect to it. Settling rates are input as a

settling speed and the segment-to-segment interfacial area over which it applies. Settling rates may be specified as time- and space-variable functions.

The WASP model incorporates the ability to input settling rates (and subsequent deposition if settling is from a water column to a sediment segment) of up to three (3) types of solids. Additionally, up to three (3) chemical constituent state variables may be associated with any of the solids state variables through user-specified equilibrium partitioning methods, and thus settle through the water column along with the solids on which they are sorbed.

The fact that WASP can simulate up to three types of solids does allow the model to mimic the mechanistic aspects of particle settling to a limited degree because gross settling rates for each type of solids may be specified based on their representative physical properties (e.g., grain size differences or potential for floc formation). However, this capability, by itself, is still insufficient to fully represent settling and deposition behavior for the range of particles that may be represented within each size class.

The relatively generic approach utilized in WASP to simulate solids settling also means that the code can be exploited in order to enhance its capability to treat this process in a more mechanistically-oriented fashion. For example, the number of solids variables could be increased to better mimic the range of particle classes that exist in a real system. Alternatively, WASP can be coupled (or linked) to an independent sediment transport model used to generate the solids settling and deposition rates needed by WASP.

B4.2 SETTLING AND DEPOSITION IN EFDC

EFDC is designed to allow a user to select from several different settling and deposition options. The model is set up in a way that facilitates the addition of new options as methods develop. The current EFDC model allows the user to specify a constant settling velocity or select from a variety of semi-empirical expressions that relate cohesive particle settling velocity to concentration and/or bed shear stress. The semi-empirical expressions are intended to approximate the effects of floc formation and disaggregation on cohesive settling, while avoiding the computational intensity of first principles mathematical modeling of these processes. While the expressions utilize much of the research discussed in Section B2, none of the semi-empirical expressions include an explicit time-dependency to represent the rate at which flocs form and disaggregate.

Once the settling velocity is computed, deposition to the bed is based on the settling velocity (w_s), the near-bed solids concentration (S_d), and a probability of deposition function (T_d):

$$J_o^d = \begin{cases} -w_s S_d \left(\frac{\tau_{cd} - \tau_b}{\tau_{cd}} \right) = -w_s T_d S_d & : \tau_b \leq \tau_{cd} \\ 0 & : \tau_b \geq \tau_{cd} \end{cases} \quad (2)$$

The probability of deposition function is based on the concept that under quiescent conditions all solids settling near the bed will reach and remain on the bed, while at some threshold flow-induced bed surface stress (τ_{cd}) none of the solids settling near the bed will reach and remain on the bed. Absent site-specific data, this critical deposition stress is generally treated as a calibration parameter with a wide range of reported values from laboratory and field observations of 0.06 to 1.1 N/m² (Tt tech memo Cht 7). The near-bed solids concentration (S_d) is also an estimated value, computed in EFDC as a function of either the bottom layer concentration (in 3D model applications) or depth-average water column concentration (in 1D and 2D models).

B4.3 EROSION IN WASP

The WASP model incorporates erosion in the same manner as it handles settling, relying on user-specified rates of erosion for each solids type in the model. The erosion rate inputs can vary in time and space. As discussed for WASP settling, this is a flexible approach that lends itself well to either very simple representation of sediment dynamics or to coupling of the WASP model to an independent sediment transport model for more sophisticated representation.

B4.4 EROSION IN EFDC

The EFDC model provides several options for erosion representation, ranging from a simple constant erosion rate to a representation of erosion as a function of shear stress and bed properties, which can vary in time and space.

Bed erosion is computed as the rate of resuspension (w_r) times the sediment concentration or dry density of the sediment bed (S_r). This resuspension flux (J') is generally represented in EFDC in the following form:

$$J'_o = w_r S_r = \frac{dm_e}{dt} \left(\frac{\tau_b - \tau_{ce}}{\tau_{ce}} \right)^\alpha : \tau_b \geq \tau_{ce} \quad (3)$$

where dm_e/dt is the “base erosion rate” expressed as a rate per unit surface area of the bed and τ_{ce} is the critical stress for surface erosion. The base erosion rate, critical stress, and the parameter α are generally determined from laboratory or *in situ* field studies. Base erosion rates ranging from 0.005 to 0.1 g/s-m² have been reported in the literature (TetraTech, 2002, Chapter 7).

EFDC allows the base erosion rate and critical stress to be user-defined constants or predicted values based on sediment properties (bulk density or void ratio). Selection of the sediment-dependent formulations requires use of the EFDC bed consolidation simulation to predict time and depth variation in these bed properties. The sediment dependent formulations in EFDC result in decreasing the base erosion rate and increasing the critical stress with increases in bulk density and decreases in the void ratio.

In addition to the surface erosion process described above, EFDC has an option for mass erosion. Mass erosion is intended to represent a rapid erosion process where the flow-induced bed stress exceeds the depth-varying shear strength of the bed at some depth below the surface. Under these conditions, the mass erosion flux in EFDC is simply the dry sediment mass per unit area of the bed having a shear strength less than the bed stress, divided by a user-specified time scale for this bulk mass transfer of sediment. Researchers have found maximum rates of mass erosion are on

the order of 0.6 g/s-m^2 (Tt tech memo Cht 7). The mass erosion option may have limited applicability and appears to be deactivated in a recently obtained version of the EFDC code.

Sediment bed armoring, which is a decrease in the erodibility of the sediment bed over time, can be simulated in a variety of ways using EFDC.

- ❑ Coarsening of the bed due to preferential erosion of lighter particles or the deposition of heavier particles;
- ❑ Specification of an empirical “hiding factor”; and
- ❑ Consolidation of the bed, increasing bulk density and decreasing the void ratio.

Simulation of bed coarsening in EFDC results from: (1) use of multiple particle classes with differing settling and resuspension properties and (2) a bed handling routine that allows time-variation in the mix of particles present in the surface layer of the sediment bed. Under certain flow conditions, it is possible that only the more easy-to-erode particles will be resuspended and/or only coarse particles will settle, resulting in a greater portion of difficult-to-erode particles in the surface layer of the sediment bed. This bed coarsening results in a decrease in erosion over time. EFDC also includes a specific armoring option that speeds the armoring process by representing a very thin active layer at the top of the sediment bed. This thin layer can coarsen very quickly as it may be only a few particle diameters thick.

Another means of bed armoring available in EFDC is the use of a “Hiding Factor”. This is a user-specified empirical value that reduces the amount of cohesive sediment resuspension computed in Equation (3) by a factor, based on the following equation:

$$\text{Cohesive Resuspension Factor} = \text{Cohesive fraction of sediment} ^ \text{Hiding Factor} \quad (4)$$

A Hiding Factor equal to zero results in no adjustment to the cohesive resuspension. For a given non-zero Hiding Factor, decreases in the cohesive fraction of sediment result in decreases in the Cohesive Resuspension Factor, which simulates armoring of the bed due to larger non-cohesive particles protecting (“hiding”) smaller cohesive particles from resuspension forces.

Consolidation of the sediment bed is the final means by which armoring is represented in EFDC. As discussed above, the base erosion rate and critical shear stress may be predicted based on sediment properties (bulk density or void ratio). The methodology for representing sediment bed consolidation is described in TetraTech, Chapter 5 (2002). As the bed consolidates (increasing bulk density and decreasing void ratio), the base erosion rate decreases and the critical shear stress increases. This decreases the erodibility of a consolidated sediment bed.

B5. PREDICTIVE UNCERTAINTY

Recent research has identified properties with important effects on transport of cohesive sediments. These relationships have been built into sediment transport models, and progress has been made in laboratory studies to quantify their magnitudes. As yet, however, there is no adequate general theory sufficient to make *a priori* predictions of settling, deposition, or erosion without site-specific measurements. In heterogeneous sediment transport environments, multiple measurements are needed to reflect the effects of differences in grain size, bulk density, and other key attributes. Measurements are highly sensitive to the method employed, especially in the case of erodibility measurement. Field measurements of suspended sediment and bed elevation changes can support calibration of *net* deposition in sediment transport models, but not separate calibration of deposition and erosion. For these reasons, predictive modeling of settling, deposition, and erosion as separate processes is subject to a high degree of uncertainty. Because net deposition can be measured directly in the field, it is less uncertain, and can be reproduced with reasonable accuracy using existing fate and transport models.

B6. REFERENCES

- Ambrose, R. B. 1987. "Modeling Volatile Organics in the Delaware Estuary." ASCE, J Env Eng 113(4): 703-721.
- Ambrose, R. B. 1988. WASP4, A Hydrodynamic and Water Quality Model - Model Theory, User's Manual, and Programmer's Guide. USEPA, Athens, GA. EPA/600/3-97-039.
- Ambrose, R. B., T. A. Wool, and J. L. Martin. 1993. The Water Quality Analysis Simulation Program, WASP5. Part A: Model Documentation. Environmental Research Laboratory, Athens, GA. September 20.
- Ariathuri and Krone. 1976. "Finite Element Model for Cohesive Sediment Transport." ASCE J. Hydr. Div. 102(3): pp. 323-388.
- Burban, P.Y., Y. Xu, J. McNeil, and W. Lick. 1990. "Settling Speeds of Flocs in Fresh Water and Seawater." Journal of Geophysical Research 95(C10): pp. 18213-18220.
- Burd, and Jackson. 1997. "Predicting Particle Coagulation and Sedimentation Rates for a Pulsed Input. Journal of Geophysical Research 102(C5): pp. 10545-10561.
- Butman, C.A. and R.J. Chapman. 1989. "The 17-Meter Flume at the Coastal Research Laboratory, Part 1: Description and User's Manual." WHOI Tech. Rep. 89-10, 31 pp.
- Cheng, Nian-Sheng. 1997a. "Simplified Settling Velocity Formula for Sediment Particles." J Hydr Eng 123(2) ASCE:149-152.
- Cheng, Nian-Sheng. 1997b. "Effect of Concentration on Settling Velocity of Sediment Particles." J Hydr Eng 123:728-731.
- DiToro, D. M. and J. P. Connolly. 1980. Mathematical Models of Water Quality in Large Lakes Part 1: Lake Huron and Saginaw Bay. EPA-600/3-80-056. pp. 28-30.
- Droppo, I.G. and E.D. Ongley. 1994. "Flocculation of Suspended Sediment in Rivers of Southeastern Canada." Water Research 28: 1799-1809.
- Dyer, K. T. L. and A. J. Manning. 1998 "Observation of the Size, Settling Velocity, and Effective Density of Flocs, and their Fractal Dimensions." Journal of Sea Research. 41L: 87-95.
- Farley, Kevin and Francois Morel. 1986. "Role of Coagulation in the Mechanics of Sedimentation". Environmental Science and Technology 20: 187-195.
- Gmachowski, Lech. 1999. "Comment on 'Hydrodynamic Drag Force Exerted on a Moving Floc and its Implication to Free-Settling Tests' by Wu and Lee." Water Research 33(4):1114-1116.

- Grossart, H. P. and M. Simon. 1997. "Formation of Macroscopic Organic Aggregates (Lake Snow) in a Large Lake: The Significance of Transparent Exopolymeric Particles, Photoplankton and Zoo-plankton." *Limnology and Oceanography* 42(8): 1651-1659.
- Gust, G. and M.J. Morris. 1989. "Erosion Thresholds and Entrainment Rates of Undisturbed *In Situ* Sediments." *J. Coastal Research* 5:87-99.
- Hamrick, J.M. 1996. User's Manual for the Environmental Fluid Dynamics Computer Code. Special Report No. 331 in Applied Marine Science and Ocean Engineering. Department of Physical Sciences, School of Marine Science, Virginia Institute of Marine Science, Gloucester Point, VA.
- Henderson, F.M. 1966. *Open Channel Flow*. McMillan, New York.
- Ibad-zade, Y. A. 1992. *Movement of Sediment in Open Channels*. S. P. Ghosh, translator, Russian Translations Series, Vol 49, A. A. Balkema, Rotterdam, The Netherlands.
- Ives, K. J. 1978. "Rate Theories," in The Scientific Basis of Flocculation, ed. K. J. Ives, pp. 37-61. Alpen aan den Rijn, The Netherlands: Sijthoff and Noordhoff International Publishers, B. V.
- Jepsen, R., J. Roberts, and W. Lick. 1997. "Effects of Bulk Density on Sediment Erosion Rates." *Water Air and Soil Pollution* 99(1-4):21-31.
- Jepsen, R., J. McNeil, and W. Lick. 2000. Effects of Gas Generation on the Density and Erosion of Sediments from the Grand River." *J. Great Lakes Research*, pp. 209-219.
- Johnson, Clifford P., Xiaoyan Li, and Bruce E. Logan. 1996. "Settling Velocities of Fractal Aggregates." *Environmental Science and Technology* 30:1911-1918.
- Jones, C., and W. Lick. 2000. "Effects of Bed Coarsening on Sediment Transport." *Estuarine and Coastal Modeling*.
- Jones, C. and W. Lick. 2001. "SEDZLJ: A Sediment Transport Model." Dept. of Mech. and Env. Eng., U-C Santa Barbara, May 29.
- JRB, Inc. 1984. Development of Heavy Metal Waste Load Allocations for the Deep River, NC. JRB Associates, McLean, VA, for USEPA Office of Water Enforcement and Permits, DC.
- Krone, R.B. 1962. "Flume Studies of the Transport of Sediment in Estuarial Processes." Final Report, Hydraulic Engineering Laboratory and Sanitary Engineering Research Laboratory, University of California, Berkeley.

- Lau, Y.L. and B.G. Krishnappan. 1994. "Does Reentrainment Occur During Cohesive Sediment Settling?" *Journal of Hydraulic Engineering (ASCE)* 120(2): 236-244.
- Lee, S-C. and A.J. Mehta. 1994. "Cohesive Sediment Erosion." Dredging Research Program (DRP) 94-6, US Army Corps of Engineers.
- Lick, Wilfred. 1982. "The Entrainment Deposition and Transport of Fine-Grained Sediments in Lakes. Interactions Between Sediments and Fresh Water, ed. P. G. Sly, *Hydrobiologia* 91: 31-40, Dr. W. Junk Publ., The Hague, Netherlands.
- Lick, Wilfred, J. Lick, and C.K. Ziegler. 1992. Flocculation and its Effects on the Vertical Transport of Fine-Grained Sediments. *Hydrobiologia* 235: 1-16.
- Lick, W., Huang, H. and R. Jepsen. 1993. "Flocculation of Fine-Grained Sediments Due to Differential Settling." *Journal of Geophysical Research* 98(C6): 10279-10288.
- Lick, W., Y.J. Xu, and J. McNeil. 1995. "Resuspension Properties of Sediments from the Fox, Saginaw, and Buffalo Rivers. *J Great Lakes Res* 21: 257-274.
- Lick, W., J. Gailani, C. Jones, E. Hayter, L.Bburkhard, and J. McNeil. 2005. Class Notes: The Transport of Sediments and Contaminants in Surface Waters. UC-Santa Barbara, January.
- Mehta, A.J. and E. Partheniades. 1975. "An Investigation of the Depositional Properties of Flocculated Fine Sediments." *J Hydr Res* 12(4): 361-368.
- McNeil, J., C. Taylor, and W. Lick. 1996. "Measurement of the Erosion of Undisturbed Bottom Sediments with Depth." *J Hydraul Eng* 122: 316-324.
- Milligan, T.G. and P.S. Hill. 1998. "A Laboratory Assessment of the Relative Importance of Turbulence, Particle Composition, and Concentration in Limiting Maximal Floc Size and Settling Behavior." *Journal of Sea Research* 39: 227-241.
- Mints, D. M. and S. A. Shubert. 1957. *Hydraulics of Granular Materials*. Y. J. Hui and H. M. Ma, translators, Water Resources Press, Beijing, China (in Chinese).
- Neale, G., N. Epstein, and W. Nader. 1973. "Creeping Flow Relative to Permeable Spheres." *Chemical Engineering Science* 28: 1865-1874.
- Partheniades, E. R. H. Cross and A. Ayora. 1968. "Further Results on the Deposition of Cohesive Sediments." *Proceedings, 11th Conference on Coastal Engineering, London, England, Vol. 2: 723-742.*
- Ravens, T. and P. Gschwend. 1999. "Flume Measurements of Sediment Erodibility in Boston Harbor." *J. Hydraulic Engin.* 125(10):998-1005

- Ravens, T. 2004. "Cohesive Sediment Stability." Background paper for Contaminated Sediments Workshop, SERDP-ESTCP, Charlottesville, VA, August 10.
- Roberts, J., Jepsen, R, and J. Gailani. 2001. Measurements of Bedload and Suspended Load in Cohesive and Non Cohesive Sediments. *Proceedings of the World Water and Environmental Resources Congress*. May, 2001.
- Sha, Y.Q. 1956. "Basic Principles of Sediment Transport." J Sediment Res (Beijing, China) 1(2):1-54 (in Chinese)
- Stolzenbach, K.D. 1993. "Scavenging of Small Particles by Fast-Sinking Porous Aggregates." Deep-Sea Research 40: 359-369.
- Thomann, R. V. 1975. Mathematical Modeling of Phytoplankton in Lake Ontario, 1. Model Development and Verification. USEPA, Corvallis, OR. EPA-600/3-75-005.
- Thomann, R. V. R. P. Winfield, D. M. DiToro, and D. J. O'Connor. 1976. Mathematical Modeling of Phytoplankton in Lake Ontario, 2. Simulations Using LAKE 1 Model. USEPA, Grosse Ile, MI, EPA-600/3-76-005.
- Thomann, R. V., R. P. Winfield, and J. J. Segna. 1979. Verification Analysis of Lake Ontario and Rochester Embayment Three Dimensional Entrophication Models. USEPA, Grosse Ile, MI, EPA-600/3-79-094.
- Tsai, C. H. and W. Lick. 1986. A Portable Device for Measuring Sediment Resuspension. J Great Lakes Res 12(4): 314-21.
- TetraTech, Inc. 2002. EFDC Technical Memorandum: Theoretical and Computational Aspects of Sediment and Contaminant Transport in the EFDC Model. 3rd Draft. Prepared for USEPA, Office of Science and Technology, May.
- Van Rijn, L. C. 1989. Handbook: Sediment Transport by Currents and Waves. Rep. H461, Delft Hydraulics, Delft, The Netherlands.
- Wool, T. A., R. B. Ambrose, J. L. Martin, E. A. Comer. 2001. Water Quality Analysis Simulation Program (WASP), Version 6.0, Draft Users Manual.
- Wu, R.M. and D.J. Lee. 1998. "Hydrodynamic Drag Force Exerted on a Moving Floc and its Implication to Free-Settling Tests." Water Research 32(3): 760-768.
- Young, R.A. 1975. "Flow and Sediment Properties Influencing Erosion of Fine-Grained Marine Sediments: Sea Floor and Laboratory Experiments." PhD dissertation, Woods Hole Oceanographic Institution, Woods Hole, MA, 202 pp.
- Zhang. 1989. Sediment Dynamics in Rivers. Water Resources Press (in Chinese).

Zhu, L. J. and N. S. Chang. "Settlement of Sediment Particles." Resp. Rep., Dept of River and Harbor Eng., Nanjing Hydr. Res. Inst., Nanjing, China (in Chinese).

Ziegler, C. K. and W. Lick. 1986. "A Numerical Model of the Resuspension, Deposition, and Transport of Fine-Grained Sediments in Shallow Water." UCSB Report ME-86-3.

Ziegler, C. K. and B.S. Nisbett. 1994. Fine Grained Sediment Transport in Pawtuxet River, Rhode Island. ASCE J Hyd Engr 120(5): 561-576.

APPENDIX C: EBULLITION

C1. INTRODUCTION

The impact of biogenic gases on uncapped or capped sediments has rarely been incorporated into the modeling and/or remediation decision making at contaminated sites. This is in part due to the assumption that these gases would have a negligible impact on the system, relative to other fate processes. While ebullition may be insignificant at some sites, many sites show evidence that biogenic gases can have an impact on both physical and chemical stability of sediments, and also capped sediments. However, probably a more important reason that gas ebullition is neglected is the dearth of information concerning the various mechanisms through which these gases can affect contaminant stability/fate. For example, gas bubbles rising through the sediment column have been shown to strip contaminants from the porewater, carrying them through the sediment, to the water column and into the atmosphere. The presence of gas bubbles decreases bulk density, making the sediment more susceptible to erosion, while gas bubbles rising through the sediment can directly mix and transport buried sediments to the surface by entraining sediment particles in the wake of the bubble. Accordingly, ebullition may in part explain observed excess contaminant fluxes due to non-resuspension processes (e.g. Hartman and Hammond, 1984; Erickson et al., 2005). Thus, ebullition can modify natural recovery rates, and in the case of a cap, ebullition can increase the effective thickness of a cap, as well as dictate the type of suitable capping material (e.g. organic content, grainsize).

The potential importance of gas formation has been observed at the following sites. Cap failure due to methane ebullition in freshwater environments has been experienced at the EPA/Manistique and the Oxbow, WI sites, where successive geotextile layers were lifted and exposed by methane formed in the contaminated sediment (Palermo et al., 2002). Methane outgassing has been observed at the Simpson-Tacoma site as well, where it did not cause physical disruption of the cap, but concerns of chemical transport by the gases prompted additional sampling of the gases (Stivers and Sullivan, 1994). The outcome of this follow-up sampling is currently unpublished. Cap design that accounted for ebullition was demonstrated at the Stryker Bay Superfund site in Duluth, Minnesota, on the St. Louis River just upstream of Lake Superior. At this site, ebullition actively transported both PAHs and NAPL to the water surface. A transient model of post-capping sediment consolidation and associated porewater movement, groundwater advection and gas ebullition predicted that a 3-ft thick cap would be necessary to suppress methanogenesis to levels at which groundwater advection of dissolved gases and sediment strength would prevent the formation of free-phase gases (Huls et al., 2003).

C2. THEORETICAL PROCESS UNDERSTANDING

Ebullition is the result of a series of processes in which excess gases are generated by micro-organisms from organic matter. Free-phase gases form when saturation concentrations are reached, bubbles migrate upward when pressures allow (building tubes and cracks if the sediment is weak enough), and finally escape into the water column. The gas bubbles can interact chemically with the dissolved contaminants and physically with the sediment matrix. The total flux of contaminants due to gas ebullition across the sediment-water interface will reflect the following coupled processes:

- gas generation and consumption,
- gas bubble formation and growth,
- gas bubble migration and escape,
- three-phase partitioning between solid, gas and aqueous phases in gas voids, ebullition tubes and the water column (subsequent advection/escape to the atmosphere),
- physical transport of particles carrying contaminants by microcurrents in the wake of gas bubbles, (subsequent desorption, uptake or resuspension), and
- resuspension as enhanced by the lower bulk density of gassy sediments.

Figure C1. shows how the various processes of gas generation and sediment stability are related. The left side shows the processes involved in gas generation, bubble formation and migration, and the right half shows the chemical and physical processes that lead to the transport of contaminants across the sediment-water and water-air interfaces.

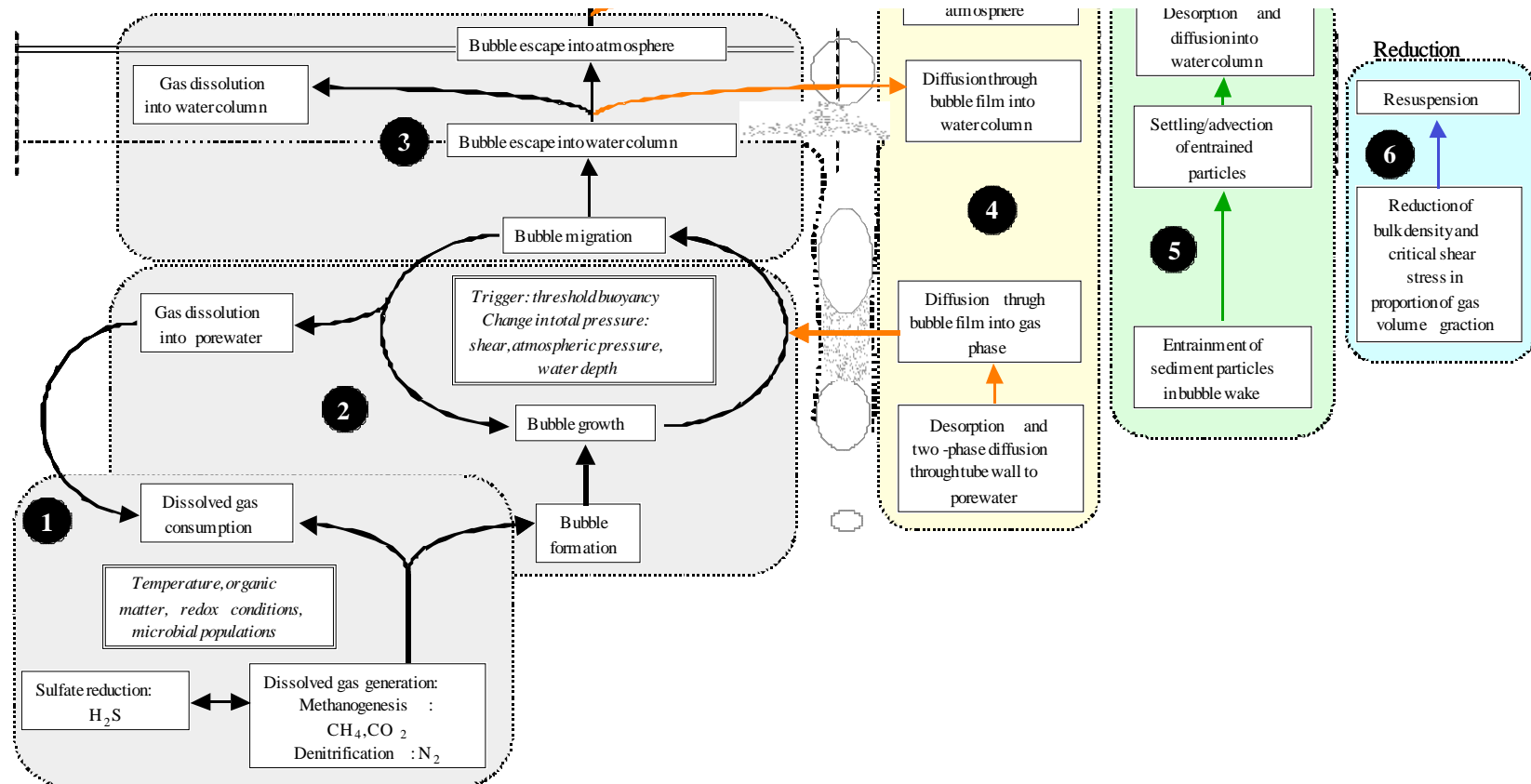


Figure C1. Gas bubble generation processes and the impact of gas bubbles on sediment and contaminant stability

C2.1 GAS GENERATION

Biogenic gas bubbles are the result of microbial decomposition of organic materials through a series of anaerobic metabolic processes, including hydrolysis, fermentation, and methanogenesis. Gas bubbles generated from naturally occurring organic matter are composed of varying combinations of methane (46-95%), nitrogen (3-50%), and trace amounts of hydrogen, carbon dioxide, ammonia, and hydrogen sulfide (Fendinger et al., 1992; Casper et al., 2000; Vroblesky and Lorah, 1991). The gases stem from the balance of metabolic interactions of fermentative, sulfidogenic, methanogenic, denitrifying, and aerobic microorganisms. The methane in the gas bubbles represents excess dissolved methane gas that has escaped oxidation/mineralization (Strayer and Tiedje, 1978). Although aerobes, sulfidogens and methanogens can co-exist when there is a sufficiently large supply of hydrogen from fermentation of organic material, in general, sulfate reducers and aerobic organisms suppress methanogens and also consume dissolved methane (Liikanen et al., 2002; Whiticar, 2002; Henrichs and Reeburgh, 1987; Martens and Klump, 1980). In freshwater environments, sulfate is in limited supply and methanogens usually dominate in most of the anoxic sediment zone. In saline environments, more sulfate is available to greater depths, and methanogens become dominant in highly reducing, deeper sediments where sulfate is sufficiently depleted. Thus the top-most sediment layer (i.e. the first 0-10 cm) may be oxic, followed by a layer of sulfate reduction (50-150 cm thick, in particular in saline environments) and a layer of methane generation and carbon dioxide generation (DiToro, 2001; Whiticar, 2002). Bubbles that have already formed in deeper layers, however, can travel through the upper layers with only small losses (Fendinger et al., 1992).

Methane generation occurs in organic-rich sediments of all aquatic environments, but is most pronounced in freshwater systems. In estuarine and marine sediments methanogenesis is important where organic carbon supply is the greatest: in shallow, highly anoxic environments, bays, estuaries, and high sedimentation shelves (Henrichs and Reeburgh, 1987). In these areas, ebullition fluxes can be comparable to fluxes in freshwater environments (Martens and Klump, 1980). Methanogenesis rates depend on the amount of organic matter in the sediment, the temperature (Matsumoto et al., 1992), sediment depth, redox conditions and the composition of microbial populations.

C2.2 BUBBLE FORMATION AND GROWTH

Methanogenesis will have an impact on contaminant fate, if sufficient dissolved gases accumulate in the porewater to form bubbles. Gas bubbles in sediments are produced when the sum of the partial pressures of dissolved gases exceeds the atmospheric pressure plus hydrostatic pressure of the overlying water (i.e. the solution is saturated) (Fendinger et al., 1992; Casper et al., 2000; Trayer and Tiedje, 1978). In many environments, methane gas dominates in gas bubbles. Relative to carbon dioxide, methane is most likely to be lost through ebullition, while carbon dioxide tends to be lost through diffusion (Casper et al., 2000; Liikanen et al., 2002). The depth to which bubbles occur varies with conditions, but information is limited. Martens and Klump (1980) observed bubbles from the sediment surface to a depth of 30 cm in marine sediments. Joyce and Jewell (2003) found that most ebullition originates from the upper 10-20 cm of the sediment column. Sediments with a high degree of gas generation and ebullition exhibit gas voids that can represent 5% (Jepsen et al., 2000) to 8% (Richardson, 1998) of the

volume (Jepsen et al., 2000). However, values up to 2% are more common (Richardson, 1998). The gas bubbles are not released immediately. Rather, they slowly grow until another pressure threshold is reached: they have to build up a certain amount of buoyancy to overcome the (locally variable) cohesive strength of the sediment and migrate upward. In general, sediments exhibit a wide and heterogeneous scattering of bubbles and channels of varying sizes through the matrix (show one of Danny's pictures of this and x-ray from Martens). The size (volume) of the bubbles will vary not only with the amount of gas they contain, but also with ambient temperature and pressure. For example, an upward migrating bubble will continually expand as pressure decreases, and as a consequence it will also accelerate. Marten and Klump (1980) found bubble sizes to range between 0.062 and 0.37 cm with a mean volume of 0.104 ml at a water depth of 7.5 m. Richardson (1998) reports bubble sizes between 0.04 and 0.5 cm within soft, marine sediments. The mechanism of growth and growth rate of gas bubbles has not been investigated in the literature. It may be an important factor in the overall residence time of bubbles within the sediments, and thus the time that contaminants have available for partitioning into the gas phase.

C2.3 BUBBLE MIGRATION AND RELEASE

Bubble migration is a highly localized process, which depends on sediment grain size and cohesive strength. Sandy sediments could act as a diffuser and force bubbles to migrate through the available interstitial pores, thus breaking up larger bubbles into many small ones. This would result in an increased surface area between the gas and the liquid phase, both in the porewater and in the water column. In fine-grained sediments, the expanding bubbles fracture the sediment rather than move around the grains. These fractures combine to make channels to the surface (Huls et al., 2003; Richardson, 1998; WL-Delft, 2004b). These bubbling tubes and cracks are maintained during periods of active ebullition, are distributed randomly, and can have a density of 50-170 tubes/m² (Martens and Klump, 1980). In this case, the contact area between the sediment solids and the water column is increased, facilitating diffusion.

Ebullition tends to occur episodically, triggered by changes in shear stress and/or pressure. Increased shear stress due to water currents, weather-related decreases in atmospheric pressure, reduced hydrostatic pressure due to tides, seiches, or water level management will lead to a sudden release of gas bubbles followed by a period in which continued microbial activity replenishes the methane to levels leading to new bubble formation (Joyce and Jewell, 2003). Thus, in tidal systems, gas release begins during falling tide 60 to 90 minutes prior to low water and stops abruptly when the tide starts to rise. Gas then builds up during high tide. These tidal bubbling episodes release less than 10% of the sedimentary bubble reservoir (defined as the sum of all bubbles that can be released with stirring) (Martens and Klump, 1980; Chanton and Martens, 1988). In non-tidal systems, wind- and water-induced shear stresses tend to control ebullition (Hartman and Hammond, 1984; Chanton and Martens, 1988).

Gas bubbles that have escaped into the water column will continue to rise until they reach the surface. Some proportion of the gases in the bubble will diffuse into the water column. This is a transient process, and the extent of dissolution depends on the depth of the water and its temperature. Martens and Klump (1980) reported that 15% of the methane within bubbles re-dissolved after release at a depth of 8.5 m and summer time water column temperatures near 25 °C.

It is in the latter phases of bubble accumulation, migration, and escape that ebullition can potentially interact with contaminants, sediments, and capping materials to alter expected rates of contaminant fluxes and attenuation rates. (The dissolved phase of biogenic gases is assumed not to affect contaminant stability.) Table C1 summarizes rates of methane ebullition reported in the literature, Figure C2 shows the data in graphical format.

Table C1. Ebullition rates reported in the literature.

Salinity	Ebullition Rates in cm/d				N(data)	% CH ₄	Notes	Source
	Min	Max	Avg	Stdev				
fresh	0.03	0.03	-	-	7	44	88 induced by rapidly falling barometric pressure	Casper et al. (2000)
fresh	-	0.26	-	-	-	-	- cited from Ward and Frear, 1979	Adamset al. (1990)
fresh	-	0.02	-	-	-	-	- cited from Chau et al., 1977	Adamset al. (1990)
fresh	-	0.26	-	-	-	-	- cited from Howard et al., 1971	Adamset al. (1990)
fresh	-	0.10	-	-	-	-	-	Adamset al. (1990)
fresh	-	-	3.22	0.56	3	-	- flowthrough microcosm in laboratory, with SO ₄ , numbers estimated from graph	Liikanen et al. (2002)
fresh	0.02	0.08	0.05	0.02	33	73	100 June-October, recalculated from graph	Strayer and Tiedje, (1978)
fresh	-	0.92	0.08	0.16	143	-	- June and July measurements, recalculated from graphs	Joyce and Jewell (2003)
fresh	6.72	44.80	-	-	-	-	- Outbursts during pressure release	Richardson (1998)
fresh	-	-	10.54	-	-	-	- daily, cited from Cicerone and Shetter, 1981	Chanton and Martens (1988)
fresh	0.32	47.45	-	-	-	-	- daily, range from many environments	Chanton and Martens (1988)
tidal fresh	0.01	0.01	0.01	0.00	-	-	- annual rate	Chanton and Martens (1988)
estuarine	-	10.07	-	-	10	85.5	85.5	Martens and Klump (1980)
marine	-	-	0.06	-	10	82	90 June-October	Martens and Klump (1980)
marine	-	3.12	-	-	10	82	90 same as above, converted to mmol	Martens and Klump (1980)
-	-	-	-	-	-	46	95 cited from Kuznetsov, 1968; Howard et al., 1971; Chen et al., 1972, Ward and Frear, 1979; Chanton et al., 1988	Fendinger et al. (1992)

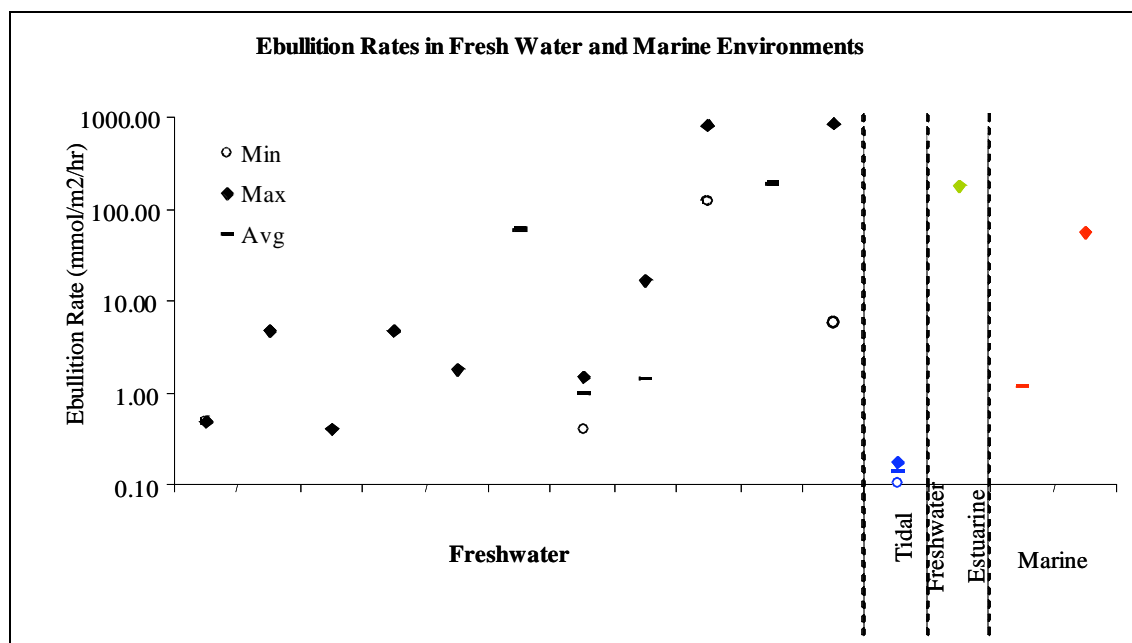


Figure C2. Ebullition rates reported in the literature.

C2.4 THREE-PHASE PARTITIONING

As gas bubbles grow and migrate within the sediment, they create a matrix that is filled with gas voids of different sizes as well as ebullition tubes that lead to the overlying water column. Escaping bubbles can strip hydrophobic contaminants from the interstitial waters, similar to engineered air stripping columns. In addition, the tubes represent a surface along which deeper anoxic sediments are exposed to the water column with potentially accelerated solid-to-water diffusion due to increased concentration gradients.

Gas bubbles will exchange hydrophobic contaminants in a 3-phase system including the solid phase of sediment particles with sorbed contaminants, the gas phase inside the bubble, and the

liquid phase. Depending on the contaminant, dissolved organic carbon (DOC) may need to be considered as a 4th phase. Solid-liquid desorption has been observed to proceed in two steps, an initial, fast desorption step with quick establishment of equilibrium, followed by a slow step modeled with intraparticle diffusion (Gong and DePinto, 1998). The liquid phase may include porewater surrounding gas voids inside the sediment, a mixture of porewater and overlying water in the ebullition tubes, and the water column during bubble escape. The partitioning process may be modified by dissolved organic carbon, which can chelate organic contaminants and make them unavailable for partitioning. Voids, tubes and water column are locations with different driving forces for diffusion, with different temperatures, bubble residence times, redox properties, and dissolved concentrations of contaminants and DOC. Upward advecting groundwater/hyporheic water will also modify the partitioning process, in particular by decreasing residence times of both dissolved and free phase gases.

Bubbles in the sediment accumulate hydrophobic contaminants through partitioning from the porewater through the bubble film boundary layer and into the bubble itself. The diffusion of contaminants into the gas bubbles is controlled by properties such as aqueous solubility, vapor pressure, Henry's law constant, diffusivity coefficient, and the presence of modifying materials such as organic films, electrolytes, and emulsions (Vroblesky and Lorah, 1991; Fendinger et al., 1992). Given sufficient residence time of the gas (i.e. depending on gas generation and ebullition rates), the three-phase system may have time to establish equilibrium with the solid phase before the gas escapes. However, for highly sorptive contaminants (high K_{oc}) it is likely that the stripping process is transient.

In addition to the gas voids, the ebullition process creates and maintains tubes. The penetration of water from the water column into the ebullition tubes creates a greater surface area through which contaminants can diffuse, and an increased gradient by dilution of the porewater with water from the overlying water column. The result is an enhanced diffusion and subsequent advection of this dissolved phase by the bubbles into the water column. Martens and Klump (1980) observed that apparent methane diffusivities increased by a factor of 1.2 (fall)-3.1 (summer) relative to theoretical diffusivities in the presence of the tubes.

Depending on water depth and bubble size, some of the contaminants carried by rising bubbles can diffuse into the water column. Martens and Klump (1980) reported that in 8 m-deep water, 15% of the methane in gas bubbles diffused into the water. For hydrophobic contaminants however, the bubbles may rise too fast for appreciable chemical exchange (deAngelis and Scranton, 1993). Most of the gas phase contaminants can be expected to be released to the atmosphere, constituting a mode for attenuation of the sediment/water system.

The impact of the chemical partitioning process in freshwater sediments was investigated by Fendinger et al. (1992) and Adams et al. (1990). They estimated annual fluxes for 6 organic compounds in Hamilton Harbour sediments based on equilibrium partitioning into gas bubbles given average ebullition rate and porewater concentrations. The annual flux varied from much less than 1 kg for pyrene (Henry's law constant (HLC) = 4.8×10^{-4}) to 124 kg for dichloromethane (HLC = 0.1). These values are likely overestimates in as much as they assume equilibrium and no interference from DOC in porewater. The majority of this flux ends up in the atmosphere, while some small proportion dissolves into the water column. Lower chlorinated PCBs and dioxins have HLCs comparable to pyrene and can also be expected to partition to gas

bubbles. For example, mono- di- and tri-chlorinated dioxins have been reported to accumulate at the air-water interface (Lohmann et al., 2003). Huls et al. (2003) observed that NAPLs were transported to the water-air interface and accumulated there.

C2.5 PHYSICAL TRANSPORT OF PARTICLES IN THE WAKE OF GAS BUBBLES

Bubbles rising through the sediment matrix exert an erosive force along their path, and as a result have the potential to mix buried sediments and move them to the surface, similar to bioturbation (Liikanen et al., 2002). The entrained particles are released into the water column upon the bubble's exit from the tube, and settle near the tube exit or are advected depending on the strength of the bottom currents (Martens and Klump, 1980). Huls et al (1980) trapped such particles in glass wool suspended in water just above the sediment-water interface in experiments involving undisturbed cores of sediments with high ebullition rates. They measured PAH flux, and found that increasing bubble production increased the amount of PAH gathered on the glass wool. This process accounted for 100% of the total PAH flux from the sediment, and amounted to 2,478 ug/m²/month in an uncapped core under ambient conditions that included upward groundwater advection. Other than such empirical observations, however, the mechanism and rate of this physical process is completely unknown. These observations do indicate, that bubble mixing may have a dominant impact on contaminant fluxes into the water column relative to gas phase transport.

C2.6 RESUSPENSION AS ENHANCED BY THE LOWER BULK DENSITY OF GASSY SEDIMENTS

The effect of the gas voids in the sediment matrix is to increase sediment porosity and reduce bulk density, thus decreasing the critical shear stress for resuspension during periods of high flow, wave activity, or storms (Joyce and Jewell, 2003; Jepsen et al., 2000; Richardson, 1998). Because gas generation and bubble formation are temperature dependent, fluctuations of bulk density, critical shear stress, and erosion rates may also follow changes in temperature. Jepsen et al. (2000) found that at 20° C, gas bubbles decreased sediment densities by up to 10%, increased erosion rates by up to a factor of 60, and decreased the critical shear stress by up to a factor of 20. At lower temperatures, these effects decreased significantly. These changes were also a function of gas void ratio (volume of gas/total volume). In sediments with 3-4% gas, erosion rates increased by a factor of 2-4 relative to sediments with no gas. The maximum erosion rate increase, 20- to 60-fold, was measured for sediments with 8% gas.

C2.7 CONTROLLING FACTORS AND SCALES OF VARIATION

Many factors influence the rate of methane generation, bubble formation, and bubble transport to the surface. Sediment accretion rate and the burial rate of organic material correlate positively with ebullition fluxes (Henrichs and Reeburgh, 1987; Richardson, 1998). The composition of microbial populations also affects gas generation rates as well as the composition of gases (Fendinger et al., 1992).

Temperature strongly affects both microbial activity rates and the saturation concentration of the methane. As a result, in temperate latitudes, methanogenesis and ebullition is highly seasonal (Joyce and Jewell, 2003). In some cases, it has been shown that seasonal temperature variations led to seasonal bubble formation due to changes in the saturation concentration, without affecting

methanogenesis rates (Richardson, 1998). Martens and Klump (1980) found that in the winter, bubbles were completely absent from the sediment matrix. Ebullition was observed to occur within a sediment temperature range of 17-27 °C. In a Michigan freshwater lake, ebullition was observed in the winter, under ice as well at 4% of the summer rate (Strayer and Tiedje, 1978). An example of the seasonality of ebullition is shown in Figure 3. Diurnal cycles in ebullition fluxes were also observed, with night time ebullition near 10% of total daily fluxes (Joyce and Jewell, 2003) in a freshwater lake at depths up to 6 m. The reason for such diurnal cycling is unknown.

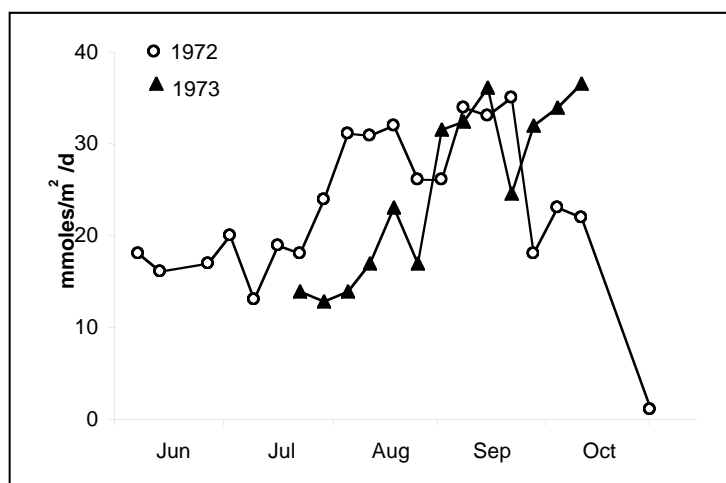


Figure C3. Ebullition fluxes as measured by Strayer and Tiedje, 1978 in a Michigan freshwater lake.

Changes in pressure due to tidal water level fluctuations, wind-induced shear, and barometric pressure changes affect the saturation concentration and can induce or stop bubbling. Small barometric pressure changes of 1-2 percent are capable of causing bubbles to move in or out of solution (Joyce and Jewell, 2003). Shear stress will temporarily weaken the sediment column to trigger the release of bubbles that cannot escape by their buoyancy alone (Joyce and Jewell, 2003). Joyce and Jewell (2003) reported correlations of ebullition fluxes (represented by their square root) with wind velocity in a small freshwater lake to be as high as 0.63, while correlation with current velocity was as high as 0.84.

Greater water depth leads to higher pressures and greater saturation pressures. It will also moderate daily and seasonal fluctuations of temperature (Fendinger et al., 1992). Joyce and Jewell (2003) reported minor ebullition rates in water deeper than 5 m, while Martens and Klump (1980) observed high ebullition rates under 8 feet of water. Deeper water also increases the time available for contaminants to diffuse from the bubbles into the water column (Fendinger et al., 1992; Martens and Klump, 1980).

In saline environments, macrofaunal activity and bioturbation affect redox zonation by irrigation of deeper sediments with oxygenated water containing sulfates. In this way, they drive methanogenesis to greater sediment depths, while encouraging oxidation of methane diffusing toward the surface (Martens, 1976). The activity of these organisms also physically controls bubble transport (Martens, 1976). For example, they can affect sediment structure through pelletization, which in turn increases the ease with which bubbles can travel through the

sediment matrix. In addition, bioturbation can influence the availability of ebullition tubes through which bubbles can escape. With a very high supply of organic matter, however, the sediments may become too reduced for colonization. In the case of the estuarine Cape Lookout Bight on the North Carolina coast, methanogenesis and bioturbation alternate in a seasonal pattern (summer and rest of year, respectively) in some locations, but do not coexist. In other locations, where macroinfauna continue to inhabit the sediment, ebullition is never observed (Martens and Klump, 1980).

Colonization of shallow, fresh, and estuarine sediments by plants affects the route through which methane leaves the sediment. Depending on the density of the vegetation, some to almost all methane may pass to the atmosphere through plants, potentially eliminating ebullitive fluxes (Bazhin, 2004) in such environments.

The effects of ebullition can enhance or be suppressed by groundwater seepage. On the one hand, ebullition may increase the permeability of the sediment matrix, thereby facilitating groundwater flow and advection of sediments and/or contaminants. On the other hand, if groundwater advection is high enough, dissolved methane will be removed from the system, thus decreasing the potential for bubble formation. Both effects were observed at the Stryker Bay Superfund Site (Huls et al., 2003). Groundwater advection may also moderate the seasonal temperature variation. The balance between these two processes may vary seasonally, with an initial dominance of dilution by groundwater, onset of ebullition with higher summer temperatures, and a final phase in which groundwater may flow more freely through the sediment.

Due to the interaction of the above mentioned factors, ebullition fluxes vary both temporally and spatially. The literature cited above includes temporal variation from 0.5 to 2.5 times the mean yearly flux, and 2-4 times as great as spatial variation (based on data from Joyce and Jewell, 2003 and Martens and Klump, 1980). Daily ebullition rates over the course of a year appear to have a bimodal distribution (Figure C4.)

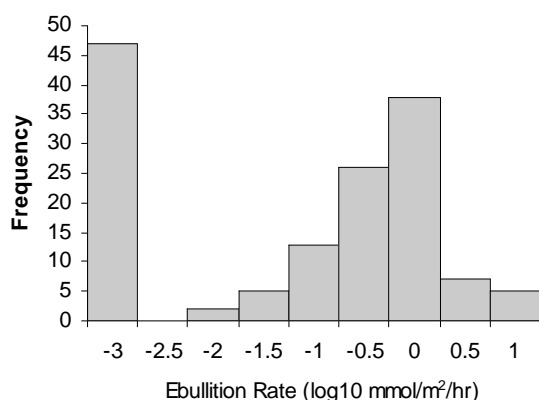


Figure C4. Distribution of hourly ebullition rates over the course of 1-2 days. (data from Joyce and Jewell, 2003).

C2.7.1 Impact of Caps on Ebullition

Huls et al. (2003) and Costello et al. (2003) have directly measured the impact of caps on ebullition combined with groundwater advection in undisturbed cores covered with layers of three different capping materials: two types of sand, and a mixture of sand and organoclay to act as a sorbent of escaping organic contaminants. One effect of the dense, coarse-grained cap material is that it fills existing gas channels in the fine grained sediment during application. Within the coarse grained cap, ebullition tubes are probably transient or may not occur at all. The gas is instead forced to break up into much smaller bubbles. The weight of the cap also compresses the underlying fine sediment, providing increased pressures and thus a higher threshold pressure for bubble formation. Capping also suppresses ebullition by attenuating temperatures, which is an important driver of ebullition rates (higher temperatures lower the saturation concentration, while stimulating methanogenesis). Finally, capping eliminates the organic matter supply, so methanogenesis rates gradually decrease, as the available organic matter is depleted over time.

Through modeling a site with significant upward groundwater seepage, contaminated with PAHs and free-phase NAPL, Huls et al. and Costello et al. determined that a three-foot thick cap would be required to completely suppress ebullition through a combination of all the above processes. All caps reduced the PAH and NAPL flux to below detection. While the cap with the organoclay additive stimulated methanogenesis in the lab, it was equally effective in reducing contaminant flux in bench-top experiments.

Three-foot thick caps are often not a realistic option due to shallow overlying water, navigation requirements, and resource constraints. This indicates, that at least in some cases, if not taken into account, ebullition could compromise predicted cap performance and lead to failure of remedial actions. However, these experiments did not separate the effect of groundwater advection, so it is possible that if groundwater advection had not been present, a thinner cap

thickness would have been sufficient. It is clear that a cap applied onto sediments with high ebullition rates must decrease the rate of gas formation quickly enough to prevent failure. Otherwise, pressures could eventually build up and be released through localized “eruptions”.

C3. DATA AVAILABILITY

Site-specific quantitative data on gas ebullition are not generally available. An exception is the Stryker Bay Superfund site in Duluth, Minnesota, where ebullition was demonstrated to be an important mass transfer mechanism. Measurements were made on columns in the laboratory using cores from the site augmented with various capping materials. Measurements included gas and contaminant flux into the water, as well as contaminant migration into the capping material over time. These measurements were not directly used in a modeling framework, but they served to demonstrate performance of capping materials for the site.

C4. REPRESENTATION IN LEADING FATE AND TRANSPORT MODELS

Two of the most common model frameworks for contaminated sediment fate are WASP and EFDC. The effect of bubble ebullition is not simulated in a mechanistic fashion by either model. Rather, ebullition and other processes are lumped into an “enhanced” sediment-water exchange rate that is typically determined empirically from site-specific data (e.g. a mass balance over a reach during conditions where resuspension is negligible) or as a calibration parameter (Imhoff et al., 2003).

In WASP there is no direct approach for including gas transport. WASP models the sediment bed as discrete layers and then simulates advective and diffusive transport between layers assuming 100% saturation. However, as long as the magnitude by which ebullition enhances chemical and physical exchange can be estimated, ebullition can be accounted for by adjusting porewater and particle mixing coefficients, as well as sediment bulk properties, accordingly.

HEM3D is a model that includes eutrophication processes and sediment biogeochemical processes (diagenesis). HEM3D is an extension of EFDC and allows the modeling of consolidation, methane generation, and the fluxes of ammonium, nitrate, phosphate and silica. The eutrophication kinetics and sediment processes are based on those in CE-QUAL-ICM. The model can compute the total amount of gas release from the sediment bed, but without simulating the movement of a separate gas phase and its various feedbacks on diffusion rates.

At least one modeling framework has been developed that explicitly includes ebullition and the effects of the gas phase on contaminant transport and sediment bulk properties at WL-Delft Hydraulics, an independent research institute and specialist consultancy based in the Netherlands. DELWAQ-G models sediment diagenesis by incorporating decomposition of organic matter, consumption of electron-acceptors (oxygen, nitrate, sulfate and methanogenesis), oxidation, precipitation and dissolution of sulphide; oxidation, ebullition and volatilisation of methane; and mass transport in the sediment by bioturbation, bio-irrigation, burial, digging and seepage (WL-Delft, 2004a). DELWAQ does not compute water movement, so a coupling with models such as WASP or EFDC is necessary for full modeling of fate and transport.

DELCON, an earlier version of DELWAQ, has been used by Service Engineering Group and Soil Technology, Inc. to model the impact of capping at the Stryker Bay Superfund Site in Duluth, Minnesota (WL-Delft, 2004b). The model was used to determine the minimum cap thickness required to suppress ebullition and associated contaminant transport. The system was modeled in transient mode, and the resulting consolidated system was used in a dynamic estuary model (DEM) in which long-term contaminant fluxes were estimated (Huls et al., 2003; Costello et al., 2003). A cap thickness of 3 ft was predicted to prevent gas ebullition due to isolation from warm temperatures.

In summary, given the uncertainties about various mechanisms and rates that describe ebullition and associated contaminant fluxes, existing modeling frameworks, such as WASP and EFDC provide sufficient opportunities to incorporate empirically determined impacts of ebullition into the modeling process. The development of a mechanistic framework for ebullition driven contaminant fluxes would be premature due to the magnitude of uncertainties (discussed below) regarding potentially important mechanisms, such as physical mixing through bubbling.

Information on the impacts of gas ebullition on contaminant stability can be incorporated into the existing models by allowing decisions to be made about the magnitude of lumped mass transfer coefficients. The apparent similarity of some of ebullitions impact to processes such as bioturbation also justifies such an approach.

C5. PREDICTIVE UNCERTAINTY

Large knowledge gaps exist about the ebullition process about both the mechanistic/ theoretical aspect of processes and empirical measurements of rates and their dependence of environmental factors.

Among the six conceptual processes that have been described, the greatest uncertainties surround the process of bubble formation and growth and the physical transport of contaminants. Bubble sizes and residence times are unknown, but would be important in order to properly estimate the extent of contaminant partitioning into the gas phase, especially when equilibrium is unlikely to be reached. The rate at which migrating bubbles mix sediments is also an important uncertainty, since it could contribute substantially to total fluxes. Finally because gas generation rates are the driving force behind ebullition, it is important to better define the microbial, chemical and physical factors that affect it on all spatial and temporal scales. Because temporal variations can be significant, properly incorporating time-variability of underlying factors can be critical in reducing model uncertainty. This includes diurnal, seasonal and weather related variabilities. Spatial variabilities can also be important since gas generation is often associated with shallower, depositional zones. How much variation exists on a local scale, within such zones, is unknown.

The interaction between groundwater seepage and ebullition can be a critical factor, because the two can act in synergy, enhancing contaminant flux pathways. It is not known how different factors could predict the direction in which these two processes would interact, or to what extent they would jointly enhance total fluxes from the sediment.

Reducing the above uncertainties would greatly facilitate the incorporation of ebullition into existing frameworks. However, much more needs to be learned for the mechanistic modeling of ebullition-driven contaminant fluxes. A fate and transport model that fully and mechanistically incorporates ebullition has to account for chemical transport inside the bubbles, physical transport of particles by rising bubbles, and reduction of bulk density/critical shear stress. The following parameters would have to be specified: bubble generation rate and depth, bubble escape rate, bubble residence time, gas void ratio, porewater to bubble partitioning, gas-bubble surface area, the rate of particle transport by bubbles. These would have to be linked to temperature, sediment grain-size distribution, shear stress, etc. Currently, the uncertainties are too large to support such a model framework.

C6. REFERENCES

- Adams, D.D., N.J. Fendinger, and D.E. Glotfelty, 1990, Biogenic gas production and mobilization of in-place sediment contaminants by gas ebullition. In: R. Baudo, J.P. Giesy and H. Muntau (Eds.) *Sediments: Chemistry and Toxicity of In-Place Pollutants*. Lewis Publishers, Inc.
- Adams, D.D., M. Naguib, and D.H. Brown, 1987, Cycling of methane in acidified freshwater environments. In: R. Perry, R. M. Harrison, J. N. B. Bell and J. N. Lester. (Eds.) *Acid Rain: Scientific and Technical Advances*. London, Publ. Division, Selper Ltd: 451-456.
- Bazhin, N.M. (2004) Influence of plants on the methane emission from sediments. *Chemosphere*, **54**(2):209-15.
- Casper, P., S.C. Maberly, G.H. Hall, and B.J. Finlay. 2000. Fluxes of methane and carbon dioxide from a small productive lake to the atmosphere. *Biogeochem.* 49: 1-19.
- Chanton, J.P., C.S. Martens (1988) Seasonal variations in ebullitive flux and carbon isotopic composition of methane in a tidal freshwater estuary. *Global Biogeochemical Cycling*, **2**(3):289-298.
- Costello, M., H. Huls, and E. Hedblom (Service Engineering Group), 2003, Design Level Evaluation of a Remedial Wetland Cap. Presented at: In-Situ Contaminated Sediment Capping Workshop, Cincinnati, OH. May 12-14, 2003.
- Erickson, M., C.L. Turner, L.J. Thibodeaux (2005) Field observation and modeling of dissolved fraction sediment - Water exchange coefficients for PCBs in the Hudson River. *Environmental Science and Technology*, **39**:49-556.
- Fendinger, N.J., D.D. Adams, D.E. Glotfelty (1992) The role of gas ebullition in the transport of organic contaminants from sediments. *The Science of the Total Environment*, **112**:189-201.
- Gong, Y. and J.V. DePinto, 1998, Desorption rates of two PCB congeners from suspended sediments – I. Experimental Results. *Water Research*, **32**(8):2507-2517.
- Gong, Y. and J.V. DePinto, 1998, Desorption rates of two PCB congeners from suspended sediments – II. Model Simulation. *Water Research*, **32**(8):2518-2532.
- Hartman, B. and D.E. Hammond, 1984, Gas exchange rates across the sediment-water and air-water interfaces in South San Francisco Bay. *Journal of Geophysical Research*, **89**(C3)3593-3603.
- Henrichs, S.M. and W.S. Reece, 1987, Anaerobic mineralization of marine sediment organic matter: rates and the role of anaerobic processes in the oceanic carbon economy. *Geomicrobiology Journal*, **5**(3/4):191-239.
- Huls, H., M. Costello (Service Engineering Group), and Richard Sheets (Soil Technology, Inc.), 2003, Bench Test Design Evaluation of a Remedial Wetland Cap (with regard to ebullition and its control).
- Imhoff, J.C., A. Stoddard, E.M. Buchak, and E. Hayter (2003) Evaluation of Contaminated Sediment Fate and Transport Models – Final Report. NATIONAL Exposure Research Laboratory - Office of Research and Development, U.S. Environmental Protection Agency, Athens, Georgia.
- Jepsen, R., J. McNeil, and W. Lick, 2000, Effects of gas generation on the density and erosion of sediments from the Grand River. *Journal of Great Lakes Research*, **26**(2):209-219.
- Jones, W.J. and M.J.B. Paynter, 1980, Populations of methane-producing bacteria and in-vitro methanogenesis in salt marsh and estuarine sediments. *Applied and Environmental Microbiology*, **39**(4):864-871.
- Joyce, J. and P.W. Jewell, 2003, Physical controls on methane ebullition from reservoirs and lakes. *Environmental and Engineering Geoscience*, **IX**(2):167-178.
- Liikanen, A., H. Tanskanen, T. Murtoniemi, and P.J. Martikainen, 2002, A laboratory microcosm for simultaneous gas and nutrient flux measurements in sediments. *Boreal Environment Research*, **7**:151-160.

- Lohmann, R., E. Nelson, S.J. Eisenreich, and K. Jones. 2000. Evidence for dynamic air-water exchange of PCDD/Fs: A study in the Raritan Bay/Hudson River Estuary. *Environmental Science and Technology* **34**:3086-3093
- Matsumoto, Y., Ishii, Y., Shimura, K. (1992) Gas generation in canals of Tokyo Port. In: Proceedings on the 12th U.S./Japan Experts Meeting: Management of Bottom Sediments Containing Toxic Substances, 11-14 November 1986, Yokohama, Japan. T.R. Patin (ed.) United States Army Corps of Engineers, Water Resources Support Center.
- Martens, C.S. (1976) Control of methane sediment-water bubble transport by macrofaunal irrigation in Cape Lookout Bight, North Carolina. *Science*, **192**:998-1000.
- Martens, C.S. and J.V. Klump (1980) Biogeochemical cycling in an organic-rich coastal marine basin – I. Methane sediment-water exchange processes. *Geochimica et Cosmochimica Acta*, **44**: 471-490.
- Palermo, M.R., Thompson, T.A., Swed, F. (2002) White Paper No. 6B – Is-Situ capping as a remedy component for the lower Fox River. Response to a document by the Johnson Company: Ecosystem-based rehabilitation plan – An integrated plan for habitat enhancement and expedited exposure reduction in the lower Fox River and Green Bay. December 2002.
- Richardson, M.D. (1998) Coastal Benthic Boundary Layer: A Final Review of the Program. NRL Memorandum Report. Marine Geosciences Division – Naval Research Laboratory. September 1, 1998
- Stayer, R.F. and J.M. Tiedje, 1978, In situ methane production in a small, hypereutrophic, hard-water lake: Loss of methane from sediments by vertical diffusion and ebullition. *Limnology and Oceanography*, **23**(6):1201-1206.
- Stivers, C.E. and Sullivan, R. (1994) Restoration and capping of contaminated sediments. In: Dredging '94, Proceedings of the Second International Conference on Dredging and Dredged Material Placement, 14-16 November 1994, Orlando, Florida. E.C. McNair, Jr. (ed.) American Society of Civil Engineers, New York, New York. p. 1017-1025.
- USGS-SMIC (2004) Surface Water and Water Quality Models Information Clearinghouse. EFDC/HEM3D. http://smig.usgs.gov/cgi-bin/SMIC/model_home_pages/model_home?selection=efdc
- Vroblesky, D.A., and Lorah, M.M., 1991, Prospecting for zones of contaminated ground-water discharge to streams using bottom-sediment gas bubbles: *Ground Water*, v. 29, p. 333-340.
- Whiticar, M.J. (2002) Diagenetic relationships of methanogenesis, nutrients, acoustic turbidity, pockmarks and freshwater seepages in Eckernförde Bay. *Marine Geology*, **182**(1-2):29-53.
- WL-Delft (2004a) Project: Sediment-water exchange of substances. <http://www.niwi.knaw.nl/nl/oi/nod/onderzoek/OND1288096/toon>.
- WL-Delft (2004b) Gas enhanced transportation from contaminated sediment at Stryker Bay, Duluth – Project description. <http://www.wldelft.nl/proj/pdf/4uk00225.scherm.pdf>

APPENDIX D: GROUNDWATER SEEPAGE

D1. INTRODUCTION

Groundwater seepage or upwelling through the sediment bed is frequently observed to occur in contaminated sediment system. However, the degree to which groundwater-surface water interaction serves as a significant factor affecting ecological exposure and contaminant losses from sediments is typically poorly understood. This section describes the current theory and process understanding of groundwater seepage and the groundwater-surface water interface (GSI) in general; assesses the adequacy of typical site-specific data; reviews how GSI processes are represented in leading fate and transport models; and assesses the relative uncertainties in predicting GSI behavior.

D2. THEORETICAL PROCESS UNDERSTANDING

Contaminant transport through the groundwater-surface water interface (GSI) is governed by a combination of complex hydraulics in and around the sediment bed, and a transport environment in the sediment bed that frequently exhibits sharp gradients in temperature, salinity, redox chemistry, biological population, and physical disruption. A brief discussion of the major factors affecting transport in the GSI follows, focusing on the hydraulics of the groundwater-surface water interaction zone and mass exchange processes related to groundwater contaminant fluxes.

D2.1 HYDRAULICS OF GROUNDWATER-SURFACE WATER INTERACTION

Groundwater seeps exist in a wide array of different hydraulic environments, from free-flowing riverine environments, to river impoundments and lakes, to coastal environments. In these different environments, the mechanisms of groundwater flow and exchange with surface water may differ significantly, depending strongly on local hydraulic behavior and local bio- and geochemistry.

In mountainous systems, groundwater is typically tightly connected with surface waters, with relatively highly conductive surface soils and frequent, highly variable rainfall. Groundwater systems in these areas are typically recharged by a combination of rainfall and snowmelt.

In lower-gradient riverine systems, groundwater flow in the vicinity of surface waters is often a mix of larger-scale regional groundwater flow and local groundwater systems that follow smaller scale topography. In particular, relatively flat river systems can have very dynamic interactions with adjacent floodplains, including groundwater-mediated floodwater recession (Winter *et al.*, 1998). Consequently, such systems typically have highly heterogeneous groundwater seepage behavior (McBride and Pfannkuch, 1975, Conant, 2004, Conant *et al.*, 2004). An informative review of the state of knowledge of groundwater hydrology and exchange processes in riverine systems can be found in Hayashi and Rosenberry (2002).

In coastal systems, groundwater discharge rates are typically strongly correlated with tidal activity, with periods of highest groundwater discharge corresponding with periods of low tide. The periodic nature of tides in many marine systems can result in “tidal pumping” of marine sediments, resulting in a relatively deep zone of mixed fresh- and marine water in the GSI (Cartwright and Nielsen, 2003; Cable *et al.*, 1996, Chadwick, 2003). Coastal systems also typically exhibit high groundwater discharge in nearshore areas, and lower rates of discharge further from shore (Robinson *et al.*, 1998). A very detailed and descriptive summary of groundwater-surface water interactions across many different hydrologic environments can be found in Winter *et al.* (1998).

Groundwater interactions with surface water typically fall into three different regimes: either a surface water receives inflow from a groundwater system (e.g., a gaining river), a surface water drains or infiltrates to a groundwater system (losing river), or the surface water system is a mixture of both upwelling and downwelling connections with the local groundwater system. It is important to note that the direction of groundwater-surface water interaction can vary significantly across different scales: a river may show net gains of groundwater across some

reaches and losses along others, while point measurements of groundwater seep may show significant variability, including upwelling and downwelling areas, at scales of as little as meters apart (e.g., Conant *et al.*, 2004, Conant, 2004; Cable *et al.*, 1997; Cable *et al.*, 1995)

D2.2 MASS EXCHANGE PROCESSES IN THE GROUNDWATER-SURFACE WATER INTERFACE

Mass transfer between the sediment bed and the overlying surface water can be attributed to a wide range of processes, including:

- molecular diffusion of dissolved phase or colloid-bound porewater PCB;
- hydrodynamically-induced advective pumping through the near-surface interstices in the sediment bed;
- biologically-enhanced porewater and particulate transport within the sediment bed and at the sediment-water interface;
- emergence and uprooting of macrophytes;
- physical disturbance from wind-driven waves, fish activity, or human activity;
- gas ebullition;
- direct desorption from surface sediments to the water column; and
- groundwater advection through the sediment bed

A general expression for sediment-water mass transfer that lumps all of the above processes into a single expression is given by:

$$\frac{\partial M}{\partial t} = \frac{EA}{L} (C_{pw} - C_w) \quad (1)$$

where:

M	= mass of constituent
E	= sediment/water exchange coefficient (L^2/t)
A	= interfacial area for mass transfer (L^2)
L	= characteristic length over which mass transfer occurs (L)
C_{pw}	= constituent concentration in pore water (M/L^3)
C_w	= constituent concentration in surface water (M/L^3)

The bulk exchange coefficient can also be expressed as a mass transfer rate coefficient with units of length per time, as:

$$K_f = \frac{E}{L} \quad (2)$$

As stated above, the focus of this section is exchange of groundwater by pure advection (upwelling) of groundwater through the sediment-water interface. Neglecting other possible

sources of sediment-bed mass exchange, flux of contaminant mass due to groundwater upwelling alone is simply described by:

$$\frac{\partial M}{\partial t} = qAC_{pw} \quad (3)$$

where q is the Darcy velocity (seepage rate) of groundwater into the system (L/t). Equating this with the above expression for bulk mass exchange, it can be shown that:

$$K_f = \frac{qC_{pw}}{C_{pw} - C_w} \quad (4)$$

Note that when surface water concentrations are significantly lower than pore water concentrations ($C_w \ll C_{pw}$), the above expression reduces to:

$$K_f = q \quad (5)$$

This condition is expected to be satisfied in most systems, due to the effect of surface water dilution of the upwelling groundwater.

The porewater concentration (C_{pw}) of the constituent of interest is a function of the constituent's partitioning behavior, as represented by the equilibrium partitioning coefficient:

$$K_d = \frac{C_s}{C_{pw}} \quad (6)$$

where C_s is the solid phase (sorbed) concentration of contaminant, with units of M/M, giving a partitioning coefficient with units of L³/M. Use of such a partitioning coefficient requires the assumption of local equilibrium partitioning behavior. Implicit in this assumption is the requirement that contact time between the solid and aqueous phases is sufficiently long that local equilibrium can be reached. While this assumption may be appropriate for simple bounding calculations, it is likely that transport through a relatively thin sediment bed may not be sufficiently long to allow conditions of local equilibrium to be reached. Departure from local equilibrium partitioning would likely result in significantly lower pore water concentrations than would be predicted based on the assumption of local equilibrium.

D3. ADEQUACY OF TYPICAL SITE-SPECIFIC INFORMATION

As described in the previous section, contaminant flux via groundwater advection through the sediment bed is dependent on both the hydrodynamics of the groundwater-surface water interaction zone and the processes governing partitioning between the sediment solid phase and the aqueous (pore water) phase. Estimation of groundwater-mediated fluxes for any particular system will require measurement of groundwater seepage and associated contaminant porewater concentrations, both of which present significant challenges. This section describes measurement techniques available for measurement of large-scale seepage rates, local seepage rates, and porewater concentrations, and assesses the adequacy of such measurements for estimation of groundwater fluxes.

D3.1 MEASUREMENT OF LOCAL GROUNDWATER SEEPAGE

Methods for estimation of local groundwater seepage typically involve placement of an inverted barrel or funnel over a section of sediment bed, making it possible to isolate a portion of the sediment-water interface and monitor flow through that interface. Such a device was first described by Lee (1977). Most seepage studies performed in the 1980's and 1990's used simple bags to collect flow crossing the sediment-water interface, allowing estimating of a net volumetric inflow across the sediment bed. Use of a partially pre-filled bag allows estimation of both upwelling and downwelling groundwater flow, as limited by the available capacity in the bag. These simple but effective groundwater seepage monitors allowed for highly precise measurements of net inflow/outflow over relatively short periods of time (e.g., Cable *et al*, 1996; Cable *et al*, 1997; Robinson *et al*, 1998; review of historical coastal studies by Taniguchi *et al*, 2001)

More recently, seepage meters with the same inverted funnel design have been fitted with highly precise flow meters placed in the narrow section of the funnel, allowing precise measurements of inflows and outflows, with much less constraint on the range of measureable flows (Chadwick, 2002). These meters have been particularly useful in marine systems, where time-dependent tidally-drive flows can now be measured directly and recorded as time series, showing more clearly than ever the relationship between tidal fluctuation and seepage.

Local seepage rate measurements are often performed in tandem with groundwater potentiometric measurements, typically performed with sets of nested piezometers. These tools can be used to detect horizontal and vertical gradients in groundwater adjacent to surface waters (e.g., Robinson *et al*, 1998, Conant 2004, Conant *et al*, 2004). The available body of data now available on local groundwater seepage rates, at virtually all sites where sufficient measurements have been made to characterize variability, consistently shows a high variability in rates. In fact, the most well-characterized sites tend also to show the most significant variability, in terms of both the magnitudes of seepage rates and the direction of seepage (e.g., Conant, 2004 – glacial riverine environment, Cable *et al*, 1997 – coastal environments, Choi and Harvey, 2000 - Everglades). Seepage meter and piezometer studies also show a high degree of temporal variability, both seasonally and with tidal fluctuation.

D3.2 MEASUREMENT OF LARGE-SCALE GROUNDWATER INTRUSION

Due to the considerable spatial and temporal variability typically observed in point measurements of groundwater seepage, many studies of groundwater intrusion now employ methods that measure seepage over larger spatial and temporal scales that serve to integrate the observed variability into more useful bulk measurements of inflow or outflow. Available methods fall into a few basic categories:

- Explicit modeling of groundwater-surface water flow (e.g., Choi and Harvey, 2000, Jobson and Harbaugh, 1999);
- The use of tracers such as radon, radium, nutrients, salinity, deuterium, methane, and heat, often supplemented with mass-balance modeling (e.g., Robinson *et al.*, 1998; Cartwright and Nielsen, 2003; Bugna *et al.*, 1996; Katz *et al.*, 1997; Choi and Harvey, 2001; Harvey *et al.*, 2000); and
- Hydrograph separation techniques that allow separation of groundwater-related baseflow from runoff-driven peaks (e.g., Holtschlag and Nicholas, 1998, **other ref**)
- Remote sensing techniques (e.g., McVicar *et al.*, 1994, **other ref**).

The most conclusive studies are ones that use multiple lines of investigation to quantify groundwater seepage across a range of temporal and spatial scales, and support the measurements with numerical models that simulate hydraulics and balance water and tracer mass. An argument for “intercalibration” of different measurement approaches can be found in Burnett *et al.* (2001).

As observed in the literature describing point measurements of groundwater seepage, studies of large-scale groundwater intrusion also show significant variability. The following section presents a discussion of the ranges of measured seepage rates in studies employing both point- and large-scale measurement methods.

D3.3 RANGES OF MEASURED SEEPAGE RATES

While a comprehensive review of all seepage rate studies performed to date is out of the scope of this paper, an extensive review of coastal seepage studies can be found in Cable *et al.* (1996), Taniguchi *et al.* (2002), and Burnett, *et al.* (2001). Seepage rates reviewed in these papers are summarized in Table D1, by study area, methods used, and sediment type.

Although this summary is not necessarily statistically representative of all coastal systems, some conclusions can be drawn from the data. The data show a wide range of measured seepage rates, spanning more than four orders of magnitude, from 0.01 to 124 cm/day. In general, it appears that the highest seepage rates are associated with the highest conductivity formations (sands and coarse sands), and lower rates of seepage are associated with lower conductivity silts and silty sands. It is also instructive to note that methods that integrate seepage estimates over a larger scale show median seepage rates that are lower than those obtained by point measurements, possibly due to the effect of averaging out localized high-rate seeps.

The data are also presented as a histogram in Figure D1, indicating an approximately log-normal distribution for the pooled set of all data, measured with both direct and indirect methods. As

noted above, the higher end of the distribution is dominated by point measurements, again suggesting an effect of spatial integration that minimizes the effect of localized, high-end seepage rates.

D3.4 MEASUREMENTS OF PORE-WATER CONTAMINANT CONCENTRATIONS

As described by equation (3), flux of contaminant mass via the groundwater seepage pathway is controlled by the seepage rate and the pore water concentration of contaminant. Porewater concentrations of hydrophobic contaminants sequestered in the solid phase are typically governed by partitioning between the solid and aqueous phase (equation 6). As noted in Section 2.2 above, aqueous-phase concentrations of partitioned contaminant can be significantly decreased by non-equilibrium partitioning between the solid and aqueous phases. The significance of non-equilibrium partitioning in sediments is treated in greater detail in Appendix A.

D3.4.1 Measurement methods

A variety of methods exist for determining pore water contaminant concentrations, including direct analysis of porewater withdrawn from the sediments, semi-permeable membrane and diffusive film devices that equilibrate with pore water concentrations, and other methods that infer porewater concentrations from secondary measurements.

A commonly employed semipermeable membrane device is the Hesslein sampler, or “peeper”, which allows a small, contained volume of water to equilibrate with pore water contaminants through a semipermeable dialysis membrane. Membranes can be selected to target specific size ranges of contaminants, allowing limited selectivity with the devices. A major limitation of peeper devices is the long equilibration times required, on the order of 1-6 months for equilibration with pore waters. Such devices have been extensively tested and evaluated by the USGS in terms of equilibration times and comparability with conventional porewater sampling (Lyford *et al*, 2000).

Pore water concentrations can also be measured with devices that operate by absorption or adsorption of pore water contaminants to various media. Adsorption to low-density polyethylene (LDPE) strips has recently been used to characterize distributions of PCBs, PAHs, and HCB in porewaters (Booij *et al.*, 2003). Very recently emerging methods involve absorption of solutes into thin layers of gel resin deployed in the sediment bed, including diffusive equilibration in thin films (DET), and diffusive gradients in thin films (DGT) (Fones *et al.*, 2001). These methods offer the possibility of much more detailed characterization of vertical porewater profiles than has previously been possible.

Similarly to the literature described above with respect to seepage rates, the most detailed and spatially dense studies of pore water concentrations available show very high variability in contaminant concentrations. Conant *et al* (2004) describe a very detailed study of the intersection of a well-characterized groundwater plume with a stream bed, involving SPMDs, multilevel sampling, ground penetrating radar, streambed temperature mapping, piezometers, and sediment coring and testing. The study concluded that the near-river zone strongly modified the distribution, concentrations, and composition of plume contaminants prior to discharge into

the surface water, resulting in significant short-scale variability in discharge concentrations, with variations in concentrations from 100 to 5000 times over distances of a few meters.

This substantial degree of observed variability suggests that characterization efforts should focus on methods that integrate spatially and temporally, rather than driving investigations to progressively smaller and smaller scales.

D4. PROCESS REPRESENTATION IN LEADING FATE AND TRANSPORT MODELS

As described in Section 3, contaminant flux via groundwater seepage into surface water systems tends to be complex, in terms of both the hydraulics of the groundwater-surface water interface and the physical and chemical processes that govern mass exchange and transport through the sediment bed. Measurement and analytical techniques appropriate for characterizing such fluxes are at an early stage of development, providing sufficient data to show the very high spatial and temporal variability in both groundwater seepage rates and contaminant fate and transport processes.

Consequently, the level of representation of groundwater seepage processes currently possible in groundwater flow and contaminant transport models is limited, both by the level of understanding of the full suite of processes that operate in the GSI, and by the limited data typically available at contaminated sediment sites. While groundwater seepage is increasingly recognized as an important part of many surface water systems, most current models acknowledge the lack of data to effectively constrain the degree of groundwater contribution, and lump groundwater contributions into source terms with relatively coarse spatial characterization. In many cases, groundwater contributions are further lumped with other, often unrelated processes that may govern transport of contaminants through the sediment bed (Section 2.2).

Modeling of the groundwater seepage problem is further complicated by a gulf between the surface water and groundwater modeling disciplines. Model developers have historically developed either groundwater or surface water models, with source terms that allow rough linkage of the models, typically without explicit representation of the temporally and spatially dynamic nature of the GSI. An early perspective on the need for better representation of the continuum of catchment, stream, and groundwater was presented in the early 1990s by Bencala (1993) and Bencala *et al.* (1993).

Since that time, some of the leading groundwater models have started to include explicit coupling routines that link groundwater and surface water components. In 1999, the USGS introduced a linkage between the very widely used MODFLOW groundwater model and DAFLOW (Jobson and Harbaugh, 1999), a simplified dynamic wave equation model of surface water flow. Although the surface water component of this pair of models has significant limitations, the MODFLOW/DAFLOW combination does allow for dynamic simulation of the GSI. A more recently release package, the MODFLOW SFR1 package, also allows limited surface water routing within the MODFLOW environment, but with even more limited surface water hydrodynamics than DAFLOW (Prudic *et al.*, 2004). While some more advanced models of variable-density flow and transport exist (e.g., Kooi and Groen, 2001), these models are typically confined to research applications.

In the areas of sediment and surface water modeling, groundwater seepage is commonly represented as a term following Equation 3, or is lumped together with a wide range of other sediment bed transport parameters into a single bed mass exchange coefficient, following Equation 1. The lumped expression presented in (1) shows resistance to mass exchange occurring in response to the limitation of the mass exchange rate, as represented by the mass exchange coefficient, K_f (Equation 2), and also due to the degree of partitioning that occurs

between the pore water and solid phases (Equation 6). Equation 1 can be restated on a flux per unit area (N) basis as:

$$N = K_f \left(\frac{C_s}{K_d} - C_w \right) \quad (7)$$

Assuming that the solute concentration in water is small relative to the pore-water concentration, C_w can be neglected and (7) can be expressed as:

$$\frac{N}{C_s} = \frac{K_f}{K_d} \quad (8)$$

This derivation follows that of Thibodeaux (2003), and shows the linear dependence of concentration-normalized chemical flux on the mass exchange coefficient, K_f , and the distribution coefficient, K_d . The following section describes how this relationship can be used to place groundwater seepage rate contributions to sediment bed transport within a general context by which contributions from the range of relevant processes can be evaluated.

D5. PREDICTIVE UNCERTAINTY

Developing an assessment of the significance of groundwater seepage as it impacts transport and exposure in surficial sediments requires understanding the uncertainty in estimates of seepage rates and transport, as described in the previous sections. Further developing this assessment also requires placing groundwater seepage in the appropriate context: understanding the significance of groundwater seepage relative to other transport processes operating in the sediment bed, and understanding the importance of seepage as it affects the ultimate endpoints of contaminant exposure, such as exposure half-times, risk contributions, or whatever else may be of importance at the sediment site.

While development of such an assessment will necessarily be a site-specific endeavor, some generalizations can be made based on the data collected in this review. As described above, Equation 8 provides a simplified depiction of the dependence of solute flux through the bed on the mass exchange coefficient, K_p , and the distribution coefficient, K_d . This relationship is graphically depicted as a “map” of varying chemical stability, following Thibodeaux (2003), in Figure D2. Diagonal lines on the map represent lines of constant concentration-normalized chemical flux (left side of Equation 8), a useful measure of chemical stability. The map illustrates the range of possible zones of chemical stability, from very low stability (high flux) where the distribution coefficient is low and the mass exchange coefficient is high (lower right), to high stability corresponding to low exchange and strongly bound contaminants (upper left).

Groundwater seepage data from Table D1 is plotted on Figure D2 as mass exchange rate coefficients, following Equation 5. A box and whisker plot is superimposed on the data, with horizontal box dimensions representing the upper and lower quartiles of the distribution and whiskers showing the range of the entire dataset. The vertical dimensions of the box represent the range of PCB distribution coefficients, assumed here to be $10^4 - 10^5$ cm³/g. As plotted, the data span approximately 6 orders of magnitude of normalized flux rates.

Defining what portions of this map constitute zones of chemical stability or instability would require more knowledge of the nature of a specific site, and what mass flux rate would be acceptable at the site. This assessment may depend on the degree of dilution available in the surface waters, the mass of contaminants in the bed and the acceptable half-times for recovery, or other factors relating to specific targets or endpoints judged to be significant at the site.

The plot can be used to illustrate the range of effectiveness of different capping alternatives. When simple reduction of flux is a primary goal, a dramatic change in the degree of chemical stability can be achieved by emplacing a low permeability cap, thus modifying the hydraulic conductivity at the bed surface and decreasing seepage velocities through the bed by several orders of magnitude. This would result in a leftward shift in the location of the data plotted in Figure 2, moving toward an area of substantially increased chemical stability. Adding reactivity to the cap through addition of chemical sorbents could enhance the improvement by simultaneously increasing the value of the distribution coefficient K_d , resulting in an upward shift in the location of plotted data. Conversely, addition of a sand cap that does not substantially alter the rate of groundwater seepage or adsorption properties could have little or no impact on the degree of chemical stability.

Table D1: Reported Measurements of Seepage Rate

Point measurements

Study Area	Method	Estimated Discharge	Units	Sediment Type	Reference
NE Gulf Mexico	Seepage Meters	0.10	cm/day	-	Rasmussen (1998)
Narrow Lake, Alberta	Piezometer	0.01	cm/day	-	Shaw et al. (1990)
Cape Cod, MA	Seepage Meters	3.07	cm/day	Mud and sand	Giblin and Gaines (1990)
Cape Cod, MA	Seepage Meters	3.56	cm/day	Mud and sand	Giblin and Gaines (1990)
Chesapeake Bay, VA	Seepage Meters	1.51	cm/day	Sandy loam	Galagher et al. (1996)
Chesapeake Bay, VA	Seepage Meters	0.05	cm/day	Sandy loam	Rcay et al. (1992)
Chesapeake Bay, VA	Seepage Meters	8.85	cm/day	Sandy loam	Rcay et al. (1992)
East coast of FL (Indian River)	Seepage Meters	6.58	cm/day	Silty sand	Zimmermann et al. (1985)
East coast of FL (Indian River)	Seepage Meters	8.77	cm/day	Silty sand	Zimmermann et al. (1985)
Great South Bay, NY	Seepage Meters	4.00	cm/day	Sand, silty sand	Bokuniewicz (1980)
Keys and Florida Bay, FL	Seepage Meters	0.99	cm/day	Limestone	Corbett et al. (1999)
Keys and Florida Bay, FL	Seepage Meters	2.93	cm/day	Limestone	Corbett et al. (1999)
Laholm Bay, Sweden	Seepage Meters	20.55	cm/day	Sand	Vanek and Lee (1991)
NE coastal Gulf of Mexico, FL	Seepage Meters	0.10	cm/day	Silty sand	Rasmussen (1998)
NE coastal Gulf of Mexico, FL	Seepage Meters	1.01	cm/day	Silty sand	Rasmussen (1998)
Northeast Gulf of Mexico, FL	Seepage Meters	2.44	cm/day	Silty sand	Cable et al. (1997b)
Northeast Gulf of Mexico, FL	Seepage Meters	0.28	cm/day	Silty sand	Cable et al. (1997a)
Northeast Gulf of Mexico, FL	Seepage Meters	5.10	cm/day	Silty sand	Cable et al. (1997a)
Northeast Gulf of Mexico, FL	Seepage Meters	1.42	cm/day	Silty sand	Bugna et al. (1996)
Northeast Gulf of Mexico, FL	Seepage Meters	11.51	cm/day	Silty sand	Bugna et al. (1996)
Off the coast, Wilmington (NC)	Seepage Meters	0.60	cm/day	Continental shelf	Simmons (1992)
Off the coast, Wilmington (NC)	Seepage Meters	2.00	cm/day	Continental shelf	Simmons (1992)
Saltmarsh estuaries, SC	Seepage Meters	0.36	cm/day	Silt/silty sand	Whiting and Childers (1989)
Saltmarsh estuaries, SC	Seepage Meters	1.81	cm/day	Silt/silty sand	Whiting and Childers (1989)
South of Osaka Bay, Japan	Seepage Meters	12.05	cm/day	Sand	Taniguchi (2000)
South of Osaka Bay, Japan	Seepage Meters	37.26	cm/day	Sand	Taniguchi (2000)
Barbados, West Indies	Seepage Meters	73.42	cm/day	Sand	Lewis (1987)
Barbados, West Indies	Seepage Meters	124.38	cm/day	Sand	Lewis (1987)
Lake Biwa, Japan	Seepage Meters	2.59	cm/day	-	Taniguchi and Fukuo (1993)
Lake Biwa, Japan	Seepage Meters	23.33	cm/day	-	Taniguchi and Fukuo (1993)
Narrow Lake, Alberta	Seepage Meters	0.04	cm/day	-	Shaw et al. (1990)
NE Gulf Mexico (FL)	Seepage Meters	20.88	cm/day	-	Cable et al. (1997)
NE Gulf Mexico (FL)	Seepage Meters	0.29	cm/day	-	Cable et al. (1997)
Off the coast, FL Keys	Seepage Meters	0.55	cm/day	Limestone	Simmons (1992)
Off the coast, FL Keys	Seepage Meters	0.74	cm/day	Limestone	Simmons (1992)
	median:	2.44			
	min:	0.01			
	max:	124.38			

Large-scale measurements

Study Area	Method	Estimated Discharge	Units	Sediment Type	Reference
Tokyo Bay, Japan	Groundwater temp - depth	0.01	cm/day	Silty sand	Taniguchi et al. (1998)
Tokyo Bay, Japan	Groundwater temp - depth	0.12	cm/day	Silty sand	Taniguchi et al. (1998)
North slope of AK	Heat flow	0.02	cm/day	Sandstone (Tertiary)	Deming et al. (1992)
Sagami Bay, Japan	Heat flow	0.02	cm/day	Philippine Sea Plate	Tsunogai et al. (1996)
Sagami Bay, Japan	Heat flow	0.03	cm/day	Philippine Sea Plate	Tsunogai et al. (1996)
Cape Cod, MA	Hydraulic dynamics	0.58	cm/day	Mud and sand	Giblin and Gaines (1990)
NE coastal Gulf of Mexico, FL	Numerical modeling	0.44	cm/day	Silty sand	Rasmussen (1998)
NE coastal Gulf of Mexico, FL	Numerical modeling	0.74	cm/day	Silty sand	Rasmussen (1998)
NE Gulf Mexico	Numerical Modeling	1.00	cm/day	-	Rasmussen 1998
Puck Bay, Baltic Sea	Nutrient, isotope	4.11	cm/day	Sand	Pickarek-Jankowska (1996)
Northeast Gulf of Mexico, FL	Radium/Radon Tracers	2.52	cm/day	Silty sand	Cable et al. (1996b)
Northeast Gulf of Mexico, FL	Radium/Radon Tracers	9.89	cm/day	Silty sand	Cable et al. (1996b)
Northeast Gulf of Mexico, FL	Radium/Radon Tracers	6.96	cm/day	Silty sand	Cable et al. (1996b)
Cape Cod, MA	Salinity budget	3.15	cm/day	Mud and sand	Giblin and Gaines (1990)
Cape Cod, MA	Salinity budget	6.36	cm/day	Mud and sand	Giblin and Gaines (1990)
Coastal bays of New England	Salinity, seepage meter	4.79	cm/day	Coarse sand	Valiela et al. (1990)
Coastal bays of New England	Salinity, seepage meter	9.59	cm/day	Coarse sand	Valiela et al. (1990)
Cape Cod, MA	Water balance	0.66	cm/day	Mud and sand	Giblin and Gaines (1990)
Cape Cod, MA	Water balance	0.85	cm/day	Mud and sand	Giblin and Gaines (1990)
Narrow Lake, Alberta	Water budget	0.09	cm/day	-	Shaw et al. (1990)
	median:	0.79			
	min:	0.01			
	max:	9.89			

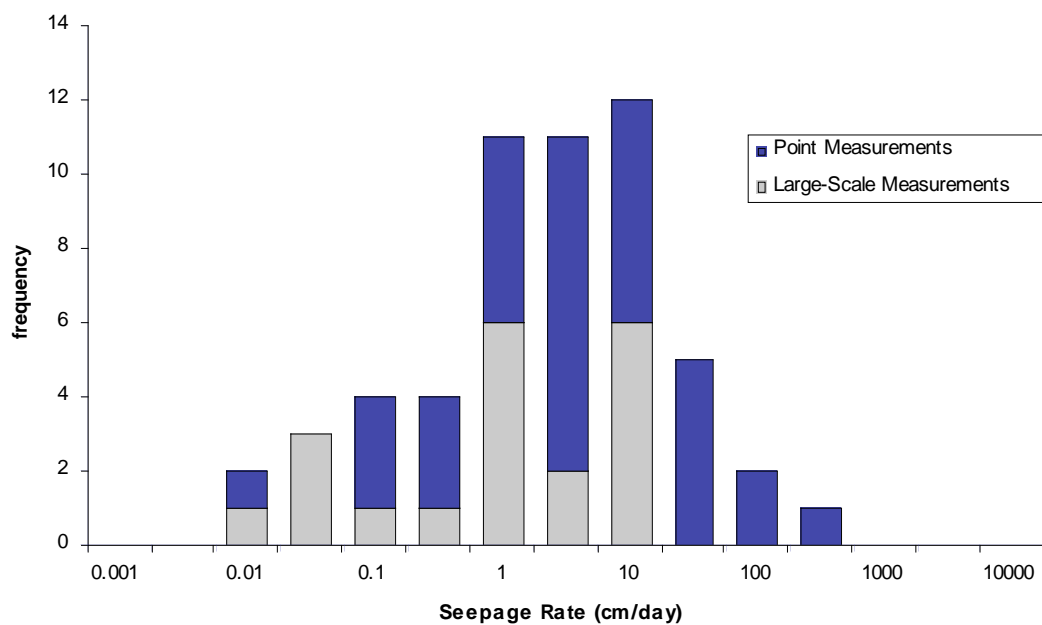


Figure D1: Distribution of Seepage Rate Measurements

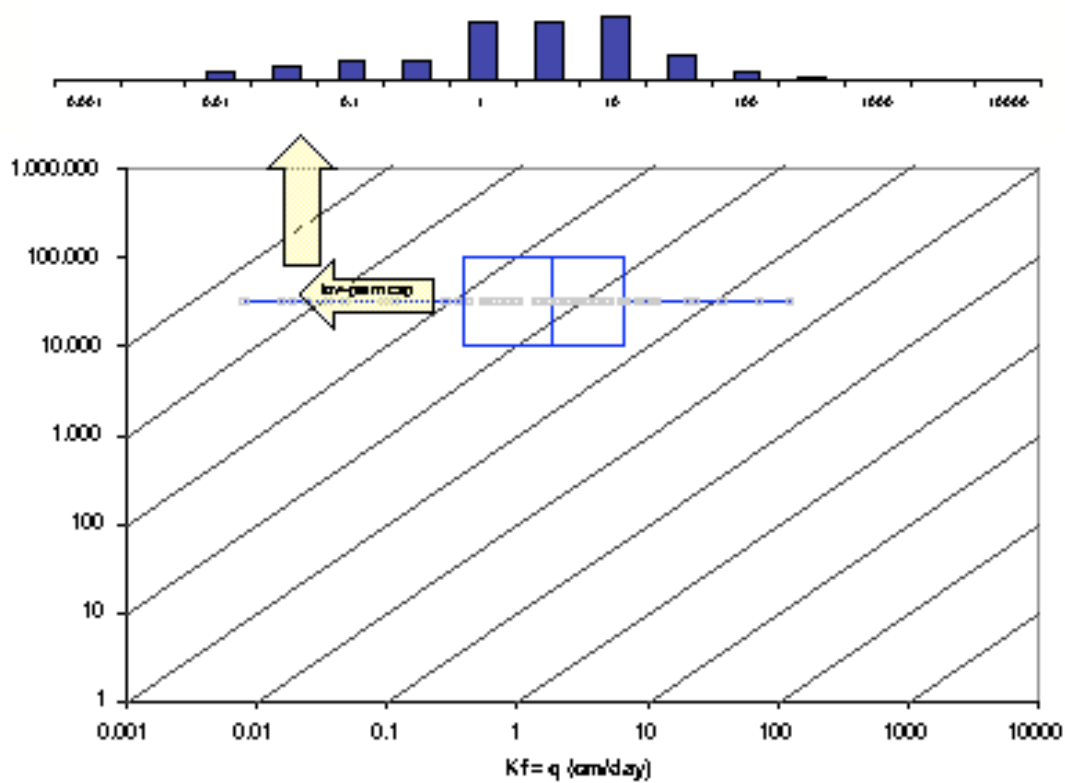


Figure D2: Groundwater Seepage Flux: Chemical Stability Map for PCB.

D6. REFERENCES

- Bencala, K.E., 1993. A perspective on stream-catchment connections. *J. N. Am. Benthol. Soc.* 12(1): 44-47.
- Bencala, K.E., J.H Duff, J.W. Harvey, A.P Jackman, and F.J Triska, 1993. Modelling within the stream-catchment continuum. In: *Modeling Change in Environmental Systems*, Edited by: A.J Jakeman, M.B. Beck and M.J McAleer. John Wiley and Sons: 1993.
- Bugna, G.C., J.P Chanton, J.E. Cable, W.C. Burnett, and P.H. Cable, 1996. The importance of groundwater discharge to the methane budgets of nearshore and continental shelf waters of the northeastern Gulf of Mexico. *Geochimica et Cosmochimica Acta*, 60(23):4735-4746.
- Booij, K, J.R. Hoedemaker, and J.F. Bakker, 2003. Dissolved PCBs, PAHs and HCB in poer waters and overlying waters of contaminated harbor sediments. *Environ Sci Technol.*, 37(18):4213-4220.
- Burnett, W.C., M. Taniguchi, and J. Oberdorfer, 2001. Measurement and significant of the direct discharge of groundwater into the discharge zone. *Journal of Sea Research* 46: 109-116.
- Cable, J.E., G.C. Bugna, W.C Burnett, J.P Chanton. Application of ^{222}Rn and CH_4 for assessment of groundwater discharge to the coastal ocean. *Limnology and Oceanography* 41(6):1347-1353.
- Cable, J.E., W.C. Burnett, J.P. Chanton, D.R. Corbett, and P.H Cable. 1997. Field Evaluation of Seepage Meters in the Coastal Marine Environment. *Estuarine, Costal, and Shelf Science* 45: 367-375.
- Cable, J.E., W.C. Burnett, J.P. Chanton. 1997. Magnitude and variations of groundwater seepage along a Florida marine shoreline. *Biogeochemistry* 38:189-205
- Cartwright, N., and P. Nielsen. Dynamics of the Salt-Freshwater Mixing Zone in Ocean Beaches. *Proceedings, Second International Conference of Saltwater Intrusion and Coastal Aquifers*. Merida, Mexico, March 30-April 2, 2003.
- Chadwick, D.B., 2002. Coastal Contamination Migration Monitoring. *Proceedings of Remediation Technologies Development Forum Workshop on Groundwater-Surface Water Interaction*, Seattle, WA. October, 2002
- Choi, J., and J.W. Harvey, 2001. Quantifying time-varying groundwater discharge and recharge in wetlands of the northern Florida Everglades. *Wetlands* 20(3): 500-511.
- Conant Jr., B, J.A. Cherry, and R.A Gillham. 2004 A PCE groundwater plume discharging to a river: Influence of the streambed and near-river zone on contaminant distributions. Accepted Feb 3, 2004, *Journal of Contaminant Hydrology*
- Conant Jr., B. 2004. Delineating and quantifying groundwater discharge zones using streambed temperatures. *Ground Water* 42(2):243-257.
- Fones, G.G., O Holby, and B. Thamdrup, 2001. High resolution metal gradients measured by insitu DGT/DET deployment in Black Sea sediments using an autonymous benthic lander. *Limnol. Oceanogr.* 46(4):982-988.

- Harvey, J.W., J.M Jackson, R.H Mooney, and J Choi. Interaction between groundwater and surface water in Taylor Slough and vicinity, Everglades National Park, South Florida: Study Methods and Appendices. *U.S. Geological Survey Open-File Report 00-483*. Reston, VA.
- Hayashi, M., and D.O. Rosenberry. Effects of ground water exchange on the hydrology and ecology of surface water. *Ground Water* 40(3): 309-316.
- Holtschlag, D.J., and J.R. Nicholas, 1998. Indirect ground-water discharge to the great lakes. *U.S. Geological Survey Open-File Report 98-579*. Lansing, Michigan.
- Jobson, H.E. and A.W. Harbaugh, 1999. Modifications to the diffusion-analogy surface-water flow model (DAFLOW) for coupling to the modular finite-difference ground-water flow model (MODFLOW). *U.S. Geological Survey Open-File Report 99-217*. Reston, VA.
- Katz, B.G., R.S. DeHan, J.J. Hirten, and J.S. Catches, 1997. Interactions between groundwater and surface water in the Suwannee River Basin, Florida. *Journal of the American Water Resources Association*, 33(6): 1237-1254.
- Kooi, H., and J. Groen, 2001. Offshore continuation of coastal groundwater systems; predictions using sharp interface approximations and variable-density flow modeling. *Journal of Hydrology* 246: 19-35.
- Lee, D.R., 1977. A device for measuring seepage flux in lakes and estuaries. *Limnology and Oceanography* 22:140-147.
- Lyford, F.P., R.E. Willey, and S. Clifford, 2000. Field tests of polyethylene-membrane diffusion samplers for characterizing volatile organic compounds in stream-bottom sediments, Nyanza chemical waste dump superfund site, Ashland, Massachusetts. *U.S. Geological Survey Water Resources Investigation Report 00-4108*. Northborough, MA.
- McBride, M.S. and H.O Pfannkuch, 1975. The distribution of seepage within lake beds. *United States Geological Survey J. Res.* 3: 505-512.
- McVicar, T.R., D.L.B. Jupp, A Hei, V.K. Choubey, and L. Lingtao, 1994. Multi-scale remote sensing of ground and surface water interactions. *Proceedings, 15th Asian Conference on Remote Sensing*, 1994.
- Prudic, D.E., L.F. Konikow, and E.R. Banta, 2004. A new streamflow-routing (SFR1) package to simulate stream-aquifer interaction with MODFLOW 2000. *U.S. Geological Survey Open-File Report 2004-1042*. Carson City, Nevada, 2004.
- Robinson, M, D Gallagher, and W. Reay., 1998. Field observations of tidal and seasonal variations in groundwater discharge to tidal estuarine surface water. *Ground Water Monitoring Review*, Winter 1998: 83-92.
- Taniguchi, M, W.C. Burnett, J.E. Cable, and J.V. Turner, 2002. Investigation of submarine groundwater discharge. *Hydrol. Process* 16:2115-2129.
- Thibodeaux, L.J., 2003. In-bed transport processes that will enhance or suppress chemical stability. Presentation at workshop: *Environmental Stability of Chemicals in Sediments*, 8-10 April 2003, San Diego, CA.
- Vroblesky, D.A., and M.M Lorah, 1991. Prospecting for zones of contaminated ground-water discharge to streams using bottom-sediment gass bubbles. *Ground Water* 29(3): 333-340.

Winter, T.C., J.W. Harvey, O.L. Franke, and W.M. Alley. 1998. Ground Water and Surface Water: A Single Resource. *US Geological Survey Circular 1139*. Denver CO 1998.

APPENDIX E: NON-RESUSPENSION MEDIATED SEDIMENT MASS TRANSFER AND THE ROLE OF BIOTURBATION

E1. INTRODUCTION

For the purposes of this discussion, diffusion is defined as the mass transfer of a chemical due to nonequilibrium conditions. In the context of contaminated sediments, diffusion is the mass transfer of a chemical of concern from sediment porewater to the overlying water column as a result of a concentration gradient. Typically higher concentrations are seen in the sediment porewater, lower concentrations in the overlying water column, and a net transfer due to diffusion from the sediment to the water column.

Molecular diffusion occurs at any temperature above absolute zero. Individual molecules move continually at random, apparently independently of each other. Frequent collisions occur and a single molecule will follow an arbitrary path. However, an aggregation of diffusing particles has an observable drift, from places of higher to places of lower concentrations. For this reason diffusion is known as a transport phenomenon.

This molecular process can be greatly enhanced by accompanying physical processes. Sediment mixing by benthic invertebrates, herein referred to as bioturbation, influences both material transport and chemical reaction rates. Bioturbation is not a single process but the net effect of locomotion, feeding, and tube construction activities of the host of benthic organisms that inhabit the seafloor and bottom sediments. Bioturbation has the effect of enhancing the rate of diffusion, or diffusivity, of a chemical in sediment porewater.

Much of the material presented is taken from two literature sources that include a comprehensive assessment of diffusion in sediment porewater and the effects of bioturbation. These sources are:

Environmental Chemodynamics: Movement of Chemicals in Air, Water, and Soil. Second Edition. Thibodeaux, L. J. 1996. John Wiley & Sons, Inc. New York.

WERF. 1995. *Models for Alteration of Sediments by Benthic Organisms*. Project 92-NPS-2. Water Environment Research Foundation.

E2. THEORETICAL PROCESS UNDERSTANDING

The distribution of chemicals in the watery portion of the benthic boundary layer below the water-sediment interface is a function of the chemistry of the underlying sediments, factors that disturb the sediment-water interface, and the physics of transport within the bottom water. As a result of a large ratio of solid surface to interstitial water volume (especially in fine-grained muds), chemical concentrations in porewater may change appreciably and give rise to large concentration gradients between sediments and the overlying water. This in turn results in fluxes of dissolved constituents and colloids to and from the sediments.

E2.1 MOLECULAR DIFFUSION

Molecular diffusion is a phenomenon caused by kinetic energy of molecules and by concentration gradients. Molecules undergo random motion which is caused by internal energy of the molecules. This phenomenon is known as *Brownian motion* and the movement of the particles is termed *Brownian diffusion*. The net transfer of mass by random molecular motion is molecular diffusion. This net mass transfer is caused by gradients in concentrations of a diffusing substance.

Diffusion in a medium with a constant diffusion coefficient is often described using the equation (Carslaw and Jaeger, 1967; Crank, 1956; Kirkham and Powers, 1976):

$$\frac{\partial c}{\partial t} = D \frac{\partial^2 c}{\partial x^2} \quad (1)$$

where $c = c(x,t)$ is the concentration of the substance at position x and time t and D is the diffusion coefficient. The diffusion coefficient of a solute in a dilute solution can reasonably be taken as constant. Diffusivities of chemicals in water are readily available in the literature and are on the order of 5 to $50 \times 10^{-6} \text{ cm}^2 \text{ s}^{-1}$ (Thibodeaux, 1996 and Li and Gregory, 1974). Natural organic colloids, to which hydrophobic organic chemicals and trace metals absorb, may be much smaller than pore openings in the bed-sediment ($>1\mu\text{m}$) and are therefore subject to diffusion as well. Transport of colloids by molecular diffusion within the bed and through the sediment-water interface can occur, provided that the particle surface chemistry is such that there is no attraction (i.e., electrical charge) with the fixed solid phase. Diffusivities have been estimated based on average particle radius, but only limited experimental data of effective diffusivities of colloids in bed-sediment have been made.

Molecular diffusivity alone is not sufficient to describe the diffusion within porous solids that have interconnected voids or pores in the solid. The diffusion is greatly affected by the size and type of the voids. Two factors operate to make the effective diffusion coefficient less than the molecular diffusivity. The interfacial area through which the chemical moves is reduced because the free or open cross section for diffusion is but a fraction of the total due to fill particles. The diffusivity is also effectively reduced because the diffusion distance along the tortuous path is

greater. Alternative methods exist for estimating the effective diffusion coefficient. Thibodeaux (1996) suggests that the effective diffusion coefficient can be estimated as:

$$D_{\text{eff}} = D \frac{\varepsilon}{\tau} \quad (2)$$

where D_{eff} is the effective diffusion coefficient, ε the void fraction (porosity), and τ the tortuosity factor, introduced to allow for the fact that the diffusion path is greater than the distance traveled normal to the face, and for varying cross section of the pores, which are not straight, round tubes. This correction factor must normally be obtained experimentally except for fill of exceedingly uniform structure and pore size. Values obtained from experimental data show that τ varies from unity to more than 6. (Smith, 1970). If it is assumed that on average, the pore makes an angle of 45 degrees with the vertical y direction in a resultant two-dimensional path, then $\tau = 2^{0.5}$, or 1.414. Thibodeaux (1996) also suggested that, based on work by Millington and Quirk (1961), the effective diffusion coefficient can be determined by:

$$D_{\text{eff}} = D \varepsilon^{4/3}. \quad (3)$$

Alternatively, Sweerts et al. (1991) and Berner (1980) suggest that

$$D_{\text{eff}} = D \frac{\varepsilon}{\tau^2}. \quad (4)$$

Vertical fluxes of solutes between sediments and the interface with the overlying water column can then be calculated from Fick's first law as described by Sweerts et al. (1991) and Berner (1980):

$$J = D_{\text{eff}} \frac{\partial c}{\partial x}, \quad (5)$$

where J is the flux in $\text{mol cm}^{-2} \text{ s}^{-1}$, the effective diffusion coefficient, D_{eff} , is in $\text{cm}^2 \text{ s}^{-1}$, and $\delta c / \delta x$ is the initial concentration gradient in $\text{mol cm}^{-3} \text{ cm}^{-1}$.

Chemical flux from the sediment-water interface into the bulk water column is also retarded by a benthic boundary layer, where turbulent mixing is limited by the drag of the sediment bed on flow. Transport within about 1mm of the bed is governed by molecular diffusion (Thibodeaux, 1996). This diffusive sublayer is contained within a viscous sublayer (Wimbush, 1976). Outside of the diffusive sublayer and within the viscous sublayer, the dominant transport process is mixing due to the viscosity of moving water. The viscous sublayer extends to a height of about 1 cm (Thibodeaux, 1996), beyond which transport is dominated by turbulence. Higher shear stresses and turbulence tend to reduce the thicknesses of both viscous and diffusive sublayer, while the thickness of the diffusive sublayer is also less for contaminants with lower free liquid diffusivities.

E2.2 ROLE OF BIOTURBATION

In addition to molecular diffusion, benthic invertebrate activity, or bioturbation, can enhance the mass transfer or “diffusion” of solutes and colloids in sediment porewater. A complete theoretical description of bioturbation would be beyond the scope of this review, due to its vast complexity. Bioturbation occurs in several different ways and can affect a number of important mass transfer processes and characteristics, including resuspension, particle mixing in the bed-sediment, mixed depth, and porewater diffusion. Bioturbation can modify patterns of horizontal stratification and affect the transport of particles, their sorbed ions, organic molecules, and entrapped porewater in both the horizontal and vertical directions. Some organisms, such as crabs and snails, mix surface sediment simply by crawling or plowing through it. More importantly, other organisms, especially polychaete worms and bivalves, burrow into sediment and ingest the sediment particles. Such burrowing can extend to several tens of centimeters. Once their burrows are constructed, some organisms remain in them and flush the burrows with overlying water. This process is referred to as bioirrigation; it involves only the porewater and not the enclosing particles and is the focus of this review.

Bioirrigation is widely recognized to be more rapid than molecular diffusion-driven processes for solute transport (Rutgers van der Loeff et al., 1984; Matisoff et al., 1985; Wang and Matisoff, 1997; Wheatcroft et al., 1990; Van Rees et al., 1996; Berelson et al., 1999; Bird et al., 1999; Matisoff and Wang, 2000). Burrowing fauna can increase the flux of solutes into overlying waters by as much as an order of magnitude (Rutgers van der Loeff et al., 1984). With regard to contaminant flux, bioirrigation may be more important for nutrients than for chemical species with high partition coefficients (Christensen et al., 1984). The partition coefficient K_d is defined as the concentration of a chemical species in the particulate phase divided by the concentration of the chemical in the aqueous phase at equilibrium. Chemical species with high K_d s are strongly associated with particulate matter.

Benthic organisms enhance diffusion by burrowing (providing holes) and by actively pumping water through the sediments (Berelson et al., 1999). Infaunal chironomids *Coelotanypus* sp. and *Chrionomus* sp., and the mayfly nymph (Ephemera: Ephemeroptera) irrigate burrows up to 10 cm below the sediment-water interface (SWI) (Matisoff and Wang, 2000). Benthic organisms can also affect solute fluxes indirectly. Bioturbation is known to modify the sediment fabric, increase mineral dissolution, alter sediment water content, and enhance organic matter decomposition (McCall and Tevesz, 1982; Matisoff et al., 1985); these transformations increase the rate of solute transport in sediments. In addition, some organisms produce stable tubes, which can function as conduits, enabling direct solute transport from deep in the sediments to the water column (Matisoff et al., 1985). In summary, benthic organisms directly enhance diffusion by increasing the advection of water and solutes through interstitial spaces and indirectly through modification of sediment structure (McCall and Tevesz, 1982; Ebenhöh et al., 1995).

Although most benthic organisms are capable of increasing fluid advection, chironomids and unionid clams have been shown to be the largest contributors to biogenic fluid advection in Lake Erie (Fisher, 1982). Some benthic organisms may be locally important for bioirrigation. For example, burrowing by the large freshwater tubificid oligochaete, *Branchiura sowerbi*, not only affects sediment movement but also solute transport. *B. sowerbi* burrowing produces effective

diffusivities of 91.69 and 234.9 cm²/y at population densities of 4000 and 8000 individuals/m², respectively. For comparison, the control diffusivity—where benthic activity does not occur—was 49.17 cm²/y. Hence, benthic processes greatly enhance that solute transport relative to molecular diffusion (Wang and Matisoff, 1997). In the coastal environment, ghost shrimp and heart urchins are recognized as important organisms for direct bioirrigation (e.g., Widdicombe and Austen, 1998; Berelson et al., 1999).

As mentioned above, the impact of bioturbation on contaminant flux may be great (Karickhoff and Morris, 1985; Reible et al., 1996; Thibodeaux and Bierman, 2003). Bioturbation is generally the most important mechanism for reworking sediments and releasing contaminants in sediments not subject to erosion and resuspension (Reible et al., 1991). Dissolved silicate flux was found to be 2-10 times greater with bioturbation than with molecular diffusion (Rutgers van der Loeff et al., 1984). Where biological activity is absent, molecular diffusion is considered to be the most important process for the flux of contaminants (Van Rees et al., 1996). Van Rees et al. (1996) also found nutrient (solute) transport was elevated (~1.6-15 times) with benthic activity in Lake Okeechobee (Florida, USA) sediments. Moreover, in a fresh water environment laboratory experiment, ninety percent (90 %) of added hydrophobic chemicals (hexachlorobenzene, pentachlorobenzene, and trifluran) were transported to the sediment surface by oligochaete bioturbation. This was 4-6 times greater than in the experimental control sediment without worms (Karickhoff and Morris, 1985). It should be noted that pollutant release from intact fecal pellets can be retarded by sorption. In the above experiment, less than 20% of pollutants retained in the pellet were released, during a typical pellet resuspension time at the sediment surface. Because fecal pellets entrap sorbed contaminants, they may be mitigating factor for contaminant release with bioturbation (Karickhoff and Morris, 1985).

The importance of bioturbation is recognized at highly contaminated sites and for notable chemicals of concern (e.g., Cd). For instance, bioturbation was found to be principally responsible for the slow decline in surface Cd concentrations at the Foundry Cove Superfund site (Hudson Estuary, New York, USA) over the period 1972-1989 (Thomann et al., 1993). This work was accomplished using a model of Cd fate calibrated to the post-Cd loading period (1972-1989). The initial model calibration with no biological sediment mixing did not fit the observed data. Continually high Cd concentrations were observed in surface sediments of this marshy brackish area, even though peak Cd loadings place most of the high Cd concentrations deep in the sediments. It is thought that vertical mixing of Cd contaminated sediments by benthos (e.g., oligochaetes mixing in the upper 10 cm) maintains high Cd concentrations in the surface sediments and therefore increases the Cd flux out of the cove. The increased Cd mass released from the cove is obtained from the deeper sediment. Thomann et al. (1993) determined that the current Cd transport rate out of the sediments is approximately 0.9 kg Cd/day. The flux of Cd is increased by an order of magnitude compared with no biological mixing (Thomann et al., 1993).

The release of PCBs (a particle reactive compound) and other hydrophobic chemicals from sediments with bioturbation may be several orders of magnitude more rapid than molecular-driven processes, when considered on a porewater concentration gradient basis (Larsson, 1983; Bosworth and Thibodeaux, 1990; Schaffner et al., 1997). In a laboratory model system, Larsson (1983) measured the transport of ¹⁴C-labeled PCB compounds from sediments to water (to air). Mixing and irrigation by chironomids and tubificids transferred PCBs, whether in a dissolved form or attached to particles, from sediments to water. The importance of bioturbation was more

pronounced for more highly chlorinated PCBs (e.g., octa- and hexachlorobiphenyls). This is not surprising, because highly chlorinated PCBs have a more lipophilic character and are more strongly adsorbed to particulates. Other, less chlorinated PCB compounds, such as tetachlorobiphenyls, are less particle reactive and may diffuse from sediments without bioturbation. Nevertheless, benthic activity can increase solute transport (dissolved PCBs) relative to molecular diffusion-driven processes. Under anaerobic conditions, the movement of PCBs is governed primarily by desorption processes. In conclusion, Larsson (1983) stated that bioturbation could increase the mobility of PCB compounds in sediments to other parts of riverine and lacustrine ecosystems. Moreover, bioturbation processes could mean increased availability of sediment-bound PCBs entering aquatic food chains. Larsson (1983) also suggested that areas with contaminated bottom sediments like the Baltics and the Great Lakes could act as a source for PCBs rather than a sink.

Bioturbation processes are variable over temporal and spatial scales. Seasonal changes in temperature can influence bioturbation (Rhoads and Boyer, 1982). Bioturbation is also affected by temporal variations in the sedimentation rate and flux of organic matter reaching the sediment surface from phytoplankton production or algal blooms in the water column. High sedimentation rates (>3 cm/yr) can restrict the abundance of colonies of infaunal organisms, as do excessively erosional conditions (Schaffner et al. 1987). Therefore, episodic erosion or deposition events and spatially variable bottom currents result in patchy distributions of organisms.

E3. ADEQUACY OF TYPICAL SITE-SPECIFIC INFORMATION

Site-specific data to support an assessment of the mass transfer rate of a chemical in sediment porewater and across the sediment-water interface due to diffusion and related bioturbation effects include:

- Diffusion coefficient of the chemical of concern in water (molecular diffusivity);
- Presence, population densities, and activity of benthic invertebrates and dependence on seasonality or temperature; and
- Field and laboratory measurements of benthic activity

Each of the above process related parameters or measurements will be discussed further in this section. Chemical transport due to diffusion and bioturbation is very complex, and site-specific data are generally not sufficient to fully characterize local process parameters. The following discussion summarizes factors affecting mixing rates, measurement techniques, and results reported in scientific literature.

E3.1 MOLECULAR DIFFUSIVITY

Empirical relationships are often used to predict the molecular diffusion coefficient, D . These relationships account for solvent-solute interactions. A popular empirical relationship is the Wilke-Chang correlation (Thibodeaux, 1996).

$$D = 7.48 \times 10^{-8} \frac{(\Psi M_B)^{0.5}}{\mu V_A^{0.6}} \quad (6)$$

M_B = molecular wt of solvent

V_A = molar volume of solute in cm^3/mol

Ψ = association factor for solvent, 2.6 for water

μ = viscosity of solution in centipoises.

This parameter is readily computed, based on tabulated parameters for the chemical of concern. Table E1 presents examples. Based on these values, a representative range of cohesive sediment porosities of about 0.5 to 0.9, and equation 3 above, this translates into a typical range of effective diffusivities of about 0.4 to $0.5 \times 10^{-5} \text{ cm}^2/\text{sec}$.

Table E1: Estimated Molecular Diffusivities for Selected Contaminants

Substance	Temperature	D (cm ² /sec)
2-Chlorobiphenyl	25	0.648 E-5
Chlorpyrifos	25	0.467 E-5
p. Cresol	25	0.871 E-5
2,4-Cresol	25	0.649 E-5
DDT	25	0.485 E-5
Mercury	23.6	2.9 E-5
Methanol	20	1.28 E-5
Monochlorobenzene	25	0.909 E-5
Phenol	20	0.84 E-5
2,4,2',4'- Tetrachlorobiphenyl	25	0.552 E-5
1,2,4-Trichlorobenzene	25	0.757 E-5

(Thibodeaux, 1996)

E3.2 BIOTURBATION

Bioturbation is controlled by a variety of biotic (organism size, population density, organic matter, food availability, and species diversity) and abiotic (hydrodynamics, temperature, and sediment chemistry) factors.

E3.2.1 Community Structure

Benthic community structure is thought to be an important control on bioturbation (Berelson et al., 1999). Subtle changes in infaunal and epifaunal community makeup—numbers, biomass, and species diversity—not only affect the depth and rate of bioturbation but also the nature of its effect (e.g., Robbins et al., 1977; Wheatcroft et al., 1994; Petersen et al., 1998; Berelson et al., 1999). In the Chesapeake Bay, biologically induced mixing depths were found to range from 17-25 cm at site CS to 21-40 cm at site WT. Bioturbation (biodiffusion) rates were also measured to be 80-172 cm²/y and 6-30 cm²/y at sites CS and WT, respectively (Dellapenna et al., 1998). Dellapenna et al. (1998) posit that observed mixing depth and rate differences reflect dominance of head-down feeding polychaetes at site CS and deep-burrowing shrimp at site WT (Dellapenna et al., 1998). It is important to note that an increase in mixing depth with changing species composition does not necessarily accompany an increase in mixing rate. In fact, the study by Dellapenna et al. (1998) demonstrates the opposite: higher mixing rates occur with lower mixing depths.

It is again valuable to emphasize consideration of multiple factors when investigating bioturbation rates and mixing depths (e.g., Dellapenna et al., 1998). Species density as well as individual organism size may affect mixing depth and rate. For instance, bioturbation rates have been observed to increase with increasing density of a community and organism size within the same species (Widdows et al., 1998). Community density (biomass) rather than organism size may be more important in prediction of bioturbation rate (Breukelaar et al., 1994). Accordingly, Retraubun et al. (1996) observed that bioturbation (sediment turnover) was higher where

lugworms were not the largest, but were the most abundant (Retraubun et al., 1996). Nonetheless, some laboratory studies have found reductions in feeding rates under high population abundances (Wheatcroft et al., 1998). Declines in bioturbation rates at high densities are thought to reflect decreasing quality and quantity of food (Retraubun et al., 1996; Wheatcroft et al., 1998). Wheatcroft et al. (1998) caution against studies seeking to transfer laboratory-based measures of deposit-feeding rates to the field. It may not be valid to transfer a deposit-feeding rate measured at density to another.

Benthic community structure may influence the nature of the bioturbation effect on sediment chemistry (Berelson et al., 1999). For example, Matisoff et al. (1985) investigated the impact of three important freshwater organisms (tubificid oligochaetes, chironomid larvae, and unionid bivalves) on nutrient release from sediments. They found tubificids increased ammonia, bicarbonate, and silicate fluxes; chironomids elevated nitrate, bicarbonate, and silicate fluxes; and bivalves only enhanced chloride and nitrate fluxes. Matisoff et al. (1985) hypothesized that observed differences in nutrient flux reflect functional differences in each organism's life mode. That is, tubificids increase mass transport via conveyor-belt feeding, chironomids mix sediments by more or less continuously pumping overlying water through burrows, and unionids episodically inject water to sediments to aid in burrowing (Matisoff et al., 1985).

Benthic communities often exhibit temporal as well as spatial patchiness (Gerino et al., 1998; Berelson et al., 1999). In a coastal marine environment (Long Island Sound, USA), benthic community composition has been observed to markedly change throughout a year. Benthic community was relatively small (3.8 ± 0.8 indiv/dm²) and was dominated by carnivores during winter. By June, organism numbers had increased considerably to 215.4 ± 17.0 individuals/dm² (Gerino et al., 1998). Moreover, subsurface deposit feeders (bivalves *Nucula proxima*, *Yoldia limatula*, and polychaete *Nephris incisa*) became the dominant organism group, comprising 72.8-79.4% of all organisms present at the site in June. Species diversity continued to change throughout the study period. The polychaete *Mediomastus sp.* became the most important species at the end of the summer (Gerino et al., 1998). Although bivalves are not conveyor-belt species, both bivalves and polychaetes eat at depth and defecate at the surface; these bioadvective actions increase the rate of surface sediment subduction. In summary, between winter and summer, organism numbers increased and the feeding mode transformed from biodiffusive to bioadvective. Such seasonal changes within a benthic community can have important consequences for how and to what extent sediments are mixed (Gerino et al., 1998).

Likewise, removing top predators from the food chain may influence community structure. In a severely eutrophied lake (Lake Rindgsjön, Sweden), the cyprinid population (mainly bream and roach) was reduced. Consequently, the lake which was dominated by oligochaetes and chironomids became repopulated by the following groups: Amphipoda, Ephemeroptera, Coleoptera and Mollusca. This more diverse group reappeared in numbers similar to those found before the lake entered its worst stage of eutrophication in 1968 (Svensson et al., 1999).

Many studies have emphasized the importance of capturing the spatial patchiness when ascribing a bioturbation rate (biodiffusion or otherwise) and mixing depth to a larger sediment area (e.g., Van Rees et al., 1996; Berelson et al., 1999). Benthic populations are known to be heterogeneous. In addition, temporal variations must also be considered, for a population can transform from biodiffusive mixers to conveyor-belt feeders within a year. Moreover, changes

in trophic structure should be considered. Therefore, caution must be exercised when applying measured bioturbation rates from other study sites, for estimates are controlled by the variability in macrobenthos activity rather than the physical characteristics of the sediments themselves (Van Rees et al., 1996).

E3.2.1.1 Benthic Community and Organic Matter

A faunal community once established will modify its environment by bioturbation (Dauwe et al., 1998). However, it is the quality (nutritional value), quantity, and vertical distribution of organic matter (OM) that will influence the type of benthic community that develops (e.g., Smith et al., 2000). Dauwe et al. (1998) investigated the relation between TOC (total organic carbon) and benthic community in North Sea sediments. Vertical benthic distribution was found to follow TOC (Dauwe et al., 1998). Where large amounts of high-quality OM occurred, most organisms (interface or suspension feeders) were found at shallow depths, feeding on freshly deposited or resuspended material. Small-sized, deeply penetrating fauna (up to 20 cm)—primarily deep-living deposit feeders and endobenthic predators—predominated where large amounts of refractory (low quality) OM occurred. The highest diversity of trophic groups, largest individuals, and deepest distribution were found in sediment with OM of intermediate quality and quantity (Dauwe et al., 1998). To reiterate, highest levels of bioturbation (biodiffusion coefficient) were found with the OM of intermediate quality and quantity (Dauwe et al., 1998).

E3.2.1.2 Food Availability

Carp and bream feeding behavior has been observed to increase resuspension of sediments (nutrients and chlorophyll *a*). In a controlled pond experiment, carp and bream primarily engaged in benthivory (feeding in the benthos). However, if zooplankton were abundant, carp and bream might switch to planktivory (feeding on planktonic organisms). This transformation—from feeding in the sediments to feeding in the water column—would decrease sediment resuspension by carp and bream. The switch by bream and carp to planktivory likely depends on the aquatic community at large. For example, if perch were abundant, these fish might continue to eat in the benthos (Breukelaar et al., 1994).

E3.2.2 Hydrodynamic Stress

Physical perturbations coupled with low quantities of OM may deter the establishment of benthic communities (Dauwe et al., 1998). Where the seabed is highly disturbed or stream velocities are moderate to high, benthic communities are often restricted; the net effect of bioturbation is therefore low (e.g., Bosworth and Thibodeaux, 1990). In the York River paleochannel (Virginia, USA), mixing depths range from 40-120 cm (Dellapenna et al., 1998). Dellapenna et al. (1998) reported that bioturbation by opportunistic, shallow-living and/or surface feeding organisms can be intense in the upper few centimeters of sediment. However, physical mixing can extend deep into the bottom sediments, erasing evidence of any biological mixing that might take place. Thus, where hydrodynamic stress is high, the relative importance of bioturbation in overall sediment mixing is low (Dellapenna et al., 1998).

E3.2.3 Oxygen Effect

Oxygen stress reduces the depth and rate of bioturbation (Thibodeaux, 1996; Smith et al., 2000). Reible et al. (1996) investigated the effect of oxic and hypoxic conditions on the feeding life

mode of tubificid oligochaetes (*T. tubifex*). They found that oxygen levels not only altered the oligochaetes' relative position in sediments, but also influenced the rate of contaminant flux. At high DO levels, *T. tubifex* remained completely within the oxic zone of the contaminated sediment, defecating below the sediment-water interface; no noticeable mounds were observed at the surface. Fluxes of 37 and 70 ng cm²/d were measured for the contaminants pyrene and phenanthrene, respectively (Reible et al., 1996). With hypoxia, worms moved up in the sediments towards the surface. The tails of the worms were positioned at or above the sediment water surface. Defecation was observed at the surface and produced noticeable mounds. This change in relative sediment position led to a significant increase in contaminant fluxes—380, 490, and 940 ng cm²/d for pyrene, phenanthrene and dibenzofuran, respectively (Reible et al., 1996). The increased flux of more soluble contaminants likely reflects more rapid release from sediment surface and the increased importance of porewater pumping as compared with sediment particle reworking for migration of these compounds. Although a significant increase in contaminant flux with changing Eh has been observed, the ecological importance of this increased flux is unknown (Reible et al., 1996).

Minimal oxygen penetration into the sediments can influence the type of benthic community established (Smith et al., 2000). (Moreover, the lack of oxygen in sediments will prevent a macrofaunal community from establishing itself at all (Thibodeaux, 1996). The certitude of this argument has led Rutgers van der Loeff et al. (1984) to employ an asphyxiation technique to measure biologically mediated transport at the SWI. Dissolved silicate fluxes were found to be 2-10 times greater under experimental aerobic conditions than anoxic conditions (Rutgers van der Loeff et al., 1984). Under anoxic conditions, molecular diffusion is recognized as the dominant mechanism of transport (Taghon et al., 1984).

E3.2.4 Seasonal Effect

The seasonal importance of bioturbation has been recognized by many researchers (e.g., Hines et al., 1984; Hines and Jones, 1985; Wheatcroft et al., 1990; Wright et al., 1997b; Rowden et al., 1998). Bioturbation increases with temperature and decreases without oxygen. Existing data indicates that biodiffusion coefficients increased by a factor of two (2) for each 10°C rise in temperature (Thibodeaux, 1996). The abovementioned studies show that flux, mixing, and subduction rates increase in summer and spring relative to winter. For instance, Hines and Jones (1985) found sulfate reduction rates were considerably slower in winter relative to spring and summer (Hines and Jones, 1985). The increased rates of sulfate reduction may have implications for the sequestration of metals in summer; sulfide precipitation with metals (e.g., Cd) enables the sediments to function as a sink rather than a source.

While seasonal dependence on bioturbation is recognized, few studies have quantitatively measured such values. In fact, many offer conflicting results regarding when the bioturbation maximum occurs. Where bioturbation does follow temperature, it likely reflects an optimal temperature of the specific benthic community rather than a temperature maximum. For example, Retraubun et al. (1996) observed fecal cast production was fastest in spring and slow in autumn and winter.

Accompanying lab tests indicated that factors other than temperature maximum influence bioturbation rates—i.e., optimal temperature for the benthic community (Retraubun et al., 1996). Here, fecal cast production increased with increasing temperatures to a maximum of 14-20° C.

At higher temperatures, fecal cast production rates declined. Food availability may explain the higher rate in spring than in summer as well (Retraubun et al. 1996). Likewise, Hymel and Plante (2000) found that temperature is less important when food concentration is very low. At 100% food levels, egestion rate increased almost monotonically with temperature, and presumably absorption rates were not overwhelmed by sediment processing rates (Hymel and Plante, 2000).

Gerino et al. (1998) also observed an increase in bioturbation with the pulsed increase in OM and chlorophyll *a* input and the temperature rise that accompanied the phytoplankton bloom and post-bloom period. They found D_b (biodiffusion coefficient) increased <2-3 times; v_b (bioadvection coefficient) increased approximately 10-50 times—both lab and *in situ* (Gerino et al., 1998). D_b and v_b measure bioturbation intensity and are defined in sections 5.4 and 5.5, respectively. Temperature and seasonal anoxia are also important influences on bioturbation in freshwater environments. High mixing rates were calculated for mouths of the Detroit and Maumee Rivers. The rates reflect high tubificid abundance, high bottom temperature, and a lack of seasonal anoxia. For comparison, lower bioturbation rates were measured in the central region of Lake Erie, where lower tubificid abundances, lower bottom temperatures, and seasonal anoxia occur (Fisher et al., 1980).

In certain environments, bioturbative mixing is considered to be non-existent in the winter (-1°C) (Taghon et al., 1984); molecular diffusion and physical mixing processes are recognized to predominate (Dellapenna et al., 1998). In the Chesapeake Bay, Dellapenna et al. (1998) found that physical mixing is more dominant in winter, when the seabed is less susceptible to erosion and wave energy is at a maximum. Physical mixing probably occurs throughout the year, however, evidence of physical mixing is only observed in winter when bioturbation is minimal. In autumn and spring, when shear stresses are lower, physical mixing is reduced and biological activity is at intermediate intensity. Evidence of physical mixing is quickly obliterated by intense bioturbation in summer (Dellapenna et al., 1998). Moreover, biological roughness is at maximum and critical bed shear stress is at a minimum in summer; sediment transport is therefore high (Dellapenna et al., 1997; Wright et al., 1997b). Dellapenna et al., (1998) conclude that biological mixing is the likely control of long-term sediment mixing in Chesapeake Bay stem plains. Lowest critical stress values coincided with the most intense bioturbation (Wright et al., 1997b).

From the above, it is clear that seasonal responses by benthic organisms must be considered when investigating benthic processes. Hymel and Plante (2000) posit understanding seasonal influences is critical for the study of deposit feeders and their roles in soft sediment environments. Thus, future work needs focus on the relative importance of temperature, algal blooms, and food availability (see Wheatcroft et al., 1994).

E3.2.5 Contamination

Highly contaminated sediments reduce both the mixing rate and depth of benthic activity (e.g., Mohanty et al., 1998). In grossly polluted sediments, the benthic community (if any) is severely restricted. Species diversity and abundance occur at very low levels. Tolerant species (e.g., some worms) are typical of contaminated sediments (Rhoads, 1982). Contaminated sediments reduce worm feeding rates, which in turn results in reduced pellet production and reduced

surface sediment deposition—i.e., reduced sediment subduction rates (Madsen et al., 1997). Madsen et al. (1997) found sediment subduction rates were reduced by approximately 19 % in sediments contaminated with fluoranthene (~ 10 ppm in the top 3 mm of sediments). Wheatcroft and Martin (1996) also investigated the effect of pollution on bioturbation. On the Palos Verdes margin (S. California), historical and ongoing wastewater discharges have created an along-shelf gradient in trace metals and other pollutants (e.g., DDT). At moderately contaminated sites, bioturbation intensities were 5-7 times greater than those measured in severely affected sediments (Wheatcroft and Martin, 1996). The results from negligibly affected sediments were inconclusive.

E3.2.6 Summary

Bioturbation is controlled by a variety of biotic (organism size, population density, and species diversity) and abiotic (temperature and sediment chemistry) factors. Organism diversity and population density can have profound influences on bioturbation intensity and mixing depths at a site. Benthic communities are naturally heterogeneous. Therefore, temporal changes and spatial patchiness should be considered when investigating benthic processes. Hydrodynamic stress, for example, may direct the type of benthic community, if any, that establishes itself.

Organic matter and food quality also have a strong influence on benthic biological activities. The highest levels of bioturbation have been found when OM of intermediate quality and quantity occurs. Moreover, food availability in the water column can affect organism activity in the sediments. For instance, if zooplankton are abundant in the water column, certain fish like carp may not resort to benthivory. Their importance to bioturbation is thereby reduced. Although the spatial and temporal heterogeneity of benthic communities are complex, there are certain environmental controls that should be emphasized. Bioturbation and bioirrigation increase with increasing temperature and decrease with decreasing oxygen levels. Benthic processes are also greatly diminished or nonexistent in highly contaminated sediments.

E3.3 TRACERS

E3.3.1 Radionuclides

Radionuclide profiles (i.e., ^{210}Pb , ^{137}Cs , and $^{239,240}\text{Pu}$) obtained from sediment cores can be used quantify the following bioturbation parameters—biodiffusive coefficients, bioadvective coefficients, and biological mixing depths (Stordal et al., 1985; Sharma et al., 1987; Dellapenna et al., 1998; Gerino et al., 1998; Smith and Schafer, 1999). The post-depositional mobility of these particle-reactive radioisotopes is essentially negligible with molecular diffusion; thus, their distribution can be correlated with macrofaunal distribution in sediments (Robbins et al., 1977; Robbins, 1978). The down-core radionuclide distribution (vertical tracer profile) can also be used to estimate sediment accumulation rates.

Particle-reactive radioisotopes are commonly used to estimate sediment processes in both coastal and freshwaters. ^{210}Pb and ^{137}Cs are among the most frequently measured radioisotopes in sediments. Naturally-occurring ^{210}Pb is a member of the ^{238}U decay series and is loaded from the atmosphere at a basically constant rate. In relatively undisturbed sediments, ^{210}Pb —that is measurement of atmospherically deposited ^{210}Pb decay ($t_{1/2} = 22.3$ years)—has been used to determine sediment accumulation rates over the last 100 years or so. Artificial ^{137}Cs , in contrast,

has a finite source (nuclear weapons testing in the 1950s and 1960s). In the northern hemisphere, peak ^{137}Cs fallout is associated with 1963 and can be correlated with specific sediment layers (e.g., Robbins and Edginton, 1975). ^{137}Cs has also been used to study sediment mixing *in vitro* by freshwater suspension feeding bivalves in a temperature-regulated aquarium (McCall et al., 1995). Recently, the nuclear accident at Chernobyl has provided a new radiotracer source, i.e., ^{134}Cs , for *in situ* bioturbation studies (Kramer et al., 1991; Robbins and Jasinski, 1995).

In coastal and marine sediment studies, ^{228}Th ($t_{1/2} = 1.7$ years) is a useful tracer (Silverberg et al., 1986; McCall et al., 1995). Its parent ^{228}Ra is found in marine sediments and is soluble in saline waters. With diffusion and bioirrigation, ^{228}Ra is released from sediments. ^{228}Ra then decays to ^{228}Th in the water column. ^{228}Th is rapidly scavenged by particulate matter and is subsequently deposited in the bottom sediments (Hancock and Hunter, 1999). Like ^{228}Th , ^7Be has a relatively short-half life ($t_{1/2} = 53$ days) and is deposited from the atmosphere to both fresh- and saltwater environments. Short-lived tracers such as ^7Be are essential if shallow mixing events are to be captured. For instance, Dellapenna et al. (1998) used ^7Be to differentiate between mixing mechanisms across seasons in Chesapeake Bay. In winter, physical mixing was deemed to dominate, since physical laminations were observed to a depth of 3 cm, which was equivalent to the ^7Be penetration depth. In the autumn and the spring, physical mixing was reduced and shear stresses were low; the depth of ^7Be was at a minimum and biological activity was of intermediate intensity (Dellapenna et al., 1998).

Radionuclides have also been used in the laboratory to quantitatively investigate the mechanisms and rates of sediment mixing by infaunal chironomids and mayfly nymphs (Matisoff and Wang, 2000). Matisoff and Wang (2000) used a multiple ^{137}Cs tracer layer technique, previously used by Wang and Matisoff (1997), Matisoff et al. (1999), and Matisoff and Wang (1998).

E3.3.2 Importance of Multiple Tracers

Multiple tracers are necessary to provide evidence of mixing on different time scales. Relatively short-lived isotopes (e.g., ^{234}Th and ^7Be) integrate only a small number of mixing events and may reflect very recent changes in benthic systems (Boudreau, 1994). Additionally, recent mixing events may have a disproportionate effect on the observed tracer profile of short-lived radioisotopes. ^{234}Th will not provide evidence of deeper mixing that can be observed with a slowly decaying radioisotope, e.g., ^{210}Pb . For the aforementioned reasons, multiple tracers should be measured in sediment cores. In fact, ^{137}Cs and ^{210}Pb are nearly always measured in conjunction. The maximum depth of ^{137}Cs below the intensely mixed surface layer has been used as a test for the possibility of deep, slow mixing which could affect the ^{210}Pb accumulation rate. Moreover, ^{137}Cs is frequently relied upon to provide an adjunct measure of mixing depth if the ^{210}Pb profile is inconclusive (e.g., Dellapenna et al., 1998).

Radiotracers only provide evidence where sediments are not dramatically disturbed. Highly dynamic systems will not supply clear geochemical profiles, since deep mixing will reset the decay profile. Similarly, intense biological mixing will inhibit the use of geochemical techniques. For example, in John Brewer Reef (Australia), Callianassid shrimp are the dominant endofauna and bioturbation agents. Walbran (1996) suggests that rapid and deep mixing by shrimp makes geochronology inappropriate for shallow coastal reef settings.

Modeling variability in ^{210}Pb and sediment cores may sometimes be problematic (Paulsen et al., 1999). For example, the Palos Verdes Shelf (California) near the Whites Point outfalls has been subjected to significant anthropogenic influences since 1930s, including increased sediment, contaminant, and OC fluxes. Until recently, bioturbation was thought to extend 18-28 cm into the sediments. Paulsen et al. (1999) have revisited questions regarding sedimentation rates and contaminant flux at the Palos Verdes Shelf. To simulate sediment, metal, and ^{210}Pb fluxes into the sediments, they developed a model using annual depth increments. The model relies upon known particle and metal emission rates from the outfalls and ^{210}Pb fluxes to the seafloor. The model was developed to reproduce tracer profiles (i.e., zinc and copper) observed in sediments, to provide estimates of sediment deposition rates, and to discern the importance of bioturbation in the development of sediment tracer concentration profiles (Paulsen et al., 1999).

In Palos Verdes Shelf sediments, there is a well-recognized anomaly in ^{210}Pb (Paulsen et al., 1999). The ^{210}Pb anomaly is likely due to elevated ^{210}Pb fluxes, which are caused by the dilution of shelf waters with outfall effluent containing enhanced ^{210}Pb -scavenging particles. In their model, Paulsen et al. (1999) assumed ^{210}Pb fluxes are a direct function of enhanced particle sedimentation rate, which changes over time with outfall effluent. In contrast, most ^{210}Pb models include assumptions of constant ^{210}Pb fluxes or constant ^{210}Pb concentrations on settling particles. Paulsen et al. (1999) suggest that such models are problematic for Palos Verdes Shelf sediments and cause an overestimation of bioturbation depth, e.g., 18-28 cm. Instead, Paulsen et al. (1999) propose that shallow bioturbation occurs in this area. Best fits to their model were obtained by mixing the top 6, 7, 4 and 2-3 cm, which is equivalent to the mixed layer depths measured by ^{234}Th penetration (2-6 cm) (Paulsen et al., 1999). Moreover, the Paulsen et al. (1999) model provides excellent agreement with natural sedimentation rates, especially when more recent results are considered (1960 to core collection).

E3.3.3. Tracer Considerations

While radionuclides such as ^{210}Pb have provided many useful results with regard to sediment mixing and sediment accumulation, they do have some shortcomings with regard to bioturbative studies (Wheatcroft et al., 1994). Radionuclides (e.g., ^{210}Pb) integrate processes over relatively long time periods (~ 100 years) and may not be sensitive indicators of biological activities that occur over short time periods (days, months). Short-lived radioisotopes like ^7Be and ^{234}Th may be difficult to detect. It is therefore important to have additional measures of bioturbative processes. Chlorophyll *a*, and luminophores (painted fluorescent particles) have been used in conjunction with radiotracers to determine mixing rates and depths in sediments. Pulsed inputs of chlorophyll *a* and luminophores have demonstrated rapid biogenic burial of surface sediments not resolved with ^{234}Th (Gerino et al., 1998). Chlorophyll *a*, a naturally-occurring tracer, is useful only when it occurs in large concentrations, i.e., phytoplankton blooms.

In addition to luminophores, other tracers have been added to sediment systems to measure bioturbation. A rare earth element (samarium oxide) has been used in Lake Superior to measure sediment accumulation rates and biological and physical mixing. This study provided a description of *in situ* sediment reworking in the Great Lakes, data which are largely unavailable (Krezoski, 1989). With this technique, samarium oxide is spread on the lake floor at higher concentrations than are observed in nature (Krezoski, 1989). Similarly, magnetite has been proposed to provide evidence of particle mixing (Thibodeaux, 2000, pers. comm.). In the field

and laboratory, glass beads have also been used to study bioturbation (Wheatcroft, 1992; Madsen et al., 1997). For the above adjunct tracers, all are pulsed inputs which are useful for studying particle mixing on short time scales; only chlorophyll *a* is not added by researchers to trace a measured system.

When estimating and comparing bioturbation parameters, e.g., D_b , it is important to identify which tracer(s) were used. Both biological mixing depth (L) and intensity (D_b) are operationally dependent on the method/tracer used to define them (Wheatcroft et al., 1990; Boudreau, 1994). For radioisotopes, particle association may pose a problem as well. For example, ^{234}Th may be associated with highly reactive organic particles (food) (Boudreau, 1994). ^{210}Pb has also been observed to mix at a slower rate than $^{239,240}\text{Pu}$. Stordal et al. (1985) posit that the more rapid mixing rate of $^{239,240}\text{Pu}$ and ^{137}Cs compared with ^{210}Pb reflects its association with food particles (Stordal et al., 1985).

Particle shape and chemistry—size, shape, specific gravity, surface texture and chemical composition—may affect how particles are mixed. These factors are important to consider when selecting a tracer, because particle selection is common among deposit feeders. The presence of radionuclides will not affect particle mixing per se, because radioisotopes will not influence particle selection by deposit feeders. However, the association of radionuclides with high organic matter may influence its mixing dynamics. There is conflicting evidence over whether or not fresh organic matter is mixed at the same rate as other particulates (e.g., Stordal et al., 1984, mixed at different rates; Gerino et al., 1998, mixed at the same rate). The value of artificial particles—e.g., luminophores and glass beads—has also been questioned for bioturbation studies (Wheatcroft et al., 1994). Deposit feeders may preferentially reject such tracers, thus limiting their applicability to measure bioturbation. The difficulty in enumerating tracers such as glass beads is also a concern when choosing a particle tracer (Wheatcroft et al., 1994).

An additional consideration with tracers is their ability to provide some mechanistic understanding of bioturbation in natural systems. Radionuclides cannot be used to directly track particles of a particular type or size, nor can they be used to distinguish between different mixing modes—biodiffusive or bioadvective. Thus, additional tracers are needed to accurately quantify and elucidate multiple bioturbation processes in the field. In the last decade, Olmez and Pink (1994) have developed an exciting ‘deliberate particle-labeling’ technique for use in physical and biological studies. Using a thermal diffusion method, natural sediments were labeled with gold (silts) and silver (sands). The technique does create ‘artificial’ sediments—e.g., luminophores—and therefore should not affect mixing dynamics. The labeled-sediments are sprinkled on the seabed. This technique allows mixing by particle size to be tracked, which is important for understanding bioturbation processes. Furthermore, this pulsed input allows short-term mixing processes on seasonal scales to be resolved.

The above ‘deliberate particle technique’ has been used to study seasonal and particle-size dependent bioturbation in Massachusetts Bay (32 m depth) (Wheatcroft et al., 1994). In spring, Wheatcroft et al. (1994) found silts (Au) were mixed down to 15 cm depth with multiple subsurface maximums; sands (Ag) were confined to the upper 5 cm and showed monotonic decreases in concentrations with depth (Wheatcroft et al., 1994). The tracers showed more congruent profiles with near surface maximums and several subsurface peaks in autumn. Two non-local bioturbation modes were suggested by tracer data—reverse conveyor belt and head-

down deposit feeding or excavation. This technique has allowed reverse conveyor-belt feeding to be identified in the field. The extent to which advective transport occurs is unknown, since most techniques are unable to identify it.

For both experiments, silts (Au) were transported out of the surface layer at a rate approximately a factor of two faster than sands. This result suggests that particle-size-dependent dispersal rates may vary less than a simple application of physical sediment transport models would suggest, and that contaminants bound to fine-grained particles can accumulate in the near field, even under episodically high energy conditions (Wheatcroft et al., 1994). The accumulation of fine-grained particulates may have important implications for contaminants, because contaminant concentration is typically related to particulate size. In summary, bioturbation may preferentially subduct particle sizes and types while returning other particulates to the surface where they are available for resuspension. Few studies have addressed temporal mixing; this technique may allow such factors (e.g., particle size mixing) to be better elucidated in the field (Wheatcroft et al., 1994).

Of all animal activities, deposit feeding has been postulated to be the dominant sediment transport mechanism (Wheatcroft et al., 1990). Thus, if preferential mixing of particles occurs, it is most likely due to this activity. The direction of particle size preference is also most clear for this animal activity. Deposit feeders on the whole actively select and displace finer particles. A higher displacement frequency (or shorter rest period in the nomenclature of Wheatcroft et al., 1990) for fine particles does not necessarily mean that they will penetrate farther into the sediments in a given unit of time, because, at least in shallow-water environments, many deposit feeders (both surface and subsurface types) egest material on the sediment surface (Wheatcroft, 1992). At the Santa Catalina Basin, data demonstrate that vertical bioturbation rates are particle size-dependent. The data suggest preferential selection of the finer fraction, and biodiffusion rate increases with decreasing tracer (particle) size. The likely cause is preferential ingestion and downward transport of fine particles by deposit feeders (Wheatcroft, 1992).

E3.3.4 Visual Techniques

Visual techniques are valuable for identifying and quantifying bioturbation in the field. For example, x-rays have been used to identify biological mixing in Chesapeake Bay (Dellapenna et al., 1998). Recently, X-ray techniques using a contrasting agent such as molybdenum carbide have been seen as particularly useful for bioturbation studies of soft lacustrine muds. Charbonneau (1997) was able to provide evidence for the extensive burrowing and mottling by insects. There was no preservation of physical stratification below the surface, i.e., no laminations, indicating the layer was completely reworked over time (Charbonneau, 1997). Divers also commonly take box-cores. Epifaunal and infaunal organisms at a study site can be later characterized and quantified with box-core dissection. This data is typically used to support tracer findings. In addition, sediment profile imaging cameras (in-bed pictures), surface camera systems, and diver cameras have been used to identify benthic activity (Wright et al., 1997b; Wright et al., 1999; Cutter and Diaz, 2000). In fact, photos are probably the most practical means to provide evidence of bioturbative activities by demersal fish. Indeed, photos, video, and/or x-ray techniques (with sediment cores) serve as valuable tools to document bioturbative processes in the bed sediments; these techniques provide graphical evidence of organisms and their activities (tube structures, mounds) as they occur in the field (e.g., Wright et al., 1997a). In

addition, side-scan sonar have been used to observe bed features (e.g., on the northern California continental shelf, Wright et al., 1999).

The sediment profile camera is a specialized remote still camera system. Such a device was used in the STRATAFORM study of the continental shelf of northern California. They used a Benthos model 3731 system (381 Edgerton Deep Sea) standard camera, designed to provide unparalleled detail for an in situ image of the SWI and subsurface 22 cm of sediment. (See Cutter and Diaz (2000) for further details). The camera was modified to take two photos at adjustable delay and timing. Image clarity is assured irrespective of bottom clarity. Profile images convey sediment-mixing depths. They are estimated as the deepest extent to which recent biological evidence was seen. Generally it includes depths of active and oxidized infaunal burrows, open feeding voids, organisms presence and mottling of otherwise uniform sediment layers (Cutter and Diaz, 2000).

Regional measurements of bottom roughness were made using side-scan-sonar surveys and more detailed local measurements were made using plan-view and sediment water interface-profiling cameras (Wright et al., 1999). Infaunal feeding voids, burrows, and occasional worms can be observed from the profiling-cameras (Wright et al., 1999).

E3.3.5 Bioirrigation Tracers

Tracers (e.g., ^{224}Ra , ^{234}Ra and $^3\text{H}_2\text{O}$) are also used to estimate bioirrigation rates (or solute flux) in laboratory and field environments (e.g., Sweerts et al., 1991). Bioirrigation tracers are unaffected by sediment chemical reactions. Naturally-occurring ^{224}Ra and ^{223}Ra have been used to investigate the effect of burrowing activities of ghost shrimp (*Neocallichirus limosus* and *Biffarius arenosus*) and heart urchin (*Echinocardium cordatum*) on dissolved substances flux across the water-sediment interface. Deuterium enriched tracers have also been introduced into benthic chambers on the seafloor (Berelson et al., 1999). Sweerts et al. (1991) found that the effect of faunal activity only has a slight effect on solute movement up to $1,600 \text{ indiv/m}^2$ (Chironomidae, *Chaoborus*, Oligochaeta), but at $12,000 \text{ indiv/m}^2$ faunal activity has a large impact. In addition, ^{22}Na has been used as a soluble tracer (bioirrigation) to determine solute exchange between sediments and freshwater in vitro (Wang and Matisoff, 1997).

E3.3.6 Summary

Many techniques have been used to quantify bioturbation and bioirrigation. Radionuclides are the most commonly used tracers to investigate sediment processes. As was demonstrated above, multiple radioisotope measures are necessary when estimating bioturbation parameters, since radioisotopes integrate over different periods and thus capture different mixing events.

Radioisotopes are often unable to capture short-lived or shallow mixing events. Thus, a variety of adjunct tracers have been utilized in the laboratory and the field to study bioturbation. One of these techniques—deliberate particle labeling (Olmez and Pink, 1994)—demonstrates promise for future bioturbation studies. It not only provides evidence for different mixing mechanisms (i.e., reverse conveyor belt), it also tracks mixing by different particle sizes. Both are important processes to understand when investigating contaminant fate and transport.

E3.4 BIOLOGICAL MIXING DEPTH (L)

The biological mixing depth (L) is defined as the thickness of surficial sediments that are most frequently mixed (Boudreau, 1994). This depth is also called the tracer identified mixing layer, since it is delineated by a perceived break in the slope of a vertical tracer profile (Boudreau, 1997b). Statistical methods are rarely used to define the mixing layer (Boudreau, 1997b).

Boudreau (1994) found that the worldwide average for deposit-feeding organisms is 9.8 ± 4.5 cm (1- σ error). Using a simple model that accounts for resource (food) availability and bioturbation intensity, Boudreau (1998) calculated L to be 9.7 cm, confirming his 1997 estimate. Boudreau (1998) contends that L is independent of burial velocity. Furthermore, speculation that the invariance of the mixed depth is a result of the feedback between food dependence of bioturbation and the decay of that resource appears to be true or at least consistent with observations (Boudreau, 1998). L is limited by increasing energy costs of reworking and excavating deeper than 10-cm. L is not likely to be a function of water depth (Boudreau, 1998). It is important to recognize that Boudreau's (1994) estimate is primarily based on work done in the marine realm. Similar relations may hold in the lacustrine environments, but at present it is not known if they will hold true. Because physical mixing may be more common in lakes, this may inhibit attempts to develop similar equations for the lacustrine systems (Boudreau, 1998).

E3.4.1 Biological Mixing Depth (L) Estimates

Although some organisms may burrow deeply—e.g., ghost shrimp tunnel to depths of 50 cm in Port Phillip Bay, Australia (Berelson et al., 1999); most biological mixing occurs in the top 1-20 cm (Boudreau, 1994). Biological mixing depths (Ls) may vary considerably between sites. Differences may be great even in the same sites in the same water body. In the Chesapeake Bay, for example, L has been reported to vary between 17-30 cm depth (Dellapenna et al., 1998).

Biological mixing depths have been extensively reviewed by a number of researchers: e.g., Matisoff (1982); McCall and Tevesz, (1982); Thoms et al. (1995). To augment Boudreau's reviews of marine mixing depths, freshwater biological mixing depths (Ls) from the aforementioned reviews will be highlighted. These reviews should be referenced for specific study results. Where freshwater Ls do exist, they are typically reported for lakes. Bioturbation studies in rivers are virtually nonexistent. In fresh water, McCall and Tevesz (1982) note that oligochaetes are among the most important organisms. Ninety percent of oligochaetes mix in the top 10-12 cm. Matisoff (1982) also reports $L = 6$ cm in Lake Huron and $L = 5-6$ cm in Lake Erie. More recently, Thoms et al.'s (1995) review cites a number of freshwater studies where $L \leq 10$ cm; only two freshwater studies are listed with estimates of $L \geq 10$ ($L = 12$ and 16 cm). In addition, one riverine study was named in this review. L was estimated to be 6 cm in Nipigon River, a tributary to Lake Superior (Bukaka and Bobba, 1984; cited in Thoms et al., 1995).

Charbonneau (1997) found Mayfly nymphs *Hexagenia* mix lacustrine sediments at depths less than 11 cm. Similarly, Matisoff and Wang (2000) found infaunal and chironomids (*Coelotanypus* sp.) and *Chironomus* sp. and mayfly nymphs construct and irrigate burrows up to 10 cm below the sediment. Freshwater oligochaetes have been observed to mix sediments at depths of 5-7 cm in the field and 6-8 cm (Fisher et al., 1980). Similarly, Robbins et al. (1977) found oligochaetes and amphipods mixed sediments to depths of 3-6 in Lake Huron. Using fallout ^{134}Cs from Chernobyl, Robbins and Jasinski (1995) reported that wind driven currents and bioturbation

mixed sediments to a depth of 10 cm within a year and 14-24 cm in two years (Lake Snairdwy, Poland). In the lab, burrows of *Branchiura sowerbyi* large freshwater tubificid oligochaetes extend to 20 cm (Wang and Matisoff, 1997).

In summary, bioturbators appear to generally mix freshwater sediments to depths of 10 cm or less. Regardless, a number of factors must be considered when comparing bioturbation parameters like L . These bioturbation parameters are not only affected by abiotic (temperature, oxygen) and biotic (community structure) factors, they are also influenced by the tracer method used. For this reason, caution must always be employed when applying L from other sites or from different seasons. Unfortunately, many studies do not account for temporal changes when estimating biological mixing depths (L) or rates (e.g., D_b). Furthermore, many studies do not quantitatively describe the benthic population at the study site, if they describe it at all. Such inadequacies in the site description may make it difficult if not impossible to apply bioturbation parameters from other studies. Also, many published estimates are based on controlled populations in laboratory environments. Bioturbation parameters estimated from similar populations in the lab and in the field have been found to differ (e.g., Fisher et al., 1980). The above considerations should also be weighed when evaluating D_b estimates.

E3.5 BIODIFFUSION COEFFICIENT (D_b)

Biodiffusion coefficients characterize the intensity of bioturbation in sediments. There is a general trend of D_b decreasing with depth. General differences are in the organic-poor deep sea deposits from oligotrophic reigns having less intense bioturbation than organic rich shallow water deposits (Aller et al., 1998). Initially, decreasing D_b was associated with decreasing biomass of organisms at depth (Robbins et al., 1977; Christensen and Bhunia, 1986). More recently the depth dependence of D_b has been correlated with increasing energy costs of burrowing at depth. The drag imposed by the sediment-water mixture increases with depth as water content decreases and lithostatic pressure increases (Wheatcroft et al., 1990).

Two-layer bioturbation models have been developed to account for the depth dependence of D_b . For example, Silverberg et al. (1986) used a model which included an order of magnitude decrease in mixing intensity (biodiffusion coefficient) to explain the observed radiotracer profile. Other models have accounted for decreasing mixing rate with depth with a continuously decreasing D_b (e.g., Dauwe et al., 1998). Regardless, some exceptions do occur; increasing mixing rates have been observed with depth. In Port Phillip Bay, Australia, high mixing rates were found in the deepest regions of the biological mixing zone (Hancock and Hunter, 1999). Hancock and Hunter (1999) hypothesized that the increased mixing rates reflect the predominance of worms and shrimp at depth. Advective transport with tunneling and feeding may in fact lead to the anomalous mixing rates at depth. This example—increasing mixing rate at depth—emphasizes the inadequacy of using D_b as a default parameter when quantifying bioturbation by natural populations, especially when non-local mixing might occur.

E3.5.1 D_b Estimates

While D_b typically decreases with depth, D_b estimates vary widely between sites and over time (McCall and Tevesz, 1982). Reviews by Matisoff (1982), McCall and Tevesz (1982), and Thoms et al. (1995) contain the most comprehensive lists of D_b s. For example, Matisoff (1982) has quantified more than 80 different biodiffusion coefficients (D_b); D_b s were found to vary over

four orders of magnitude. D_b estimates are difficult to compare between sites. Differences in biodiffusion rates may reflect subtle changes in biota among other factors. For example, Robbins et al. (1977) reported $D_b = 4.4 \times 10^{-8} \text{ cm}^2/\text{s}$ ($L = 6 \text{ cm}$, oligochaetes) and $D_b = 1.8 \times 10^{-7}$ to $1 \times 10^{-7} \text{ cm}^2/\text{s}$ ($L = 3\text{-}6 \text{ cm}$, tubificids and amphipods) in Lake Huron. Again, freshwater studies of bioturbation are relatively scarce, therefore only a few studies will be highlighted herein. In the Great Lakes, deposit feeders (e.g., oligochaetes) are thought to be dominant mixers; however, suspension feeders may be locally important (McCall et al., 1995). In a study of freshwater bivalves, McCall et al. (1995) found whole cell D_b s were 2.6×10^{-8} – $6.7 \times 10^{-8} \text{ cm}^2/\text{s}$ and $1.7 \times 10^{-8} \text{ cm}^2/\text{s}$ for *A. grandis* (unionid) and *S. striatinum* (a typical pisidiidae), respectively. Adjusted for equal populations, *A. grandis*' mixing rate was 11–27 times greater; this is most likely reflects its greater size. No general trend when freshwater and marine organisms of similar size and feeding mechanism were compared (McCall et al., 1995). Very few bioturbation studies are conducted in rivers; D_b in a tributary to Lake Superior was estimated to be $9.5 \times 10^{-7} \text{ cm}^2/\text{s}$ ($L = 6 \text{ cm}$) (Bukaka and Bobba, 1984; cited in Thoms et al., 1995).

Using a multiple ^{137}Cs tracer layer technique (laboratory), Matisoff and Wang (2000) studied mixing rates of infaunal midges *Coelotanypus* sp. and *Chironomus* sp. and mayfly nymph *Hexogenia* spp. They found biodiffusion to be strongly depth dependent. Only *Chironomus* sp. mix sediments by biodiffusion (random) mixing at rates comparable to conveyor-belt deposit feeding oligochaete worms on a per individual basis. Individual rates of non-local mixing by feeding (directed particle motion) for the chironomid and mayfly larvae were similar to or less than those reported by oligochaetes in similar experiments. Although they are burrow irrigators, they rework sediments in a nonlocal fashion. Results indicate that sparse populations of bivalves, some chironomids (*Coelotanypus* sp.) and mayflies cause a relatively small amount of mixing compared to the more abundant amphids, tubificid oligochaetes and *Chironomus* sp. Surprising, the bioirrigator *Chironomus* sp. appears to be as important in mixing sediment as deposit feeding conveyor-belt tubificid oligochaetes (Matisoff and Wang, 2000).

Some differences in reported biodiffusion coefficients may be related to size. Wheatcroft et al. (1990) noted that D_b is proportional to the distance² of particles moved and inversely with elapsed time between particle movements. Therefore, larger organisms would be expected to dominate particle movement, and this is true in general, but not for bioirrigators (Matisoff and Wang, 2000). In Lake Erie, in situ comparisons were made between unionids ($10\text{-}10^2 \text{ indiv}/\text{m}^2$ prior to zebra mussels) and for tubificid oligochaetes (up to $10^6 \text{ indiv}/\text{m}^2$) (Wang and Matisoff, 2000). Results indicate that even if individual mixing is large, sparse population of bivalves, some chironomids (*Coelotanypus* sp.) and mayflies result in a relatively small amount of mixing compared with more abundant tubificids. In particular, the amphipod. Recently, Matisoff and Wang (2000) have also named the amphipod *Diporeia* as highly important to sediment mixing in Lake Erie. It should be emphasized that macrobenthic communities are heterogeneous and dynamic, and that spatial and temporal variability should be considered when taking *in situ* measurements.

Table E2, from Thibodeaux (1996), summarizes values of biodiffusion coefficients and depths found in the literature, and shows the ranges of values found in various environments. Note that

Table E2 shows biodiffusion coefficients varying over many orders of magnitude, and that reported pore water mixing rates generally exceed particle mixing rates.

Table E2 Biodiffusion Coefficients and Depths

Location	Coefficient, D_B (cm^2/s)	Depth, L (cm)
Solid Particle Mixing		
Deep sea, various sites	3.2E-11 to 3.2E-8	10 to 48
Mid-Atlantic Ridge	6E-9	8
Long Island Sound	1.2 to 3.5E-6	4
Chesapeake Bay	1E-6	10 to 15
New York Bight	5E-7	?
Rhode Island, 0 to 1 cm	29 to 1.6E-5	1
Rhode Island, 2 to 10 cm	83 to 4.3E-6	8
La Jolla, CA	1.5E-5	30
Barnstable Harbor, MA	7.6E-8	6
Long Island Sound	3.2E-7	2
Long Island Sound	2E-6	3
Laboratory	1E-5	3
Laboratory	20 to 4.5 E-5	11
Freshwater lake, mud	4.4E-8	0 to 6
Lake Huron, mud	1.2E-7	0 to 3/6
Porewater Mixing		
Long Island Sound, mud	>2.8E-5	0 to 8
Coastal North Sea, mud	E-4	0 to 3.5
Coastal North Sea, sand	0.5 to 2E-4	0 to >15
Narragansett Bay, mud	4E-5	0 to 25

E4. REPRESENTATION IN LEADING FATE AND TRANSPORT MODELS

Models are useful in providing order-of-magnitude estimates of flux, lifetime, and concentration of chemicals in sediment porewater.

The most common type of model in use for describing bioturbation is a model based on a diffusion analogy that assumes uniform random mixing and is described by a biodiffusion coefficient and mixing depth. More than 240 values of the biodiffusion coefficient are reported for various locations and organisms in the literature. Far fewer parameters are available for models that simulate pore water mixing and reactions or nonlocal particle mixing such as that caused by conveyor-belt-feeding organisms. A model developed by Dr. John Robbins in 1986 is particularly versatile because it can simulate both kinds of organism mixing processes for both sediments and pore waters (WERF, 1995).

E4.1 WATER QUALITY ANALYSIS SIMULATION PROGRAM (WASP) AND ENVIRONMENTAL FLUID DYNAMICS CODE (EFDC)

In WASP applications, dispersive mixing coefficients can be specified between adjoining segments representing pore water diffusion. Diffusion coefficients are multiplied internally by cross-sectional areas divided by characteristic mixing lengths, and are treated as flows that carry dissolved toxicants between benthic segments and the water column. The user may specify diffusive transport of dissolved chemicals in benthic-segment pore water. The user supplies a time function giving dispersion coefficient values (in m²/sec) as they vary in time. For each exchange in the group, the user must supply an interfacial area, a characteristic mixing length, and the segments between which exchange takes place. The characteristic mixing length is typically the distance between two benthic segment midpoints (multiplied internally by the tortuosity, which is roughly the inverse of porosity). For pore water exchange with a surface water segment, the characteristic mixing length is usually taken to be the depth of the surficial benthic segment. The interfacial area is the surficial area of the benthic segment (which is input by the user) multiplied internally by porosity.

There may be several surficial benthic segments underlying a water column segment, representing discrete benthic deposits (or habitats). The diffusing concentration of chemical is the dissolved fraction per unit pore water volume. The actual diffusive exchange between benthic segments *i* and *j* at time *t* is given by:

$$\frac{\partial M_i}{\partial t} = \frac{E_{ij}(t) \cdot A_{ij}}{L_{cij}} (C_j - C_i) \quad (7)$$

where:

M_i = mass of state variable in segment *i* (g);

C_i = dissolved or colloid-bound state variable concentration in segment *i* (g/m³);

C_j = dissolved or colloid-bound state variable concentration in segment *j* (g/m³);

$E_{ij}(t)$ = diffusion coefficient time function for exchange “ij” (m^2/day);

A_{ij} = interfacial area shared by segments i and j (m^2); and

L_{cij} = characteristic mixing length between segments i and j (m).

The diffusion coefficient may also be expressed as a mass transfer rate by dividing the diffusion coefficient by the characteristic mixing length:

$$v_{ij}(t) = \frac{E_{ij}(t)}{L_{cij}} \quad (8)$$

where:

$v_{ij}(t)$ = mass transfer rate for exchange between segments i and j (m/day).

EFDC provides a linkage to WASP for simulation of water quality and benthic layers and would, therefore, incorporate the same pore water diffusion processes as described above for WASP.

E4.2 OTHER MODELS

Time-averaged bioturbation is most commonly modeled as a one-dimensional (vertically) diffusive process (e.g., Robbins et al., 1977; Aller, 1982; Boudreau, 1986a; Officer and Lynch, 1989; Wheatcroft, 1992; Dauwe et al., 1998). Such models typically describe local mixing by deposit feeders. In a (bio)diffusion model, bioturbation is characterized numerically by an intensity coefficient (D_b) and by the depth over which bioturbation occurs (L) (Boudreau, 1998). D_b , termed the biodiffusion coefficient, is analogous to a standard Fickian diffusivity. As discussed above, D_b enables complex mechanisms of sediment mixing—e.g., feeding, burrowing, and tube building—to be parameterized as a single factor (Wheatcroft et al., 1990; Madsen et al., 1997). L , namely the biological mixing depth, is defined as the thickness of surficial sediments that are most frequently mixed (Boudreau, 1994). It is important to note that L does not refer to the maximum depth of biological mixing, since some organisms mix sediments to depths of a meter or more (Bird et al., 1999). Biodiffusion coefficients (D_b) are estimated by fitting regression lines to the down-core tracer distribution. Biological mixing depths (L) are identified by the slope break in a tracer profile (Boudreau, 1994). Sediment tracers were discussed in detail in section 5.2.

Biodiffusive mixing is generally described by Equation 9 below. Here, the steady-state distribution of a solid species subject to first-order decay (e.g., a radionuclide tracer) in a constant porosity sediment with negligible advection is given as:

$$D_b \frac{\partial^2 C}{\partial^2 x^2} - \lambda C = 0 \quad (9)$$

where D_b is the biodiffusion coefficient ($\text{length}^2 \text{time}^{-1}$), C is the concentration of the species in the solid phase, x is depth, and λ is a rate (decay) constant (time^{-1}) (Boudreau, 1998). While porosity modification has been ascribed to the actions of bioturbators (Boudreau, 1986a), the

effect of porosity modification has not been found to significantly influence model results (Mulsow et al., 1998). Consequently, constant porosity is generally considered with bioturbation models.

Equation 9 has proven to be remarkably good at fitting the data (describing tracer profiles) (Boudreau, 1998). Nevertheless, this model is limited in its capacity to provide mechanistic understanding or prediction about bioturbation processes (Boudreau, 1998). This is notwithstanding extensive research efforts (e.g., Boudreau, 1986a,b; Boudreau and Imboden, 1987; Wheatcroft et al., 1990).

Biodiffusion models are inadequate when the time scale of observation is short relative to the rate for mixing or when organisms advect sediments in preferential directions—e.g., conveyor-belt mixers (Boudreau, 1986b; Boudreau and Imboden, 1987; Officer and Lynch, 1989; Wheatcroft et al., 1990). Simulations have demonstrated that drastically different types of bioturbation (e.g., diffusive versus advective) can, given sufficient time, produce similar tracer profiles (Boudreau 1986a,b; Boudreau and Imboden, 1987). This convergence does not mean that these mixing styles are equivalent geochemically, since reaction kinetics of many chemical species are markedly affected by the type of sediment mixing (Wheatcroft et al., 1990). For this reason, bioturbation models must address the fact that many mechanisms of sediment displacement are not diffusive, even though they may combine to produce apparently diffusive tracer profiles (Wheatcroft et al., 1990). Biodiffusion models have been used to model bioirrigation (e.g., Berelson, 1999), and there has been some criticism of its use. For example, Boudreau (1997b) noted that bioirrigators do not mix porewaters in a diffusional manner; therefore, a 1-D biodiffusion model does not appropriately describe bioirrigation (Boudreau, 1997b).

Nonlocal (advective) mixing has also been modeled though less frequently than biodiffusive mixing (e.g., Boudreau, 1986b). Biodiffusion models, as discussed earlier, are commonly used to model local mixing by deposit feeders. Furthermore, they are employed as a default when little is known about the natural population. In contrast, advective mixing models are selectively used to describe bioturbation by conveyor-belt feeders in controlled environments. Nonlocal models have been used to estimate subduction rates of surficial sediment due to the activity of conveyor-belt mixers (Boudreau, 1986b; Wheatcroft et al., 1990). The vertical advective transport coefficient (v_b) is used to describe the intensity of nonlocal mixing.

In some cases, biodiffusive-bioadvective models have been utilized to describe sediment mixing by a natural (and diverse) benthic population (Christensen and Bhunia, 1986). These models are hybrids of biodiffusion and bioadvective models (e.g., Silverberg et al., 1986; Gerino et al., 1998). For instance, steady-state and non-steady state models have been developed to quantify biodiffusive transport (D_b) and vertical advective transport (v_b) (Gerino et al., 1998). Equation 3 is a fundamental model equation used to describe advective-diffusive transport when compaction is ignored (Gerino et al., 1998),

$$\frac{\partial^z C}{\partial t} = D_b \frac{\partial^2 C}{\partial z^2} - v_b \frac{\partial C}{\partial z} - kC \quad (10)$$

where: D_b = biodiffusive coefficient;
 v_b = bioadvective coefficient;
 t = time;
 z = depth, positive into deposit;
 C = tracer concentration or activity; and
 k = first order reaction constant (depends on the tracer used)

It is important to note that equation 10 only approximates complex nonlocal transport by conveyor-belt feeders. Other nonlocal transport processes, i.e., reverse conveyor belt feeding, are ignored. Boudreau (1998) has developed a simple (food) feedback, diffusive-advective model of bioturbation. It is derived from the steady-state mass balance equation for a tracer subject to the effects of biodiffusion, advective transport, and first order decay in the mixed layer. This equation also predicts a finite depth of the biological mixing zone in sediments. Boudreau (1998) stated that it would be unlikely that his diffusive-advective equation would supplant the basic biodiffusion equation (equation 9), since researchers are reluctant to use numerical methods and a simple analytical solution was not readily available. In the interim, Swaney (1999) has provided analytical solutions to Boudreau's (1998) model corresponding to two different standard boundary conditions.

E5. PREDICTIVE UNCERTAINTIES

Chemical transport within the upper layers of bed sediments is a very complex process that will continue to challenge the efforts of environmental chemists, benthic biologists, and engineers for decades. The laboratory and field data needed to verify models, which includes both fluxes and concentration site-specific profiles, appear to be very limited.

Based on literature values, biodiffusion coefficients range between about 10^{-8} and 10^{-4} cm²/sec. The upper end of this range, which is attributed primarily to porewater mixing by benthic organisms, exceeds the range of effective molecular diffusivities by about an order of magnitude. This suggests that bioturbation can dominate molecular diffusion in the biologically mixed layer, which typically extends to about 10cm below the sediment-water interface.

While molecular diffusivity can be predicted with reasonable accuracy based on chemical characteristics and sediment porosity, biodiffusion is much more difficult to predict without extensive knowledge of local benthic populations and processes. For this reason, low-flow contaminant releases to the water column at rates exceeding molecular diffusion by as much as an order of magnitude must be considered, unless ruled out by site-specific benthic studies. To the extent that bioturbation is an important transport mechanism, a permanent cover in excess of the biologically mixed layer will mitigate against contaminant release to the water column.

E6. REFERENCES

- Aller, R. C., 1982. The effects of macrobenthos on the chemical properties of marine sediment and overlying water. *Animal-Sediment Relations* (Eds. P. L. McCall and M.J.S. Tevesz). Plenum, New York: 53-102.
- Aller, R.C., Hall, P.O.J., Rude, P.D., and Aller, J.Y., 1998. Biogeochemical heterogeneity and suboxic diagenesis in hemipelagic sediments of the Panama Basin. *Deep-Sea Research I*, 45: 133-165.
- Berelson, W.M., Townsend, T., Heggie, D., Ford, P., Longmore, A., Skyring, G., Kilgore, T., and Nicholson, G., 1999. Modelling bio-irrigation rates in the sediments of Port Phillip Bay. *Marine and Freshwater Research*, 50: 573-579.
- Berner, R. A. 1980. *Early diagenesis: A theoretical approach*. Princeton.
- Bird, F.L., Ford, P.W., and Hancock, G.J., 1999. Effect of burrowing macrobenthos on the flux of dissolved substances across the water-sediment interface. *Marine and Freshwater Research*, 50: 523-532.
- Bosworth, W.S., and Thibodeaux, L.J., 1990. Bioturbation: a facilitator of contaminant transport in bed sediments. *Environmental Progress*, 9(4): 211-217
- Boudreau, B.P., 1986a. Mathematics of tracer mixing in sediments: I. Spatially dependent, diffusive mixing. *American Journal of Science*, 286: 161-198.
- Boudreau, B.P., 1986b. Mathematics of tracer mixing in sediments: II. Nonlocal mixing and biological conveyor-belt phenomena. *American Journal of Science*, 286: 199-238.
- Boudreau, B.P., 1994. Is burial velocity a master parameter for bioturbation? *Geochimica et Cosmochimica Acta*, 58(4): 1243-1249.
- Boudreau, B.P., 1998. Mean mixed depth of sediments: The wherefore and the why. *Limnology and Oceanography*, 43(3): 524-526.
- Boudreau, B.P. and Imboden, D.M., 1987. Mathematics of tracer mixing in sediments: III. The theory of nonlocal mixing with in sediments. *American Journal of Science*, 287: 693-719.
- Breukelaar, A., Lammens, E.H.R.R., Breteler, J.G.P.K., and Tátrai, I., 1994. Effects of benthivorous bream (*Abramis brama*) and carp (*Cyprinus carpio*) on sediment resuspension and concentrations of nutrients and chlorophyll *a*. *Freshwater Biology*, 32: 113-121.

- Carslaw, H. S. and J. C. Jaeger, 1967. Conduction of heat in solids. Oxford University Press, New York, p. 54-56.
- Charbonneau, P., Hare, L., and Carignan, R., 1997. Use of x-ray images and a contrasting agent to study the behavior of animals in soft sediments. *Limnology and Oceanography*, 42(8): 1823-1828.
- Christensen, E.R., and Bhunia, P.K., 1986. Modeling radiotracers in sediments: Comparison with observations in Lake Huron and Michigan. *Journal of Geophysical Research*, 91: 8559-8571.
- Christensen, J.P., Devol, A.H., and Smethie, W.M., Jr., 1984. Biological enhancement of solute exchange between sediments and bottom water on the Washington continental shelf. *Continental Shelf Research*, 3: 9-23.
- Crank, J., 1956. The mathematics of diffusion. Oxford University Press, New York, p. 12-15.
- Cutter, G.R., Jr., Diaz, R.J., 2000. Biological alteration of physically structured flood deposits on the Eel margin, northern California. *Continental Shelf Research*, 20: 235-253.
- Dauwe, B., Herman, P.M.J., and Heip, C.H.R., 1998. Community structure and bioturbation potential of macrofauna at four North Sea stations with contrasting food supply. *Marine Ecology Progress Series*, 173: 67-83.
- Dellapenna, T.M., Kuehl, S.A., and Schaffner, L.C., 1998. Sea-bed mixing and particle residence times in biologically and physically dominated estuarine systems: a comparison of lower Chesapeake Bay and the York River subestuary. *Estuarine, Coastal, and Shelf Science*, 46: 777-795.
- Ebenhöh, W., Kohlmeier, C., and Radford, P.J., 1995. The benthic biological submodel in the European Seas Ecosystem Model. *Netherlands Journal of Sea Research* 33: 423-452.
- Fisher, J.B., 1982. Effects of macrobenthos on chemical diagenesis of freshwater sediments. *Animal-Sediment Relations* (Eds. P. L. McCall and M.J.S. Tevesz). Plenum, New York: 105-176.
- Fisher, J.B., Lick, W.J., McCall, P.L., and Robbins, J.A., 1980. Vertical mixing of lake sediments by tubificid oligochaetes. *Journal of Geophysical Research*, 85: 3997-4006.
- Gerino, M., Aller, R.C., Lee, C., Cochran, J.K., Aller, J.Y., Green, M.A., and

- Hirschberg, D., 1998. Comparison of different tracers and methods used to quantify bioturbation during a spring bloom: 234-thorium, luminophores and chlorophyll *a*. Estuarine, Coastal and Shelf Science, 46: 531-547.
- Hancock, G.J., and Hunter, J.R., 1999. Use of excess ^{210}Pb and ^{228}Th to estimate rates of sediment accumulation and bioturbation in Port Phillip Bay, Australia. Marine and Freshwater Research, 50: 533-545.
- Hines, M.E., and Jones, G.E., 1985. Microbial biogeochemistry and bioturbation in the sediments of Great Bay, New Hampshire. Estuarine, Coastal, and Shelf Science, 20: 729-742.
- Hines, M.E., Lyons, W.B., Armstrong, P.B., Orem, W.H., Spencer, M.J., Gaudette, H.E., and Jones, G.E., 1984. Seasonal metal remobilization in the sediments of Great Bay, New Hampshire. Marine Chemistry, 15: 173-187.
- Hymel, S.N., and Plante, C.J., 2000. Feeding and bacteriolytic responses of the deposit-feeder *Abarenicola pacifica* (Polychaeta: Arenicolidae) to changes in temperature and sediment food concentration. Marine Biology, 136: 1019-1027.
- Karickhoff, S.W., and Morris, K.R., 1985. Impact of tubificid oligochaetes on pollutant transport in bottom sediments. Environmental Science and Technology, 19: 51-56.
- Kirkham, D. and W. L. Powers, 1972. Advanced soil physics. Wiley-Interscience, A division of John Wiley & Sons, Inc., New York.
- Kramer, K.J.M., Misdorp, R., Berger, G., and Duijts, R., 1991. Maximum pollutant concentrations at the wrong depth: a misleading pollution history in a sediment core. Marine Chemistry, 36(1-4): 183-198.
- Krezoski, J.R., 1989. Sediment reworking and transport in eastern Lake Superior: *in situ* rare earth element tracer studies. Journal of Great Lakes Research, 15: 26-33.
- Larsson, P., 1983. Transport of 14C-labelled PCB compounds from sediment to water and from water to air in laboratory model systems. Water Research, 17: 1317-1326.
- Li, Y. H. and S. Gregory. 1974. Diffusion of ions in sea water and in deep-sea sediments. Geochim. Cosmochim. Acta 38: 703-714.
- Madsen, S.D., Forbes, T.L., and Forbes, V.E., 1997. Particle mixing by the polychaete *Capitella* species: coupling fate and effect of a particle-bound organic contaminant (fluoranthene) in a marine sediment. Marine Ecology Progress Series, 147: 129-142.
- Madsen, S.D., Forbes, T.L., and Forbes, V.E., 1997. Particle mixing by the

- polychaete *Capitella* species: coupling fate and effect of a particle-bound organic contaminant (fluoranthene) in a marine sediment. Marine Ecology Progress Series, 147: 129-142.
- Matisoff, G., Fisher, J.B., and Matis, S., 1985. Effects of benthic macroinvertebrates on the exchange of solutes between sediments and freshwater. *Hydrobiologia* (Neth.), 122: 19-33.
- Matisoff, G., and Wang, X., 2000. Particle mixing by freshwater infaunal bioirrigators: midges (Chironomidae: Diptera) and mayflies (Ephemerae: Ephemeroptera). *Journal of Great Lakes Research*, 26(2): 174-182.
- Matisoff, G., Fisher, J.B., and Matis, S., 1985. Effects of benthic macroinvertebrates on the exchange of solutes between sediments and freshwater. *Hydrobiologia* (Neth.), 122: 19-33.
- McCall, P.L., and Tevesz, M.J.S., 1982. The effects of benthos on physical properties of freshwater sediments. *Animal-Sediment Relations* (Eds. P. L. McCall and M.J.S. Tevesz). Plenum, New York: 105-176.
- McCall, P.L., Tevesz, M.J.S., Wang X., and Jackson, J.R., 1995. Particle mixing rates of bivalves: *Anodonta grandis* (Unionidae) and *Sphaerium striatinum* (Pisidiidae). *Journal of Great Lakes Research*, 21(3): 333-339.
- Millington, R. J. and J. P. Quirk. 1961. *Trans. Faraday Soc.*, 57, 1200.
- Mohanty, S., Reible, D.D., Valsaraj, K.T., and Thibodeaux, L.J., 1998. A physical model for the simulation of bioturbation and its comparison to experiments with oligochaetes. *Estuaries*, 21(2): 255-262.
- Mulsow, S., Boudreau, B.P., and Smith, J.N., 1998. Bioturbation and porosity gradients. *Limnology and Oceanography*, 43(1): 1-9.
- Officer, C.B., and Lynch, D.R., 1989. Bioturbation, sedimentation, and sediment-water exchanges. *Estuarine, Coastal, and Shelf Sciences*, 28: 1-12.
- Olmez, I., and Pink, R., 1994. New particle-labeling technique for use in biological and physical sediment transport studies. *Environmental Science and Technology*, 28: 1487-1490.
- Paulsen, S.C., List, E.J., and Santschi, P.H., 1999. Modeling variability in ²¹⁰Pb and sediment fluxes near the Whites Point outfalls, Palos Vedes Shelf, California. *Environmental Science and Technology*, 33: 3077-3085.

- Petersen, K., Kristensen, E., Bjerragaard, P., 1998. Influence of bioturbating animals on flux of cadmium into estuarine sediment. *Marine Environmental Research*, 45(4/5): 403-415.
- Reible, D.D., Vlasaraj, K.T., and Thibodeaux, L.J., 1991. Chemodynamic models for transport of contaminants from sediment beds. *The Handbook of Environment Chemistry, Volume 2, Part F* (Ed. O. Hutzing). Springer-Verlag, Berlin, pp. 187-227.
- Reible, D. D., Popov, V., Valsaraj, K.T., Thibodeaux, L.J., Lin, F., Dikshit, M., Todaro, M.A., and Fleeger, J., 1996. Contaminant fluxes from sediment due to tubificid oligochaete bioturbation. *Water Resources*, 30(3): 704-714.
- Retraubun, A.S.W., Dawson, M., and Evans, S.M., 1996. Spatial and temporal factors affecting sediment turnover by the lugworm *Arenicola marina* (L.). *Journal of Experimental Marine Biology and Ecology*, 201: 23-35.
- Rhoads, D. C., and L. F. Boyer. 1982. The Effects of Marine Benthos on Physical Properties of Sediments: a Successional Perspective, in *Animal-Sediment Relations*, P. L. McCall and M. J. S. Tevesz (eds.), Plenum Press.
- Robbins, J.A., 1978. Geochemical and geophysical applications of radioactive lead. *The Biogeochemistry of Lead in the Environment* (Ed. J.O. Nriagu). Elsevier/North-Holland: 285-393.
- Robbins, J.A. & D.N. Edgington. 1975. Determination of recent sedimentation rates in Lake Michigan using Pb-210 and Cs-137. *Geochimica et Cosmochimica Acta* 39: 285-304.
- Robbins, J.A., and Jasinski, A.W., 1995. Chernobyl fallout radionuclides in Lake Sniardwy, Poland. *Journal of Environmental Radioactivity*, 26(2): 157-184.
- Robbins, J.A., Krezoski, J.R., and Mozley, S. C., 1977. Radioactivity in sediments of the Great Lakes: post-depositional redistribution by deposit-feeding organisms. *Earth and Planetary Science Letters*, 36: 325-333.
- Rowden, A.A., Jones, M.B., and Morris. 1998. The role of *Callianassa subterranean* (Montagu) (THALASSINIDEA) in sediment resuspension in the North Sea. *Continental Shelf Research*, 18: 1365-1380.
- Rutgers van der Loeff, M.M., Anderson, L.G., Hall, P.O.J., Iverfeldt, Å., Josefson, A.B., Sundby, G., and Westerlund, S.F.G., 1984. The asphyxiation technique: an approach to distinguishing between molecular diffusion and biologically mediated transport at the sediment-water interface. *Limnology and Oceanography*, 29: 675-686.

- Schaffner, L. C., R. J. Diaz, C. R. Olsen, and I. L. Larsen. 1987. Faunal Characteristics and Sediment Accumulation Processes in the James River Estuary. *Estuar. Coast. Shelf Sci.*, 25, 211.
- Schaffner, L.C., Dickhut, R.M., Mitra, S., Lay, R.W., and Brouwer-Riel, C., 1997. Effects of physical chemistry and bioturbation by estuarine macrofauna on the transport of hydrophobic organic contaminants in the benthos. *Environmental Science and Technology*, 31: 3120-3125.
- Sharma, P., Gardner, L.R., Moore, W.S., and Bollinger, M.S., 1987. Sedimentation and bioturbation in a salt marsh as revealed by ^{210}Pb , ^{137}Cs , and ^7Be studies. *Limnology and Oceanography*, 32(2): 313-326.
- Silverberg, N., Nguyen, H.V., Delibrias, G., Koide, M., Sundby, B., Yokoyama, Y., and Chesselet, R., 1986. Radionuclide profiles, sedimentation rates and bioturbation in modern sediments of the Laurentian Trough, Gulf of St. Lawrence. *Oceanologica Acta*, 9: 285-290.
- Smith, C.R., Levin, L.A., Hoover, D.J., McMurtry, G., and Gage, J.D., 2000. Variations in bioturbation across the oxygen minimum zone in the northwest Arabian Sea. *Deep-Sea Research II*, 47: 227-257.
- Smith, J.N., and Schafer, C.T., 1999. Sedimentation, bioturbation, and Hg uptake in the sediments of the estuary and Gulf of St. Lawrence. *Limnology and Oceanography*, 44(1): 207-219.
- Smith, J. M. 1970. *Chemical Engineering Kinetics*, 2nd ed., McGraw-Hill, New York, p. 414.
- Stordal, M.C., Johnson, J.W., Guinasso, N.L., Jr., and Schink, D.R., 1985. Quantitative evaluation of bioturbation rates in deep ocean sediment. II. Comparison of rates determined by ^{210}Pb and $^{239,240}\text{Pu}$. *Marine Chemistry*, 17: 99-114.
- Sundby, G., and Westerlund, S.F.G., 1984. The asphyxiation technique: an approach to distinguishing between molecular diffusion and biologically mediated transport at the sediment-water interface. *Limnology and Oceanography*, 29: 675-686.
- Svensson, J.M., Bergman, E., and Andersson, G., 1999. Impact of cyprinid reduction on the benthic macroinvertebrate community and implications for increased nitrogen retention. *Hydrobiologia*, 404: 99-112.
- Swaney, D.P., 1999. Analytical solution of Boudreau's equation for a tracer subject to food-feedback bioturbation. *Limnology and Oceanography*, 44(3): 697-698.

- Sweerts, J-P.R.A., Kelly, C.A., Rudd, J.W.M., Hesslein, R., and Capenberg, T.E., 1991. Similarity of whole-sediment molecular diffusion coefficients in freshwater sediments of low and high porosity. *Limnology and Oceanography*, 36(2): 335-342.
- Taghon, G.L., Nowell, A.R.M., and Jumars, P.A., 1984. Transport and breakdown of fecal pellets: biological and sedimentological consequences. *Limnology and Oceanography*, 29: 64-72.
- Thibodeaux, L. J. 1996. *Environmental Chemodynamics: Movement of Chemicals in Air, Water, and Soil*. John Wiley & Sons, Inc. New York.
- Thibodeaux, L. J. and V. J. Bierman. 2003. The bioturbation-driven chemical release process. *Environmental Science and Technology*. July 1, 2003.
- Thomann, R.V., Merklin, W., and Wright, B., 1993. Modeling cadmium fate at superfund site: impact of bioturbation. *Journal of Environmental Engineering*, 119 (3): 424-442.
- Thoms, S.R., Matisoff, G., McCall, P.L., and Wang, X., 1995. Models for Alteration of Sediments by Benthic Organisms (Project 92-NPS-2). Water Environment Research Foundation, Alexandria, VA.
- Van Rees, K.C.J., Reddy, K.R., and Rao, P.S.C., 1996. Influence of benthic organisms on solute transport in lake sediments. *Hydrobiologia*, 317: 31-40.
- Walbran, P.D., 1996. ^{210}Pb and ^{14}C as indicators of callianassid bioturbation in coral reef sediment. *Journal of Sediment Research*, 66(1): 259-264.
- Wang, X. and Matisoff, G., 1997. Solute transport in sediments by a large freshwater oligochaete, *Branchiura sowerbyi*. *Environmental Science and Technology*, 31(7): 1926-1933.
- WERF. 1995. *Models for Alteration of Sediments by Benthic Organisms*. Project 92-NPS-2. Water Environment Research Foundation.
- Wheatcroft, R.A., and Martin, W.R., 1996. Spatial variation in short-term (^{234}Th) sediment bioturbation intensity along an organic-carbon gradient. *Journal of Marine Research*, 54: 763-792.
- Wheatcroft, R.A., Jumars, P.A., Smith, C.R., and Nowell, A.R.M., 1990. A mechanistic view of the particulate biodiffusion coefficient: step lengths, rest periods and transport direction. *Journal of Marine Research*, 48: 177-207.
- Wheatcroft, R.A., Olmez, I., and Pink, F.X., 1994. Particle bioturbation in Massachusetts Bay: preliminary results using a new deliberate tracer technique. *Journal of Marine Research*, 52: 1129-1150.

- Wheatcroft, R.A., Starczak, V.R., Butman, C.A., 1998. The impact of population abundance on the deposit feeding rate of a cosmopolitan polychaete worm. *Limnology and Oceanography*, 43(8): 1948-1953.
- Widdicombe, S., and Austen, M.C., 1998. Experimental evidence for the role of *Brissopsis lyrifera* (Forbes, 1841) as a critical species in the maintenance of benthic diversity and the modification of sediment chemistry. *Journal of Experimental Marine Biology and Ecology*, 228: 241-255.
- Widdows, J., Brinsley, M.D., Salkeld, P.N., and Elliott, M., 1998. Use of annular flumes to determine the influence of current velocity and bivalves on material flux at the sediment-water interface. *Estuaries*, 21(4A): 552-559.
- Wimbusch, M. 1976. The Physics of the Benthic Boundary Layer in I. N. McCave, Ed., The Benthic Boundary Layer. Plenum Press, New York, pp. 3-10.
- Wright, L.D., Kim, S.-C., and Freidrichs, C.T., 1999. Across-shelf variations in bed roughness, bed stress and sediment suspension on the northern California shelf. *Marine Geology*, 154: 99-115.
- Wright, L.D., Schaffner, L.C., and Maa, J.P.-Y., 1997b. Biological mediation of bottom boundary layer processes and sediment suspension in the lower Chesapeake Bay. *Marine Geology*, 141: 27-50.
- Wool, T. A., R. B. Ambrose, J. L. Martin, E. A. Comer. 2003?. *Water Quality Analysis Simulation Program (WASP), Version 6.0, Draft: User's Manual*. United States Environmental Protection Agency.

APPENDIX F: BIOCHEMICAL TRANSFORMATIONS

F1. INTRODUCTION

In an aquatic environment, an organic compound partitions between dissolved and particulate phases and may be degraded by a number of processes. The biochemical transformations can occur due to chemical processes (such as ionization, precipitation, dissolution, hydrolysis, photolysis, oxidation, and reduction) and biological processes (such as biodegradation, mineralization, and bioconcentration). The breakdown of a compound by the enzyme systems in bacteria is referred as bacterial degradation, microbial transformation, or biodegradation.

F2. THEORETICAL PROCESS UNDERSTANDING

A potentially significant factor governing the long-term fate of contaminants in aquatic systems is the microbially-induced transformations of compounds in bottom sediments. A significant amount of research on the biodegradation of hydrophobic contaminants has been conducted in recent years. Two types of biodegradation are recognized: growth metabolism, and catabolism. Growth metabolism occurs when the organic compound serves as a food source for the bacteria. Adaptation times can vary from 2 to 20 days (Mills et al. 1985). Adaptation may not be required for some chemicals or in chronically exposed environments. Adaptation times may be lengthy in environments with a low initial density of degraders (Mills et al. 1985). For cases where biodegradation is limited by the degrader population size, adaptation is faster for high initial microbial populations and slower for low initial populations. Following adaptation, biodegradation proceeds at fast first-order rates. Cometabolism occurs when the organic compound is not a food source for the bacteria. Adaptation is seldom necessary in cometabolism, and the transformation rates are slow compared with growth metabolism.

For environmental transformations, redox reactions are particularly important. Surface water sediments behave as a highly reducing environment where oxic conditions and reduction potential quickly diminish with depth. In coastal sediments, particularly in estuarine and contaminated harbor sediments, oxygen is rapidly depleted due to the abundance of organic matter that is deposited from both land-driven runoff and autochthonous sources, which leads to high biochemical oxygen demand. Thus, alternate electron acceptors including iron (III), manganese (II) and bicarbonate, nitrate, and sulfate are utilized in the degradation of organic compounds in all but the very top layer (~0.5 cm) of sediment. Of these, sulfate is the least energetically favored (Libes 1992), but is the most abundant acceptor in marine sediments, being derived from sulfate in seawater. Because of the high sulfate concentrations in saline environments (20-30 mM), sulfate-reduction is often the dominant process in carbon metabolism in marine sediments (Capone and Kiene 1988), although fermentation (Ollivier et al. 1994), denitrification (Bonin et al. 1994; Nowicki 1994), iron reduction (Lovley 1991), and methanogenesis (de Angelis and Scranton 1993; Ollivier et al. 1994) have been demonstrated. These conditions are conducive to reduction reactions such as dechlorination of PCBs and dioxins (Adriaens et al. 1999), and aromatic ring destabilization of PAHs. Natural dechlorination rates for these compounds range from one chlorine removed every seven to ten years, depending on the rates of carbon turnover in the sediments (10^2 - 10^{-2} mmole $\text{CH}_2\text{O}/\text{L}/\text{y}$) (Murphy and Schramke, 1998).

Hydrolysis is the degradation of a compound through reaction with water. Since hydrolysis can be mediated by enzymes (enzymatic hydrolysis), in natural waters hydrolysis may also be a biochemical degradation process. During hydrolysis, both an organic compound molecule and a water molecule are split, and the two water molecule fragments (H^+ and OH^-) join to the two pollutant fragments to form new chemicals. The hydrolysis products may be less toxic than the original compound. In general, the hydrolysis is a second-order reaction because of dependence on the molar concentration of $[\text{H}^+]$, $[\text{OH}^-]$, or water mediator. A chemical compound can undergo biochemical transformations depending on contaminant properties, the conditions and the environment. For example, the reactivity of halogenated aromatic compounds (also known as aryl halides) in sediments is a function of intrinsic chemical and thermodynamic properties of the compound, biochemical properties of the sedimentary environment and the microbial metabolic

diversity and interactions. Together, these biochemical factors determine the predominant fate reactions, rates, pathways and products.

The behavior and congener pattern of PCBs in river systems can be modified by bacteria through biochemical transformations. In general, those congeners with fewer chlorine atoms (1-4 Cl) PCBs tend to be more readily biotransformed under aerobic conditions, and the higher chlorinated congeners are more readily biotransformed under anaerobic conditions. However, microbially mediated anaerobic dehalogenation is required to promote degradation of higher chlorinated PCBs. Studies on microbial degradation in sediments (Brown et al. 1987, David et al. 1994) have elucidated a shift in the sediments from higher chlorinated congeners to lower chlorinated congeners which has been attributed to anaerobic dechlorination (Brown et al. 1987; Weigel and Wu 2000). Rhee et al. (1999) also documented dechlorination of PCBs in sediments, but concentrations had to be high, and the responsible bacteria were not identified.

Dehalogenation of dioxins and PCBs by *dehalococcoides ethanogenes* strain 195, a halorespiring bacterium, has been demonstrated in the laboratory (Fennell et al. 2004). Ishiguro et al. (2000) investigated the aerobic degradation of dibenzofuran (DBF) and dioxins by a *Pseudomonas aeruginosa* and a *Xanthomonas maltophilia* strain. *Ps. Aeruginosa*, which had a high growth rate with DBF as a C source, and showed high growth rates in the presence of such dioxins as dibenzo-p-dioxin. Under the same conditions, growth rates were different for different compounds. The results suggested that there is a correlation between growth and the ability to biodegrade dioxins. Several researchers studied PCB dechlorination in freshwater sediments (Abramowicz et al. 1993; Alder et al. 1993; Bedard and Quensen 1995; Brown et al. 1987a; Quensen et al. 1990; Sokol et al. 1994), and others studied biotransformation potential in marine and estuarine sediments under anaerobic conditions (Brown and Wagner 1990; Lake et al. 1991; Ofjord et al. 1994; Kuo et al. 1999). Various reviews have been written on PCB biodegradation (Brown et al. 1987; Abramowicz 1990; Boyle et al. 1992; Higson 1992; Mohn and Tiedje 1992; Haluska et al. 1993; Tiedje et al. 1993).

Lesser chlorinated compounds have been shown to migrate out of the sediments into the water column or upper sediment layers (Gevao et al 1997, Lohmann et al. 2000; Fu et al. 2001). The establishment of the terminal electron-accepting processes (TEAPs) tends to be limited by the availability of hydrogen from fermentation reactions (Kerner 1993, Postma and Jakobsen 1996). More reducing TEAP conditions are conducive to reductive dehalogenation reactions of aryl halides as they provide a competitive environment (more negative reduction potential) than that of halogenated compound.

Processes which are poorly understood or incompletely characterized include the following:

- The growth kinetics of degrading bacteria;
- The effects of naturally binding organic complexing agents on transformation rates; and
- Congener-specific differences in half-lives of chemical mixtures like PCBs.

F2.1 IMPACTS OF BIOCHEMICAL PROCESSES

The long-term biochemical transformation of contaminants is important to consider for evaluating the long-term performance of in-situ sediment remediation technologies. Microbial activities can impact contaminant mobility in both positive and negative ways (Apitz 2002a), by influencing chemical sorption, by causing the ebullition of various gases, and by chemically

altering the contaminants themselves (Adriaens et al. 1999, 2003). Biochemical transformations can detoxify and mineralize toxins and diffuse potential toxins, but they can also activate potential toxins. Rhee et al. (1993) documented significant dechlorination of PCBs within the buried sediments in the Thompson Island Pool in the Hudson River, NY, resulting in a shift in the original congener patterns. In most cases, dechlorination of PCBs renders them less toxic. These transformations depend on the contaminant and on the pathways. Ebullition of gases can destabilize the sediment or cap matrix, while gases such as methane and carbon dioxide can induce desorption of organic contaminants into the (organic) gas and facilitate convective and diffusive transport (Palermo et al. 2002). The formation and migration of biogenic gas in marine sediments, its effect on sediment bed morphology and (in)stability, and emissions into the water column and atmosphere have been well documented (Claypool and Kvenvolden 1983; van Weering et al. 1997, Casper et al. 2000).

F2.2 RATES OF BIOCHEMICAL PROCESSES

The haloaromatic compounds have been shown to dehalogenate by microbial methanogenic bacteria (Sulfito et al. 1983; Brown et al. 1984; Tiedge and Quenson 1988). However, the reductive dehalogenation processes mediated by bacteria have been observed to be specific to certain PCBs. For example, monochlorinated biphenyls have been degraded by certain microorganisms, leaving the higher chlorinated congeners untouched (Shiaris and Saylor 1982). PCB congeners with the chlorine on the ortho carbon (that ring position closet to the bond connecting the two rings) tend to be more difficult to biotransform than those with the chlorine atom in the meta or para positions, the one farther away from the connecting bond. Furukawa et al. (1978) reported the rates of biodegradation of 31 chlorobiphenyl congeners by two species of microbes. Tetra- and penta-PCBs were shown to have very low rates of biodegradation. 2,4,4'- and 2,4',5-tri PCBs degraded between 6 and 25 times faster than the 2,2',5-tri PCBs. There remains uncertainty in establishing rates of processes that are chemical specific and highly site dependent. Davis (2004) compared PAH and PCB loss rates in San Francisco Estuary found that the PAH loss rate was considerably more rapid. The time required for half the original mass of PCB 118 to be loss was estimated at about 20 years, more than threefold slower than the slowest PAHs.

In many modeling studies, such as in the Lake Michigan Mass Balance Study (LMMB) and the Hudson River study, the PCB biodegradation process is neglected as the concentrations of PCBs were below the threshold level which causes reductive dechlorination (Kim and Rhee 1997; Cho et al. 2002). The degradation rates for PCBs and dioxins are low as reported in the studies by Gobas et al. (1995) and Davis (2003 and 2004). In literature, these rates are used as representative of one particular degradation pathway or a combination of degradation processes. The degradation rate could vary considerably depending on the binding strength and the nature of particulate material that can affect bioavailability of hydrophobic contaminants. The half-lives of contaminants in a system are governed by the partitioning of the contaminants in the aqueous phase and the dissolved phase. In general, hydrophobic contaminants bind strongly to sediment solids.

Based on representative rates from the literature, illustrative degradation half-lives were calculated for the dissolved phase by using $T_{1/2} = \ln 2 / (k F_d)$ and $T_{1/2} = \ln 2 / k$ for the particulate phase of the compound, where F_d is the dissolved fraction and k is the biochemical degradation rate. The estimated half-lives for the dissolved PCBs are thousands of years, while for

particulate phase they are about 55.8 years. These were calculated based on a degradation rate of 3.4×10^{-5} (1/day). The half-life estimates were conducted with particle densities of 2.0, 2.25, 2.5 g/cm³, porosity of 0.8, 0.9, 0.95 ($V_{\text{porewater}}/V_T$), sediment organic carbon content (f_{oc}) = 0.01, 0.025, 0.05 (g_{oc}/g_{dw}), and log (organic carbon partition coefficient) (Log (K_{oc})) = 4.5, 5.5, 6.5.

F3. ADEQUACY OF TYPICAL SITE-SPECIFIC INFORMATION

Integration of fate and transport processes for organic compounds in computer models requires reasonably accurate representation of the chemical and biological processes. These processes are described by rate equations, which may be quantified by first-order constants or by second-order chemical specific constants and environment-specific parameters that may vary in space and time. The range and significance of these processes are influenced by site-specific information. Extensive site-specific data gathering is required to adequately represent the processes occurring in a system to understand the fate and transport of chemicals in sediments. High-resolution sampling of both parent compounds and potential daughter products with measurements over time is essential for understanding the transformation processes. Rarely are data available in sufficient spatial and temporal resolution to represent chemical process rates in modeling frameworks. Moreover, PCB congener half-lives in aquatic environment are not well quantified. Therefore, the degradation rates used for modeling PCBs do not accurately represent all congeners.

All sediments exhibit significant variability in their characteristics, with vast changes in the sediment environment over vertical distances of a few millimeters and over horizontal distances of meters or less (Reible and Thibodeaux 1999). The assessment of chemical transformations over long time periods is especially difficult in the face of the composited samples that are normally collected. Moreover, the transformation processes in near-surface solids tend to be faster than in deep sediments. Aerobic biodegradation processes are generally faster than anaerobic processes, and degradation rates depend on the presence of sufficient nutrients and substrate components. Generally, enough information is not available to characterize all processes at fine spatial scales.

The biochemical properties and conditions (i.e. availability of electron acceptors and donors, organic matter composition, salinity, mineral compositions, co-contaminants, microbial consortia) are highly heterogeneous in space and variable in time, leading to variations in the fate processes of contaminants (e.g., transformation, exchange of contaminants between the sediment phase and the water column). Moreover, each site is different and physical environments of each site are highly variable. For example, sediment texture, water depth and flow velocities, temperature effects and climatographic effects might be important in combination with chemical and biological environment to understand the dynamics of chemical transformations.

In toxic chemical models, the representation of processes, such as biodegradation, is generally simplistic as described below. Though biochemical transformation is considered as a remedial option in the contaminated sites, complete information is rarely known regarding the nature of reactions due to complex characteristics of organic chemicals and the environmental conditions.

F4. PROCESS REPRESENTATION IN LEADING FATE AND TRANSPORT MODELS:

F4.1 WASP

TOXI5, toxic chemical model of the WASP model (version 5), simulates the transport and transformation of chemicals and one to three types of particulate material (solid classes). Transformation processes included in the TOXI5 are biodegradation, hydrolysis, photolysis, and oxidation (Ambrose et al.1993). The model does not include representations of reduction and precipitation-dissolution reactions. Sorption is treated as an equilibrium reaction. The simplified transformation processes are described by first-order rate equations. There are some limitations to these assumptions: first, these assumptions are valid when chemical concentrations are near trace levels, i.e., below half the solubility or 10^{-5} molar. At higher concentrations, the assumptions of linear partitioning and transformation begin to break down. Chemical density may become important, particularly near the source, such as in a spill. Large concentrations can affect key environmental characteristics, such as pH or bacterial populations, thus altering transformation rates.

TOXI5 allows users to specify simple first-order reaction rates for the transformation reactions of each of the chemicals simulated. It provides two options for including chemical transformations.

F4.1.1 Option 1: Total lumped first order decay

First order rates may be applied to the total chemical and varied by segment. Because the rate is representative of all processes (lumped decay reactions), chemical transformations to daughter products cannot be simulated.

$$\frac{\partial C_{ij}}{\partial t} = K_{ij} C_{ij}$$

where:

K_{ij} = lumped first order decay constant (day^{-1}) for chemical i in j segment

C_{ij} = concentration of total chemical i in segment j

F4.1.2 Option 2: Individual first order transformation

This option allows the user to input a global first-order reaction rate constant separately for each of the following processes: volatilization, water column biodegradation, benthic degradation, alkaline hydrolysis, neutral hydrolysis, acid hydrolysis, oxidation, and photolysis. The total reaction rate is then based on the sum of each of the individual reactions as given by:

$$\frac{\partial C_{ij}}{\partial t} = \sum_{k=1}^N K_{ki} C_{ij}$$

where:

K_{ki} = first order transformation constants (day^{-1}) for reaction k of chemical i .

The user may input half-lives rather than first-order decay rate constants. If half-lives are provided for the transformation reactions, they will be converted internally to first order rate constants and used as above:

$$K_{ki} = 0.693/T_{HKi}$$

where:

T_{HKi} = half-life of reaction k for chemical i , days.

Transformation and daughter products. The chemicals that may be simulated by TOXI5 may be independent, or may be linked with reaction yields, such as a parent compound-daughter product sequence. Linked transformations may be implemented by simulating two or three chemicals and by specifying appropriate yield coefficients for each process:

$$\begin{aligned} S_{kc1} &= \sum_c \sum_k K_{kc} C_c Y_{kc1}, & c=2,3 \\ S_{kc2} &= \sum_c \sum_k K_{kc} C_c Y_{kc2}, & c=1,3 \\ S_{kc3} &= \sum_c \sum_k K_{kc} C_c Y_{kc3}, & c=1,2 \end{aligned}$$

where:

S_{kci} = production of chemical “ i ” from chemical “ c ” undergoing reaction “ k ”, mg_i/L-day

K_{kc} = effective rate coefficient for chemical “ c ” reaction “ k ”, day⁻¹

Y_{kci} = yield coefficients for production of chemical “ i ” from chemical “ c ” undergoing reaction “ k ”, mg_i/mg_c

Biodegradation Reactions. In TOXI5, first order biodegradation rate constants or half lives for the water column and the benthos may be specified. If these rate constants have been measured under similar conditions, this first-order approach is likely to be as accurate as more complicated approaches. If first-order rates are unavailable, or if they must be extrapolated to different bacterial conditions, then the second-order approach may be used. It is assumed that bacterial populations are unaffected by the presence of the compound at low concentrations. Second-order kinetics for dissolved, DOC-sorbed, and sediment-sorbed chemical are considered:

$$\begin{aligned} K_{BW} &= P_{bac}(t) \sum_i \sum_j K_{Bij} f_{ij}, & j=1,2 \\ K_{BS} &= P_{bac}(t) \sum_i \sum_j K_{Bij} f_{ij}, & j=3 \end{aligned}$$

where:

K_{BW} = net biodegradation rate constant in water, day⁻¹

K_{BS} = net biodegradation rate constant in sediment, day⁻¹

K_{Bij} = second order biodegradation rate constant for species i , phase j , ml/cell-day

$P_{bac}(t)$ = active bacterial population density in segment, cell/ml

f_{ij} = fraction of chemical as species i , phase j .

In TOXI5, the biodegradation rate may be adjusted by temperature as:

$$K_{Bij}(T) = K_{Bij} Q_{Tij}^{(T-20)/10}$$

where:

Q_{Tij} = “Q-10” temperature correction factor for biodegradation of species i , phase j .

T = ambient temperature in segment, °C.

The temperature correction factors represent the increases in the biodegradation rate constants resulting from a 10°C temperature increase. Values in the range of 1.5 to 2 are common.

F4.2 AQUATOX

Microbial degradation is modeled by entering a maximum biodegradation rate for a particular organic toxicant, which is subsequently reduced to account for suboptimal temperature, pH, and dissolved oxygen. For those organic chemicals that undergo hydrolysis, neutral, acid-, and base-catalyzed reaction rates are entered into AQUATOX as applicable.

The process of biodegradation of pollutants, whether they are dissolved in the water column or adsorbed to organic detritus in the water column or sediments, is modeled using the same equations as for decomposition of detritus, substituting the pollutant and its degradation parameters for detritus:

$$MicrobialDegrn = KMDegrn_{phase} \cdot DOCorrection \cdot TCorr \cdot pHCorr \cdot Toxicant_{phase}$$

where

$MicrobialDegrn$ = loss due to microbial degradation ($g/m^3 \cdot d$)

$KMDegrn$ = maximum degradation rate, either in water column or sediments (1/day)

$DOCorrection$ = effect of anaerobic conditions (unitless)

$TCorr$ = effect of suboptimal temperature (unitless)

$pHCorr$ = effect of suboptimal pH (unitless)

Toxicant = Concentration of organic toxicant (g/m^3)

Microbial degradation proceeds more quickly if the material is associated with surficial sediments rather than suspended in the water column (Godshalk and Barko 1985); thus, in calculating the loss due to microbial degradation in the dissolved phase, the maximum degradation rate is set arbitrarily to 25 percent of the maximum degradation rate in the sediments. The model assumes that reported maximum microbial degradation rates are for suspended slurry or wet soil samples; if the reported degradation value is from a flask study without additional organic matter, then the parameter value that is entered should be four times that reported.

Hydrolysis:

Neutral and acid- and base-catalyzed hydrolysis are modeled using the approach of Mabey and Mill (1978) in which an overall pseudo-first-order rate constant is computed for a given pH, adjusted for the ambient temperature of water:

$$Hydrolysis = KHyd \cdot Toxicant_{phase}$$

where

$$K_{Hyd} = (K_{AcidExp} + K_{BaseExp} + K_{Uncat}) \cdot Arrhen$$

and where:

K_{Hyd} = overall pseudo-first-order rate constant for a given pH and temperature (1/d)

$K_{AcidExp}$ = pseudo-first-order acid-catalyzed rate constant for a given pH (1/d)

$K_{BaseExp}$ = pseudo-first-order base-catalyzed rate constant for a given pH (1/d)

K_{Uncat} = the measured first-order reaction rate at pH 7 (1/d)

$Arrhen$ = temperature adjustment (unitless).

F4.3 EFDC

EFDC allows first order water column and sediment bed decay of toxicant variables at rates in units of 1/sec.

F5. PREDICTIVE UNCERTAINTIES

The degradation rate is an important parameter for understanding the fate of contaminants in water and sediments, and is poorly understood. Degradation rates for different PCB congeners can be expected to vary considerably, in inverse proportion to the degree of chlorination. Often models that have been used for specifying the biodegradation processes contain simplifications and site-specific assumptions that facilitate their application and interpretation with limited data. Below are potential sources that can cause uncertainty in determining the fate of contaminants in sediments:

- The growth kinetics of bacterial populations degrading the chemicals are not well-understood;
- The presence of competing substrates and of other bacteria, the toxicity of the chemical to the degrading bacteria, and the possibilities of adaptation to the chemical and co-metabolism make quantification of changes in the population difficult;
- Often, measured first order biodegradation rate constants from other aquatic systems are used directly in other systems;
- Toxic chemical models assume a constant biological activity rather than modeling the bacteria directly;
- Natural organic complexing agents (such as humic and fulvic acids) found in sediments can bind contaminants. There remains uncertainty in determining binding of contaminants and chemicals undergoing transformations;
- The transformations of chemicals can be influenced by environmental factors other than temperature. Bacterial population size can limit degradation rates. In addition, nutrient limitation can be significant in oligotrophic environments. Low concentrations of dissolved oxygen can also cause reductions in biodegradation rates. This effect is generally not simulated in models such as WASP5. The rates start to decrease for DO concentrations below 1 mg/L. When anoxic conditions prevail, most organic substances are biodegraded more slowly. Because biodegradation reactions are generally more difficult to predict than physical and chemical reactions, site-specific calibration becomes more important.
- PCB congener half-lives are not well quantified: the modeling studies use one value for degradation of PCBs that may be applicable to a group of congeners but not to all.
- The scale and matrix complexity at which data are collected may not be fully representative.

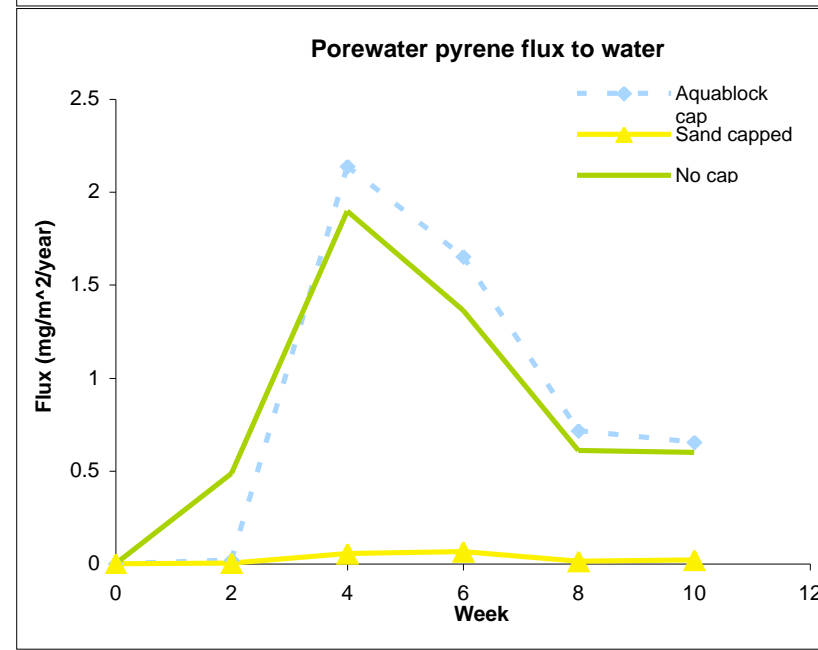
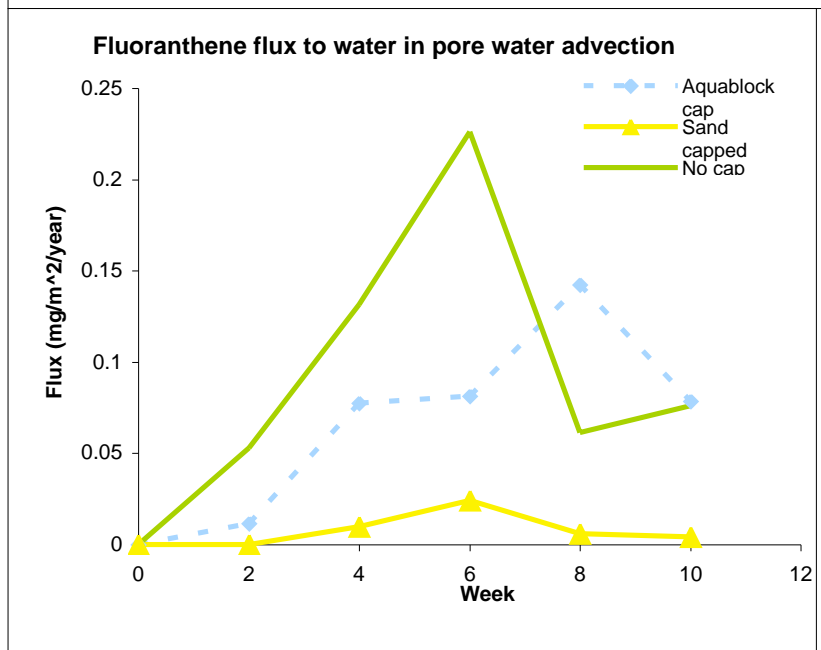
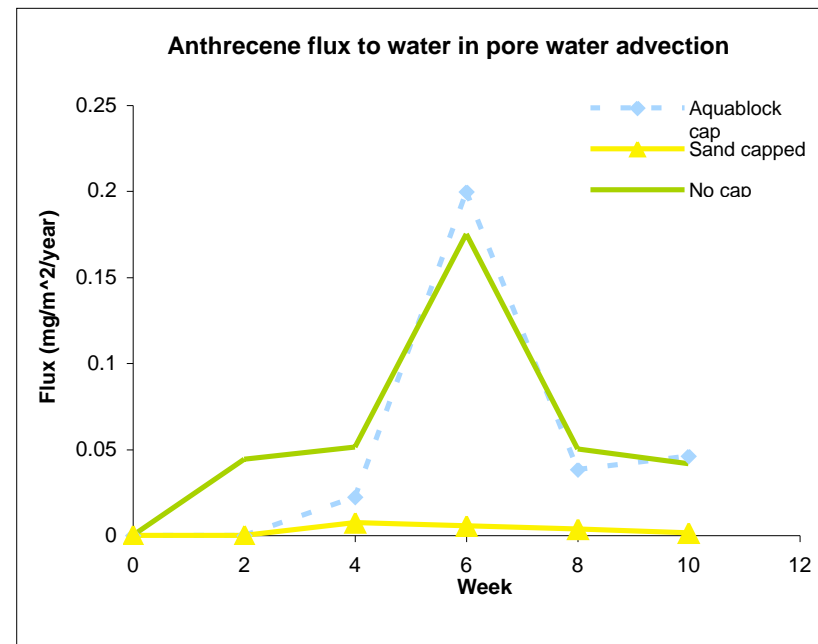
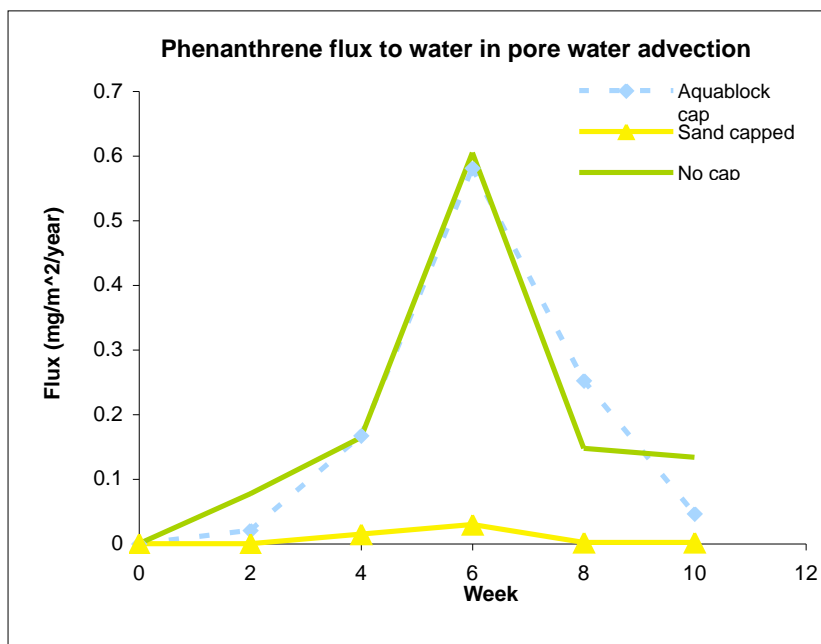
Given the extremely wide range of degradation rates, there remains uncertainty in predicting the fate of contaminants in various systems. Care must be taken in using laboratory-measured rates in field situations. For example, Delos et al. (1984) commented that the basic problem is the extrapolation of laboratory hydrolysis rate (usually in distilled water) to environmental conditions with associated potential complex interactions with organic chemicals and metals and a natural biota. To confidently forecast the recovery of any ecosystem from contamination, understanding of the biodegradation processes and the environment is essential. Research is required on degradation rates for various chemicals and seasonal variations of those rates, the influence of horizontal heterogeneity, the influence and type of contaminants and other environmental factors on the diversity and functioning of *in-situ* microbial communities.

F6. REFERENCES

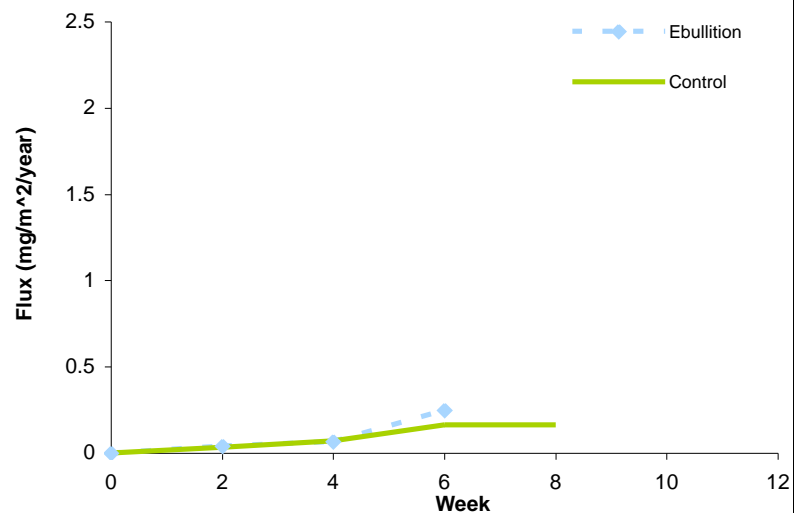
- Abramowicz, D.A. 1990. Aerobic and anaerobic biodegradation of PCBs: a review. *Crit. Rev. Biotechnol.* 10(3):241-251.
- Abramowicz, D.A., and Brennan, M.J. 1991. Anaerobic and aerobic biodegradation of endogenous PCBs. In Jafvert C.T., and Rogers J.E. (eds): *Biological remediation of contaminated sediment with emphasis on Great Lakes*. Environment Research Laboratory, Office of research and development, U.S. EPA, Athens, GA. EPA/600/9-91/001, pp. 78-86.
- Adriaens, P. A.L. Barkovskii, and I.D. Albrecht. 1999. Fate of Chlorinated Aromatic Compounds in Soils and Sediments. In D.C. Adriano, J.-M. Bollag, W.T. Frankenberger, and R. Sims (Eds), *Bioremediation of Contaminated Soils*, Soil Science Society of America/American Society of Agronomy Monograph, Soil Science Society of America Press, Madison WI. pp. 175-212.
- Adriaens, P., Gruden, C., and M.L. McCormick. (2003). Biogeochemistry of Organohalides. In: *Treatise of Geochemistry*, Kluwer, The Netherlands, In Press.
- Alder, A.C., Haggbloom, M.M., Oppenheimer, S.R., and Young, L.Y. 1993. Reductive dechlorination of polychlorinated biphenyls in anaerobic sediments. *Environ. Sci. Technol.* 27:530-538.
- Ambrose, R.B., Wool, T.A., Martin, J.L. September 1993. The Water Quality Analysis Simulation Program, WASP5, Part A: Model Documentation. Environmental Research Laboratory. Athens, GA.
- Apitz, S.E., Davis, J.W., Finkelstein, K., Hohreiter, D.L., Hoke, R., Jensen, R.H., Jersak, J., Kirtay, V.J., Mack, E.E., Magar, V., Moore, D., Reible, D., Stahl, R. (2002) *Critical Issues for Contaminated Sediment Management*, MESO-02-TM-01. <http://meso.spawar.navy.mil/docs/MESO-02-TM-01.pdf>
- Bedard, D.L., and Quensen III, J.F. 1995. Microbial reductive dechlorination of polychlorinated biphenyls. P. 127-216. In L.Y. Young and C. Cerniglia (eds). *Microbial transformation and degradation of toxic organic chemicals*. Wiley –Liss Division, John Wiley and Sons, Inc., NY.
- Bonin, P.; Ranaivoson, E.R.; Raymond, N.; Chalamet, A.; Bertrand, J.C. *Mar. Pol. Bull.* 1994, 28, 89-95.
- Boyle, A.W., Silvén, C.J., Hassett, J.P., Nakas, J.P., and Tenenbaum, S.W. 1992. Bacterial PCB biodegradation. *Biodegradation* 3(2/3):285-298.
- Brown, J.F., Wagner, R.E., Bedard, D.L., Brennan, M.J., Carnahan, J.C., May, R.J., and Tofflemire, T-J. 1984. PCB transformations in upper Hudson river sediments. *Northeast Env. Sci.* 3:167.
- Brown, J.F. Jr., Bedard, D.L., Brennan, M.J., Carnahan, J.C., Feng, H., and Wagner, R.E. 1987. Polychlorinated biphenyl dechlorination in aquatic sediments. *Science* 236:709-712.
- Brown, J.F. Jr., Wagner, R.E., Feng, H., Bedard, D.L., Brennan, M.J., Carnahan, J.C., and May, R.J. 1987a. Environmental dechlorination of PCBs. *Environ. Toxicol. Chem.* 6(8):579-594.
- Brown, J.F., Jr., and Wagner, R.E. 1990. PCB movement, dechlorination, and detoxification in the Acushnet estuarine. *Environ. Toxicol. Chem.* 9:1215-1233.
- Capone, D.G.; Kiene, R.P. *Limnology and Oceanography*. 1988, 33, 725-749.
- Casper, P., S.C. Maberly, G.H. Hall, and B.J. Finlay. 2000. Fluxes of methane and carbon dioxide from a small productive lake to the atmosphere. *Biogeochem.* 49: 1-19.
- Cho, Y.-C., Sokol, R.C., and Rhee, G-Y. 2002. Kinetics of polychlorinated biphenyl dechlorination by Hudson River, New York, USA, Sediment microorganisms. *Environ. Toxicol. And Chemistry*, 21(4):715-719.
- Claypool, G.E. and K.A. Kvenvolden. 1983. Methane and other hydrocarbon gases in marine sediments. *Ann. Rev. Earth Planet. Sci.* 11: 299-327.
- Davis, J. A. 2003. The long term fate of PCBs in San Francisco Bay. San Francisco Estuary Institute, Oakland, CA, 47 pp.

- Fennell, D.E., Nijenhuis, I., Wilson, S.F., Zinder, S.H., and Haggblom, M.M. 2004. Dehalococcoides ethanogenes Strain 195 reductively dechlorinates diverse chlorinated aromatic pollutants. Environ. Sci. Technol. 38(7):2075-2081.
- Fu, Q.S., A.L. Barkovskii, and P. Adriaens. 2001. Dioxin Cycling in Aquatic Sediments: The Passaic River Estuary. *Chemosphere*, In Press.
- Furukawa, K., Tomizuka, N., and Kamibayashi, A. 1978. Effect of chlorine substitution on the biodegradability of polychlorinated biphenyls. Appl. Environ. Microbiol. 35: 223.
- de Angelis, M.A.; Scranton, M.I. Global. Biogeochem. Cycles 1993, 7, 509-523.
- Delos, C.G. et al. 1984. Technical guidance manual for performing wasteload allocations, Book II. Streams and Rivers, chapter 3, Toxic substances. USEPA, Washington D.C., EPA-440/4-84-022.
- Gevao B, HamiltonTaylor T, Murdoch C, et al. (1997) Depositional time trends and remobilization of PCBs in lake sediments. Environmental Science and Technology 31, 3274-3280.
- Gobas, F.A.P.C., Z'Graggen, M.N., and Xhang, X. 1995. Time response of the Lake Ontario ecosystem to virtual elimination of PCBs. Environ. Sci. Technol. 29: 2038-2046.
- Godshalk, G.L., and Barko, J.W. 1985. Chapter 4, Vegetative succession and decomposition in reservoirs. In D. Gunnison (ed.), Microbial Processes in Reservoirs, Dordrecht:Dr. W. Junk Publishers, pp. 59-77.
- Haluska, L., Balaz, S., and Dercova, K. 1993. Microbial degradation of polychlorinated-biphenyls. Chemike Listy 87(10):697-708.
- Higson, F.K. 1992. Microbial degradation of biphenyl and its derivatives. Adv. Appl. Microbiol. 37:135-164.
- Ishiguro, T.O.Y., Nakayama, S. et al. 2000. Biodegradation of dibenzofuran and dioxins by *Pseudomonas aeruginosa* and *Xanthomonas maltophilia*. Environ. Technol. 21:1309-1316.
- Kerner, M. 1993. Coupling of microbial fermentation and respiration processes in an intertidal mudflat of the Elbe Estuary. Chemosphere 38:314-330.
- Kim, J. and Rhee, G. 1997. Population dynamics of polychlorinated biphenyl-dechlorinating microorganisms in contaminated sediments. Appl. Environ. Microbio 63(5), 1771-1776.
- Kuo, C-E., Liu, S-M., and Liu, C. 1999. Biodegradation of coplanar polychlorinated biphenyls by anaerobic microorganisms from estuarine sediments. Chemosphere 39(9):1445-1458.
- Lake, J.L., Pruett, R.J., and Osterman, F.A. 1991. Dechlorination of polychlorinated biphenyls in sediments of New Bedford Harbor, p. 173-197. In R.A. Baker (ed), Organic substances and sediments in water. Lewis Publishers, Inc. Chelsea, MI.
- Lake, J.L., Pruett, R.J., and Osterman, F.A. 1991. An examination of dechlorination processes and pathways in New Bedford Harbor sediments. Mar. Environ. Res. 33:31-47.
- Libes, S.M. 1992. Marine biogeochemistry. John Wiley and Sons, Inc., New York, Chap. 12.
- Lohmann, R., Nelson, E., Eisenreich, S.J., and Jones, K. 2000. Evidence for dynamic air-water exchange of PCDD/Fs: A study in the Raritan Bay/Hudson River Estuary. Environ. Sci. Technol. 34:3086-3093.
- Lovley, D.R., Klug, M. *Applied Environmental Microbiology*. 1982, 43, 552-560.
- Mabey, W., and Mill, T. 1978. Critical review of hydrolysis of organic compounds in water under environmental conditions. J. Phys. Chem. Ref. Data., 7:383-415.
- Mills, W.B., Porcella, D.B., Unga, M.J. Gherini, S.A., Summers, K.V., Mok L., Rupp, G.L., Bowie, G.L., and Haith, D.A. 1985. Water Quality Assessment: A screening procedure for toxic and conventional pollutants, Parts 1 and 2. U.S. Environmental Protection Agency, Athens, GA. EPA-600/6-85-002a and b.

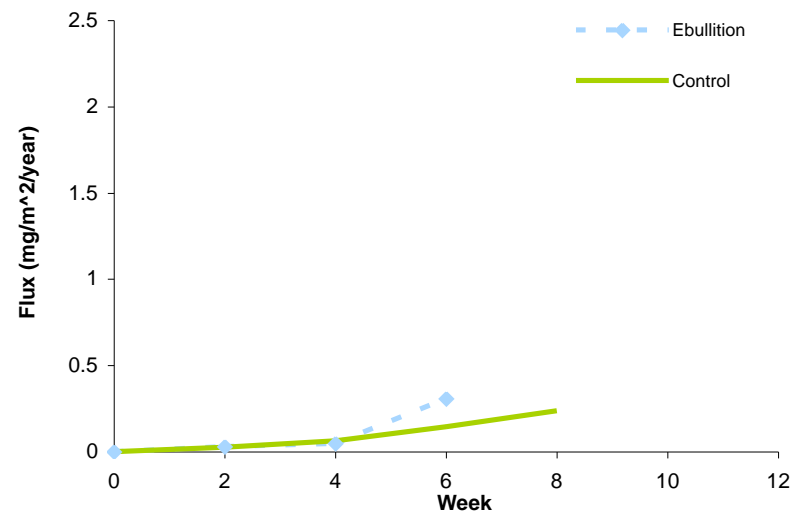
- Mohn, W.W. and Tiedje, J.M. 1992. Microbial reductive dehalogenation. *Microbiol. Rev.* 56(3):482-507.
- Nowicki, B.L. *Est. Coast Shelf Sci.* 1994, 38, 137-156.
- Ofjord, G.D., Puhakka, J.A., and Ferguson, J.F. 1994. Reductive dechlorination of Aroclor 1254 by marine sediment cultures. *Environ. Sci. Technol.* 28:2286-2294.
- Ollivier, B.; Caumette, P.; Garcia, J.-L.; Mah, R.A. (1994) *Microbiological Reviews*, 58, 27-38.
- Palermo, M.R., Thompson, T.A., Swed, F. (2002) *White Paper No. 6B – Is-Situ capping as a remedy component for the lower Fox River*. Response to a document by the Johnson Company: Ecosystem-based rehabilitation plan – An integrated plan for habitat enhancement and expedited exposure reduction in the lower Fox River and Green Bay. December 2002.
- Potsma, D., and Jakobsen, R. 1996. Redox zonation: equilibrium constraints on the Fe(III)/SO₄²⁻ reduction interface. *Geochimica et Cosmochimica Acta* 60:3169-3175.
- Quenson, J.T. and Tiedje, J.M. 1998. Reductive dechlorination of polychlorinated biphenyls by anaerobic microorganisms from sediments. *Science* 247:752.
- Quenson, J.F. III, Boyd, S.A., and Tiedje, J.M. 1990. Dechlorination of four commercial polychlorinated biphenyl mixtures (Aroclors) by anaerobic microorganisms from sediments. *Appl. Environ. Microbiol.* 56:2360-2369.
- Reible, D.D., and Thibodeaux, L.J. 1999. Using natural processes to define exposure from sediments.
- Rhee, G.Y., Sokol, R.C., Bush, B., and Bethony, C.M. 1993. Long-term study of the anaerobic dechlorination of Aroclor 1254 with and without biphenyl enrichment. *Environ. Sci. Technol.* 27:714-719.
- Shiari, M.P. and Saylor, G.S. 1982 Biotransformation of PCBs by natural assemblages for freshwater microorganisms. *Environ. Sci. Technol.* 16:367.
- Sokol, R.C., Kwon, O.S., Bethoney, C.M., and Rhee, G.Y. 1994. Reductive dechlorination of polychlorinated biphenyls in St. Lawrence River sediments and variations in dechlorination characteristics. *Environ. Sci. Technol.* 28:2054-2064.
- Sulfit, J.M., Robinson, J.A., and Tiedje, J.M. 1983. *Appl. Environ. Microbiol.* 45:1466.
- Reible and Thibodeaux 1999
- Tiedje, J.M., Quenson, J.F. III, Chee-Sanford, J., Schimel, J.P. and Boyd, S.A. 1993. Microbial reductive dechlorination of PCBs. *Biodegradation* 4(4):231-240.
- Van Weering, T.C.E., G.T. Klaver, and R.A. Prins. 1997. Gas in marine sediments – and introduction. *Marine Geology* 137: 1-3.
- Wiegel, J., and Wu, Q. 2000. Microbial reductive dehalogenation of polychlorinated biphenyls. *FEMS Microbiology Ecology* 32(1):1-15.



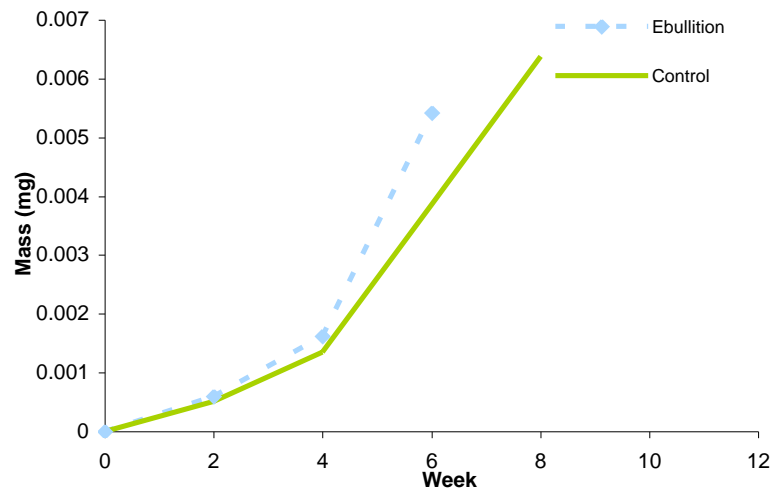
Phenanthrene flux to water



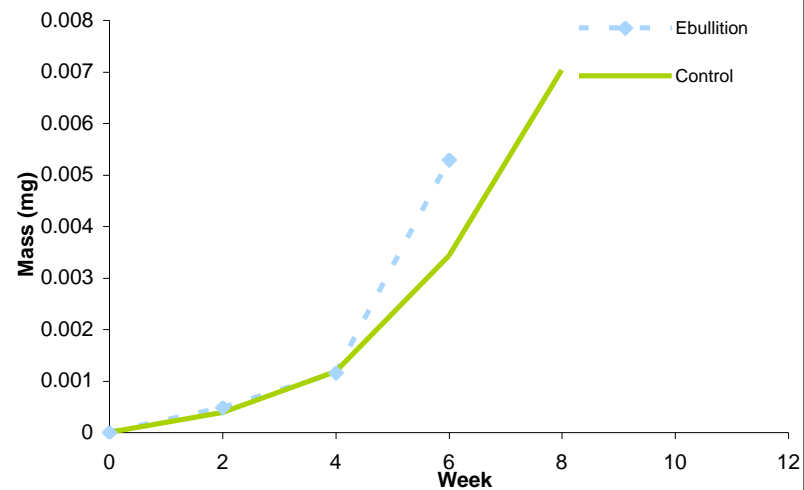
Anthracene flux to water



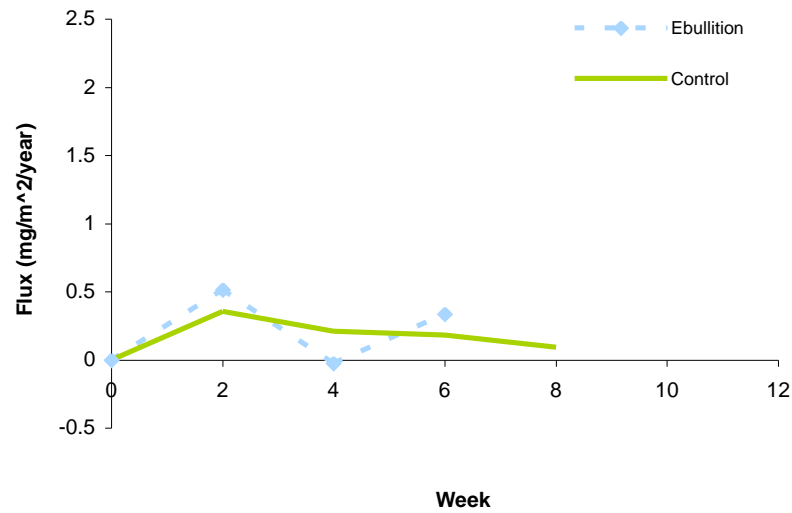
Cumulative phenanthrene mass in SPMD



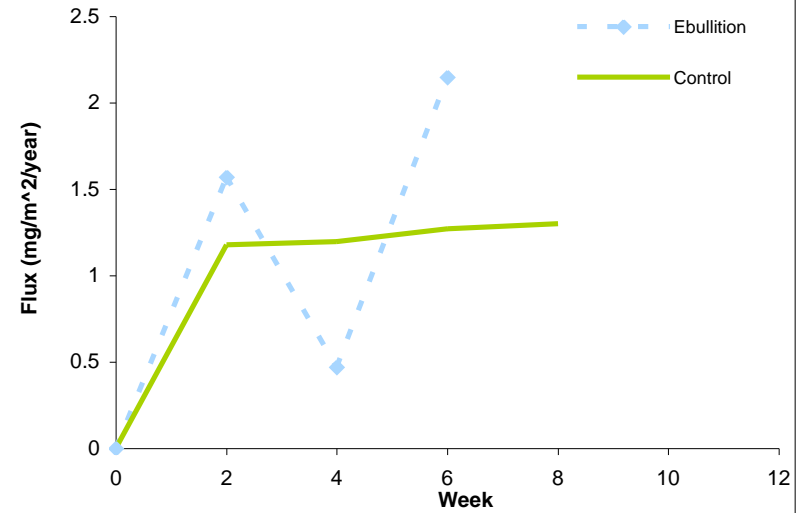
Cumulative Anthracene mass in SPMD



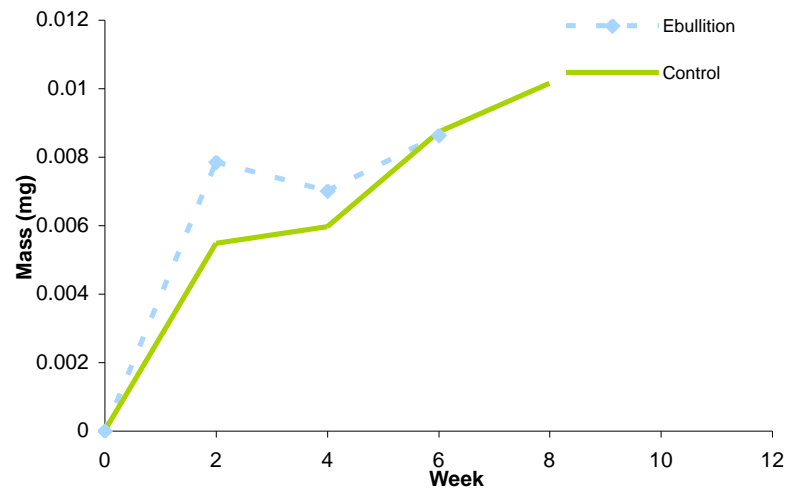
Fluoranthene flux to water



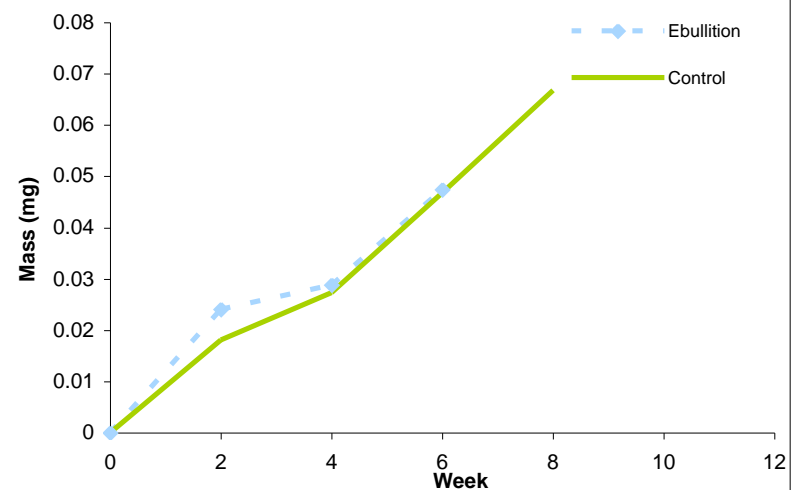
Pyrene flux to water

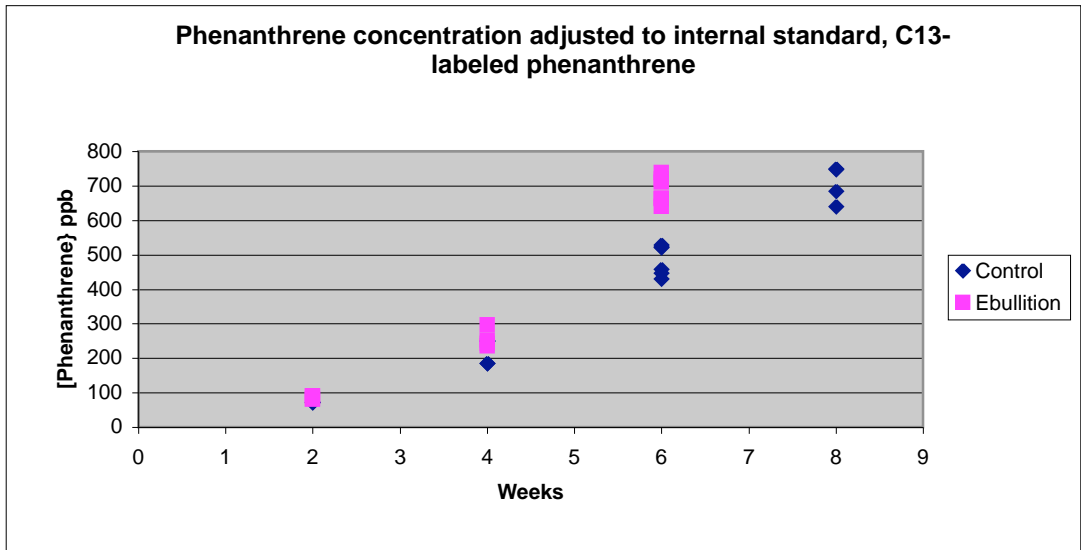
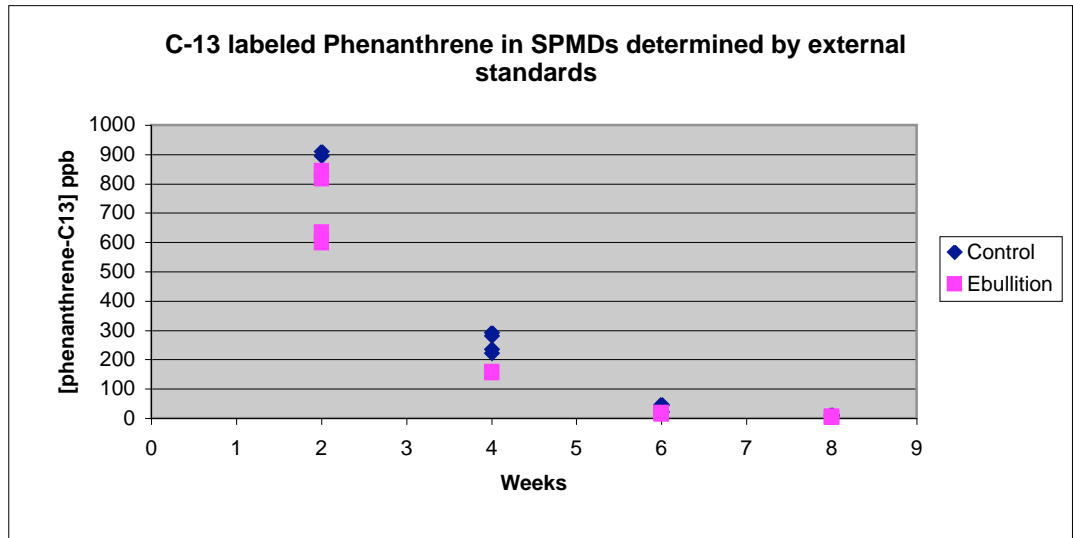
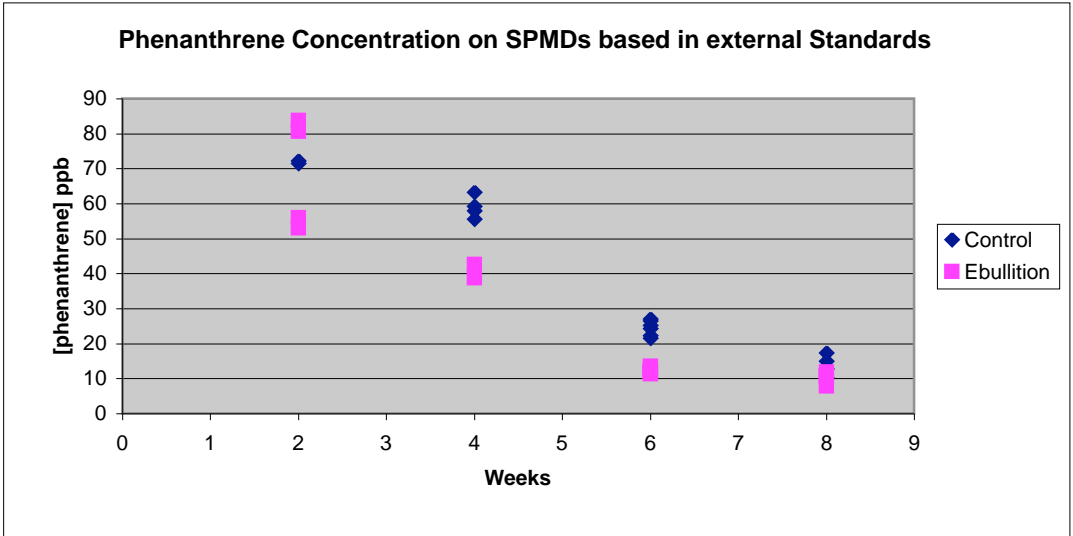


Cumulative Fluoranthene mass in SPMD

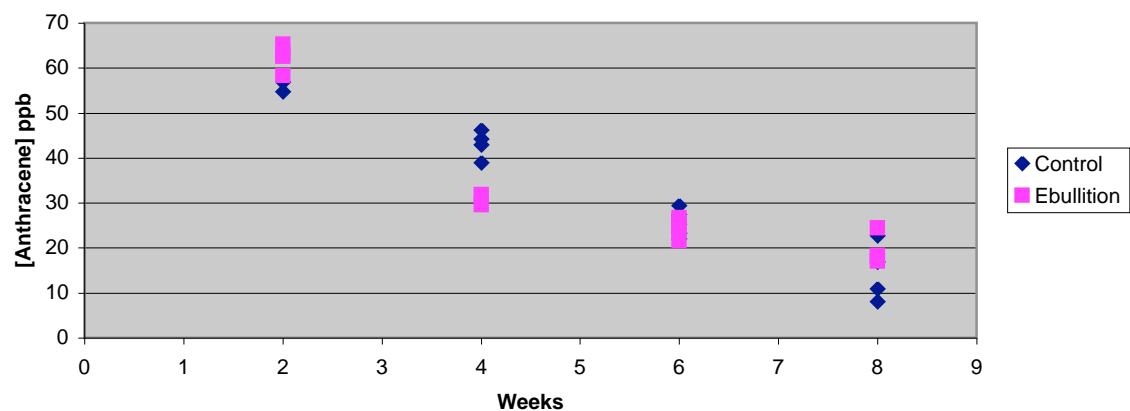


Cumulative pyrene mass in SPMD

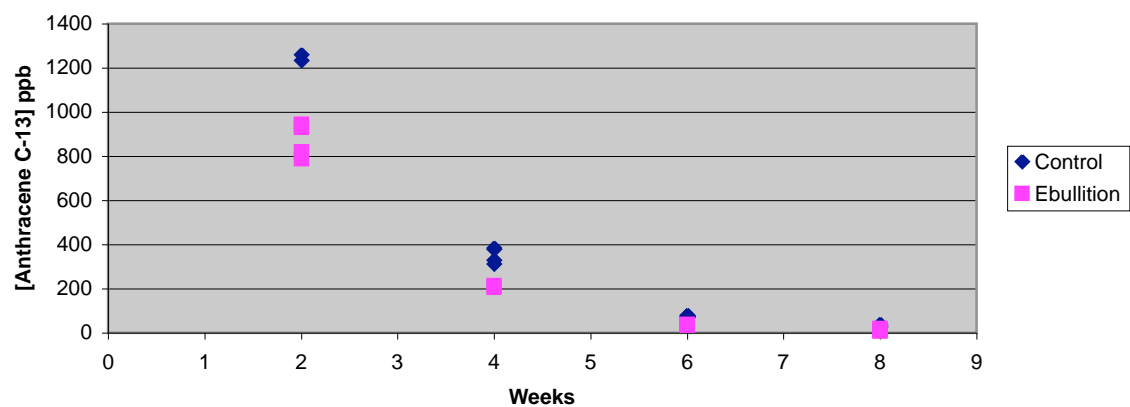




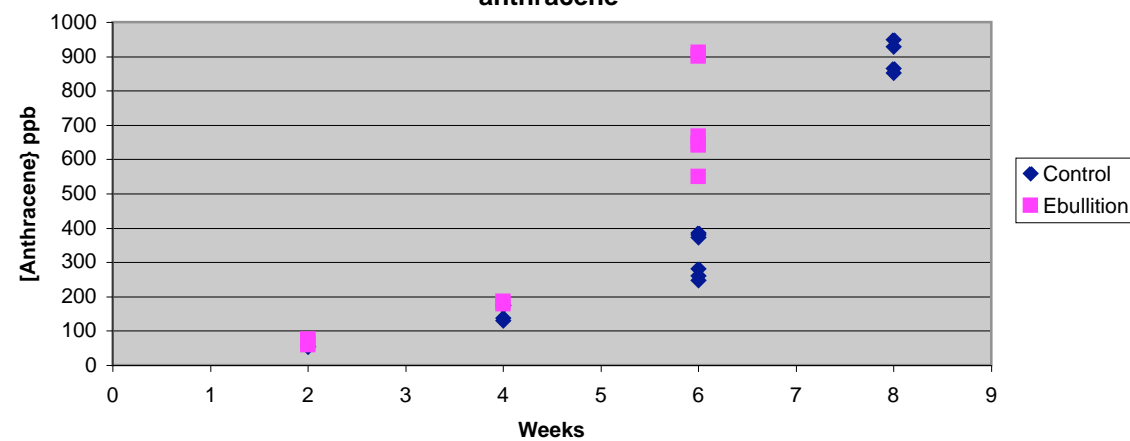
Anthracene Concentration in SPMDs based on external standards

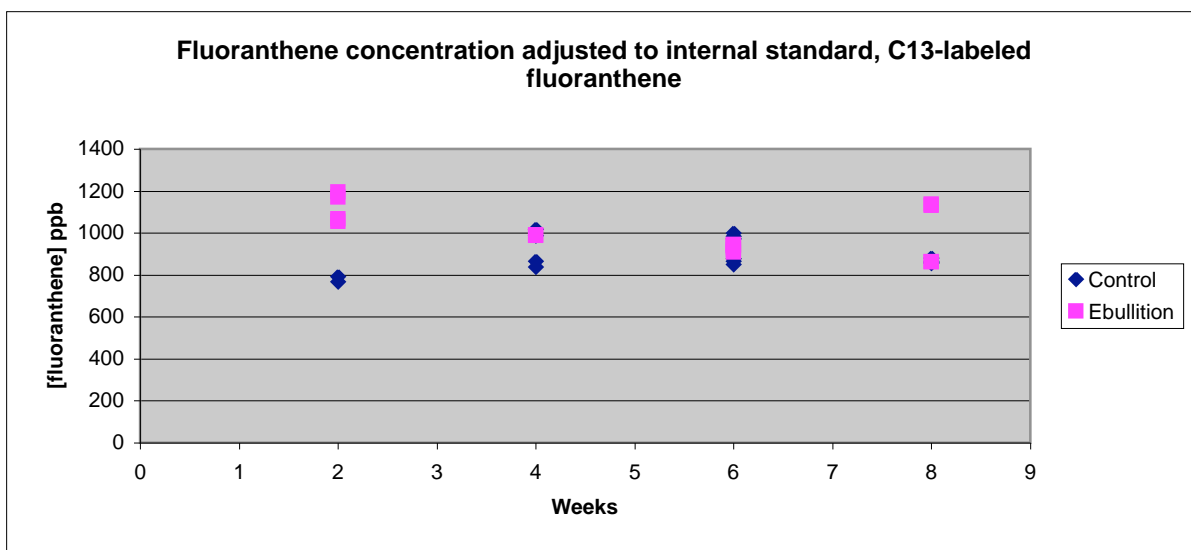
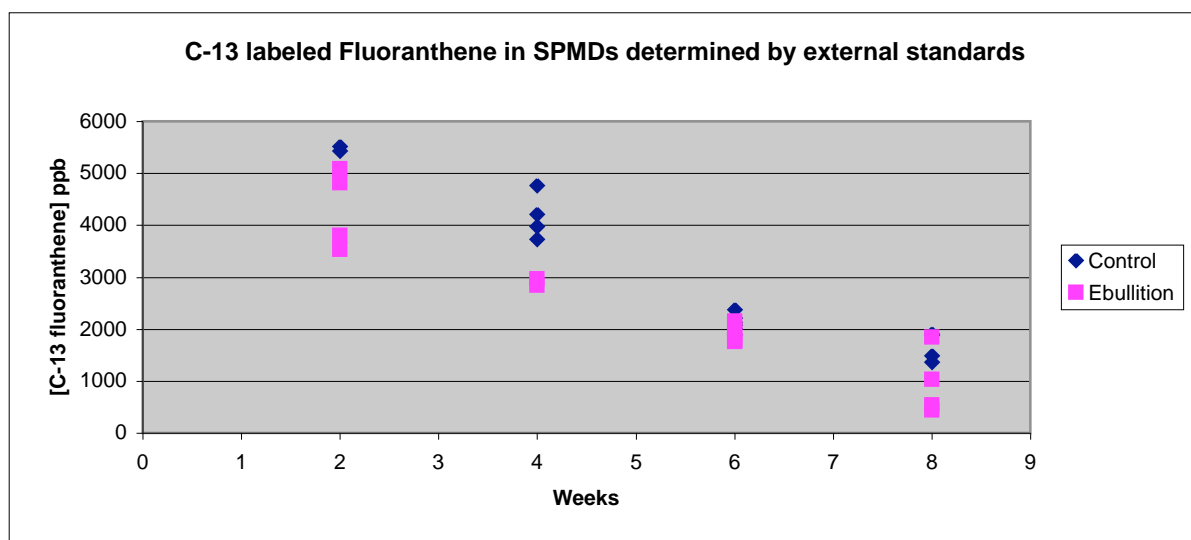
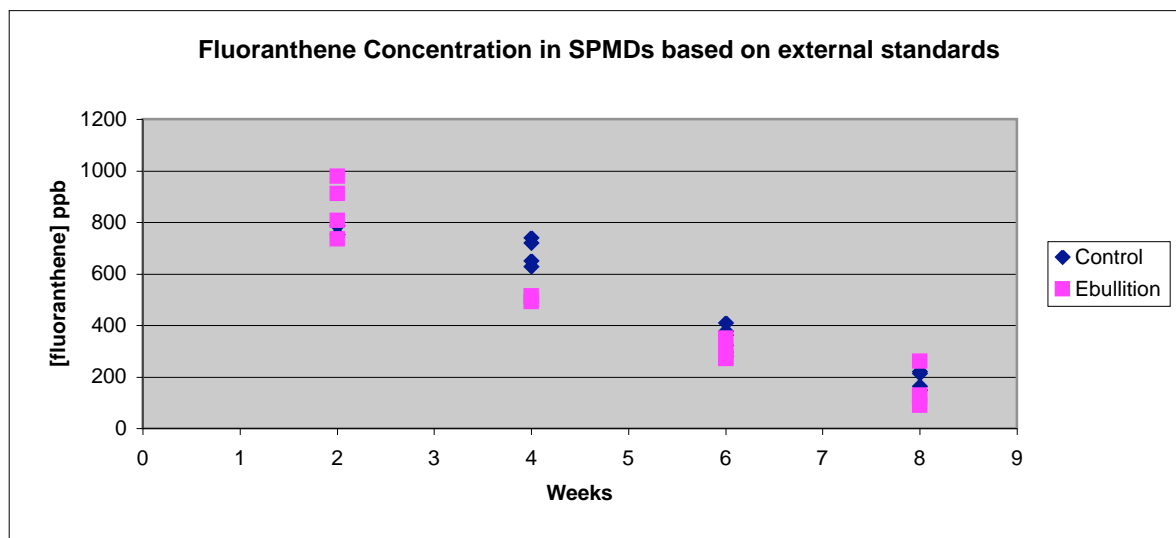


C-13 labeled Anthracene in SPMDs determined by external standards

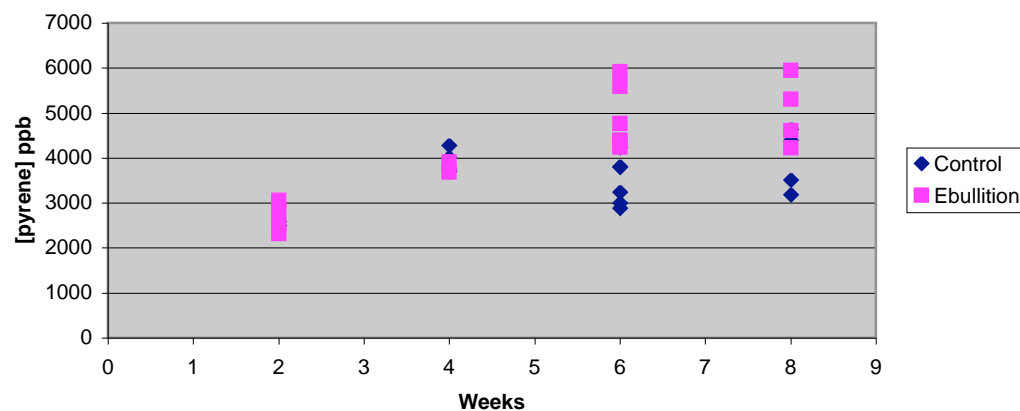


Anthracene concentration adjusted to internal standard, C13-labeled anthracene

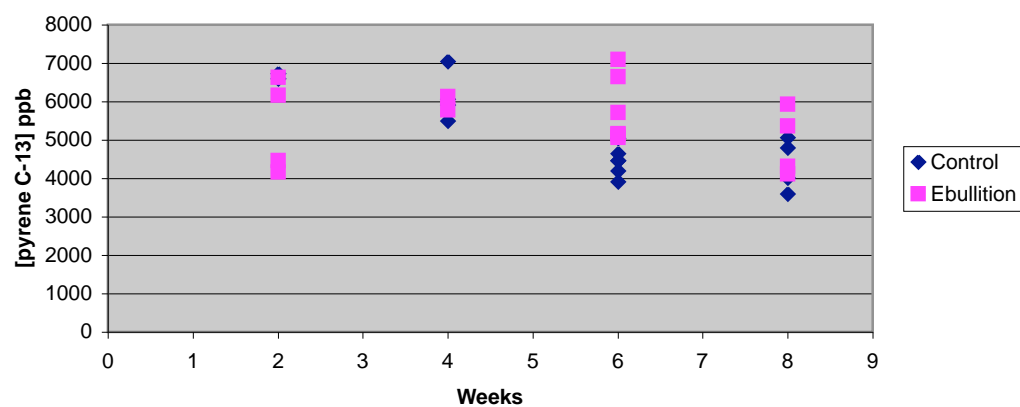




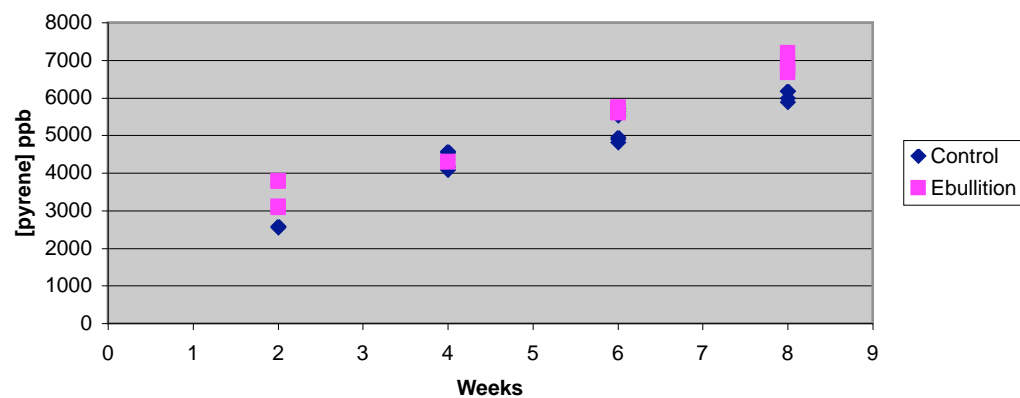
Pyrene Concentration in SPMDs based on external standards



C-13 labeled Pyrene in SPMDs determined by external standards



Pyrene concentration adjusted to internal standard, C13-labeled pyrene



C. PUBLICATIONS AND PRESENTATIONS

Dissertations

1. M.Y. Li. 2008. The M-Scale Model: Scaling Process Uncertainty in Contaminated Sediments. The University of Michigan, Ann Arbor.
2. P. Cakir. 2008. Effect of Advective Flow, Pore Water Transport and Ebullition on the Stability of Capped and Uncapped Cohesive Sediments. The University of Michigan, Ann Arbor.
3. Q. Wang. 2007. The Effect of Capping Regime on the Microbial Communities and the Biogas Formation Potential of Contaminated Surface Sediments (Defended November 2007).

Manuscripts to Date

1. Adriaens, P., A. Michalak and M-Y. Li. 2006. Scaling of Sediment Bioremediation Processes and Applications. *Eng. Life Sci.* 6 (3), 217-227.
2. Adriaens, P., and M.Y. Li. 2006. Scaling and Uncertainty of in Situ Biotransformation of Chlorinated Dioxins in Sediments of US Rivers and Lakes. *Proceed. International Summer School Biomonitoring, bioavailability and microbial transformation of pollutants in sediments and approaches to stimulate their biodegradation. Italian Inter-University Consortium "Chemistry for the Environment" INCA, Genoa, Italy.*
3. Cakir, P. and S. J. Wright. 2006. Stability of Non-cohesive Sediments under Conditions of Pore Water and Gas Fluxes. *World Environmental and Water Resources Congress, ASCE Proceedings, Omaha Nebraska.*
4. Li, M.Y., A.M. Michalak, and P. Adriaens. 2007. M-Scale Model: A Linear Estimation to Reproduce Spatial Variation. *Math. Geol.* In Resubmission.
5. M.Y. Li, A.M. Michalak, and P. Adriaens. 2007. Spatial Interpolation of Dioxin Contamination and Reactive Processes in Passaic River Sediments. *Environ. Sci. Technol.* In Review.
6. Wang, Q., C. Windnagle, and C. Gruden. 2008. "The Impact of Capping and Sediment Depth on Ebullition in Freshwater Sediments." In preparation for submission to *Water Science and Technology*.
7. Wang, Q., I. Kassem, V. Sigler, and C. Gruden. "The Short Term Effect of Capping on the Microbial Communities in Contaminated Sediments." *Water Environment Research*. Accepted September 2008.
8. M.Y. Li, A.M. Michalak, and P. Adriaens. 2007. Scaling Laboratory and Field Scale Experiments Through Microscale Variability. *Environ. Sci. Technol.* In Review.
9. Wang, Q., Windnagle, C., and C. Gruden. 2009. "The Impact of Environmental Conditions on Biogas Production in Contaminated Freshwater Sediments." Under preparation for submission to *Water Research*.
10. Cakir, P., and S.J. Wright. 2008. Stability of Non-cohesive Sediment Beds Subject to Bed Seepage (in review *Journal of Hydraulic Engineering*).

Abstracts

1. Gavril, M., Li, M-Y., Koning, K., Wright, S.J., and P. Adriaens. Scaling of Microbial Activity and Contaminant Transport in Capped and Uncapped Sediments. *Soc. Environ. Toxicol. Chem – Asia/Pacific, Beijing, China* (9/06).
2. Adriaens, P., A. Michalak and M-Y. Li. 2006. Scaling of Sediment Bioremediation Processes and Applications. *Int. Symp. Environ. Biotechnol., Leipzig, Germany* (7/06).
3. Li, M.-Y., N. Barabas, and P. Adriaens. "M-Scale: A Novel Tool for Uncertainty-Based Multi-Scale Site Characterization", *Battelle Conf., Monterey, CA.* (May, 2006).

4. Wang, Q., Kassem, I., Sigler, V., and Gruden, C.L. May 2006 "The Effect of Different Capping Regimes on Microbial Communities in Contaminated Sediments" 106th General Meeting of the American Society for Microbiology, Orlando, FL
5. Vannela, R., S. Jain, P. Adriaens, Q. Wang, O. Mileyeva-Bebiesheimer, and C. Gruden "Microbial Characterization and Projected Ebullition-Driven Contaminant Transport in Sediments", Battelle Conf., Monterey, CA. (May, 2006).
6. Wang, Q., Kassem, I., Sigler, V., and Gruden, C.L. May 2007. "The Effect of Capping on the Ebullition Potential and Microbial Ecology of Contaminated Surface Sediments" 107th General Meeting of ASM, May 21-25, 2007, Toronto, ON.
7. Cakir, P., and S.J. Wright. 2009. Effects of Pore Water Flux on Sediment Resuspension. Battelle Conference, Jacksonville, FL.
8. Redder, T., J. DePinto, J. Wolfe, P. Adriaens, S. Wright, and C. Gruden. 2009. Gas Ebullition in Sediments: Mechanisms, Impacts and Representation in Models. Proceed. 2009 Battelle Sediment Conference, Jacksonville, FL.
9. Adriaens, P., S. J. Wright, T. Redder, J. Wolfe, J. DePinto and N. Barabas. 2009. Integrating Site and Laboratory Data Using an Uncertainty-Based Sediment Capping Model. Proceed. 2009 Battelle Sediment Conference, Jacksonville, FL.
10. Cakir, P., and S.J. Wright. 2009. Experimental Results on the Stability of Non-Cohesive Sediment Beds Subject to Vertical Pore Water Flux paper accepted for Environmental and Water Resources Institute Congress, Kansas City, May 2009.
11. Cakir, P., and S.J. Wright. 2009. Effects of Gas Ebullition on Cohesive Sediment Resuspension and Cap Stability paper accepted for Environmental and Water Resources Institute Congress , Kansas City, May 2009